THE UNIVERSITY
of EDINBURGH

Investigating the Role of Thiosulfate Sulfurtransferase in Adipose Tissue Dysfunction in Obesity

Clare Elizabeth Mc Fadden

Thesis for the Degree of Doctor of Philosophy (PhD)

University of Edinburgh

2018

Declaration

I hereby declare that all work carried out during this PhD was performed by me, unless otherwise stated, under the supervision of Prof. Nicholas Morton and Dr. Roderick Carter. This thesis has not previously been submitted for any other degree or qualification.

_____

Clare Elizabeth Mc Fadden

Abstract

Obesity is associated with dysfunction of adipose tissue due to oxidative stress and inflammation, leading to insulin resistance. Thiosulfate sulfurtransferase (*Tst*) was previously identified as an adipose-expressed anti-diabetic gene that protects against diet-induced metabolic impairment when upregulated in adipose tissue of mice. TST is a mitochondrial enzyme involved in the metabolism of cyanide, reactive oxygen species (ROS) and endogenous hydrogen sulfide (H_2S). This thesis tested the hypothesis that TST maintains metabolic health in the face of dietary obesity. To do this, I investigated the adipose-tissue phenotypes and metabolic consequences of *Tst* gene deletion ($Tst^{-/-}$ mice) and of adipose tissue-specific overexpression of human TST (Ad-hTST mice) after exposure to high fat diet (HFD).

After 20 weeks of HFD, $Tst^{-/-}$ mice exhibited impaired glucose tolerance despite unchanged adipose tissue inflammatory cell infiltration, protein carbonylation and unfolded protein response activation. However, levels of mRNA encoding mitochondrial antioxidant enzymes including superoxide dismutase 2 and peroxiredoxin 3 were lower in $Tst^{-/-}$ mice on HFD. Unexpectedly, chow-fed $Tst^{-/-}$ mice had lower body weight and fat mass than wild-type controls highlighting a potential effect of *Tst* on fat accumulation with age.

A new mouse model with high expression of human TST genetically targeted to adipose tissue (Ad-hTST) was developed using the LoxP / Cre recombinase expression system, with a parent line expressing Cre under the control of the adiponectin promoter to confer adipose specificity. The Ad-hTST mice were found to gain a similar amount of weight and fat mass to control mice when exposed to 6 weeks of HFD. However, Ad-hTST mice had impaired glucose tolerance with no change in inflammatory cell infiltration, mRNA levels of antioxidant enzymes or unfolded protein response genes. Thus, unexpectedly, overexpression of human TST in adipose tissue of mice results in a detrimental metabolic phenotype.

In vivo and *in vitro* experiments were conducted to test the hypothesis that TST protects against ROS accumulation. Paraquat was tested as an inducer of oxidative stress *in vivo* in wild-type, $Tst^{-/-}$ and $Tst^{+/-}$ mice. At the doses used (25mg/kg and under), mice became unwell and lost weight, with no increase in markers of oxidative

stress in adipose or lung. The production of mitochondrial ROS in response to exogenous hydrogen peroxide (H_2O_2) exposure was increased in primary adipocytes from *Tst*$^{-/-}$ mice *in vitro*. However, primary hepatocytes showed reduced mitochondrial ROS production in response to H_2O_2 exposure. ROS production in hepatocytes was unaffected by pre-incubation with a H_2S donor, an inhibitor of H_2S-producing enzyme CSE or N-acetyl-cysteine, an antioxidant. TST may therefore influence mitochondrial ROS production differently in cell types such as adipocytes and hepatocytes. Disposal of exogenous H_2O_2 was unchanged in primary adipocytes from *Tst*$^{-/-}$ and Ad-hTST mice, and this was not affected by pre-incubation with sodium thiosulfate, a TST substrate.

Metabolic changes in response to HFD may be influenced by alteration in TST expression, however the current data suggest it is unlikely to occur through the prevention of excessive local ROS accumulation in adipose tissue. Mice lacking the *Tst* gene globally and mice with adipose-specific overexpression of the human TST gene have a similarly impaired metabolic response to HFD. The phenotype of adipose-specific human TST-overexpressing mice does not recapitulate the protective metabolic phenotype produced by overexpression of the endogenous mouse *Tst* gene. In conclusion, TST may influence adipose tissue due to its role in the oxidation of H_2S, however, by the current means, it does not appear to substantially impact the response of this tissue to oxidative stress.

Lay Summary

The prevalence of obesity has increased greatly over the last three decades, and because of this, diseases that are associated with increased weight, such as diabetes are on the rise. In obesity, fat tissue expands to store excess nutrients, but this can often lead to damage to fat cells causing them to make damaging reactive oxygen species (ROS), stop functioning properly and die. When this happens, the fat tissue no longer responds to insulin which is telling it to absorb sugar from the blood, a state that is called insulin resistance that can lead to diabetes. Whether someone who is obese will get diabetes or not is often influenced by how well their fat cells survive and respond to this large expansion, and genes in the fat cells can affect this. TST is one gene that was found to protect mice against gaining weight and becoming diabetic when it was increased in fat tissue.

This project aimed to find out how changing the levels of TST in fat tissue could protect against damage of the tissue caused by obesity. It is thought that TST could protect fat cells because it might be able to break down ROS, which are made by damaged fat cells, and which cause more damage. To test this idea, mice without TST and mice with higher amounts of human TST introduced into their fat tissue were put on a high fat diet to make them obese. Mice lacking TST became overweight to the same level as normal mice that had the gene, but they had slightly more sugar in their blood. There were no major differences in damage to their fat tissue however, and so lacking TST in fat tissue was probably not causing the diabetes. The other mice with higher amounts of TST in their fat tissue, gained weight as normal when given a high fat diet. Surprisingly however, these mice showed a slight worsening of their diabetes. They also had no major differences in damage to their fat tissue, and so I could not confirm that having high amounts of human TST in fat tissue protected the mice from becoming diabetic when they were obese.

Isolated fat cells from mice lacking TST and mice with high TST in fat were used to test if these cells made more ROS than normal fat cells, or if they could break down ROS better. Fat cells lacking TST made more ROS than normal cells, but when repeated with liver cells, the opposite result was found. Fat cells lacking TST and fat

cells with more TST broke down ROS at the same rate as normal fat cells. Therefore, TST likely does not help protect cells against damaging ROS and so it might not be able to protect fat tissue damaged in obesity.

This project was important because it found out that increasing TST in fat tissue probably won't prevent diabetes in obese people. Future work focusing on understanding the functions of TST in other tissues may help us uncover a way to target this enzyme to prevent diabetes.

Acknowledgements

At times it seemed like I might not reach the end of this PhD, and now that I sit with the final version in front of me, I feel a great sense of gratitude to the people who helped me get to this point, and to the friends for life I have made along the way.

I must first thank my supervisors for their support, encouragement and guidance throughout. Thank you to my primary supervisor, Nik Morton, for his imagination and optimism, which helped me to find my motivation and hope when I thought there was no way forward. Thank you to Rod Carter, who as my secondary supervisor was always there to help figure out practical solutions to overcome the bumps in the road, and for who's support during tough times I will forever be grateful.

I would also like to thank the other members of the molecular metabolism group who were always there for practical and emotional support. I am grateful to Rhona Aird, our lab manager for keeping the lab running despite the occasional chaos, and for always lending a hand or an ear when needed. To my fellow PhD students, Dr. Katharina Schraut & Dr. Matthew Gibbins, I am both proud of what they achieved during our time toiling away in lab together, and thankful that I had such great people to share my PhD successes and troubles with.

My PhD experience was enriched by the friends I made during my time in Edinburgh. I made it through my first year, during which I acclimatised to a new city and struggled with the workload of a Masters course mainly because of the friendship of Raphaël Castellan. That year, we struggled to settle in together as international students and kept each other sane, and in the following years, Raphaël was there to listen to my woes, both scientific and personal, and my time in Edinburgh would have been undoubtedly more difficult and less enjoyable without him. Sam Littler and Tracy Mak-Lewin were also a joy to meet when I first moved here, and I am so grateful for their friendship and support over the years. Thank you also to the other fellow PhD students who were around to lend a sympathetic ear or to encourage non-scientific distraction – Marlène, Chris, Amelia, Emma, Callam, Nicole and Julie.

Many thanks to the other people who helped me along the way with my research. I would like to thank the technicians in the animal unit for their help, especially Sandra who worked so hard to make sure the mice were happy and able to

give me the best results I could expect, and who always found the time to help, or to chat when needed. I am also grateful to Cecile Benezech and Marlène Magalhaes-Pinto for their guidance in how to do flow cytometry and how to analyse the results.

I was exceptionally lucky to have had great flatmates throughout my time in Edinburgh, and I am grateful to them all for their friendship and support. My first flatmates, Gayle and Gemma, without knowing, kept me in Edinburgh when I was ready to give up. I learned so much from them over the years, and I am grateful to them for sharing their lives with me. I am grateful to Karen for reminding me what I loved about home, and to Christine and Kelly for the fun we had while living together. My last flatmates were also my greatest support while I set out to write my thesis, and with them and their partners, Mayfield Terrace became home, for which I am so thankful. Raphaël and Marlène, you were there to help with the science and non-science dilemmas, and to make sure I always remembered to have dinner and only ever drank good wine! You brought Steven Allison and Cat Wann into the flat and my life, and I'm so grateful for the support and friendship they gave me as well.

Finally, I want to thank the people who encouraged me from the start, and who got me through the final months of my thesis and what felt like the infinite wait for my viva. My parents, Hannah and Mícheál, always encouraged me to achieve my best and believed in my ability even when I did not. They happily welcomed me home as their boomerang child, and put up with my return to adolescence as I struggled to finish the thesis and find my place in life. I will be forever grateful to them for allowing me this time to find my way through – although I will always maintain my aversion to steamed potatoes! The last person I need to thank is the one who, without a doubt has been a constant support through the hardest times in my life – including periods during this PhD where I doubted myself and my ability. She reminded me why I chose to do a PhD in the first place, and that I was able for whatever came at me, and her generosity with her time and thoughts got me to the point where I have a thesis to hand in today. Thank you, Niamh McDermott for being such a good friend.

List of Figures

Figure 1.1: Catalytic mechanism of TST activity in the detoxification of cyanide and in the assay used to measure rhodanese activity. 42
Figure 1.2: Mitochondrial sulfide oxidation pathway 44
Figure 2.1: Map of gene expression cassette at Rosa26 locus of Rosa26^{LSLhTST} mice (a) before and (b) after Cre-mediated recombination. 61
Figure 2.2: Gating strategy for analysis of SVFs from epididymal adipose tissue from *Tst*$^{-/-}$ and Ad-hTST mice. 82
Figure 3.1: Timeline of WT and *Tst*$^{-/-}$ mice on chow or HFD for 6 weeks. 89
Figure 3.2: Timeline of WT and *Tst*$^{-/-}$ mice on chow or HFD for 20 weeks. 89
Figure 3.3: Body weight of *Tst*$^{-/-}$ and WT mice on chow or HFD for 6 weeks. 90
Figure 3.4: Epididymal white adipose weight of *Tst*$^{-/-}$ and WT mice on chow or HFD for 6 weeks. 91
Figure 3.5: Immune cell populations in stromal vascular fraction (SVF) of epididymal adipose tissue in *Tst*$^{-/-}$ and WT mice on chow or HFD for 6 weeks. 93
Figure 3.6: Body weights of *Tst*$^{-/-}$ and WT mice on chow or HFD for 20 weeks. 95
Figure 3.7: White adipose depot weights in *Tst*$^{-/-}$ and WT mice on chow or HFD for 20 weeks. 96
Figure 3.8: Plasma glucose and insulin levels of *Tst*$^{-/-}$ and WT mice on chow or HFD for 18 weeks after administration of a glucose bolus. 98
Figure 3.9: Plasma glucose levels of *Tst*$^{-/-}$ and WT mice on chow or HFD for 19 weeks after administration of an insulin bolus. 100
Figure 3.10: Plasma adiponectin levels in *Tst*$^{-/-}$ and WT mice on chow or HFD for 20 weeks. 102
Figure 3.11: Gene expression of adiponectin in mesenteric white adipose tissue of *Tst*$^{-/-}$ and WT mice on chow or HFD for 20 weeks. 103
Figure 3.12: Gene expression of key antioxidant enzymes in mesenteric adipose tissue in *Tst*$^{-/-}$ and WT mice on chow or HFD for 20 weeks. 105
Figure 3.13: Gene expression of NRF2-responsive antioxidant enzymes in mesenteric adipose tissue in *Tst*$^{-/-}$ vs. WT mice on chow or HFD for 20 weeks. 106

Figure 3.14: Carbonyl content of mesenteric adipose tissue of *Tst*$^{-/-}$ and WT mice on chow or HFD for 20 weeks. 107
Figure 3.15: Immune cell populations in stromal vascular fraction (SVF) of epididymal adipose tissue in *Tst*$^{-/-}$ and WT mice on chow or HFD for 20 weeks. 109
Figure 3.16: Gene expression of pro-inflammatory adipokines in mesenteric adipose tissue of *Tst*$^{-/-}$ and WT mice on chow or HFD for 20 weeks. 111
Figure 3.17: Gene expression of endoplasmic reticulum stress markers in mesenteric adipose tissue of *Tst*$^{-/-}$ and WT mice on chow or HFD for 20 weeks. 112
Figure 3.18: Comparison of *Tst* gene expression in mesenteric adipose tissue in WT mice after (a) 6 weeks and (b) 20 weeks of chow or HFD. 113
Figure 3.19: Gene expression of H_2S-producing enzymes in mesenteric adipose tissue of *Tst*$^{-/-}$ and WT mice on chow or HFD for 20 weeks. 115
Figure 3.20: Gene expression of sulfide oxidation genes in mesenteric adipose tissue of *Tst*$^{-/-}$ and WT mice on chow or HFD for 20 weeks. 116
Figure 4.1: Schematic of genetic structure of (a) Adipoq-Tst and (b) Ad-hTST mice. 131
Figure 4.2: Timeline of WT-LSL and male Ad-hTST mice on LFD or HFD for 6 weeks. 133
Figure 4.3: Gene expression of human TST in adipose depots of Ad-hTST and WT-LSL female mice at 8 weeks of age. 135
Figure 4.4: Gene expression of mouse *Tst* in adipose depots of Ad-hTST and WT-LSL female mice at 8 weeks old. 136
Figure 4.5: Rhodanese activity in homogenates of adipose depots of Ad-hTST and WT-LSL female mice at 8 weeks of age. 138
Figure 4.6: TST protein in adipose depots of Ad-hTST and WT-LSL female mice at 8 weeks of age. 139
Figure 4.7: Gene expression of human TST in non-adipose tissues of Ad-hTST and WT-LSL female mice at 8 weeks of age. 140
Figure 4.8: mCherry fluorescence in adipose and non-adipose tissues of Ad-hTST and WT-LSL female mice at 8 weeks of age. 143

Figure 4.9: Body weight of Ad-hTST and WT-LSL mice on LFD or HFD for 6 weeks. 144
Figure 4.10: Whole body composition of Ad-hTST and WT-LSL mice on LFD or HFD for 6 weeks. 145
Figure 4.11: White adipose depot weights of Ad-hTST and WT-LSL mice on LFD or HFD for 6 weeks. 146
Figure 4.12: Food intake and feed efficiency per week in Ad-hTST and WT-LSL mice on LFD or HFD for 6 weeks. 147
Figure 4.13: Plasma glucose and insulin levels after administration of a glucose bolus to Ad-hTST and WT-LSL mice on LFD or HFD for 5 weeks. 149
Figure 4.14: Plasma adiponectin levels of Ad-hTST and WT-LSL mice on LFD or HFD for 6 weeks. 151
Figure 4.15: Plasma adiponectin levels of Adip-cre and WT (6J) mice. 152
Figure 4.16: Adiponectin gene expression in epididymal white adipose tissue of Ad-hTST and WT-LSL mice on LFD or HFD for 6 weeks. 153
Figure 4.17: Gene expression of key antioxidant enzymes in epididymal adipose tissue of Ad-hTST and WT-LSL mice on LFD or HFD for 6 weeks. 155
Figure 4.18: Gene expression of NRF2-responsive antioxidant enzymes in epididymal adipose tissue of Ad-hTST and WT mice on LFD or HFD for 6 weeks. 156
Figure 4.19: Immune cell populations in stromal vascular fraction (SVF) of epididymal adipose tissue of Ad-hTST and WT-LSL mice on LFD or HFD for 6 weeks. 158
Figure 4.20: Gene expression of pro-inflammatory adipokines in epididymal adipose tissue of Ad-hTST and WT mice on LFD or HFD for 6 weeks. 159
Figure 4.21: Gene expression of endoplasmic reticulum stress markers in epididymal adipose tissue of Ad-hTST and WT mice on LFD or HFD for 6 weeks. 160
Figure 4.22: TST gene and protein expression in epididymal adipose tissue of Ad-hTST and WT mice on LFD or HFD for 6 weeks. 162
Figure 4.23: Gene expression of H_2S-producing enzymes in epididymal adipose tissue of Ad-hTST and WT-LSL mice on LFD or HFD for 6 weeks. 163
Figure 4.24: Gene expression of sulfide oxidation genes in epididymal adipose tissue of Ad-hTST and WT-LSL mice on LFD or HFD for 6 weeks. 164

Figure 4.25: Comparison of mouse and human TST protein sequence. 172
Figure 5.1: Chemical structure and redox cycling mechanism of paraquat dichloride (PQ) in the production of superoxide in vivo. 177
Figure 5.2: Weight loss of *Tst*$^{+/-}$ mice at 24hrs after administration of PQ (25mg/kg) or saline (0.9%). 180
Figure 5.3: White adipose tissue response in *Tst*$^{+/-}$ mice at 24hrs after administration of PQ (25mg/kg) or saline (0.9%). 181
Figure 5.4: Lung response in *Tst*$^{+/-}$ mice at 24hrs after administration of PQ (25mg/kg) or saline (0.9%). 182
Figure 5.5: Percentage of 100μM H_2O_2 in media after 5mins exposure of primary adipocytes of WT and *Tst*$^{-/-}$ mice. 183
Figure 5.6: Percentage of 100μM H_2O_2 in media after 5mins exposure of primary adipocytes of WT and Ad-hTST mice. 184
Figure 5.7: Mitochondrial superoxide and LDH activity of primary adipocytes of *Tst*$^{-/-}$ and WT mice exposed to H_2O_2 (0.5%) for 3hrs. 185
Figure 5.8: Mitochondrial superoxide and LDH activity of primary hepatocytes of *Tst*$^{-/-}$ and WT mice exposed to H_2O_2 for 2hrs. 188
Figure 5.9: Mitochondrial superoxide and LDH activity of primary hepatocytes of *Tst*$^{-/-}$ and WT mice exposed to H_2O_2 for 2hrs with or without pre-incubation with an antioxidant. 190
Figure 5.10: Mitochondrial superoxide and LDH activity of primary hepatocytes of *Tst*$^{-/-}$ and WT mice exposed to H_2O_2 for 2hrs with or without pre-incubation with a sulfide donor or CSE inhibitor. 192
Figure 7.1: Body weight of at 5 months old *Tst*$^{-/-}$ and WT mice on chow diet. 211
Figure 7.2: White adipose depot weights in 5-month-old *Tst*$^{-/-}$ versus WT mice on chow diet. 212
Figure 7.3: Weight and adipose malondialdehyde content of *Tst*$^{-/-}$ and WT mice treated with 1, 5 or 10mg/kg paraquat or saline (0.9%) for 24hrs. 213
Figure 7.4: Antioxidant gene expression in epididymal adipose tissue of *Tst*$^{-/-}$ and WT mice treated with 1, 5 or 10mg/kg paraquat or saline (0.9%) for 24hrs. 214
Figure 7.5: Timeline of WT mice exposed to paraquat for 2, 3 or 6 days. 215

Figure 7.6: Weight and adipose response of WT mice 2, 3 or 6 days after administration of PQ (20mg/kg) or saline (0.9%). 216
Figure 7.7: Lung response in WT mice 2, 3 or 6 days after administration of PQ (20mg/kg) or saline (0.9%). 217

List of Tables

Table 2.1: Composition of RM1 maintenance diet 62
Table 2.2: Composition of Surwit high fat and low fat diets. 63
Table 2.3: Gene names and TaqMan IDs for probes used for RT-PCR. 67
Table 2.4: Components of lysis buffer for extraction of protein from adipose tissue. 69
Table 2.5: Components of SDS-polyacrylamide gels 70
Table 2.6: Components of buffers for SDS-PAGE and Western blots. 72
Table 2.7: Primary and secondary antibodies for Western blots. 72
Table 2.8: Components of Full Krebs phosphate buffer (Full Krebs). 76
Table 2.9: Components of liver perfusion and digestion media for primary hepatocyte isolation 78
Table 2.10: Components of primary hepatocyte media 78
Table 2.11: Components of 10X DMEM used to make equilibrated Percoll. 78
Table 2.12: Flow cytometry antibodies used in Chapter 3 80
Table 2.13: Flow cytometry antibodies used in Chapter 4 81
Table 6.1: Summary of Results - Chapter 3 202
Table 6.2: Summary of Results - Chapter 4 203
Table 6.3: Summary of Results - Chapter 5 204
Table 7.1: Abbreviations and meanings 218
Table 7.2: Manufacturer's Details 221

Contents

Declaration **1**

Abstract **2**

Lay Summary **4**

Acknowledgements **6**

List of Figures **8**

List of Tables **12**

Chapter 1 Introduction **18**

1.1 Obesity **18**

1.1.1 Obesity Prevalence 18

1.1.2 Metabolic syndrome 18

1.1.3 Genetics of obesity 19

1.2 Adipose tissue dysfunction in obesity **21**

1.2.1 Adipose structure and function 21

1.2.2 Oxidative stress in adipose tissue 22

1.2.3 Inflammation 29

1.2.4 Endoplasmic reticulum stress 32

1.2.5 Adipose expansion, hypoxia and fibrosis 33

1.2.6 Altered adipokine secretion 34

1.3 Thiosulfate sulfurtransferase **40**

1.3.1 Discovery of Tst as a lean gene 40

1.3.2 Function of thiosulfate sulfurtransferase 41

1.3.3 Hydrogen sulfide 48

1.3.4 TST function summarised 57

1.4 Overview **57**

1.5 Hypothesis and aims **58**

Chapter 2 Materials and Methods **59**

2.1 In vivo physiology **59**

2.1.1 Animal models and maintenance 59

2.1.2 Experimental procedures 64

2.2 Molecular Biology **65**

2.2.1 Measurement of gene expression 65

2.2.2 Measurement of protein expression 68

2.2.3 Biochemical and enzyme assays 73

2.3 Cell Biology **76**

2.3.1 Primary cell isolation 76

2.3.2 In vitro cell analysis 79

2.4 Imaging **85**

2.4.1 Whole-mount staining of tissue explants 85

2.4.2 Imaging 85

2.5 Statistics **85**

Chapter 3 The effects of Tst gene knockout on glucose homeostasis and adipose tissue response to high fat diet. **86**

3.1 Introduction **86**

3.1.1 Hypothesis & aims 88

3.2 Method **89**

3.3 Results **90**

3.3.1 The effect of Tst gene knockout after 6 weeks of high fat diet. 90

3.3.2 The effect of Tst gene knockout after 20 weeks of high fat diet. 95

3.4 Discussion 117

3.4.1 Metabolic impairment of $Tst^{-/-}$ mice on HFD. 117

3.4.2 Adipose tissue dysfunction of $Tst^{-/-}$ mice on HFD. 120

3.4.3 Impact of increased sulfide on metabolic impairment of $Tst^{-/-}$ mice. 124

3.4.4 Reduced fat mass in $Tst^{-/-}$ mice on chow diet. 125

3.4.5 Limitations and future work. 127

Chapter 4 Metabolic characterisation of a new mouse model with human TST expression in adipose tissue 130

4.1 Introduction 130

4.1.1 Hypothesis & aims 132

4.2 Method 133

4.3 Results 134

4.3.1 Expression of human and mouse TST in adipose and other tissues of female Ad-hTST mice. 134

4.3.2 The effects of human TST gene overexpression in adipose on glucose homeostasis and adipose tissue response to high fat diet in Ad-hTST male mice. 144

4.4 Discussion 165

4.4.1 Metabolic impairment of Ad-hTST mice on HFD. 167

4.4.2 Adipose tissue dysfunction of Ad-hTST mice on HFD. 169

4.4.3 Impact of hydrogen sulfide on adipose tissue in Ad-hTST mice. 170

4.4.4 Limitations and future work. 171

Chapter 5 The role of thiosulfate sulfurtransferase in the response to oxidative stress. 175

5.1 Introduction 175

5.1.1 Hypothesis & Aims 178

5.2 Method 179

5.2.1 Induction of oxidative stress in vivo using paraquat 179

5.2.2 Induction of oxidative stress in vitro 179

5.3 Results 180

5.3.1 Paraquat as an inducer of adipose tissue oxidative stress in vivo. 180

5.3.2 Consumption of ROS by primary adipocytes from $Tst^{-/-}$ and Ad-hTST mice. 183

5.3.3 Mitochondrial superoxide production in primary adipocytes from $Tst^{-/-}$ mice. 185

5.3.4 Mitochondrial superoxide production in primary hepatocytes from $Tst^{-/-}$ mice. 187

5.4 Discussion 193

5.4.1 Paraquat as a model of oxidative stress in vivo 193

5.4.2 The role of TST in the response to oxidative stress in adipocytes in vitro. 195

5.4.3 Primary hepatocytes lacking Tst may be protected against oxidative stress 197

5.4.4 Limitations and future work. 198

Chapter 6 Discussion 200

6.1 TST and metabolic impairment 205

6.2 TST and oxidative stress 207

6.3 Future work 208

6.4 Concluding remarks 210

Chapter 7 Appendix 211

7.1 Body weight and adipose tissue weights of 5-month-old $Tst^{-/-}$ versus WT mice on chow diet. 211

7.2 Paraquat Pilot Results..... 213

7.2.1 Treatment of $Tst^{-/-}$ and WT mice with 1, 5 or 10mg/kg paraquat for 24hrs. 213

7.2.2 Treatment of WT mice with 20mg/kg paraquat for 2, 3 or 6 days..... 215

7.3 Abbreviations and Manufacturer's Details 218

References 227

Chapter 1 Introduction

1.1 OBESITY

1.1.1 Obesity Prevalence

Obesity is defined as having a body mass index (BMI) over 30kg/m^2, and a BMI over 25kg/m^2 is defined as overweight. A high BMI, particularly if accompanied by excessive visceral fat accumulation, is associated with increased risk of non-communicable diseases such as cardiovascular disease, type two diabetes mellitus and cancer (Renehan *et al.* 2008; Wormser *et al.* 2011). The world is in the grips of an obesity epidemic, with the prevalence of overweight and obesity increasing 27.5% for adults and 47.1% for children between 1980 and 2013 (Ng *et al.* 2014). The detrimental effect of this rapid increase in obesity on global health is seen in the doubling of diabetes prevalence between 1980 and 2014, and the increased economic burden due to healthcare costs and loss of work (Seuring *et al.* 2015; Zhou *et al.* 2016). The cause of this rapid worldwide increase in obesity is thought to be globalisation of a diet high in animal fat and protein, refined grains and added sugar, and a reduction in physical activity due to technological advances (Malik *et al.* 2012). Despite this obesogenic environment, a substantial proportion of the population has remained non-obese indicting that some protection against obesity may lie in the genetic variation of the population (Ljungvall and Zimmerman 2012). Understanding the underlying mechanisms controlling this variation may lead to the development of new interventions – pharmacological or lifestyle – that can be targeted to prevent or reverse excess weight gain and diseases associated with it.

1.1.2 Metabolic syndrome

Excess fat mass characterised by a high BMI or waist circumference is significantly associated with the most common non-communicable diseases: cardiovascular disease, diabetes and cancer (Chan *et al.* 1994; Renehan *et al.* 2008; Wormser *et al.* 2011). Central obesity, an excess of intra-abdominal visceral fat, is particularly predictive of metabolic and cardiovascular disease risk (Tchernof and Després 2013).

The metabolic syndrome is a cluster of risk factors for these diseases, and is defined as at least three of the following: dyslipidemia, hyperglycemia, elevated blood pressure, and a pro-inflammatory and pro-thrombotic state (Grundy 2016). The prevalence of metabolic syndrome is increased in obese and overweight cohorts (Park *et al.* 2003), and excess abdominal fat is positively correlated with many of these risk factors (Vega *et al.* 2006). Pathophysiological changes occur in adipose tissue in obesity, including altered secretion of many hormonal factors and pro-inflammatory cytokines that directly contribute to these features of the metabolic syndrome, and link obesity with diabetes and cardiovascular disease.

1.1.3 Genetics of obesity

BMI and other measurements of body mass such as waist circumference are heritable traits. Twin studies have estimated this heritability to be between 56% and 77% for BMI (Silventoinen *et al.* 2008; Wardle *et al.* 2008). A long history of experimental genetics in mouse lines confirms that body weight and fat mass are influenced by genes. The was illustrated by the identification of the hyperphagic *ob*/*ob* mouse as far back as 1950 (Ingalls *et al.* 1950). It took almost half a century to finally identify the *ob* gene as an adipose-derived hormone, named leptin from the Greek “lepto” for thinness, that signals in the hypothalamus to suppress appetite and energy expenditure (Zhang *et al.* 1994; Satoh *et al.* 1997). Subsequently, two cases of leptin deficiency in humans leading to severe obesity were described, with subsequent successful treatment with recombinant leptin (Montague *et al.* 1997; Farooqi *et al.* 1999). This discovery confirmed that individual susceptibility to weight gain was influenced by genetics. Subsequently, the genetic basis of obesity in other rodent models was uncovered, including the discovery of neuropeptide Y, pro-opiomelanocortin and the melanocortin-4 receptor, leading to the elucidation of neural circuits involved in the control of appetite (Dryden *et al.* 1995; Huszar *et al.* 1997; Yaswen *et al.* 1999). Rare mutations in these genes were also found to cause morbid obesity in humans (Van Der Klaauw and Farooqi 2015). As these monogenic forms of obesity explained only the severest cases, accounting for only a small proportion of the obese population,

genome-wide associated studies (GWAS) were undertaken to search for common variants with less extreme effects on obesity risk. The first gene region with variation that has a strong and replicable association with obesity was in the first intron of the FTO gene. Single nucleotide polymorphisms (SNPs) in this region associated strongly with early-onset and severe obesity, and type 2 diabetes risk through increased BMI (Dina *et al.* 2007; Frayling *et al.* 2007). A more recent meta-analysis including data from more 300,000 individuals from 125 studies identified 97 loci significantly associated with BMI (Locke *et al.* 2015). When grouped by pathway, these common obesity-associated variants confirm a major role for neural control of obesity risk, but also highlight new pathways such as insulin signalling, energy metabolism and adipogenesis. Waist to hip ratio, another surrogate measurement of obesity related to fat distribution, was associated with up to 49 loci in a genome wide association meta-analysis (Shungin *et al.* 2015). Many of the loci were distinct from those previously associated with BMI, and were in or near genes expressed highly in adipose tissue, or involved in biological processes necessary for adipose tissue expansion such as adipogenesis and angiogenesis. The success of GWAS at finding genetic variants associated with obesity has led to a wealth of information about possible causes of increased weight gain, especially through the discovery of genes involved in biological processes such as appetite regulation and adipose tissue function. However, understanding the function of many of these common variants and how, or even whether they contribute to obesity risk at a molecular and biochemical level remains a challenge.

1.2 ADIPOSE TISSUE DYSFUNCTION IN OBESITY

1.2.1 Adipose structure and function

Adipose tissue had long been thought of as only a storage organ for excess nutrient as lipid, with a huge capacity for expansion. However, in recent years the ability of adipose tissue to secrete numerous endocrine factors with a myriad of systemic effects has been recognised. Adipose tissue is now known to play a role in other vital functions including thermogenesis, reproduction and lactation, as well as helping to modulate immune responses. The main cellular component of adipose tissue is the adipocyte, a cell highly specialised to store a large quantity of triglyceride in lipid droplets, and to synthesise and secrete many hormonal factors, called adipokines. Adipose tissue contains other cell types, collectively called the stromal vascular fraction (SVF), including pre-adipocytes, endothelial cells, fibroblasts and many types of immune cells (Rosen and Spiegelman 2014). Different types of adipose tissue are specialised for different functions. Brown adipose tissue (BAT) is highly vascularised and contains adipocytes with many small lipid droplets and numerous large mitochondria with high expression of uncoupling protein 1 (UCP1)(Diaz *et al.* 2014). During cold exposure, UCP1 mediates the biochemical uncoupling of mitochondrial oxidative phosphorylation from ATP production, leading to the production of heat. It was initially thought that brown fat was only present in humans in infants, however recent discoveries of cold-triggered highly metabolically active tissues in adult humans has led to the recognition that some BAT depots are retained in adults, and can contribute to thermogenesis (Sacks and Symonds 2013). White adipose tissue (WAT) is much more abundant than BAT, and carries out the classical function of energy storage, but is also a key endocrine organ (Coelho *et al.* 2013). White adipocytes contain a single large lipid droplet, and are highly specialised to take up and convert nutrients to triglyceride for storage (lipogenesis), and to release free fatty acids by lipolysis. White adipocytes can also expand in times of excess – a process called hypertrophy – or pre-adipocytes can proliferate and differentiate to add more lipid storage capacity through hyperplasia (Rosen and Spiegelman 2014). Different white adipose depots have a different capacity to expand without causing detrimental metabolic effects, and it is

widely recognised that upper body obesity characterised by excess visceral fat is more metabolically harmful than lower-body obesity in which the subcutaneous fat expands more (Tchernof and Després 2013). A third type of adipocyte with an intermediary phenotype, the beige adipocyte, has also been described (Diaz *et al.* 2014). Beige adipocytes have several lipid droplets and UCP1-expressing mitochondria like brown adipocytes, however they are located within white adipose depots. A full understanding of their contribution to metabolic health is outside the scope of this thesis.

1.2.2 Oxidative stress in adipose tissue

Reactive oxygen species (ROS) are made during cellular processes and are essential for normal physiological activity of the cell. However, ROS can cause oxidative damage when produced in excess or when the cellular antioxidant machinery is overloaded. Oxidative stress contributes to the pathology of many diseases, including obesity. In adipose tissue, ROS are essential for differentiation of pre-adipocytes to mature adipocytes (Tormos, Anso and Hamanaka 2011). As well as playing a role in the creation of new adipocytes, ROS are produced in the mitochondria and by activation of the insulin signalling pathway in mature adipocytes, and are necessary for appropriate propagation of the intracellular insulin signal (Mahadev *et al.* 2004). Therefore, maintaining the redox balance of the cell is essential for adipose tissue to function normally. In obesity, adipose tissue exhibits oxidative stress due to increased production of ROS and overloading of the antioxidant capability of the tissue (Furukawa *et al.* 2004; Huh *et al.* 2012; Long *et al.* 2013). This contributes to dysfunction of the tissue, and is a key risk factor for metabolic disease.

1.2.2.1 Sources of cellular reactive oxygen species

Mitochondria are a major source of ROS. Both complex I and III of the electron transport chain are significant sites of superoxide anion production, as well as other mitochondrial enzymes such as pyruvate dehydrogenase, 2-oxoglutarate dehydrogenase and complex II, with the type of substrate used influencing the amount

of superoxide produced (Quinlan *et al.* 2013). Another source of cellular ROS is the NADPH oxidases (NOX), with NOX4 being the most abundant in adipose tissue. NOX4 produces hydrogen peroxide (H_2O_2) in response to insulin-stimulation in adipocytes, which acts as a second messenger in the insulin signalling cascade, and is essential for insulin-induced differentiation of pre-adipocytes (Mahadev *et al.* 2004; Schröder *et al.* 2009). In normal physiological conditions, superoxide is metabolised rapidly to H_2O_2 by the superoxide dismutase enzymes – SOD1 in the cytosol, and SOD2 in the mitochondria. Superoxide and H_2O_2 act as redox signals, reversibly oxidising redox sensitive cysteines on enzymes, and thus changing their activity or function and contributing to cellular homeostasis across a physiological range (Sies 2014). Disruption of the redox balance of the cell by production of excess superoxide and H_2O_2 can result in irreversible oxidation of redox sensitive enzymes, impairing their function. As well as direct effects, excess H_2O_2 in the presence of ferrous iron (Fe^{2+}) can be converted to the hydroxyl radical, which oxidatively damages proteins, lipids and nucleic acids (Gieseg *et al.* 1993; Cadet *et al.* 1999; Ayala *et al.* 2014). These highly reactive hydroxyl radicals cause peroxidation of lipids, resulting in the production of damaging lipid hydroperoxides and reactive aldehyde species. Reactive aldehydes – 4-hydroxy-2-nonenal (4-HNE) and malondialdehyde (MDA) for example – attach to cysteine, histidine and lysine amino acid side chains as carbonyl additions (Ruskovska and Bernlohr 2013). Protein carbonylation is increased in adipose tissue from obese individuals and causes alterations to many key enzymes, with a potential loss of function (Grimsrud *et al.* 2007).

1.2.2.2 Endogenous antioxidant machinery

Cells constantly generate ROS, and must be able to quench these ROS or reverse the damage they cause to maintain their functionality. Several enzymatic antioxidant systems maintain physiological levels of ROS and intracellular redox potential in the cytoplasm and mitochondria. These systems are triggered by activation of redox sensitive transcription factors, such as nuclear factor (erythroid-derived 2)-like 2 (NRF2). Under normal cellular conditions NRF2 is bound to Kelch-Like ECH

Associated Protein 1 (KEAP1), an actin-bound protein that mediates the ubiquitination of the transcription factor marking it for degradation (Vomhof-Dekrey and Picklo 2012). During oxidative stress, KEAP1 is oxidised at cysteine residues, freeing NRF2 to translocate to the nucleus and bind to antioxidant response elements in the promoters or regulatory regions of target antioxidant genes.

To maintain cellular ROS levels within a normal range for redox signalling and to prevent damage from oxidative stress, maintaining a normal balance of hydrogen peroxide is essential. Catalase is the main enzyme responsible for disposing of cytoplasmic H_2O_2 (Okuno *et al.* 2008). The thioredoxin and glutathione antioxidant cytoplasmic and mitochondrial systems are also involved in this process, and both are inducible by NRF2 activation. The mitochondrial thioredoxin system, comprising thioredoxin reductase 2 (TXNRD2) and thioredoxin 2 (TXN2) contributes to the control of H_2O_2 levels in mitochondria by maintaining peroxiredoxin 3 (PRX3) in its reduced form and thus capable of scavenging further H_2O_2 (Chae *et al.* 1999; Lu and Holmgren 2014). The importance of this ROS scavenging system in metabolism was highlighted by recent work which demonstrated reduced *Prx3* expression in adipose tissue in obesity and metabolic syndrome (Huh et al., 2012). In addition, *Prx3* knockout mice exhibit impaired glucose tolerance, adipocyte hypertrophy and increased adipose tissue protein carbonylation and superoxide levels.

The glutathione antioxidant system is also important for regulating the redox environment, quenching ROS and reversing oxidative damage (Quintana-Cabrera and Bolaños 2013). Glutathione is produced by the enzyme glutamate-cysteine ligase (GCL) and is a tripeptide composed of glutamate, cysteine and glycine. It is maintained in its reduced form (GSH) by glutathione reductase (GR) at very high intracellular concentrations (10-15mM) (Marí et al. 2009). NRF2 activation can induce expression of both GCL and GR, increasing the pool of reduced GSH to counteract damage from oxidative stress (Harvey et al. 2009). In the mitochondria and cytosol, GSH is used as a cofactor for glutathione peroxidase 1 (GPX1) in the reduction of H_2O_2 to water (Brigelius-Flohé and Maiorino 2013). GSH is also necessary for detoxification of lipid peroxides by glutathione peroxidase 4 (GPX4) and the metabolism of reactive

aldehydes such as 4-HNE by glutathione-S-transferase A4 (GSTA4)(Yant *et al.* 2003; Curtis *et al.* 2010). Perturbations of the antioxidant machinery contribute to dysfunction of adipose tissue in obesity (Long *et al.* 2013).

1.2.2.3 Oxidative stress in adipose tissue

Oxidative stress is a feature of dysfunctional adipose tissue in obesity. Consumption of a high fat diet for just one week can cause increased production of mitochondrial ROS, increased levels of markers of oxidative stress and impairment of glucose tolerance (Paglialunga *et al.* 2015). Similarly, a high fructose diet can also cause adipose oxidative stress and metabolic impairment (Mellouk *et al.* 2011, 2012). Exposure of the 3T3-L1 adipocyte cell line to excess nutrients from glucose and palmitate results in increased NOX4 activity and production of excess ROS (Han *et al.* 2012). Molecularly, the rate of production of superoxide is dependent on a number of factors including the availability of electron carriers such as NADH, FADH and ubiquinone, and the demand for ATP (Murphy 2009). In cells with a high demand for ATP, electron carriers are mostly oxidised and superoxide production is low. Overnutrition supplies excess electrons to the respiratory chain and lack of physical exercise reduces ATP demand, leading to increased superoxide formation (James *et al.* 2012). As well as excess superoxide production from mitochondria, hypoxia due to inadequate expansion of adipose vasculature can contribute to oxidative stress through reducing the expression of antioxidant enzymes (Lee *et al.* 2008). Hypoxia and increased ROS production can also result in the triggering of the unfolded protein response, which contributes to further ROS production and oxidative stress (Harding *et al.* 2003). As well as increased ROS production, adipose tissue from obese individuals exhibits reduced expression and activity of many key antioxidant enzymes. Superoxide dismutase activity and glutathione peroxidase activity, as well as expression of catalase are reduced in adipose tissue of genetically obese mice (Furukawa *et al.* 2004). Peroxiredoxin 3 is also reduced in adipose of obese humans and mice (Huh *et al.* 2012). Excess production of ROS in adipose tissue from obese individuals, and consequent overloading of the antioxidant machinery, leads to

dysfunction of insulin signalling, adipogenesis and contribute to local and systemic inflammation.

Oxidative stress in adipose tissue can cause irreversible damage to cellular components, interfere with normal adipocyte function, and induce local and systemic inflammation. One of the main consequences of oxidative stress is the irreversible oxidation or carbonylation of proteins leading to impaired function and degradation or aggregation. GST4A is responsible for detoxifying the reactive aldehyde 4-HNE and is reduced in adipose tissue of obese insulin-resistant individuals, resulting in an increase in carbonylation, with many of the target enzymes having roles in cellular stress response and insulin signalling (Grimsrud *et al.* 2007; Curtis *et al.* 2010). Treating 3T3-L1 adipocytes with 4-HNE caused carbonylation and degradation of the insulin receptor substrate 1 and 2 (IRS1/2) and thus, impaired insulin-stimulated glucose uptake and lipogenesis (Demozay *et al.* 2008). Oxidative stress also caused a reduction in proteasome activity, leading to aggregation of oxidised and ubiquitinated proteins, and activation of the unfolded protein response (UPR) and insulin resistance (Díaz-Ruiz *et al.* 2015). While a physiological level of ROS production by NOX4 is induced and required for insulin-mediated differentiation of pre-adipocytes (Schröder *et al.* 2009), excess ROS inhibits both proliferation and differentiation of pre-adipocytes and thus reduces the availability of new adipocytes to store excess lipid leading to hypertrophy (Carrière *et al.* 2003, 2004). Production of H_2O_2 by NOX4 under normal physiological conditions is also necessary for insulin-stimulated glucose uptake (Mahadev *et al.* 2004), however prolonged exposure to a high concentration of H_2O_2 impairs insulin-induced translocation of the glucose transporter GLUT4 to the plasma membrane and reduced glucose uptake and lipogenesis (Rudich and Kozlovsky 1997; Rudich *et al.* 1998).

Increased oxidative stress, as well as having direct effects on insulin signalling in the adipocyte, is implicated in induction of inflammatory signalling pathways and infiltration of macrophages. Oxidative stress caused an alteration in the secretome of adipokines towards a more pro-inflammatory phenotype, with a reduction observed in the anti-inflammatory, insulin-sensitising hormone adiponectin and an increase in

monocyte chemotactic protein 1 (MCP1), plasminogen activator inhibitor 1 (PAI1), and interleukin-6 (IL-6), a pro-inflammatory cytokine (Furukawa *et al.* 2004). This alteration in the adipokine secretion profile was induced in 3T3-L1 adipocytes *in vitro* by exposure to exogenous H_2O_2 or high concentrations of glucose and palmitate, which induced excess ROS production (Chen *et al.* 2009; Han *et al.* 2012). As well as direct effects of excess ROS, lipid aldehydes such as 4-HNE produced by peroxidation of lipids can also trigger activation of local inflammatory pathways (Zarrouki *et al.* 2007), and the detoxification of 4-HNE by the addition of glutathione allows it to be secreted from the cell, where it subsequently induces infiltration and activation of macrophages (Frohnert *et al.* 2014). Therefore, inflammation of adipose tissue triggered by oxidative stress is one of the main drivers of adipose dysfunction in obesity and metabolic syndrome.

1.2.2.4 Mitohormesis

While excess production of ROS leads to oxidative stress and cellular damage, at lower physiological levels, ROS can act as signalling molecules to induce cellular changes that promote resistance to stress. This concept, named mitochondrial hormesis, or mitohormesis, theorises that low doses of ROS protect cells from damage through induction of antioxidant and stress defence mechanisms, and can thus promote health and increase lifespan (Ristow and Schmeisser 2014). An understanding of the mitohormetic response is essential when considering the implications of ROS production in obesity, as variation in the ability to upregulate protective mechanisms may underlie individual susceptibility to metabolic dysfunction (Kolb and Eizirik 2012).

The mitohormetic response can be induced by various stimuli that are relevant when discussing the impact of ROS on metabolic health. Exercise, calorie restriction and hypoxia have all been shown to increase ROS production, and produce beneficial outcomes at a cellular and systemic level in certain contexts (Ristow and Schmeisser 2014). Physical activity is a long recognised trigger of the mitohormetic response, with exercise-induced ROS production leading to mitochondrial biogenesis and increased

mitochondrial function (Davies *et al.* 1982). Exercise reduces risk of diabetes, cardiovascular disease and cancer, as well as potentially delaying onset of neurodegenerative diseases (Radak *et al.* 2008), and increases lifespan in rodents (Boveris and Navarro 2008). This adaptive effect is abrogated if antioxidants such as vitamins C and E are administered prior to exercise, indicating the importance of ROS in this process (Ristow and Zarse 2009). Another trigger of the mitohormetic response proven to promote health and increase lifespan is calorie restriction (CR). Reducing nutrient intake by up to 50% without malnutrition increases lifespan in many species, including mammals, and reduces risk of age-related diseases in humans (Heilbronn *et al.* 2006; Ristow and Schmeisser 2014). CR in yeast and glucose restriction in the nematode *Caenorhabditis elegans* (*C. elegans*) increase ROS production, leading to increased antioxidant activity and prolonged lifespan (Agarwal *et al.* 2005; Schulz *et al.* 2007). Hypoxia occurs in adipose tissue in obesity due to poor vascularisation of the expanding tissue (discussed in paragraph 1.2.5 on page 33). However, transient hypoxia has also been shown to extended lifespan in *C. elegans* through ROS-mediated mechanisms (Lee *et al.* 2010). These triggers of a mitohormetic response mediate their beneficial effects through activation of various stress-response mechanisms including NRF2, a transcriptional regulator of many antioxidant genes (described in paragraph 1.2.2.2 on page 23) , AMP-activated protein kinase (AMPK), a sensor of nutrient shortage and sirtuins, histone deacetylases involved in regulation of expression of DNA repair enzymes, protein folding chaperones and autophagy (Ristow and Schmeisser 2014).

Increased production of ROS in adipose tissue in obesity is generally recognised as being detrimental to the function of the tissue, leading to impairment of insulin signalling, dysregulation of adipokines and metabolic syndrome (Rudich *et al.* 1998; Furukawa *et al.* 2004). However, early adaptation to a high fat diet may lead to induction of a mitohormetic response, which may reduce metabolic impairment in a mouse model of diet-induced obesity.

1.2.3 Inflammation

1.2.3.1 Immune cell populations in adipose tissue

As well as the lipid-storing adipocytes and their precursors, adipose tissue contains many other cell types that greatly affect the tissue microenvironment and its dysfunction in obesity. The stromal vascular fraction (SVF) of adipose tissue contains endothelial cells, fibroblasts, smooth muscle cells and immune cells. Nearly all cells of the innate and adaptive immune system have been identified in adipose tissue. Many immune cell types play roles in the maintenance of a healthy anti-inflammatory environment, and others have been found to contribute to local inflammation during the development of obesity. In a lean state, immune cells play a key role in adipose tissue homeostasis, tissue remodelling and maintenance of an anti-inflammatory environment through secretion of anti-inflammatory cytokines. Adipose tissue macrophages (ATMs) are the most common immune cell in the tissue, with both resident cells and infiltrating monocyte-derived macrophages present. In a lean individual, ATMs are mostly polarised towards an alternatively activated or M2 phenotype (Lumeng *et al.* 2007), although recent evidence indicates that macrophage activation states exist as a spectrum rather than a branched set of phenotypically distinct states (Xu *et al.* 2013; Ginhoux *et al.* 2015). ATMs in adipose tissue from non-obese individuals are characterised by anti-inflammatory cytokine production, such as increased expression of IL-10 and its receptor, and increased arginase 1 expression, which dampens down inflammatory T cell activation and prevents fibrosis (Lumeng *et al.* 2007; Pesce *et al.* 2009). A role for M2 macrophages has also been suggested in clearing apoptotic adipocytes to facilitate tissue remodelling during cold exposure and because of increased lipolysis (Lee *et al.* 2013).

This beneficial M2 cell type is supported by signals from other immune cells such as eosinophils and invariant-chain natural killer T cells (iNKT). Eosinophils are the main source of the cytokine IL-4 which is necessary for the maintenance of the ATM M2 phenotype, and they are subsequently sustained by IL-5 secretion from innate lymphoid type 2 cells (ILC2) (Wu *et al.* 2011; Molofsky *et al.* 2013). The anti-inflammatory ATM population is also regulated by iNKT cells. These are unusual T

cells in that they recognise lipids presented by CD1d antigen-presenting cells rather than peptides presented using the major histocompatibility complex (MHC)(Lynch 2014). iNKT cells mediate the function of other immune cells by rapid cytokine production, including the anti-inflammatory IL-4 and IL-10 (Lynch *et al.* 2012). Another subset of T cells, regulatory T cells (Treg) are also present in adipose tissue from non-obese individuals and secrete IL-10, helping to maintain an anti-inflammatory insulin-sensitive environment (Feuerer *et al.* 2009).

1.2.3.2 Variations in adipose tissue immune cell populations in obesity.

Chronic low-grade inflammation in adipose tissue in obesity is thought to be one of the main drivers of local and systemic insulin resistance. Inflammation can be triggered by hypoxia due to adipocyte hypertrophy, subsequent adipose tissue fibrosis and necrotic adipocyte death (Ye *et al.* 2007; Khan *et al.* 2009). Activation of the UPR and increased production of ROS in adipose tissue also lead to activation of inflammatory signalling (Furukawa *et al.* 2004; Özcan *et al.* 2004). These features of dysfunctional adipose tissue can exist simultaneously in obesity, and all result in the modification of the normal immune cell population of adipose tissue, and an increase in pro-inflammatory cytokine production leading to systemic insulin resistance.

Obesity associated with a high fat diet induces an accumulation in immune cells in adipose tissue, as well as a switch towards more pro-inflammatory cell types. These directly contribute to local insulin resistance and are responsible for increases in plasma pro-inflammatory cytokine levels. Adipose tissue in obesity lacks or has reduced numbers of many of the cell types responsible for maintaining an anti-inflammatory environment in the non-obese state. Eosinophils, ILC2 cells and Treg cells are all reduced in obesity resulting in less anti-inflammatory cytokine production (Feuerer *et al.* 2009; Wu *et al.* 2011; Brestoff *et al.* 2015), which is required to maintain the M2 ATM population (Molofsky *et al.* 2013). In contrast, neutrophil content in adipose tissue increases quickly after exposure to a high fat diet (Elgazar-Carmon *et al.* 2008). Activated neutrophils secrete elastase, a protease that has been found to degrade insulin receptor substrate 1 (IRS1) and induce insulin resistance in adipocytes

and hepatocytes, as well as activating toll-like receptor 4 (TLR4) pro-inflammatory signalling (Talukdar *et al.* 2012). $CD8^+$ effector T cells are also increased and activated in adipose tissue after high fat feeding (Nishimura *et al.* 2009). When activated, these cells secrete MCP1, encouraging the migration of monocytes into adipose tissue and their differentiation into macrophages (Kamei *et al.* 2006; Nishimura *et al.* 2009). Natural killer (NK) cells in adipose tissue increase in number with high fat feeding and act as sensors of cellular stress or infection (Wensveen *et al.* 2015). In response to upregulation of stress signals from adipocytes, NK cells increase interferon-γ (IFN-γ) production, triggering polarisation of ATM to an M1 phenotype.

Pro-inflammatory macrophages in visceral adipose tissue are thought to be the main source of the excessive production of pro-inflammatory cytokines and insulin resistance. ATMs are the most abundant immune cell in adipose tissue, and their population size is greatly increased in the obese state (Weisberg *et al.* 2003; Xu, Barnes, *et al.* 2003), due to increased expression of chemoattractant signals from adipocytes, both alive and necrotic, and other immune cells (Cinti *et al.* 2005; Nishimura *et al.* 2009; Arner *et al.* 2012). M1-polarised ATMs in obesity are found mostly around dying or dead adipocytes in clusters called crown-like structures (CLS), where they scavenge free lipid and form giant multinucleated cells (Cinti *et al.* 2005; Lumeng *et al.* 2007; Murano *et al.* 2008). The pro-inflammatory phenotype of these ATMs is characterised by increased expression of the cell surface marker CD11c, lysosome biogenesis and expression of pro-inflammatory cytokines (Wentworth *et al.* 2010; Xu *et al.* 2013). These activated ATMs are the primary source of many damaging pro-inflammatory cytokines that are increased systemically in obesity, including tumour necrosis factor alpha (TNFα), the first cytokine found to be upregulated in obese adipose tissue and associated with insulin resistance (Hotamisligil *et al.* 1993; Nguyen *et al.* 2007). ATMs also increase expression of interleukin 1 beta (IL-1β) in diet-induced obesity, leading to a rise in plasma levels of the cytokine and increased production of monocytes and neutrophils in bone marrow, a prevalent feature of obesity-associated insulin resistance (Nagareddy *et al.* 2014). As well as its systemic effects, IL-1β induces inflammatory gene expression and insulin

resistance in primary adipocytes, potentially increasing local inflammation further (Gao *et al.* 2014). The damaging local and systemic effects of these pro-inflammatory macrophages have been confirmed by ablation of $CD11c^+$ cells in obese mice (Patsouris *et al.* 2008). Without M1 macrophages, adipose expression as well as serum levels of pro-inflammatory cytokines were reduced, and whole body insulin sensitivity was restored, with a reduction in liver lipid content and macrophage markers in muscle. A reduction in adipose tissue macrophage content was also associated with improved insulin sensitivity in humans after thiazolidinedione treatment (Koppaka *et al.* 2013).

1.2.4 Endoplasmic reticulum stress

The endoplasmic reticulum (ER) is a large membranous organelle involved in protein and lipid synthesis, and with the Golgi apparatus, ensures the secretion of correctly folded proteins. Within the lumen of the ER, chaperone proteins aid in the correct folding of proteins and formation of disulfide bonds. Adipocytes are potent endocrine cells, secreting many endocrine and paracrine factors, some of which are found abundantly in serum. The ER also plays a role in triglyceride formation in adipocytes, as the enzymes required to join three fatty acids and one glycerol molecule are located in the ER lumen (Wolins *et al.* 2006) and it has been suggested to be integral to the formation of lipid droplets (Blanchette-Mackie *et al.* 1995). The ER is very sensitive to changes in the cell including glucose deprivation, increased demand for protein synthesis and secretion, excess lipid and hypoxia (Koumenis *et al.* 2002; Gregor and Hotamisligil 2007). If stressed, the ER triggers an adaptive response called the unfolded protein response (UPR). The UPR is characterised by reduced protein synthesis, enhanced secretory capability and increased expression of chaperone proteins to aid in folding proteins in the ER (Gregor and Hotamisligil 2007). As well as its effects on protein synthesis, the UPR increases production of reactive oxygen species through increased activity of endoplasmic reticulum oxidoreductase 1 (ERO1)(Harding *et al.* 2003). UPR activation has also been shown to activate pro-

inflammatory pathways and directly inhibit insulin signalling in liver cells through inhibition of insulin-stimulated phosphorylation of downstream targets (Özcan *et al.* 2004). In adipose tissue of obese mice and humans, the UPR is activated contributing to metabolic dysfunction (Özcan *et al.* 2004; Sharma *et al.* 2008).

1.2.5 Adipose expansion, hypoxia and fibrosis

Excess nutrients are stored by hypertrophy of the adipocyte population and recruitment of adipocyte precursors to differentiate and cause hyperplastic growth of the fat pad. With rapid expansion of the fat depot, the vasculature can fail to expand accordingly and adequate blood flow is not maintained, resulting in local areas of hypoxia. Obesity has been shown to reduce oxygenation of adipose tissue in humans, dogs and mice (Di Girolamo *et al.* 1971; Kabon *et al.* 2004; Hosogai *et al.* 2007). Hypoxia causes stabilisation of hypoxia inducible factor 1α (HIF1α), the key transcriptional regulator of the hypoxia response. In a classical hypoxic response, HIF1α stimulates the expression of proangiogenic genes such as vascular endothelial growth factor A (VEGFa) and its receptor. However, in adipose tissue from obese individuals, HIF1α fails to trigger this pro-angiogenic response, and instead upregulates components of the extracellular matrix (ECM) leading to deposition of fibrillar collagen and reduction of tissue plasticity (Halberg *et al.* 2009). This abnormal fibrotic response causes stress to increasingly large adipocytes, resulting in necrotic cell death, infiltration of macrophages and local inflammation and subsequently impaired glucose tolerance (Khan *et al.* 2009). As well as enacting a damaging fibrotic program of gene expression, hypoxia can also trigger activation of the UPR, reduce gene expression of antioxidant enzymes, dysregulate adipokine production and promote inflammation (Koumenis *et al.* 2002; Hosogai *et al.* 2007; Ye *et al.* 2007; Lee *et al.* 2008). Through its many detrimental effects on cellular function, and direct metabolic impairment of adipocyte function, hypoxia is a key player in the pathophysiology of dysfunctional adipose tissue in metabolic disease.

1.2.6 Altered adipokine secretion

Adipose tissue is an endocrine organ, producing many hormones and cytokines that signal the metabolic and inflammatory state of the tissue. Adipocytes and cells of the stromal vascular fraction, including pre-adipocytes and immune cells make and secrete these signals, collectively called adipokines. In obesity, secretion of beneficial adipokines such as adiponectin are reduced and pro-inflammatory adipokines, like PAI1 and TNFα are increased, and it is through disruption of the balance of these signals that dysfunctional adipose tissue can lead to systemic insulin resistance, cardiovascular disease and the metabolic syndrome.

1.2.6.1 Anti-inflammatory adipokines

Several beneficial adipokines have been identified which have pleotropic effects on insulin sensitivity, cardiovascular health, inflammation, neuroendocrine activity and food intake. Adiponectin is the most abundant adipokine in human plasma. It is expressed in all white adipose tissue and levels in plasma are reduced with obesity (Hu *et al.* 1996) and further reduced in diabetic patients (Yu *et al.* 2002). Hypoxia and oxidative stress in adipose tissue in obesity reduce adiponectin expression, and in diet-induced obesity in mice, adiponectin protein is sequestered in adipose tissue rather than secreted (Furukawa *et al.* 2004; Chen *et al.* 2006; Nakatsuji *et al.* 2014). Adiponectin is a peptide hormone produced by white adipocytes with a structure similar to complement factor C1q (Scherer *et al.* 1995). Two known receptors for this adipokine, AdipoR1 and AdipoR2, are found in both humans and rodents in many tissues and cell types including adipocytes (Blüher *et al.* 2005), hepatocytes (Neumeier *et al.* 2005), skeletal muscle cells (Staiger *et al.* 2004), cardiomyocytes (Ding *et al.* 2007), osteoblasts (Berner *et al.* 2004), immune cells (Chinetti *et al.* 2004; Alberti *et al.* 2007), pancreatic β cells (Kharroubi *et al.* 2003) and in the hypothalamus (Kubota *et al.* 2007). The widespread expression of adiponectin receptors gives some indication of its importance as an insulin-sensitising hormone and anti-inflammatory signal. In mouse models, recombinant adiponectin replacement improves insulin sensitivity and reduces hepatic steatosis (Yamauchi *et al.* 2001; Xu, Wang, *et al.* 2003). Adiponectin

enhances insulin signalling in both liver and skeletal muscle, inhibiting gluconeogenesis and increasing glucose uptake respectively (Berg *et al.* 2001; Stefan *et al.* 2002). Adiponectin also functions in an autocrine manner on adipocytes, increasing insulin-mediated glucose uptake and lipogenesis (Fu *et al.* 2005). As well as its insulin-sensitising effects, adiponectin acts as an anti-inflammatory hormone, encouraging macrophage M2 polarisation, and inhibiting pro-inflammatory cytokine production (Okamoto *et al.* 2008; Ohashi *et al.* 2010). It also supresses proliferation of monocytic precursors, phagocytosis and cytokine production in mature macrophages (Yokota *et al.* 2000), and importantly for cardiovascular risk, it prevents macrophage to foam cell transformation by preventing lipid accumulation (Ouchi *et al.* 2001). The anti-inflammatory effects of adiponectin on macrophages are suggested to be protective against atherosclerosis, along with its beneficial effects on endothelial cells through decreasing TNFα expression (Ouchi *et al.* 2000), and down-regulating leukocyte adhesion (Komura *et al.* 2013). In apolipoprotein E knockout mice, supplementation of adiponectin by adenoviral delivery reduces the formation of atherosclerotic lesions (Okamoto *et al.* 2002). Therefore, the reduced level of circulating adiponectin in obesity is directly implicated as a cause of systemic insulin resistance and cardiovascular disease.

Other beneficial adipokines are expressed and secreted by adipose tissue, although a full understanding of their mechanisms of action and regulation remains to be elucidated. The C1q/TNF-related protein (CTRP) family are structurally similar to adiponectin, and some members are mainly expressed in adipose tissue, and their expression is reduced with obesity (Wong *et al.* 2008). These CTRP proteins are associated with enhanced insulin signalling, reduced macrophage activation and improved revascularisation after cardiac ischaemic injury (reviewed in Ohashi *et al.* 2014). Other adipokines with beneficial metabolic and cardiovascular effects are secreted frizzled-related protein 5 (SFRP5) and omentin. Both are reduced in adipose tissue in mouse models of obesity and in visceral fat from obese human individuals (De Souza Batista *et al.* 2007; Ouchi *et al.* 2010). Mice lacking SFRP5 have worsened insulin sensitivity after a high fat feeding challenge, and are susceptible to increased

cardiac damage after myocardial ischemia/reperfusion injury (Ouchi *et al.* 2010; Nakamura *et al.* 2016). Omentin overexpression in apolipoprotein E knockout mice attenuated atherosclerotic lesion formation, reducing macrophage infiltration and pro-inflammatory cytokine expression in plaques (Hiramatsu-Ito *et al.* 2016). These and other beneficial adipokines exert positive effects throughout the body, and dysregulation of their expression in dysfunctional adipose tissue in obesity directly contributes to whole-body insulin resistance and other characteristics of the metabolic syndrome.

1.2.6.2 Pro-inflammatory adipokines in obesity

Leptin was the first adipokine to be discovered, and it was initially known to act as a satiety signal, with its absence leading to reduced energy expenditure, hyperphagia and extreme obesity (discussed in paragraph 1.1.3 on page 19)(Friedman and Halaas 1998). Leptin also plays a role in many peripheral processes including reproduction (Chehab *et al.* 1996), bone metabolism (Ducy *et al.* 2000), angiogenesis (Sierra-Honigmann *et al.* 1998), hematopoiesis (Bennett *et al.* 1996) and glucose homeostasis (Berti and Gammeltoft 1999). Leptin also influences the activity of the immune system contributing to systemic inflammation in obesity. Plasma leptin is increased in obesity, and correlates with fat mass in mice and humans (Frederich *et al.* 1995; Considine *et al.* 1996). Although leptin is known to signal in the hypothalamus to inhibit food intake, in most cases of severe obesity, high leptin levels fail to act as an appetite suppressant, a state that has been described as “leptin resistance”. Leptin has a similar structure to the long chain helical family of cytokines, and its receptor is a member of the class I cytokine receptor family (Tartaglia *et al.* 1995; Zhang *et al.* 1997). This receptor is expressed in the hypothalamus and other neural regions, but it is also expressed by many cells of the immune system, including monocytes, neutrophils and lymphocytes (Tartaglia *et al.* 1995; Lord *et al.* 1998; Zarkesh-Esfahani *et al.* 2001; Caldefie-Chezet *et al.* 2003). Leptin induces proliferation and expression of pro-inflammatory cytokines and chemokines in monocytes and macrophages (Gabay *et al.* 2001; Zarkesh-Esfahani *et al.* 2001; Kiguchi *et al.* 2009). It also increases chemotaxis

and ROS production in neutrophils (Caldefie-Chezet *et al.* 2003). In $CD4^+$ T cells, leptin has been found to induce proliferation and increase expression of pro-inflammatory cytokines and adhesion molecules (Lord *et al.* 1998). Leptin also increases platelet aggregation and ROS production and cytokine expression by endothelial cells, as well as encouraging macrophage to foam cell differentiation (Konstantinides *et al.* 2001; Yamagishi *et al.* 2001; O'Rourke *et al.* 2002). Therefore, these effects of leptin contribute to the chronic pro-inflammatory state in obesity, and increase the risk of developing atherosclerosis or suffering a thrombotic stroke.

Macrophages in adipose tissue are a source of many pro-inflammatory adipokines that have detrimental local and systemic effects. Dysfunctional adipose tissue in obesity overexpresses many factors that cause macrophage infiltration and activation. Tumour necrosis factor alpha (TNFα) was the first cytokine found to be expressed in adipose tissue, and this discovery established the association of inflammation with severe obesity and insulin resistance (Hotamisligil *et al.* 1993). TNFα, produced by adipocytes and macrophages, inhibits insulin signalling, as well as maintaining pro-inflammatory cytokine production, including its own production, thus creating a chronic inflammatory state (Hotamisligil *et al.* 1994; Nguyen *et al.* 2005). Monocyte chemotactic protein 1 (MCP1) is also upregulated in adipose tissue in obesity and contributes to insulin resistance in adipose tissue, liver and muscle (Kamei *et al.* 2006; Kanda *et al.* 2006a; Sell *et al.* 2006). MCP1 also acts as a chemokine, encouraging monocyte infiltration into adipose tissue. Macrophages also produce interleukin-6 (IL-6) which is associated with insulin resistance (Pradhan *et al.* 2001; Fain *et al.* 2004). Blocking IL-6 in cases of genetic or diet-induced obesity improved hepatic insulin sensitivity and prevented macrophage recruitment to adipose tissue (Klover *et al.* 2005; Kraakman *et al.* 2015). However, the function of IL-6 in metabolic processes is complex, as mice genetically lacking the gene (IL-$6^{-/-}$ mice) are more prone to developing hepatic inflammation and systemic insulin resistance than wild type controls on a standard or high fat diet (Matthews *et al.* 2010).

An increase in the expression of some adipokines is associated with cardiovascular disease. Plasminogen activator inhibitor 1 (PAI1) is increased in

plasma of obese and diabetic patients. (Landin *et al.* 1990; McGill *et al.* 1994). PAI1 is an inhibitor of fibrinolysis, a process that prevents blood clot formation, and it is produced by adipocytes and SVF cells, with its expression induced by TNFα, as well as other inflammatory factors (Alessi *et al.* 1997; Samad *et al.* 1999). Another player in the control of haemostasis, tissue factor (TF) is also dysregulated in adipose tissue in obesity. TF is a major initiator of the coagulation cascade and its expression is increased in adipose depots of *ob/ob* mice (Samad *et al.* 1998). Leptin increases expression of TF in neutrophils and monocytes (Rafail *et al.* 2008). Inhibition of fibrinolysis by PAI1 and increased risk of coagulation by TF, coupled with increased platelet activity (Konstantinides *et al.* 2001), likely underpins the increased risk for thrombotic and cardiovascular complications associated with obesity (Borch *et al.* 2011; Wormser *et al.* 2011). Adipose tissue also produces angiotensinogen, a key factor in the renin-angiotensin system (RAS) of blood pressure control. Activation of RAS is found in hypertension associated with diet-induced obesity in rats, and upregulation of angiotensinogen in adipose tissue is thought to be responsible for the increased blood pressure (Boustany *et al.* 2004).

Other adipokines increased in obesity have been associated with insulin resistance or inflammation, although less is known about their mechanisms of action. Resistin is secreted by adipocytes in mice, its plasma levels are increased in obesity and there is evidence that it impairs glucose tolerance and induced insulin resistance (Steppan *et al.* 2001). In humans, resistin is expressed by macrophages rather than adipocytes (Savage *et al.* 2001), however the development of a "humanised" mouse expressing resistin only in macrophages supported a causal link between this adipokine and adipose tissue inflammation and insulin resistance in WAT and skeletal muscle (Qatanani *et al.* 2009). Chemerin is another adipokine associated with glucose intolerance and worsened measurements of metabolic health. Chemerin is expressed in adipose tissue, enriched in the adipocytes, and its receptor is most highly expressed in adipose tissue suggesting a paracrine action (Goralski *et al.* 2007). Plasma chemerin is increased in obese individuals, and is correlated with features of the metabolic syndrome such as fasting insulin, plasma triglycerides and HDL cholesterol (Bozaoglu

et al. 2009). In obese mice, chemerin exacerbated glucose intolerance and reduced serum insulin levels (Ernst *et al.* 2010). Retinol binding protein 4 (RBP4) is also upregulated in adipose tissue of obesity mice, with increased plasma levels associated with insulin resistance (Yang, Graham, *et al.* 2005). Its role in human obesity is more controversial, as results from clinical studies measuring RBP4 in obese and diabetic subjects have given conflicting results (Kotnik *et al.* 2011), despite mouse studies showing that RBP4 increases adipose inflammation, impairs insulin signalling, and increases hepatic gluconeogenesis (Yang, Graham, *et al.* 2005; Moraes-Vieira *et al.* 2014). These and many more adipokines underlie the varied detrimental effects of obesity on metabolic health.

To summarise, in obesity adipose tissue expansion with inadequate angiogenesis leads to hypoxia, endoplasmic and oxidative stress and inflammation, impairing the ability of the tissue to store excess lipid, make and secrete adipokines and respond to insulin. These consequences of adipose dysfunction lead to an increase in systemic pro-inflammatory cytokine circulation, and a reduction in insulin sensitivity locally and in other organs.

1.3 THIOSULFATE SULFURTRANSFERASE

1.3.1 Discovery of *Tst* as a lean gene

Recent work from our laboratory sought to discover a genetic basis for healthy leanness comparing the Lean and Fat mouse lines (L and F mice), created by divergent selection for more than 60 generations for low and high body fat content (Horvat *et al.* 2000). One gene was found to be overexpressed in white adipose tissue of the L mice, thiosulfate sulfurtransferase (*Tst*) (Morton *et al.* 2016). Elevated *Tst* expression in adipose tissue co-segregated with leanness in subsequently derived congenic lines with increasingly refined "lean" chromosomal regions back-crossed onto the divergently selected counterpart F line. Conversely, adipose TST levels are low in mice with diet-induced or genetic obesity. Direct evidence that elevated TST is metabolically protective was provided by the phenotype of transgenic mice overexpressing *Tst* in adipose tissue under the adiponectin promoter, the Adipoq-*Tst* mouse. In response to high fat diet, these mice had reduced weight gain, elevated plasma adiponectin and improved glucose tolerance (Morton *et al.* 2016). In addition to a genetic increase in *Tst* expression, pharmacological activation by treatment with a TST substrate, sodium thiosulfate ameliorated diabetes in high fat diet-fed wild-type mice and genetically obese mice. Investigation of the relevance of TST to human biology found that TST mRNA was higher in adipose depots from lean compared to obese subjects in an Austrian cohort, and adipose TST mRNA correlated negatively with BMI in two other human cohorts from Iceland and Spain. Several polymorphisms in and around the TST gene were identified in a small Caucasian cohort, some of which were predicted to alter the function or stability of the enzyme or impact promoter activity, however no metabolic phenotypes were reported in these papers (Billaut-Laden *et al.* 2006; Libiad *et al.* 2015). A full understanding of the role of TST in adipose tissue function, including an investigation of the effects of common TST polymorphisms on obesity and metabolic syndrome risk has yet to be elucidated.

1.3.2 Function of thiosulfate sulfurtransferase

TST was first described as early as the 1950s as a cyanide detoxification enzymatic activity called rhodanese (Baskin *et al.* 1992). Rhodanese domain-containing proteins have since been found in all phyla, including bacteria and plants (Bordo and Bork 2002). As a sulfurtransferase, TST's main function is to catalyse the transfer of sulfane sulfur (R-S-SH) from a donor to an acceptor. TST shares up to 66% sequence similarity with another sulfutransferase, 3-mercaptopyruvate sulfurtransferase (MPST) which was first identified as the source of hydrogen sulfide (H_2S) in the brain (Nagahara *et al.* 1995; Shibuya *et al.* 2009). In the detoxification of cyanide, thiosulfate is administered as an antidote, and is used by TST as a substrate to drive the addition of sulfur to cyanide, making the less toxic thiocyanate ion. This reaction is also used as the basis of an assay to measure rhodanese activity *in vitro* as shown in Figure 1.1. Decades of research linked TST to a number of cellular processes such as donation of sulfane sulfur to iron-sulfur clusters of the respiratory complexes of the mitochondrial electron transport chain, detoxification of mitochondrial ROS, transport of ribosomal 5S RNA into mitochondria and metabolism of the endogenously-produced gasotransmitter H_2S (Bonomi et al. 1977; Nandi et al. 2000; Hildebrandt and Grieshaber 2008; Smirnov et al. 2010). The central role of TST in many mitochondrial processes suggests a number of potential biochemical mechanisms linking it to the adipose tissue-intrinsic control of fat accumulation and insulin sensitivity, and fits with evidence that oxidative stress, mitochondrial dysfunction, hydrogen sulfide signalling and inflammation play key roles in the pathogenesis of obesity and diabetes (Koh et al. 2007; Gregor and Hotamisligil 2011; Ruskovska and Bernlohr 2013).

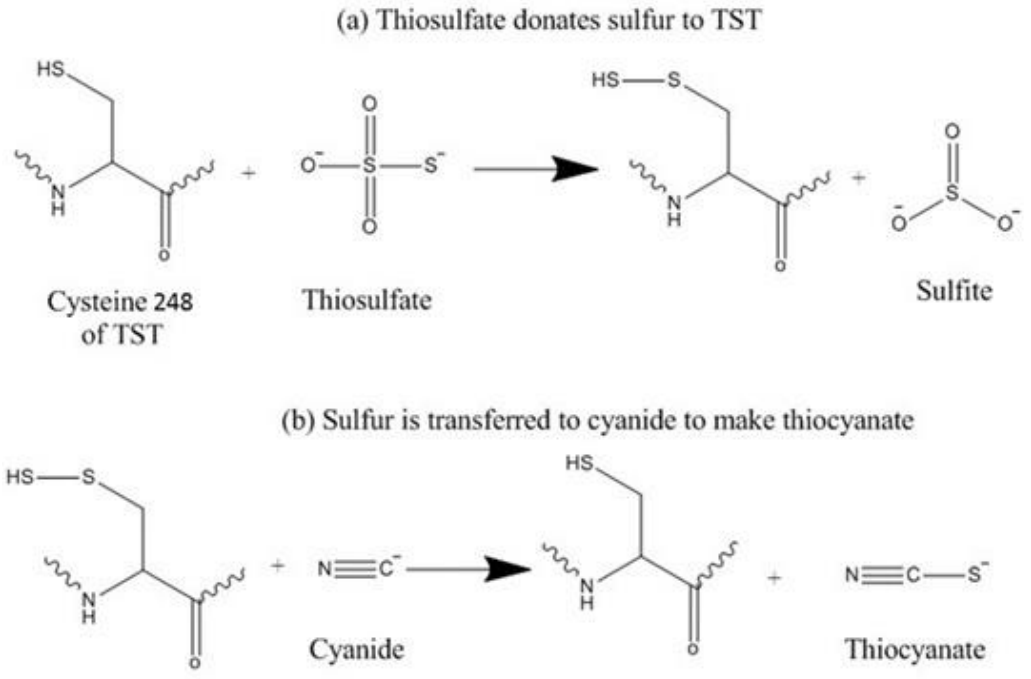

Figure 1.1: Catalytic mechanism of TST activity in the detoxification of cyanide and in the assay used to measure rhodanese activity.
(a) Thiosulfate becomes sulfite by donating a sulfur to the active site cysteine (Cys-248) of TST. (b) This sulfur is then transferred to cyanide making thiocyanate. (Image created using ChemDraw Std).

1.3.2.1 TST in hydrogen sulfide metabolism

In humans and mice, TST is implicated in the oxidation of hydrogen sulfide (H_2S) in the mitochondria, however its role and the mechanism of its action is not fully clarified. H_2S is a gasotransmitter with varied physiological effects, including vasodilation and redox and inflammatory mediation, and it may play a role in adipose tissue dysfunction in obesity (discussed in section 1.3.3 on page 48).

H_2S is metabolised in the mitochondria by enzymes of the sulfide oxidation pathway (Figure 1.2). The initial oxidation of H_2S by sulfide quinone oxidoreductase (SQR) which is bound to the inner mitochondrial membrane, results in the transfer of two electrons from sulfide to the electron transport chain (Hildebrandt and Grieshaber 2008). The remaining sulfane sulfur is transferred to glutathione, making glutathione persulfide (GSSH). This is then further oxidised to sulfite (SO_3^{2-}) by a sulfur dioxygenase, also known as ethylmalonic encephalopathy protein 1 (ETHE1) due to its discovery as the causative mutation in that fatal inherited disease (Tiranti *et al.* 2009). TST catalyses the transfer of sulfur from another molecule of glutathione persulfide to this highly reactive sulfite, neutralising it and making thiosulfate (SSO_3^{2-}) (Libiad *et al.* 2014). Sulfite can also be disposed of by sulfite oxidase (SO), which turns it into sulfate (SO_4^{2-}). Thiosulfate and sulfate are the two main products of the sulfide oxidation pathway, although the ratio of their production varies in different tissues and depending on the concentration of substrates and expression of the enzymes of the pathway. Red blood cells, lacking mitochondria, employ an alternative mechanism of sulfide metabolism using methemoglobin to oxidise sulfide, producing thiosulfate and polysulfides, which can also act as signalling molecules (Vitvitsky *et al.* 2015).

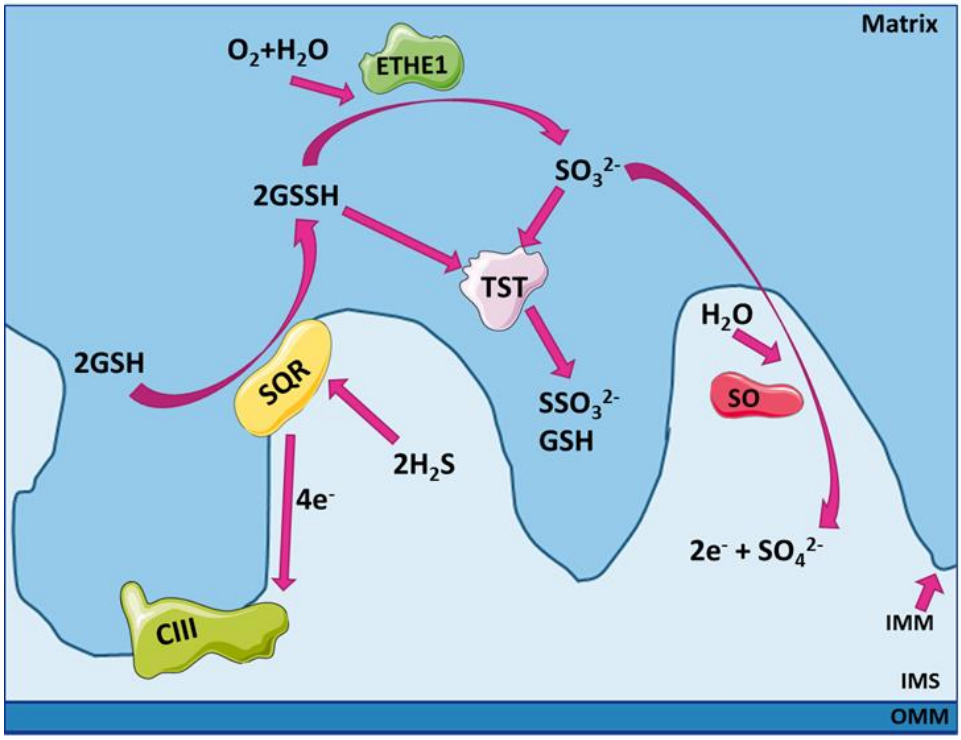

Figure 1.2: Mitochondrial sulfide oxidation pathway

Proposed model of mitochondrial sulfide oxidation. Hydrogen sulfide (H_2S); sulfide quinone oxidoreductase (SQR); Ethymalonic encephalopathy protein 1 (ETHE1); Thiosulfate sulfurtransferase (TST); Sulfite oxidase (SO); Glutathione +/- persulfidation (GSH/GSSH); Sulfite (SO_3^{2-}); Thiosulfate (SSO_3^{2-}); Sulfate (SO_4^{2-}); Complex III (CIII); Electron (e^-); Outer mitochondrial membrane (OMM); Intermembrane space (IMS); Inner mitochondrial membrane (IMM). [Protein images licenced under Creative Commons Attribution 3 from Servier Medical Art by Servier at smart.servier.com].

Some controversy exists about whether TST can directly metabolise sulfide, or whether it must first be oxidised to sulfane-sulfur, such as in glutathione persulfide and thiosulfate. This controversy is based on investigation of sulfide oxidation in the colon, where levels of sulfide can reach or exceed toxic concentrations due to production by bacteria (Macfarlane *et al.* 1992; Leschelle *et al.* 2005). Rhodanese activity (encompassing TST and MPST activity) has been measured throughout the gastroinstestinal tract, with highest activity in the colon (Picton *et al.* 2002). This study concluded that rhodanese was capable of metabolising H_2S, and was the main activity responsible for sulfide oxidation in the colonic muscosa. However, this was

subsequently challenged by another group that found that the H_2S-metabolising rate of rhodanese was up to twenty times lower than the capacity of mixed protein homogenate of colonic muscosa, and it is likely rhodanese requires the initial oxidation of H_2S by another enzyme, such as SQR, before rhodanese can use it as a substrate (Wilson *et al.* 2008). Although this was challenged by the authors of the first paper (Eggo *et al.* 2008), more recent investigations, such as that by Libiad *et al.* (2014), do not support the claim that rhodanese/TST can directly metabolise H_2S.

Preliminary results from our lab using liver tissue homogenate of *Tst*$^{-/-}$ mice have indicated that TST is involved in the breakdown of H_2S, as liver homogenate lacking *Tst* shows a lower rate of H_2S breakdown than wild type (Roderick Carter, unpublished). Also the *Tst*$^{-/-}$ mouse has increased plasma sulfide, indictating a profound alteration in sulfide oxidation (Morton *et al.* 2016). The presence of TST in many other tissues including adipose tissue, the liver and immune cells indicates a broad role for this enzyme in the metabolism of H_2S, and hence its importance in regulating the myriad physiological effects proposed for H_2S as a signalling molecule and ROS and inflammatory mediator (see 1.3.3). A full understanding of the role of TST in H_2S metabolism is still lacking, however evidence linking H_2S to oxidative stress, inflammation and insulin resistance highlights a potential mechanism for the impact of altered adipose *Tst* expression in the polygenic Lean mouse line.

1.3.2.2 TST *in ROS metabolism*

As well as its role in sulfur metabolism, TST may interact with antioxidant enzymes to aid in metabolism of reactive oxygen species (ROS). Thioredoxin, one of the main antioxidant enzymes reverses oxidation of cysteine groups by high ROS levels (described in section 1.2.2.2 on page 23). Thioredoxin is in turned recycled to its reduced form by thioredoxin reductase using NADPH. TST can be oxidised by H_2O_2 at its active site cysteine forming a sulfenic acid, and prolonged exposure to excess H_2O_2 can result in further oxidation and the formation of a disulfide bond, permanently inactivating the enzyme (Costa *et al.* 1977). However, in a cell-free system, the oxidation of one isoform of TST by the formation of a sulfenic acid at its active site

was reversed by thioredoxin, resulting in the oxidation of NADPH and the neutralisation of the attacking ROS (Nandi *et al.* 2000). Thioredoxin, thioredoxin reductase and TST are found in the mitochondrial matrix, and so excess mitochondrial ROS production as observed in dysfunctional adipose tissue may be neutralised by this pathway. While this interaction has not yet been directly observed in mammalian cells, sulfurtransferases of the plant *Arabidopsis thaliana* interacted with thioredoxins which are in close proximity within subcellular locations (Henne *et al.* 2015). In mammalian cells, the evolutionarily similar sulfurtransferase MPST can be oxidised and inactivated by H_2O_2, and this oxidation is reversed by interaction with thioredoxin (Nagahara and Katayama 2005). This inactivation of MPST by oxidative stress indirectly contributes to the restoration of the redox balance by reducing the amount of cysteine consumed by MPST and allowing it to be used as a reducing agent instead. Due to the similarity of MPST and TST, it is conceivable that TST may also be inactivated by oxidation, leading to the build-up of H_2S or glutathione persulfide, both of which may help to restore the redox balance of the cell, however this has not been investigated.

Some evidence indicating a link with TST and ROS metabolism *in vivo* in mammals has been found, although a definite role has yet to be described. TST gene and protein expression was reduced in blood monocytes of hemodialysis patients, and was negatively correlated with superoxide levels, and low levels predicted greater mortality risk (Krueger *et al.* 2010). In rats exposed to long-term low-dose radiation, TST expression was increased in liver, potentially in response to increased ROS production, however the authors failed to confirm the presence of oxidative stress (Nakajima *et al.* 2008). Our lab found that siRNA-mediated knockdown of TST in 3T3-L1 adipocytes led to increased mitochondrial ROS production after exposure to H_2O_2 (Morton *et al.* 2016). The contribution of TST to the control of ROS *in vivo* remains uncertain, but *in vitro* evidence of its ability to interact with thioredoxin suggests that the enzyme may play a part in reducing mitochondrial ROS levels, and thus could help to prevent oxidative stress and subsequent inflammation and insulin resistance.

1.3.2.3 Other functions of TST

Several other roles for TST that could impact the function of the mitochondria have been suggested. Early investigation of the sulfur-transfer function of TST led biochemists to conclude that it could increase the function of iron-sulfur cluster-containing enzymes. NADH dehydrogenase, complex I of the electron transport chain and succinate dehydrogenase, complex II can receive sulfur from TST, allowing them to function *in vitro* (Pagani *et al.* 1975; Bonomi *et al.* 1977; Pagani and Galante 1983). As well as this, a role for TST in transportation of 5S ribosomal RNA from the cytoplasm to the mitochondria has been suggested. TST was found to bind ribosomal RNA and silencing of the gene lead to a reduction in mitochondrial protein translation (Smirnov *et al.* 2010), which may impact the phenotype of genetically altered mice used in this thesis.

1.3.3 Hydrogen sulfide

1.3.3.1 H_2S is an endogenously produced gasotransmitter

Hydrogen sulfide (H_2S) was long recognised as a toxic gas with the smell of rotten eggs. Its toxicity lies in its ability to inhibit cytochrome c oxidase, complex IV, thus stopping respiration and causing cell death (Nicholls and Kim 1982). However in recent decades, H_2S has been recognised as an endogenously produced gasotransmitter, with many pleotrophic physiological effects. At estimated endogenous levels, H_2S can donate electrons to the electron transport chain, thus acting as substrate for oxidative phosphorylation (Goubern *et al.* 2007). H_2S may exert biological effects by directly interacting with ROS to make thiol intermediates, but it can also change protein function by persulfidation, a post-translational modification characterised by the addition of sulfur to the thiol side chain of cysteine residues forming a persulfide group (Li *et al.* 2011). H_2S has also been shown to mediate the beneficial effects of calorie restriction (Hine *et al.* 2015). Through direct chemical interaction or through protein modification, H_2S has been identified as a modulator of inflammation and oxidative stress, thus linking it to progression of metabolic disease in obesity.

H_2S was first discovered to be produced endogenously in mammalian brain by cystathionine β-synthase (CBS), and to modulate brain function by enhancing neurotransmitter receptor activity (Abe and Kimura 1996). Susequently, another H_2S-producing enzyme, cystathionine γ-lyase (CSE) was identified in the vasculature, and it was found that H_2S could cause vasorelaxation through inhibition of potassium ATP channel function (Zhao *et al.* 2001; Hosogai *et al.* 2007). CBS and CSE are dependant on a co-factor, pyridoxal 5' phosphate (PPP), and use L-cysteine or homocysteine as substrates. H_2S can also be made by a third enzyme, the rhodanese domain-containing 3-mercapopyruvate sulfurtransferase (MPST) which uses 3-mercaptopyruvate as a substrate and has high similarity to TST (Nagahara *et al.* 1995; Shibuya *et al.* 2009). In adipose tissue, CSE is recognised as the main source of local H_2S production (Feng *et al.* 2009). The tissue-specific expression and activity of these enzymes, as well as

substrate and co-factor availability determines the rate of H_2S production in different tissues.

Our understanding of the role of H_2S *in vivo* has been hampered by inaccurate methods of measuring and delivering the gas experimentally. It was discovered that measurements of endogenous H_2S levels in tissue were likely to be much lower than initially thought (Furne *et al.* 2008), and modern methods of sulfide measurement have been developed which substantiate this (Wintner *et al.* 2010). The most commonly used H_2S donor compounds such as disodium sulfide (Na_2S) and sodium hydrosulfide (NaHS), rapidly release large non-physiological amounts of H_2S which is quickly metabolised, putting in doubt any long-term effects. New slow-release H_2S donor compounds such as GYY4137 and the mitochondrially-targeted AP39 are being used to deliver physiological levels of the gas and to investigate its biological effects in many diseased and non-diseased states (Li *et al.* 2008; Szczesny *et al.* 2014). It is likely that improvements in our ability to measure and control delivery of H_2S will lead to a deeper understanding of its myriad physiological roles as an endogenously produced gasotransmitter and its potential as a therapeutic target for many diseases, including the metabolic syndrome.

1.3.3.2 H_2S as an antioxidant mediator

Hydrogen sulfide can help to maintain a normal cellular redox balance through several mechanisms. It may directly act to scavenge reactive species, thus preventing or reversing damage to proteins, DNA and lipids. It is likely that persulfidation of some antioxidant enzymes may increase their activity during oxidative stress. Persulfidation of specific proteins within mitochondria can also lead to reduced production of mitochondrial ROS. As well as these direct antioxidant effects, H_2S-mediated persulfidation of key transcription factors can lead to upregulation of antioxidant and anti-inflammatory genes.

H_2S can directly scavenge ROS and reactive products of their reaction with other cellular components, and may be able to reduce mitochondrial ROS production during oxidative stress. H_2S can directly scavenge superoxide *in vitro*, as well as

inhibiting superoxide production from NADPH oxidase (NOX) in aortic rings (Al-Magableh *et al.* 2014). Superoxide reacts with nitric oxide to form a reactive nitrogen compound, peroxynitrite with strong oxidising and nitrating capabilities. H_2S inhibits peroxynitrite-mediated nitration of proteins and protects against cytotoxicity in a neuronal cell line (Whiteman *et al.* 2004). Lipid hydroperoxides are found in oxidised low density lipoprotein (oxLDL) and are formed by the attack of lipids by highly reactive species such as the hydroxyl radical. These reactive lipids can be destroyed by H_2S, potentially reducing damage to the vasculature by oxLDL, which can lead to atherosclerosis (Muellner *et al.* 2009). Damage due to 4-HNE, another product of lipid peroxidation, is also inhibited by H_2S, preventing carbonylation of proteins and protecting against cell death (Schreier *et al.* 2010). H_2S can also reduce the formation of ROS from mitochondria through inhibitory persulfidation of p66Shc, a protein involved in upregulation of mitochondrial ROS (Xie *et al.* 2014). These ROS and their damaging products are found in dysfunctional adipose tissue in obesity, (discussed in paragraph 1.2.2 on page 22), therefore it is possible that local H_2S production or delivery from the blood may reduce obesity-associated oxidative stress.

H_2S can also directly modulate the function of some antioxidant enzymes. Superoxide dismutase (SOD) has cytosolic and mitochondrial forms that incorporate different metal ions. H_2S reduces the manganese ion in SOD2, the mitochondrial form, causing the inactivation of the enzyme due to release of its manganese core (Bolic *et al.* 2015). However, H_2S may lead to an overall increase in SOD2 activity during oxidative stress, as it is thought to cause an increase in its protein expression (Sun *et al.* 2012). Expression of the cytosolic form of SOD (SOD1 or CuZn-SOD) is unchanged by H_2S, but its activity is directly increased by binding of H_2S to its copper ion (Sun *et al.* 2012; Bolic *et al.* 2015). H_2S enhances protein expression and activity of other antioxidant enzymes such as catalase, glutathione S-transferase and glutathione peroxidase in response to an oxidative stress challenge (Wen *et al.* 2013).

Exogenous H_2S mediates the activity of NRF2, inducing the expression of many antioxidant enzymes. Normally NRF2 is bound to KEAP1, but increased oxidation from ROS allows its dissociation (see paragraph 1.2.2.2 on page 23). H_2S

can also cause the disassociation of NRF2 from KEAP1 through persulfidation of KEAP1 (Yang *et al.* 2013). This leads to an increase in GSH through the upregulation of GCL and GR. H_2S also decreases oxidative stress through NRF2-mediated upregulation of the antioxidant enzymes thioredoxin 1 and heme oxygenase 1 in a mouse model of cardiac ischemia reperfusion injury (Calvert *et al.* 2009).

1.3.3.3 H_2S as an inflammatory mediator

H_2S plays a role in the inflammatory process, however it is still debated whether it is anti- or pro-inflammatory. H_2S synthesising enzymes are expressed in many cells of the immune system, and their expression is increased in some inflammatory disease states. H_2S can influence many of the cardinal features of acute inflammation – increased blood flow, oedema, pain and immune cell infiltration and activation – however, some of these effects are also key to the resolution of inflammation. As a signalling molecule, H_2S can upregulate or downregulate key inflammatory and apoptotic pathways in different contexts, muddying the water further. Recent development of slow-releasing H_2S donor compounds and research on their effects on inflammatory disease models has helped bring some clarity to this complicated and contradictory field of research, and highlights a potential therapeutic role for this gasotransmitter.

H_2S can directly influence the cardinal signs of inflammation, increasing blood flow, altering leukocyte adhesion and survival (Hosoki *et al.* 1997; Pan *et al.* 2011). While the role of H_2S in mediating blood flow in inflammation has not been well-characterised, the vasodilatory effect of this gas through persulfidation of potassium ATP channels highlights a potential mechanism for increased blood flow in pathogenic states (Hosoki *et al.* 1997). This increased blood flow may contribute to oedema during inflammation, as observed in a model of limb oedema in which H_2S synthesis and plasma levels were increased, and administration of a CSE-inhibitor reduced swelling (Bhatia *et al.* 2005). However, in other studies of limb inflammation, administration of a H_2S donor reduced inflammation and blood flow, indicating a more complicated effect of this gasotransmitter on oedema (Andruski *et al.* 2008; Ekundi-Valentim *et al.*

2010). The adhesion of leukocytes to the endothelium is a key step in allowing infiltration of cells towards a site of inflammation, and H_2S suppressed this process by reducing expression of adhesion molecules in HUVEC endothelial cells, leading to reduced adhesion of monocytes (Pan *et al.* 2011). Also in limb ischemia-reperfusion, neutrophil infiltration was inhibited by treatment with H_2S (Ball *et al.* 2013). H_2S can also impact the activity of leukocytes, as well as reducing their adhesion and infiltration. Macrophages treated with H_2S show reduced expression of a chemokine CXCL1 and its receptor, and this effect was reproduced in an *in vivo* model of atherosclerosis in which H_2S treatment reduced plaque formation (Zhang, Guo, Wu, *et al.* 2012). H_2S suppressed uptake of oxLDL by macrophages *in vitro,* preventing their conversion to lipid-laden foam cells (Zhao *et al.* 2011). These effects of H_2S mediate its protective effect against atherosclerosis development (Wang *et al.* 2009). The ability of H_2S to modulate leukocyte adhesion and function is now widely accepted and has led to an understanding of the signalling pathways underlying this effect.

A deeper understanding of the mechanism of H_2S mediation of inflammatory pathways has led to a better understanding of its role in inflammatory diseases, and to the development of H_2S donor compounds that are better able to influence these pathways. Patients with inflammatory bowel diseases (IBD) such as ulcerative colitis and Crohn's disease were found to have reduced sulfide detoxification, which led to the hypothesis that accumulating H_2S is causative for these diseases (De Preter *et al.* 2012; Arijs *et al.* 2013). However, a H_2S-releasing derivative of mesalamine, a first-line therapy for IBD, reduced disease severity, neutrophil activity and pro-inflammatory cytokine expression in a mouse model of colitis, indicating that the reduced sulfide metabolism observed in these patients may be compensatory (Fiorucci *et al.* 2007). Other evidence for the benefit of H_2S in reducing gut inflammation came from the development of H_2S-releasing non-steroidal anti-inflammatory drugs (NSAIDs). This class of anti-inflammatory drug includes the common painkillers aspirin and ibuprofen, which increase risk of gastric injury, especially with long-term use. NSAIDs were found to inhibit H_2S synthesis in the gastric mucosa, highlighting

a potential mechanism of gastric injury (Fiorucci *et al.* 2005). A H_2S-releasing derivative of the NSAID diclofenac, showed a similar ability to reduce oedema and neutrophil activity as its parent drug, but with greatly reduced intestinal damage (Sidhapuriwala *et al.* 2007; Wallace *et al.* 2007). H_2S-releasing derivatives of aspirin protected against gastric injury, while also reducing plaque size in a model of atherosclerosis and hypertension and insulin levels in a model of metabolic syndrome, as well as maintaining the anti-thrombotic benefits of aspirin (Rossoni *et al.* 2010; Zhang, Guo, Zhang, *et al.* 2012). Compounds which release H_2S slowly have also been developed, such as GYY4137 which inhibited pro-inflammatory macrophage activation and supressed cytokine production in a model of endotoxic shock (Li *et al.* 2009; Whiteman, Li, *et al.* 2010). A mitochondrially-targeted H_2S donor – AP39 – has also recently been developed, and initial testing *in vivo* has shown beneficial effects in reducing neutrophil infiltration, markers of oxidative stress and tissue damage in kidney after ischaemia/reperfusion injury (Ahmad *et al.* 2016).

The potent anti-inflammatory effects of H_2S-based therapies in pre-clinical disease models has transformed our understanding of the role of H_2S in the complex biology of inflammation, and highlighted this simple molecule as a promising new target in numerous inflammatory conditions, including the chronic inflammation observed in dysfunctional adipose tissue in obesity.

1.3.3.4 H_2S in obesity and diabetes

One study found that hydrogen sulfide was reduced in the plasma of diabetic patients and obese individuals (Whiteman, Gooding, *et al.* 2010). This reduction may contribute to the metabolic consequences of these diseases, due to the loss of H_2S-mediated suppression of oxidative stress and inflammation. H_2S also exerts direct effects on metabolically important tissues such as the adipose, liver, and insulin-producing β-cells, which may be diminished due to the reduction of H_2S in obesity.

Adipose tissue expresses the enzymes responsible for H_2S production, and this gaseous signalling molecule may influence adipogenesis, insulin signalling and lipolysis, as well a potentially impacting upon the production of adipokines. A role for

H_2S in adipogenesis has been suggested, as expression of H_2S-generating enzymes is increased during adipocyte differentiation (Tsai *et al.* 2015). H_2S can also influence differentiation through persulfidation of the transcription factor Peroxisome proliferator-activated receptor gamma (PPAR-γ), a master regulator of adipogenesis (Cai *et al.* 2016a). Supplementation of differentiation media of the adipocyte cell line 3T3-L1 with H_2S or the slow-release donor GYY4137 increased nuclear translocation of PPAR-γ, with increased lipid accumulation and expression of adipocyte biomarkers. *In vivo* evidence of an important role for H_2S in adipogenesis came from studies of CBS deficient and CSE knockout mice, which both exhibited reduced fat mass (Gupta and Kruger 2011; Mani *et al.* 2011). H_2S also influences mature adipocyte function through modulation of insulin signalling and lipolysis. While initial research found H_2S inhibits insulin-mediated glucose uptake (Feng *et al.* 2009), results from more recent investigations have shown that H_2S improves insulin action in adipose through upregulation of PPAR-γ activity, and through increasing GLUT4 translocation to the membrane via activation of phophatidylinositide 3-kinase (PI3K) (Manna and Jain 2011; Xue *et al.* 2013; Cai *et al.* 2016a). H_2S inhibits basal and adrenergic-stimulated lipolysis in many models, including in our own *Tst*$^{-/-}$ mouse which has increased plasma sulfide levels (Morton *et al.* 2016). Inhibition of lipolysis by H_2S has also been observed in 3T3-L1 cells and in wild-type mice treated with the slow-release donor GYY4137, with beneficial effects on glucose tolerance when administered during a high fat diet regime (Geng *et al.* 2013; Tsai *et al.* 2015). H_2S may also impact the secretion of adipokines in adipose tissue, although this has yet to be observed *in vivo*. In 3T3-L1 adipocytes exposed to a high glucose concentration, secretion of the pro-inflammatory cytokine MCP1 was increased, and adiponectin was reduced, but these effects were partially normalised by exposure to H_2S (Manna and Jain 2011; Pan *et al.* 2014). As well as impacting the function of adipocytes, the depletion of H_2S in obesity may increase the phenotypic switching of macrophages from the tissue resident pro-resolution M2 type to the M1 pro-inflammatory type with increased production of pro-inflammatory cytokines (Velmurugan *et al.* 2015). H_2S also has pro-angiogenic and anti-fibrotic effects which may help to limit damage caused by local hypoxia during

expansion, although these are yet to be fully investigated in adipose tissue (Papapetropoulos *et al.* 2009; Zhang *et al.* 2015). These beneficial effects of H_2S on adipose tissue function may help to prevent dysfunction of the tissue, but the reduction of H_2S in obesity may contribute to the link between obesity and metabolic syndrome.

The activity of insulin in liver is influenced by H_2S levels, although current evidence suggests it has the opposite effects to H_2S in adipose tissue. The liver responds to insulin by increasing glucose uptake and its conversion to glycogen or lipid, as well as inhibiting gluconeogenesis. H_2S has the opposite effects on hepatocytes, inhibiting glucose uptake and increasing glucose production via gluconeogenesis and glycogenolysis, as well as enhancing lipid β-oxidation and inhibiting lipid synthesis (Zhang *et al.* 2013; Wu *et al.* 2015). While insulin reduces the expression of CSE in a hepatocyte cell line grown under normal conditions, when insulin resistance was induced by pre-exposure to high glucose and high insulin concentrations, CSE expression was increased, potentially contributing to the impaired insulin-responsiveness of these cells (Zhang *et al.* 2013). This insulin-mediated suppression of H_2S production by the liver may be counter-intuitively protective against liver damage by high fat diet. Exogenous H_2S administration reduced lipid synthesis and lipid droplet accumulation in mice fed a high fat diet, as well as reducing markers of oxidative stress (Wu *et al.* 2015). In human obesity, the observed reduction in plasma H_2S concentration may therefore contribute to ectopic lipid storage in the liver, contributing to the development of non-alcoholic fatty liver disease, although this has yet to be investigated.

The jump from insulin resistance to overt type 2 diabetes occurs due to failure of the pancreatic insulin-producing β cells. A protective role for H_2S has been suggested in this process, although with some controversy. In isolated primary mouse islets exposed to a high glucose concentration or oxidative stress, exogeneous H_2S exposure protected against apoptosis and preserved insulin secretion (Kaneko *et al.* 2009; Taniguchi *et al.* 2011). CSE knockout mice with reduced H_2S production were susceptible to β cell damage when put on a high fat diet, but only when older than 6 months (Okamoto *et al.* 2013). These mice exhibited impaired glucose tolerance due

to reduced insulin secretion caused by increased apoptosis in pancreatic islets, suggesting that H_2S production improves β cell survival. However, other research on CSE knockout mice concluded that H_2S contributed to β cell failure in mice exposed to streptozotocin, a commonly used model of type 1 diabetes (Yang *et al.* 2011). The contradictory effects of H_2S in these studies may be due to the differing mechanisms of β cell damage caused by high glucose and streptozotocin, indicating that H_2S may be either protective or damaging depending on the level of cellular damage caused by outside factors. In human obesity, which is more closely modelled by high fat diet exposure in rodents, the progression to type 2 diabetes may be facilitated by the reduction in H_2S observed in patients leading to β cell damage. As well the potential effect of H_2S on β cell survival, increased intracellular H_2S levels in β cells has been directly linked to suppression of insulin secretion due to H_2S-mediated activation of K_{ATP} channels and inhibition of calcium channels (Yang, Yang, *et al.* 2005; Tang *et al.* 2013). Therefore, H_2S reduction in diabetes may be a compensatory mechanism to increase insulin secretion, but ultimately contributing to β cell death.

1.3.3.5 H_2S and calorie restriction

Recently, a role for H_2S in modulating the beneficial effects of calorie restriction (CR) has been suggested. CR is a trigger of mitohormesis, with beneficial effects on health, including glucose tolerance, and lifespan (Heilbronn *et al.* 2006; Ristow and Schmeisser 2014)(described in paragraph 1.2.2.4 on page 27). CR in mice leads to increased hepatic expression of the H_2S -producing enzyme CSE, and increased production of H_2S in liver extracts (Hine *et al.* 2015). This increase in H_2S was shown to be essential for the protective effects of CR on a model of hepatic ischaemia reperfusion injury in mice, and it was associated with lifespan extension in fruit flies, yeast and the nematode, *C. elegans*. As the *Tst*$^{-/-}$ mouse used in this thesis has increased plasma sulfide levels (Morton *et al.* 2016), the potential for H_2S to impact the metabolic phenotype of these mice must be considered.

1.3.4 TST function summarised

To summarise, the mitochondrial enzyme TST may influence adipose tissue function through its ability to neutralise ROS, by enabling persulfidation of target proteins, by donating sulfur to iron-sulfur clusters of complexes of the electron transport chains, via transport of mitochondrial ribosomal RNA and through metabolism of H_2S. This gasotransmitter has anti-inflammatory and antioxidant effects, and influences the response of metabolically active tissues to insulin, and so may mediate or counteract the effect of altered TST expression.

1.4 OVERVIEW

In a polygenic model of healthy leanness, TST was found to be upregulated in white adipose tissue. A subsequent mouse model with TST specifically over-expressed in adipose under the control of the adiponectin promoter, the Adipoq-*Tst* mouse, was found to be protected against weight gain and metabolic impairment on a high fat diet. It has been suggested that TST has antioxidant capabilities through interaction with thioredoxin. As oxidative stress is a key feature of adipose tissue dysfunction in obesity, leading to inflammation, altered adipokine secretion and insulin resistance, the local antioxidant effect of TST may underlie its protective effects in this mouse model. TST also contributes to the oxidation of hydrogen sulfide, and in our *Tst*$^{-/-}$ mouse line, systemic sulfide levels are increased. H_2S can act as an antioxidant and anti-inflammatory mediator and maintain insulin action in adipose tissue, therefore its effects on metabolic parameters were considered.

1.5 HYPOTHESIS AND AIMS

Overarching hypothesis:

Thiosulfate sulfurtransferase in adipose tissue maintains metabolic health by preventing excessive local reactive oxygen species accumulation and subsequent oxidative stress and inflammation.

The sub-hypotheses of this PhD are:

- Thiosulfate sulfurtransferase gene knockout impairs metabolic health after a high fat challenge due to increased adipose oxidative stress and inflammation.
- Thiosulfate sulfurtransferase over-expression in adipose tissue protects against metabolic impairment of a high fat challenge due to increased antioxidant capability.

Aims

To test these hypotheses, the aims of this thesis were:

- To measure oxidative stress and inflammation in adipose of *Tst* knockout mice after a high fat challenge, and assess metabolic impairment.
- To characterise TST expression in a new mouse line with over-expression of human TST in adipose.
- To evaluate metabolic phenotype of Ad-hTST mice after a high fat challenge.
- To investigate response to exogenous oxidative stress in primary adipocytes from $Tst^{-/-}$ and Ad-hTST mice *in vitro* and *in vivo*.

Chapter 2 Materials and Methods

See Appendix for manufacturers' details and addresses (Table 7.2 on page 221).

2.1 *IN VIVO* PHYSIOLOGY

2.1.1 Animal models and maintenance

2.1.1.1 Maintenance conditions

Mice were housed in standard conditions of 12hrs light/dark (7am to 7pm) and room temperature (21°C) with *ad libitum* access to food, either standard chow (RM1; Special Diet Services) or experimental diets (see Table 2.2 on page 63 for experimental diet composition). All experiments and procedures were carried out in accordance with the UK Animals (Scientific Procedures) Act 1986 under a valid and active project licence (N Morton, PPL: 70/8117) and personal licence (C. Mc Fadden, PIL: IF3546C87). Approval of the named veterinary surgeon was given for all procedures. Mice were culled by CO_2 followed by cervical dislocation (schedule 1 method) or by decapitation (regulated procedure) when blood plasma was required.

2.1.1.2 *Tst*$^{-/-}$ mouse

The *Tst*$^{-/-}$ mouse is a homozygous knockout that was previously described (Morton *et al.* 2016). Briefly, this line was generated by the University of California at Davis knockout-mouse project (https://www.komp.org/geneinfo.php?geneid=85272; project VG13928; model Tst$^{tm1(KOMP)Vlcg}$, representing a definitive null allele with the whole *Tst* gene replaced by a *neo* gene). Sperm from viable heterozygote mice were used to fertilize C57BL/6N embryos at the University of Edinburgh Genetic Intervention and Screening technologies (GIST) facility. The mice were initially bred with C57BL/6J wild-type mice, and subsequently the genotypes were separated for use as wild-type and *Tst*$^{-/-}$ lines on a mixed 6N/6J genetic background for high fat-feeding experiments and paraquat administration (chapter 3 and chapter 5). Backcrossing was subsequently performed to C57BL/6J, and these mice were used for isolation of primary adipocytes for *in vitro* reactive oxygen species experiments (chapter 5).

2.1.1.3 Ad-hTST mouse

The Ad-hTST line overexpresses the human TST gene in adipose tissue. This mouse was produced using the cre-*loxP* recombination system to target overexpression to adipose tissue alone. The parent line (Rosa26^{LSLhTST}) was generated by Cyagen Biosciences by using homologous recombination to target the constitutively active Rosa26 locus in C57BL/6N embryonic stem cells for insertion of an expression cassette containing the human TST cDNA preceded by a stop cassette flanked by *loxP* sites (*loxP*-STOP-*loxP*: LSL) (Figure 2.1a). To excise the stop region, the Rosa26^{LSLhTST} mice were bred with Adiponectin-cre (Adip-cre) mice, expressing cre recombinase in adipose tissue only (Eguchi *et al.* 2011). Offspring of this cross were genotyped for the presence of cre recombinase (see 2.1.1.4). Cre-positive mice were presumed to have excision of the stop region (Figure 2.1b), and were called Ad-hTST. Cre-negative littermates were used as controls, and were called wild-type-*loxP*-STOP-*loxP* (WT-LSL). These mice were genetically indistinguishable from the parent line Rosa26^{LSLhTST}.

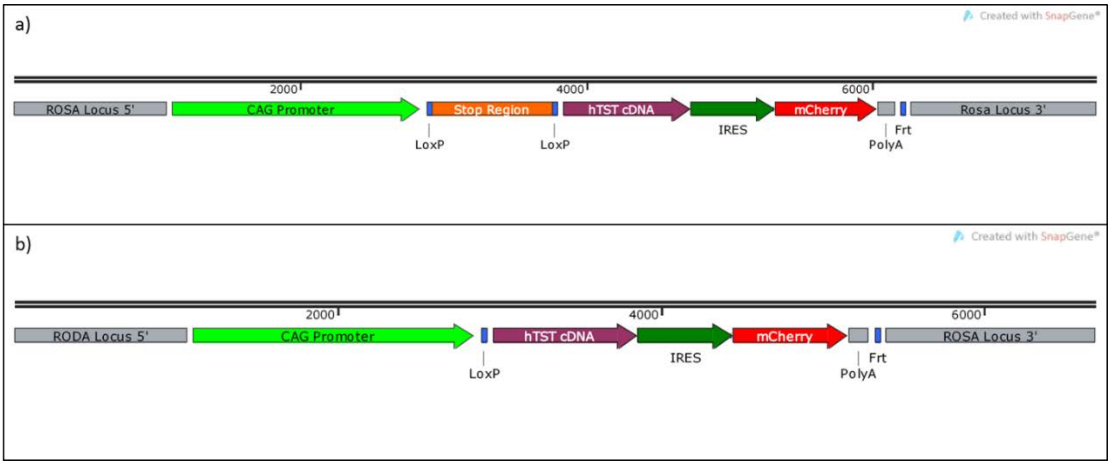

Figure 2.1: Map of gene expression cassette at Rosa26 locus of Rosa26^{LSLhTST} mice (a) before and (b) after Cre-mediated recombination.

CAG promoter: adapted from chicken β-actin promoter (Jun-ichi et al. 1989); loxP: DNA recognition sites for cre recombinase; Stop region: contains premature stop codon; hTST cDNA: open reading frame of human TST cDNA; IRES: internal ribosome entry site; mCherry: open reading frame of the mCherry fluorescence gene; PolyA: polyadenosine coding sequence; Frt: DNA recognition sites for Flp recombinase; ROSA Locus 5'/3': 5 prime and 3 prime regions of the ROSA locus. (Created using SnapGene Viewer software).

2.1.1.4 Genotyping (carried out by Transnetyx®)

At the age of three weeks, mice were weaned and ear clips were taken for identification and genotyping by animal facility staff. Ear clips were placed in 96-well plates and sent to Transnetyx (Memphis, TN, USA) for genotyping. Transnetyx used a high-throughput fully automated process to extract and purify DNA, and carry out real-time PCR with custom probes. To genotype for the presence of the cre recombinase gene, Transnetyx used the following primer sequences for forward and reverse primers:

Forward: TTAATCCATATTGGCAGAACGAAAACG

Reverse: CAGGCTAAGTGCCTTCTCTACA.

2.1.1.5 Surwit high fat and control diet composition

To induce obesity by high fat diet, mice were fed a high fat, high sucrose diet (HFD) for the length of the experiment, starting from 6 to 8 weeks of age (Surwit *et al.* 1995). Standard RM1 chow (Table 2.1) was used as a control diet in *Tst*$^{-/-}$ cohorts, however in later experiments using Ad-hTST mice it was decided to change to the comparable Surwit low fat diet (LFD) with corn-starch as the main carbohydrate source (Table 2.2).

Table 2.1: Composition of RM1 maintenance diet

RM1 Standard Maintenance Diet	
Composition	**kcal%**
Protein	17.50
Carbohydrate	75.08
Fat	7.43
Ingredients	
Wheat	Soya oil
Barley	Whey powder
Wheatfeed	Amino acids
Vitamins	Soya protein concentrate
Micro minerals	De-hulled extracted toasted soya
Macro minerals	
Breakdown of micro and macro mineral content available at http://www.sdsdiets.com/pdfs/RM1-A-P.pdf	

Table 2.2: Composition of Surwit high fat and low fat diets.

	Surwit D12331		**Surwit D12328**	
	High fat / High sucrose		Low fat / High corn starch	
Composition	**Gram%**	**kcal%**	**Gram%**	**kcal%**
Protein	23	16.4	16.8	16.4
Carbohydrate	35.5	25.5	74.3	73.1
Fat	35.8	58	4.8	10.5
Ingredients	**Gram**	**kcal**	**Gram**	**kcal**
Casein	228	912	228	912
DL-Methionine	2	0	2	0
Maltodextrin 10	170	680	170	680
Corn starch	-	-	835	3340
Sucrose	175	700	-	-
Soybean oil	25	225	25	225
Coconut oil	333.5	3001.5	40	360
Mineral mix S10001	40	0	40	0
Sodium bicarbonate	10.5	0	10.5	0
Potassium citrate	4	0	4	0
Vitamin mix V10001	10	40	10	40
Choline bitartrate	2	0	2	0
FD&C red dye #4	0.1	0	-	-
FD&C yellow dye #5	-	-	0.1	0

2.1.2 Experimental procedures

2.1.2.1 Glucose tolerance test

Mice were fasted for 4hrs prior to the start of the glucose tolerance test (GTT). A sterile glucose/saline solution was made consisting of 25% glucose and 0.9% sodium chloride. A tail vein incision was made and basal blood glucose levels measured using OneTouch Ultra® glucometer and test strips. Blood samples were also collected using Microvette CB300 EDTA-containing tubes and stored on ice. A glucose bolus (2mg per gram body weight) was administered by intraperitoneal (IP) injection at time 0. Blood glucose and a blood sample were collected at time 15mins, 30mins, 60mins and 120mins. Blood samples were centrifuged at 4^{o}C, 3,000rpm for 8mins to separate plasma, which was removed and stored at -80^{o}C for future measurement of insulin (see section 2.2.3.2 on page 74)

2.1.2.2 Insulin tolerance test

Mice were fasted for 4hrs prior to the start of the test. Fasting blood glucose was measured as in the GTT (section 2.1.2.1 above) before administration of insulin (Humulin® U-100, 1mU per gram body weight) by IP injection. Blood glucose was then measured at 15, 30, 60 and 120mins post-injection.

2.1.2.3 Measurement of lean and fat mass by time domain-NMR

Fat and lean mass were measured in awake mice using the Bruker minispec LF50 (7.5MHz, 0.175T) system. This used time domain nuclear magnetic resonance (TD-NMR) relaxometry to measure fat, lean and free body fluid (water) content while the mouse was restrained to minimise movement (Künnecke *et al.* 2004). Data was represented as a percentage of total body weight.

2.1.2.4 Paraquat administration

Paraquat dichloride in saline solution (0.9% sodium chloride) was made in Milli-Q® filtered water and filtered to sterilise. Paraquat or saline were injected by IP injection, and mice were monitored for up to 1hr before being returned to their home cages for the duration of the exposure.

2.2 MOLECULAR BIOLOGY

2.2.1 Measurement of gene expression

2.2.1.1 RNA extraction

RNA was extracted from tissues according to the following method. Frozen tissue was put in a 2ml microcentrifuge tube with a stainless steel grinding ball and kept on dry ice. For each 100mg of tissue, 1ml of QIAzol was added and the sample immediately homogenised by shaking in a Mixer Mill MM301 homogeniser at a speed of 30 shakes per second for 1min at RT. Samples were transferred to ice before being centrifuged at 12,000g for 5mins in a centrifuge 5415R at 4ºC to settle debris. For adipose tissue, this spin also caused lipid to form a clear colourless layer on top. The samples were transferred to new 1.5ml microcentrifuge tubes, avoiding the settled debris and the colourless top-layer in the case of adipose tissue. Samples were left at RT for 5min. Chloroform was added at a ratio of 200µl for every 1ml of QIAzol, and samples were shaken vigorously for 15s, then left at RT for 2mins. Samples were then centrifuged at 12,000g for 15min at 4ºC. The top aqueous layer was transferred to a new tube, isopropanol was added (500µl for every 1ml of QIAzol) and samples were vortexed for 10s before incubating at RT for 10mins. Samples were then centrifuged at 12,000g for 10-30mins to pellet RNA, and the pellets were washed in 1ml of 75% ethanol (100% ethanol diluted with RNAase/DNAase-free water) by centrifuging at 7,500g for 5mins. The wash was carried out twice and after the second wash the pellet was allowed to dry at RT for ~5mins before being resuspended in 20-30µl of RNAase/DNAase-free water. RNA quantity was assessed using the NanoDrop ND-1000 spectrophotometer by the absorbance at 260nm wavelength. The ratio of RNA/protein (A260/280) and RNA/organic compounds (A260/230) were used to assess purity of the sample.

2.2.1.2 cDNA synthesis and dilution

RNA was cleared of genomic DNA and transcribed into cDNA using QuantiTect Reverse Transcription Kit. To remove contaminating genomic DNA, RNA (750 – 1000ng) was incubated with gDNA wipeout buffer for 2mins at 42ºC. To transcribe the remaining RNA to cDNA, 1µl of QuantiTect reverse transcriptase, 1µl of RT primer mix and 3µl of RT buffer were added, and this was incubated for 15mins at 42ºC, followed by 3mins at 95ºC to inactivate the reverse transcriptase. All incubations were carried out in a thermal cycler. cDNA samples were diluted 1:20 in RNase-free water, unless otherwise states. 5µl of each sample was pooled to make a standard curve of serial dilutions ranging from 1:4 to 1:256. Standard curves were made from a pool of all samples in the group unless otherwise stated.

2.2.1.3 Real-time quantitative polymerase chain reaction

Gene expression was measured by quantifying cDNA levels using a Roche LightCycler® 480. Reactions were carried out in a white 384-well plate with the following added: 2µl of diluted cDNA, 5µl of buffer, 2.5µl of RNase-free water and 0.5µl of TaqMan® assay probe. For every gene measured, a standard curve of seven standards was also measured, as well as a negative control containing no cDNA. Plates were sealed using a clear plastic sticker and centrifuged at 2,000rpm for 2mins prior to being placed in the LightCycler®. A program for hydrolysis reaction was run as follows: Pre-incubation at 95ºC for 10mins, followed amplification for 50 cycles of 95ºC for 10s, 60ºC for 30s and 72ºC for 1s, before a final cooling at 40ºC for 30s. Reactions were performed in triplicate, and wells were excluded if standard deviation varied more than 0.2. The standard curve generated by LightCycler® software was log of concentration (X axis) against crossing point (Y axis), and it was deemed acceptable if reaction efficiency factor was between 2.8 and 3.2. Relative concentration was interpolated from the standard curve. Data is represented at relative to endogenous control genes *Tbp* or *Eef2*, and all Taqman probe IDs are listed in Table 2.3.

Table 2.3: Gene names and TaqMan IDs for probes used for RT-PCR.

Gene	Taqman ID	Gene	Taqman ID
Adipoq	Mm00456425_m1	Pai1 (AKA. Serpine1)	Mm00435858_m1
Atf4	Mm00515325_g1	Pparg	Mm00440940_m1
Cbs	Mm00460654_m1	Prx1	Mm01621996_s1
Chop (AKA. Ddit3)	Mm01135937_g1	Prx3	Mm00545848_m1
Cse (AKA. Cth)	Mm00461247_m1	Sod1	Mm01344233_g1
Eef2	Mm01171435_gH	Sod2	Mm01313000_m1
Ethe1	Mm00480916_m1	Sqrdl	Mm00502443_m1
Gpx1	Mm00656767_g1	Tbp	Mm01277042_m1
Gpx4	Mm00515041_m1	Tnfa	Mm00443258_m1
Hmox1	Mm00516005_m1	TST (human)	Hs00361812_m1
Mcp1 (AKA. Ccl2)	Mm00441242_m1	Tst (mouse)	Mm01195231_m1
Mpst	Mm00460389_m1	Txn2	Mm00444931_m1
Nqo1	Mm01253561_m1	Txrd2	Mm00496766_m1

2.2.2 Measurement of protein expression

2.2.2.1 Protein extraction from adipose tissue

Samples were kept cold at all times, on ice or in a cooled centrifuge at 4ºC. Fat samples were weighed and cut on dry ice to make all samples a similar weight. Ice-cold fat lysis buffer (described in paragraph 2.2.2.2 below) was added to each sample (2µl for every microgram) in a 2ml microcentrifuge tube containing a stainless steel grinding ball. Samples were homogenised for 1min in a Mixer Mill MM301 homogeniser. Samples were centrifuged at 4ºC for 1min at 13,000rpm to settle debris, and transferred to new tube. They were centrifuged at the same speed and tempterature for 10mins and aqueous phase was removed to a new tube. Adipose samples formed a solid fat layer which was avoided when transferring to a new tube. This was repeated a minimum of 3 times until no fat remained on top of the sample. Protein concentration was measured in samples diluted 1 in 20 using DC™ Protein assay from Bio-Rad according to the manufacturer's protocol, using bovine serum albumin (0.1mg/µl to 1.41mg/µl) in 1:20 lysis buffer to make a standard curve. Samples were then diluted to 2mg/ml in 10µl aliquots for a total of 20µg protein per sample for Western Blot analysis.

2.2.2.2 Protein lysis buffer for adipose tissue

Lysis buffer to extract protein from adipose tissue was made using the following protocol. To 800ml Milli-Q® filtered water, the components in Table 2.4 were added. When all components were dissolved, the pH was adjusted to 7.4 using concentrated hydrochloric acid (1M). The volume was adjusted to 1 litre with filtered water, before the final addition of Triton X-100. On the day of use, the final components in were added to a volume of either 50ml or 10ml as required.

Table 2.4: Components of lysis buffer for extraction of protein from adipose tissue.

Component	**Concentration**
Tris base	50mM
Sucrose	270mM
Sodium fluoride	50mM
Ethylenediaminetetraacetic Acid (EDTA)	1mM
Ethylene glycol-bis(2-aminoethylether)-N,N,N′,N′-tetraacetic acid (EGTA)	1mM
• After pH and volume adjustments:	
Triton X-100	1%
Added on day of use:	
β-mercaptoethanol	0.1%
cOmplete ULTRA Tablet (mini tablets for 10ml)	1 tablet
β-glycerophosphate	10mM
Sodium orthovanadate (Stock 100mM in water with pH > 12)	1mM

2.2.2.3 Polyacrylamide gel electrophoresis and Western blotting

Protein samples were separated using sodium dodecyl sulfate polyacrylamide gels for electrophoresis (SDS-PAGE), transferred to PVDF membrane followed by Western blotting to visualise bands.

2.2.2.3.1 Separation of proteins by SDS-PAGE:

The stacking gel to hold the samples, and separating gel in which the separation of proteins occurred were made according to the protocol in Table 2.5. Separating gel was added to gel plates and methanol was put on top to give an even surface and remove air bubbles. When the gel was set, the methanol was poured off and the stacking gel was added to the top with a comb inserted to create wells. Gel plates were assembled in gel running apparatus and cold PAGE running buffer (described in Table 2.6) was added until the space between the plates was full and the tank was filled to the necessary level. Protein samples (20µg in 10µl) were mixed with protein loading buffer (1:6) and added to the wells in the stacking gel. Pre-stained protein ladder was added to at least one well on every gel. Proteins were separated by running the gel at 100V for 2hrs.

Table 2.5: Components of SDS-polyacrylamide gels

Component	**Separating Gel**	**Stacking Gel**
Milli-Q® filtered water	8ml	5.7ml
1.5M / 0.5M Tris	pH 8.8 - 5ml	pH 6.8 - 2.5ml
10% (w/v) Sodium Dodecyl Sulfate (SDS) in water	200µl	100µl
30% Acrylamide/ Bis Acrylamide	6.7ml	1.7ml
10% Ammonium Persulfate (APS) in water	150µl	50µl
N,N,N′,N′-Tetramethylethylenediamine (TEMED)	20µl	10µl

2.2.2.3.2 Transfer of proteins to PVDF membrane

Protein was transferred to Amersham Hybond P 0.45 PVDF membrane using a Bio-Rad wet transfer system. Briefly, for each gel 4 rectangles of blotting filter paper were prepared and a piece of PVDF membrane the size of the gel was cut. The membrane was soaked in methanol for 1min, then filtered water for 1min, and finally transfer buffer (described in Table 2.6) for at least 2mins or until ready to use. Two pieces of filter paper were soaked in transfer buffer and placed in the transfer "sandwich" equipment. The gel was removed from the plates and put on top of these, then the membrane was put on top of the gel making sure to exclude air bubbles. Two more pieces of filter paper soaked in transfer buffer were added. The transfer sandwich was then placed in the transfer tank. An ice block was placed in the tank to keep apparatus cool and the tank was topped up with cold transfer buffer. The transfer was run at 200mA for 2hrs (or overnight at 125mA in the cold room at 4^{o}C).

2.2.2.3.3 Visualisation of proteins by Western blot

The membrane was removed from the transfer sandwich and rinsed in tris-buffered saline with tween (TSB-T), described in Table 2.5. It was then incubated on a shaker at RT for 1hr in blocking solution (5% skimmed milk powder in TBS-T). Membranes were washed for 15min three times in TBS-T, then incubated in primary antibody in 5% bovine serum albumin for 2hrs at RT or overnight at 4^{o}C. After a further three washes, membranes were incubated for 2hrs in fluorescent secondary antibody at a 1:10,000 dilution in 5% milk, washed three times in TBS-T. Details of antibodies are shown in Table 2.7. Fluorescence was visualised using a LI-COR Odyssey scanner and quantified using Image Studio Lite. Quantification of proteins was expressed relative to an internal control protein.

Table 2.6: Components of buffers for SDS-PAGE and Western blots.

PAGE Running Buffer (10x)	**Transfer Buffer (10x)**	**Tris-buffered Saline (TBS, 10x)**
1.9M Glycine	1.9M Glycine	500mM Tris base
250mM Tris base	250mM Tris base	1.5M NaCl
pH to 8.3 (before SDS)	pH to 8.3	pH to 7.6
1% Sodium Dodecyl Sulfate (SDS)	1x made with 20% Methanol	1x made with 0.1% Tween (TBS-T)

Table 2.7: Primary and secondary antibodies for Western blots.

Primary antibodies	**Raised in:**	**Secondary Antibody**
Anti-4 Hydroxynonenal polyclonal antibody	Rabbit	IRDye® 800RD Goat Anti-Rabbit
Anti-GAPDH polyclonal antibody	Mouse	IRDye® 680RD Donkey Anti-Mouse
Anti-TST polyclonal antibody	Rabbit	IRDye® 800RD Goat Anti-Rabbit

2.2.3 Biochemical and enzyme assays

2.2.3.1 Measurement of total and HMW adiponectin in plasma by ELISA

Total and high molecular weight (HMW) adiponectin was measured in plasma from control and high fat-fed mice using the mouse HMW and total adiponectin enzyme-linked immunosorbent assay (ELISA) from Alpco. Plasma samples were collected by decapitation using Microvette CB300 tubes (as in GTT, paragraph 2.1.2.1 on page 64) and stored at -80^{o}C until use. For HMW measured, samples were pre-treated with a protease that specifically digests medium and low molecular weight adiponectin. Undigested samples were diluted to the same degree but without protease. 50µl of adiponectin standards and diluted digested and undigested samples were then added to a 96-well plate coated with monoclonal adiponectin antibody and incubated for 1hr at RT. Wells were then washed twice with wash buffer. 50µl of biotin-conjugated polyclonal adiponectin antibody was then added to each well and the plate was incubated for 1hr at RT. The plate was washed three times before addition of 50µl of enzyme-labelled streptavidin for 30min at RT. After a further wash (x3), 50µl of the substrate solution was added and incubated for 10min at RT before addition of 50µl of the stop solution. The absorbance was then measured at a wavelength of 492nm using the Infinite® M1000 PRO microplate reader. The absorbance of the blank standard containing assay buffer only was subtracted from all other measurements.

2.2.3.2 Measurement of insulin in plasma by ELISA

Plasma samples from mice collected during GTT (section 2.1.2.1 on page 64) were used to measure insulin using the Ultra Sensitive Mouse Insulin ELISA kit. Insulin standard curve and plasma samples were measured according to the manufacturer's protocol, however samples from high fat-fed mice were diluted 1 in 5 to ensure they fell within the range of the wide-range assay. 95µl of sample diluent was added to each well of the antibody-coated microplate. 5µl of either sample or insulin standard was added and the plate was incubated at 4°C for 2hrs. All wells were washed 5 times with wash buffer, ensuring excess solution was removed after each wash. 100µl anti-insulin enzyme conjugate was added to each well and the plate was incubated at RT for 30min, followed by 7 washes with wash buffer. 100µl of enzyme substrate solution was then added to each well and the plate was incubated at RT for 40min in the dark. To stop the reaction 100µl stop solution was added and absorbance was measured at 450nm, with 630nm absorbance subtracted, using the Infinite® M1000 PRO microplate reader. Insulin concentrations were interpolated from the standard curve.

2.2.3.3 Rhodanese activity measurement in tissue homogenates

Rhodanese activity was measured in adipose tissue homogenates using the principle described in Figure 1.1 (page 42). Adipose samples were homogenised as described previously (paragraph 2.2.2.1 on page 68) in potassium phosphate (500mM, pH5.5). Homogenate (10µl) was incubated with potassium phosphate (10µl), sodium thiosulfate (10µl; 500mM) and Milli-Q® filtered water (60µl) for 2mins. Potassium cyanide (10µl; 500mM) was then added to start the production of thiocyanate, and incubated for 5-15mins. The reaction was stopped by adding 11µl of paraformaldehyde (38%). To the stopped reaction, iron (III) nitrate (125µl; 250mM) in 26% nitric acid was added, and absorbance was measured at 460nm using the Infinite® M1000 PRO microplate reader. This measurement of rhodanese activity was expressed relative to protein concentration, as measured by the DC™ Protein assay from Bio-Rad using bovine serum albumin (0.1mg/µl to 1.41mg/µl) in potassium phosphate to make a standard curve.

2.2.3.4 Measurement of thiobarbituric acid reactive substances (TBARS)

The reactive lipid aldehyde malondialdehyde (MDA) was measured in adipose and lung homogenate using the OxiSelect TBARS Assay Kit from Cell Biolabs. MDA reacts with thiobarbituric acid (TBA) to form a compound that can be measured by spectrometry. Frozen tissue was homogenised in phosphate buffered saline (PBS) containing an antioxidant, butylated hydroxytoluene using stainless steel grinding balls and a Mixer Mill MM301 homogeniser as described previously for RNA and protein extraction. In microcentrifuge tubes, 100µl of sample homogenate or control was added to 100µl of SDS lysis solution and incubated for 5mins at RT. TBA reagent (250µl) was then added and the tubes incubated at 95^{o}C for 45mins. The tubes were then placed in an ice bath for 5mins to cool before centrifuging at 3000rpm for 15mins. Supernatants (200µl) were transferred to a 96-well plate, and absorbance was measured at 532nm. MDA concentration was interpolated from a standard curve.

2.3 CELL BIOLOGY

2.3.1 Primary cell isolation

2.3.1.1 Isolation of primary adipocytes and stromal vascular fraction (SVF) from adipose tissue

Adipose depots were dissected and collected into ~10ml of warmed full Krebs buffer (described in Table 2.8). The digestion was carried out by putting the fat pad into full Krebs containing Collagenase I at a concentration of 2mg/ml. The fat was cut into small pieces using scissors and was incubated for approximately 45 minutes in a 5% CO_2, 37°C incubator, mixing every 10mins. The digestion was then filtered through plastic mesh of 500µM aperture into a falcon tube containing 10ml of fresh warm full Krebs or media. To separate the adipocytes from the SVF, the cells were centrifuged at RT for 5mins at 1500 rpm. The adipocytes settled to form a white floating layer which was removed to a 7ml bijoux containing fresh full Krebs or media using a 1ml pipette, with a cut off tip to ensure cells did not burst. SVF cells formed a pellet which was resuspended in media or phosphate buffered saline as required.

Table 2.8: Components of Full Krebs phosphate buffer (Full Krebs).

Component	**Concentration**
Milli-Q® filtered water	Make up to 1 litre
Sodium chloride	118mM
Potassium chloride	5mM
Magnesium sulfate heptahydrate	1.2mM
100mM Disodium hydrogen phosphate (Na_2HPO_4): Add 120ml	PO_4 approx.. 15-20mM
100mM Sodium dihydrogen phosphate (NaH_2PO_4): Used to adjust pH to 7.4	PO_4 approx.. 15-20mM
Added on day of use:	
Calcium chloride	1.265mM
Glucose	1mg/ml
Bovine serum albumin	1%

2.3.1.1 Primary hepatocyte isolation (carried out by Matthew Gibbins)

Mice were culled by CO_2 followed by cervical dislocation, the abdomen was opened and the portal vein nicked to release blood. The thoracic vena cava was then cannulated by puncturing the atrium with a needle attached to tubing. Warm (37^{o}C) liver perfusion media (LPM, Table 2.9) was then perfused through the tubing using a peristaltic pump for 10min, clearing red blood cells and blanching the liver. The liver was then digested by perfusing with liver digestion media (LDM, Table 2.9) for approximately 7min or until the appearance of clear sinusoidal spaces that remained after applying pressure. The digestion was then stopped by perfusing LPM for a further 10min. The liver was dissected and put into a petri dish containing warm LPM, and the gall bladder, the diaphragm and any other non-liver tissue were removed. In a cell culture hood, the liver was manually disrupted using forceps and the cells put into a 50ml centrifuge tube through a 40µm cell strainer with hepatocyte media (Table 2.10). The cells were settled by centrifuging at 500rpm for 5min and resuspended in DMEM. 50% equilibrated Percoll solution (described below) was then added underneath the cell suspension in an equal volume, and the sample centrifuged at 1000rpm for 15min to separate live hepatocytes in the pellet from dead and non-hepatocyte cells in the interface. The pellet was then washed twice in DMEM as above, and counted in a 1:1 mix with trypan blue using a haemocytometer. Cells were then plated onto collagen-coated plates and allowed to settle overnight before use.

Equilibrated Percoll was prepared in advance by making a 1 in 10 dilution of Percoll in 10X DMEM (Table 2.11). This was then diluted 1 in 2 in 1X DMEM (1:10 dilution of 10X DMEM in Milli-Q® filtered water, sterile filtered) to make 50% equilibrated Percoll solution.

Table 2.9: Components of liver perfusion and digestion media for primary hepatocyte isolation

Base Media	**Liver Perfusion Media**	**Liver Digestion Media**
Sodium chloride 140mM	Base media plus:	Base media plus:
Potassium chloride 2.6mM	EGTA 0.5mM	Calcium chloride 5mM
Disodium hydrogen phosphate 0.28mM	**pH 7.4**	Collagenase type 1 100U/ml
Glucose 5mM		**pH 7.4**
HEPES 10mM		

Table 2.10: Components of primary hepatocyte media

Hepatocyte media
Dulbecco's Modified Eagle Medium with Low glucose 1000g/L
10% (v/v) HyClone™ foetal bovine serum
1% (v/) Penicillin/streptomycin
2mM glutamine

Table 2.11: Components of 10X DMEM used to make equilibrated Percoll.

10X DMEM
Milli-Q® filtered water 100ml
DMEM 10g
Sodium bicarbonate 2.438g
1M HEPES 10mL
Penicillin/streptomycin 10mL

2.3.2 *In vitro* cell analysis

2.3.2.1 Analysis of immune cell types in SVF by flow cytometry

Cells of the stromal vascular fraction (SVF) of digested epididymal adipose tissue were resuspended in 1ml cold phosphate buffered saline with bovine serum albumin (PBS-BSA, 0.1%) and filtered through a 100µm cell strainer. Cells were pelleted by centrifuging at 1500rpm for 5min in a centrifuge cooled to 4ºC. Cells were resuspended in PBS-BSA containing anti-mouse CD16/CD32 antibody at a dilution of 1 in 300 to block FC receptors. Samples were transferred to a V-bottomed 96-well plate and incubated on ice for at least 20min. To pellet samples, the plate was centrifuged for 3min at 1700rpm. Pellets were resuspended in PBS-BSA with 10% mouse/rat serum with antibodies diluted as indicated concentrations (Table 2.12 and Table 2.13). The plate was then incubated on ice and protected from light for 30min. Samples were centrifuged and washed three times in cold PBS before being transferred into flow cytometry tubes. If secondary antibodies were needed, they were incubated for 10min before washing again. 1µl of DAPI (4',6-diamidino-2-phenylindole, 1:10,000) was added to each sample to stain dead cells just before analysis by flow cytometry using BD LSRfortessa™ cell analyser with BD FACSDiva™ software. Further analysis was carried out using FlowJo® software, following the gating strategy shown in Figure 2.2. Cells were gated in the order indicated by the black arrows. Side scatter (SSC-A) and forward scatter (FSC-A) were used to exclude debris. Single cells were gated using FSC-H (height) and FSC-A (area). From the single cells gate, live cells were identified as DAPI-negative. Hematopoetic cells were then identified as $CD45^+$, and within this population, eosinophils were distinguished based on SiglecF expression. From the $SiglecF^-$ population, macrophages (Mac) were identified as F4/80+ and CD11b+ initially, followed by $Ly6C^-$ and $MHCII^+$ (Ad-hTST cohort only). CD11c+ cells were then identified as M1-macrophages (M1).

Table 2.12: Flow cytometry antibodies used in Chapter 3

Chapter 3: *Tst*$^{-/-}$ mice on HFD for 20 weeks				
Cell type	**Antigen**	**Fluorophore**	**Dilution**	**Antigen Name**
Hematopoietic	CD45	Pacific Blue	1:200	Protein tyrosine phosphatase receptor C
Eosinophil	Siglec F	PE	1:200	Sialic acid binding IG-like lectin F
Neutrophil	Gr1	APC Cy7	1:100	Lymphocyte antigen 6 complex, locus G
Myeloid	F4/80	FITC	1:100	Adhesion G protein-coupled receptor E1
Macrophage	CD11b	PerCP Cy5.5	1:1200	Integrin alpha M
Monocytes	Ly6C	APC	1:400	Lymphocyte antigen 6 complex, locus C
M1 Mac	CD11c – Biotin (1:50)	Streptavidin PE Cy7	1:400	Integrin alpha X

Table 2.13: Flow cytometry antibodies used in Chapter 4

Chapter 4: Ad-hTST mice on HFD for 6 weeks				
Cell type	**Antigen**	**Fluorophore**	**Dilution**	**Antigen Name**
Hematopoietic	CD45	FITC	1:100	Protein tyrosine phosphatase receptor C
Eosinophil	Siglec F	PE	1:200	Sialic acid binding IG-like lectin F
Antigen-presenting	MHCII	eFlour 450	1:800	Major histocompatibility complex 2
Myeloid	F4/80	PE Cy7	1:200	Adhesion G protein-coupled receptor E1
Macrophage	CD11b	PerCP Cy5.5	1:1200	Integrin alpha M
Monocytes	Ly6C	AlexaFluor 700	1:200	Lymphocyte antigen 6 complex, locus C
M1 Mac	CD11c	Pacific Blue	1:50	Integrin alpha X

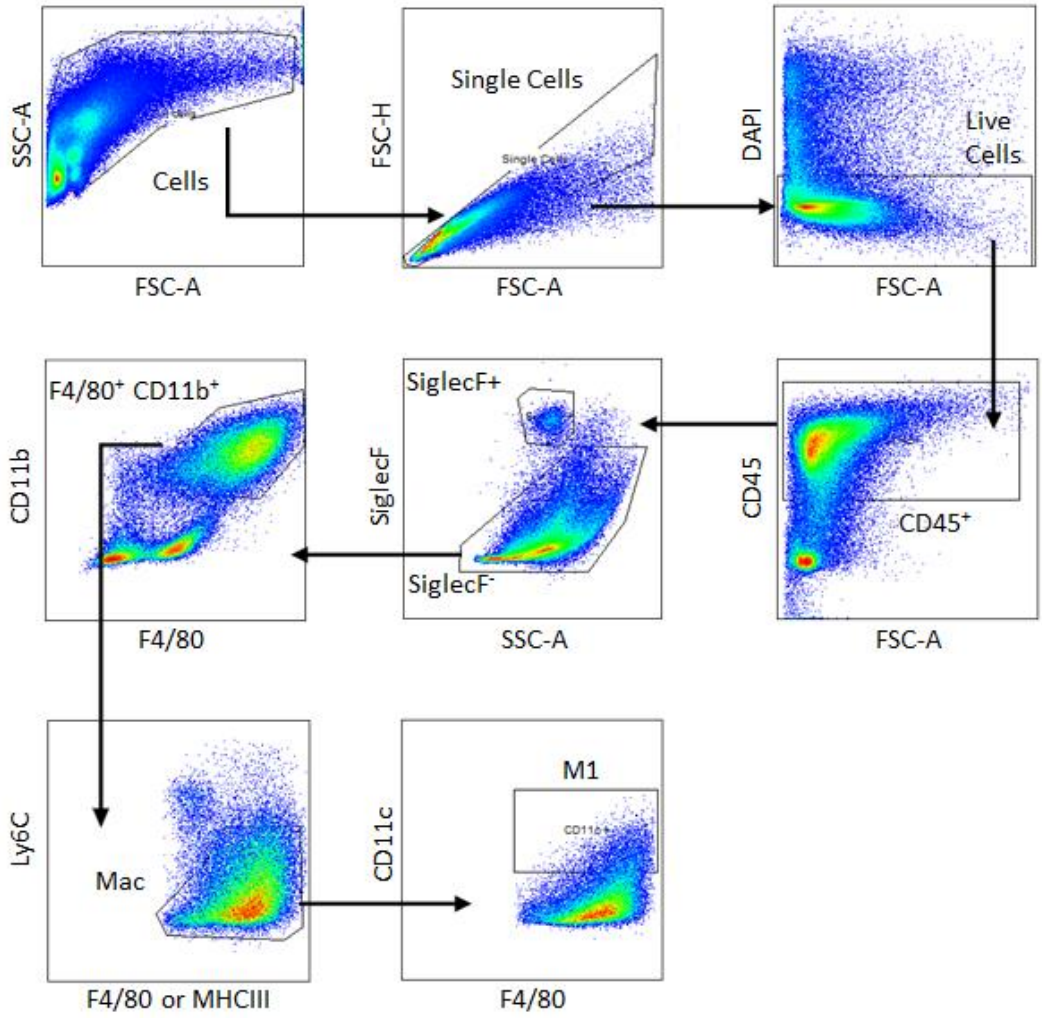

Figure 2.2: Gating strategy for analysis of SVFs from epididymal adipose tissue from Tst$^{-/-}$ and Ad-hTST mice.

Cells were gated in the order indicated by the black arrows. SSC-A: side scatter-area; FSC-A: forward scatter-area; FSC-H: forward scatter-height; DAPI: 4',6-diamidino-2-phenylindole; Mac: macrophages; M1: M1 macrophages.

2.3.2.2 Measurement of mitochondrial reactive oxygen species production

Mitochondrial ROS production was measured in primary adipocytes and primary hepatocytes. Cells were incubated with hydrogen peroxide (H_2O_2) in suitable media (full Krebs solution or hepatocyte media) for up to 2hrs to stimulate mitochondrial ROS production. This was then washed using Hank's balanced salt solution (HBSS) three times. Mitochondrial ROS was then stained using the fluorescent probe MitoSOX™ Red mitochondrial superoxide indicator by incubating for 10min in a concentration of 5μM in HBSS. The cells were then washed three times as before, and fluorescence measured using the Infinite® M1000 Pro plate reader, using excitation/emission wavelengths of 510/580nm. Fluorescence measurements for adherent cells were normalised to protein concentration as measured by SRB assay (section 2.3.2.4 on page 84).

2.3.2.3 Measurement of H_2O_2 disposal in primary adipocytes

Primary adipocytes were exposed to 100μM H_2O_2 in full Krebs media for 5 minutes, with or without pre-incubation in thiosulfate 2mM for 1hr. H_2O_2 remaining after this time period was measured using the fluorometric H_2O_2 assay kit. After incubation, 10μl of media was removed from each sample and control and added to 490μl assay buffer to make a 1 in 50 dilution. 50μl of these dilutions were put into wells of a 96-well plate and a matching volume of Master Mix was added for 30min at RT, protecting the plate from light. Master Mix contained red peroxidase substrate, horseradish peroxidase and assay buffer per the manufacturer's protocol. The fluorescence intensity was then measured using excitation/emission wavelengths of 540/590nm. H_2O_2 concentration was calculated using a standard curve.

2.3.2.4 Sulforhodamine B colorimetric assay for cellular protein content

Protein concentration of primary hepatocytes in a 96-well plate was measured using the sulforhodamine B (SRB) assay as described by Skehan *et al.* (Skehan *et al.* 1990). To wells containing 200µl of media, 50µl of 50% trichloroacetic acid (TCA, diluted from 100% TCA with filtered water) was added to fix cells, and the plate was incubated at 4ºC for 1hr. The wells were then washed with tap water ten times and air-dried. 50µl of SRB solution (SRB 0.4%w/v solution in 1% acetic acid) was added for 30min at RT to stain cells. The dye was washed out by four washes in 1% acetic acid (diluted from 100% with filtered water), and the plate was air-dried. Cell-bound dye was re-dissolved in Tris solution (10mM Tris solution pH 10.5) and absorbance was measured at 540nm.

2.3.2.5 Lactate dehydrogenase assay

Lactate dehydrogenase (LDH) activity was measured in media as a marker of cellular toxicity using the Pierce™ LDH Cytotoxicity assay kit from ThermoFisher. This kit uses NADH, which is formed by the LDH-catalysed conversation of lactate to pyruvate, to reduce a tetrazolium salt to a red formazan product, which is directly proportional to the amount of LDH in the media. For each experiment, a triplicate of wells was used as a maximum measurement of LDH activity by adding lysis buffer before the start of LDH measurement. LDH was measured by adding 50µl of each sample or control to 50µl of reaction mixture. This was incubated for 30mins at RT protected from light before 50µl of stop solution was added. Absorbance was measured at 490nm and 680nm, and the measurement of the latter was subtracted from the former.

2.4 IMAGING

2.4.1 Whole-mount staining of tissue explants

Small pieces of adipose and other tissues (10-20µg) were placed in about 500µl PBS at RT. DAPI was added at a concentration of 1 in 10,000 and incubated for 10mins at RT. Samples were washed in 1-2ml PBS three times, and pieces of tissue were then placed on plain microscope slides and mounted using Fluoromount™ Aqueous Mounting Medium. A coverslip was attached using clear nail polish, and this was left to dry overnight before imaging.

2.4.2 Imaging

Fluorescence and brightfield imaging was performed with a Hamamatsu Orca II CCD camera attached to an Olympus AX-70 Provis epifluorescence microscope, kindly provided by Prof. Margarete Heck with assistance from Dr. Kanishk Abhinav. Images were captured with SmartCapture 3 software and processed with ImageJ.

2.5 STATISTICS

GraphPad Prism 5 was used for analysis with data presented as mean ± SEM. Comparison between two groups was done using unpaired Student's *t*-test. 2-way analysis of variance (ANOVA) was used to compare between genotypes and diets, and Bonferroni multi-comparison post-hoc test was included where appropriate. Data from GTT and ITT experiments were compared using 2-way repeated measures ANOVA with Bonferroni post-hoc. Statistical significance was considered at $P < 0.05$.

Chapter 3 The effects of *Tst* gene knockout on glucose homeostasis and adipose tissue response to high fat diet.

3.1 INTRODUCTION

Previous evidence suggests that increasing *Tst* expression in adipose tissue protects mice from the metabolic impairment of a high fat diet (HFD) (Morton *et al.* 2016). The aim of this chapter was to investigate the impact of a lack of *Tst* on adipose function and metabolic outcome after a HFD. It was hypothesised that mice with a global knockout of the *Tst* gene would be more susceptible to oxidative stress in adipose tissue, and thus more metabolically impaired. To investigate this hypothesis, two cohorts of $Tst^{-/-}$ mice were exposed to HFD for 6 and 20 weeks, and subsequent effects on metabolic parameters and markers of adipose tissue dysfunction were assessed.

Our group showed previously that moderate overexpression of mouse *Tst* in adipose tissue protects these mice (Adipoq-*Tst* mouse) from gaining weight after a 6-week HFD, and prevents glucose intolerance (Morton *et al.* 2016). It was hypothesised that the antioxidant capability of TST contributed to the improved metabolic phenotype through prevention of local oxidative stress in adipose tissue, as Adipoq-*Tst* mice had increased SOD2 protein and *Prx3* mRNA in adipose tissue. Whilst there is evidence that TST interacts with and may neutralise ROS directly (Nandi *et al.* 2000), this has not been fully elucidated in mammals *in vivo*. However, some evidence indicating a link with TST and ROS metabolism has been found *in vitro*, as a siRNA-mediated knockdown of *Tst* expression in 3T3-L1 adipocytes results in increased mitochondrial ROS levels (Morton *et al.* 2016). One of the aims of this chapter is therefore to investigate if altered *Tst* expression influences the antioxidant machinery of adipocytes during oxidative stress.

To induce oxidative stress in adipose tissue, $Tst^{-/-}$ mice were exposed to HFD for either 6 or 20 weeks. WT mice on HFD typically gain weight faster than control-fed mice, and exhibit features of adipose tissue dysfunction such as increased carbonyl

content, immune cell infiltration and metabolic impairment (Matsuzawa-Nagata *et al.* 2008). This model of diet-induced obesity is commonly used to assess the impact of altered gene expression on risk of metabolic impairment. A short-term HFD challenge of only one week can increase adipose ROS production and impair insulin signalling without any difference in body weight (Paglialunga *et al.* 2015). A long-term challenge, such as for twenty-four weeks causes overt obesity, whole-body insulin resistance, an increase in adipose carbonyl content and upregulation of antioxidant enzyme expression (Matsuzawa-Nagata *et al.* 2008). The *Tst*$^{-/-}$ mouse was previously shown to have worse glucose tolerance than WT mice after 6 weeks of HFD (Morton et al., 2016), and so this time-point was chosen to carry out an intial investigation of adipose tissue dysfunction. However, it was decided to focus on the longer duration of 20 weeks of HFD to ensure chronic oxidative stress and adipose tissue dysfunction was achieved in this model.

To investigate the hypothesis of this chapter, the metabolic phenotype and adipose tissue dysfunction were assessed in *Tst*$^{-/-}$ mice after exposure to HFD. A duration of 6 weeks was initially carried out to measure immune cell infiltration, as this was thought to be good early marker for different susceptibility to adipose tissue dysfunction. This did not uncover any major differences between WT and *Tst*$^{-/-}$ mice, and so a longer duration of 20 weeks was chosen to induce greater adipose tissue dysfunction including oxidative stress and chronic inflammation, as well as further impair insulin sensitivity. Metabolic phenotype was assessed by carrying out a glucose tolerance test, insulin tolerance test and by measuring levels of the insulin-sensitising hormone adiponectin. Adipose tissue dysfunction was investigated by measuring a marker of oxidative stress and altered expression of antioxidant genes, as well as evaluating the inflammatory phenotype of the tissue. *Tst*$^{-/-}$ mice have increased plasma sulfide levels (Morton et al., 2016) which may impact the effect of HFD on both adipose function and systemic insulin sensitivity. While it was not possible to control for this potential factor in the experiments carried out in this chapter, the impact of Tst knockout and HFD exposure on the expression of genes that code for H_2S-producing enzymes and enzymes involved in H_2S breakdown was assessed.

This chapter describes the results of these two experiments for which *Tst*$^{-/-}$ mice were fed a HFD for 6 or 20 weeks. Evidence for or against the hypothesis is discussed, as well as potential limitations of this evidence. Future avenues of research for further investigating the impact of *Tst* on metabolic health are suggested, including work that followed on from these experiments and will be described in chapter 5.

3.1.1 Hypothesis & aims

In this chapter, it was hypothesised that thiosulfate sulfurtransferase gene knockout would impair metabolic health after a high fat challenge due to increased adipose oxidative stress and inflammation.

The aims of this chapter were:

- To evaluate metabolic impairment of *Tst* knockout mice after a high fat challenge.
- To assess oxidative stress and inflammation in adipose of *Tst* knockout mice after a high fat challenge.

3.2 METHOD

Male *Tst*$^{-/-}$ mice (as described in paragraph 2.1.1.2 on page 60) were used in this chapter to investigate the impact of *Tst* knockout on metabolic health when exposed to HFD for either 6 or 20 weeks. These mice were maintained as a homozygous line, having previously been maintained as heterozygotes (*Tst*$^{+/-}$) breeding with C57BL/6J wild-types (WT). Homozygous *Tst*$^{-/-}$ and control mice (WT) were generated by breeding heterozygous littermates, selecting for homozygous knockouts and WTs, and maintaining these as separate lines for 10+ generations. At the age shown in Figure 3.1 and Figure 3.2 below, *Tst*$^{-/-}$ and WT mice were separated into two groups with one maintained on RM1 standard chow (Chow; see Table 2.1 on page 62) and the other group received Surwit D12331 high fat, high sucrose diet (HFD; see Table 2.2 on page 63). Mice were maintained on these diets until the end of the study period (6 or 20 weeks), at which point they were culled by decapitation, and blood and organs were harvested.

Figure 3.1: Timeline of WT and Tst$^{-/-}$ mice on chow or HFD for 6 weeks.

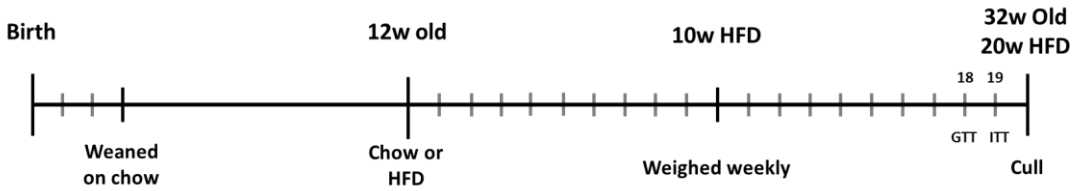

Figure 3.2: Timeline of WT and Tst$^{-/-}$ mice on chow or HFD for 20 weeks.

Glucose tolerance test (GTT) and insulin tolerance test (ITT) were carried out after 18 and 19 weeks of HFD.

3.3 RESULTS

3.3.1 The effect of *Tst* gene knockout after 6 weeks of high fat diet.

3.3.1.1 Body weight was not different in Tst$^{-/-}$ versus WT on HFD for 6 weeks, but Tst$^{-/-}$ mice had reduced body weight on chow diet.

After 6 weeks of HFD, an increase in body weight was observed in *Tst*$^{-/-}$ mice, however WT mice were largely unchanged (Figure 3.3). On chow diet, *Tst*$^{-/-}$ mice weighed less than WT mice.

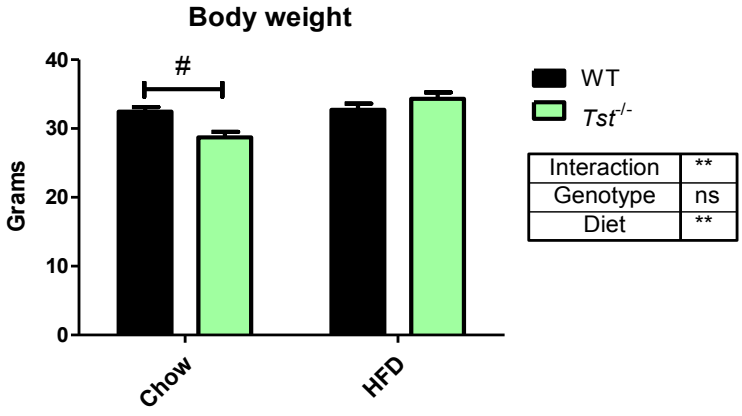

Figure 3.3: Body weight of Tst$^{-/-}$ and WT mice on chow or HFD for 6 weeks.

*Data are mean ± SEM, analysed by 2-way ANOVA: ** P < 0.01, ns = not significant; with Bonferroni post-hoc test comparing between genotypes for each diet: # P < 0.05; (chow: n = 6; HFD: n=11).*

3.3.1.2 *Epididymal adipose tissue depot weight was not different in Tst$^{-/-}$ versus WT on HFD for 6 weeks.*

6 weeks of HFD increased epididymal adipose weight to a similar extent in WT and *Tst*$^{-/-}$ mice, but no differences were observed in epididymal weight between genotypes (Figure 3.4).

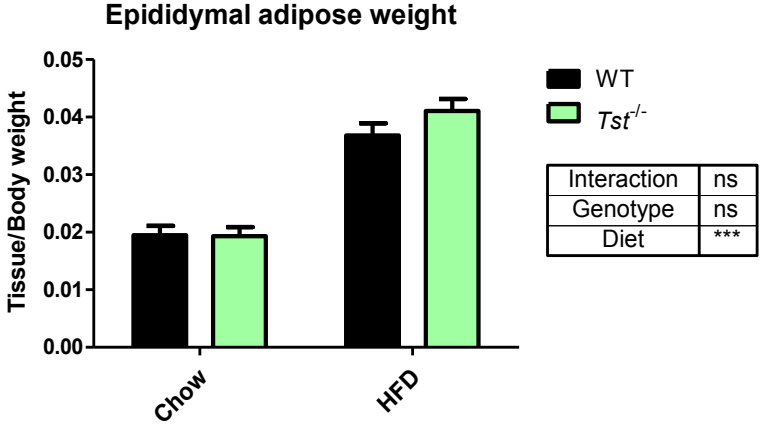

Figure 3.4: Epididymal white adipose weight of Tst$^{-/-}$ and WT mice on chow or HFD for 6 weeks.

*Data are mean ± SEM, analysed by 2-way ANOVA: *** P < 0.001, ns = not significant; (n = 6/11).*

3.3.1.3 Immune cell populations in stromal vascular fraction of adipose tissue were not different in Tst$^{-/-}$ versus WT mice on HFD for 6 weeks.

Adipose stromal vascular fraction (SVF) was isolated from control diet or HFD-fed mice by collagenase digestion of epididymal fat pads, stained with fluorescent antibodies to differentiate cell types, and analysed by flow cytometry. Macrophage (F480$^+$ CD11b$^+$ Ly6C$^-$) number as a percentage of total hematopoietic cell population (CD45$^+$ population) was unchanged by HFD in both genotypes (Figure 3.5a). The percentage of hematopoietic cells expressing the pro-inflammatory macrophage marker CD11c was increased by HFD, but no significant differences were observed between genotypes, despite a trend for increased CD11c$^+$ cells in *Tst*$^{-/-}$ mice on chow diet (Figure 3.5b). The percentage of eosinophils (SiglecF$^+$) was not significantly altered by HFD (Figure 3.5c).

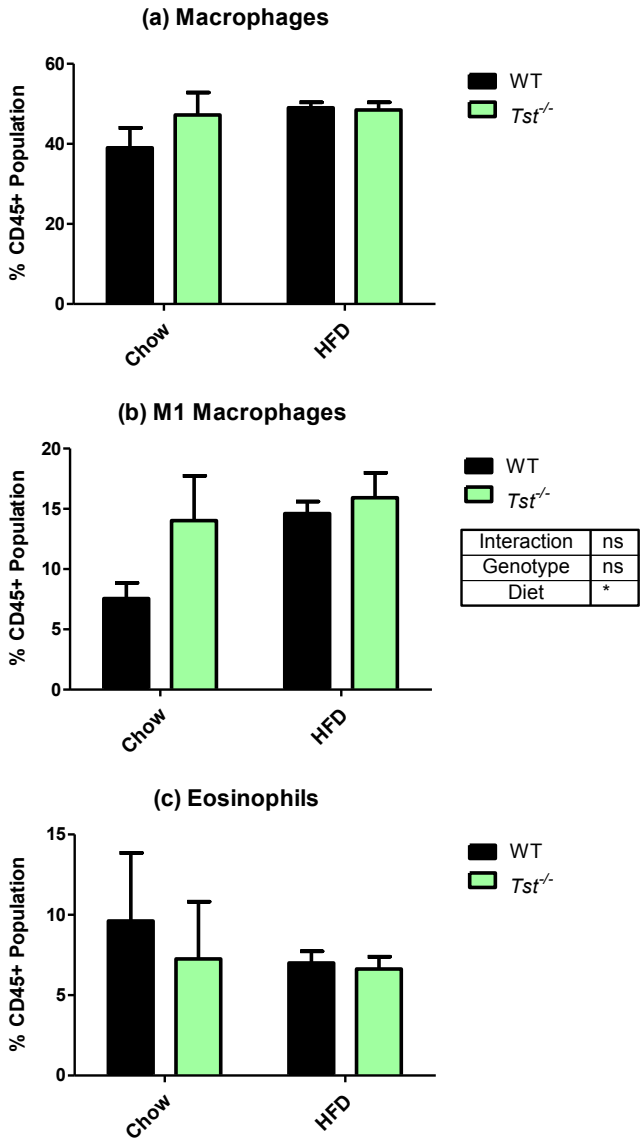

Figure 3.5: Immune cell populations in stromal vascular fraction (SVF) of epididymal adipose tissue in Tst$^{-/-}$ and WT mice on chow or HFD for 6 weeks.

*(a) Macrophages (F4/80$^+$ CD11b$^+$ Ly6C$^-$), (b) M1 macrophages (F4/80$^+$ CD11b$^+$ Ly6C$^-$ CD11c$^+$), and (c) eosinophils (SiglecF$^+$) measured in SVF of epididymal fat by flow cytometry. Results are expressed as percentage of hematopoietic population (CD45$^+$). Data are mean ± SEM, analysed by 2-way ANOVA: *** P < 0.001, ns = not significant: (n = 6/11).*

3.3.1.4 Conclusion after 6 weeks of HFD.

After exposure to HFD for 6 weeks, WT mice had not gained a significant amount of weight, and while adipose tissue had expanded, there was no significant increase in macrophage cell number in adipose tissue, a key marker of inflammation. As there were no significant differences in *Tst*$^{-/-}$ mice, which while gaining weight on HFD, largely followed the same pattern as WT on HFD in terms of fat mass gain and immune cell infiltration, it was decided to carry out a longer exposure to HFD to induce a greater extent of metabolic impairment and adipose tissue dysfunction.

3.3.2 The effect of *Tst* gene knockout after 20 weeks of high fat diet.

3.3.2.1 Body weight was not different in Tst$^{-/-}$ versus WT on HFD for 20 weeks.

After 20 weeks of HFD, all mice gained a significant amount of weight, with no difference in body weight between *Tst*$^{-/-}$ and WT groups (Figure 3.6a). Chow-fed mice also gained weight, but to a lesser extent than those on HFD (Figure 3.6b). Chow-fed *Tst*$^{-/-}$ mice did not gain significantly less weight than WT mice (Figure 3.6b).

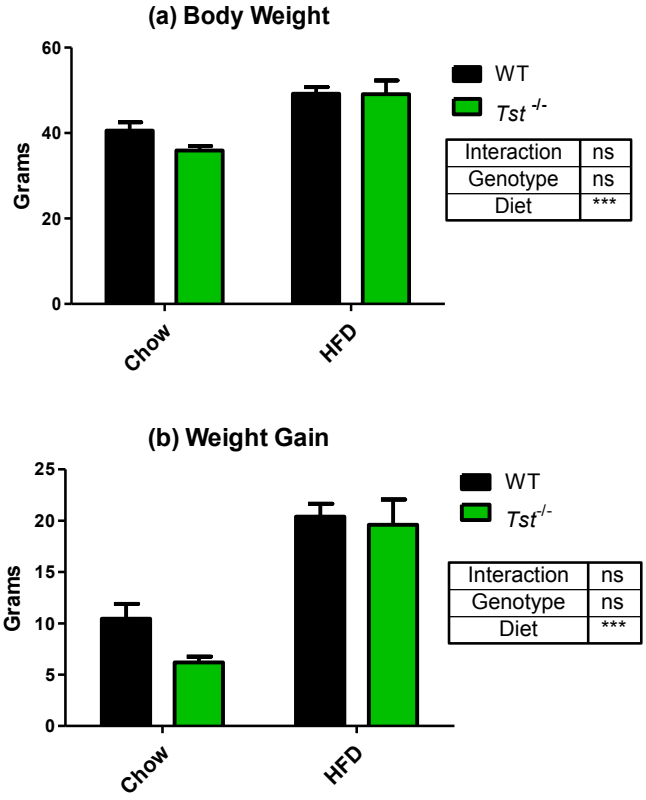

Figure 3.6: Body weights of Tst$^{-/-}$ and WT mice on chow or HFD for 20 weeks.

*(a) Body weight at cull, and (b) Weight gain between week 0 and week 20. Data are mean ± SEM, analysed by 2-way ANOVA: *** P < 0.001, ns = not significant; (n = 7-8).*

3.3.2.2 Adipose tissue depots weights were not different in Tst$^{-/-}$ versus WT on HFD for 20 weeks, but Tst$^{-/-}$ mice had less fat mass on chow diet.

Three white adipose depots were weighed after 20 weeks on chow or HFD and normalised to body weight. Epididymal, mesenteric and subcutaneous adipose depots were increased with HFD in both *Tst*$^{-/-}$ and WT mice. However, on chow diet, *Tst*$^{-/-}$ mice had less adipose tissue in all three depots than WT mice (Figure 3.7).

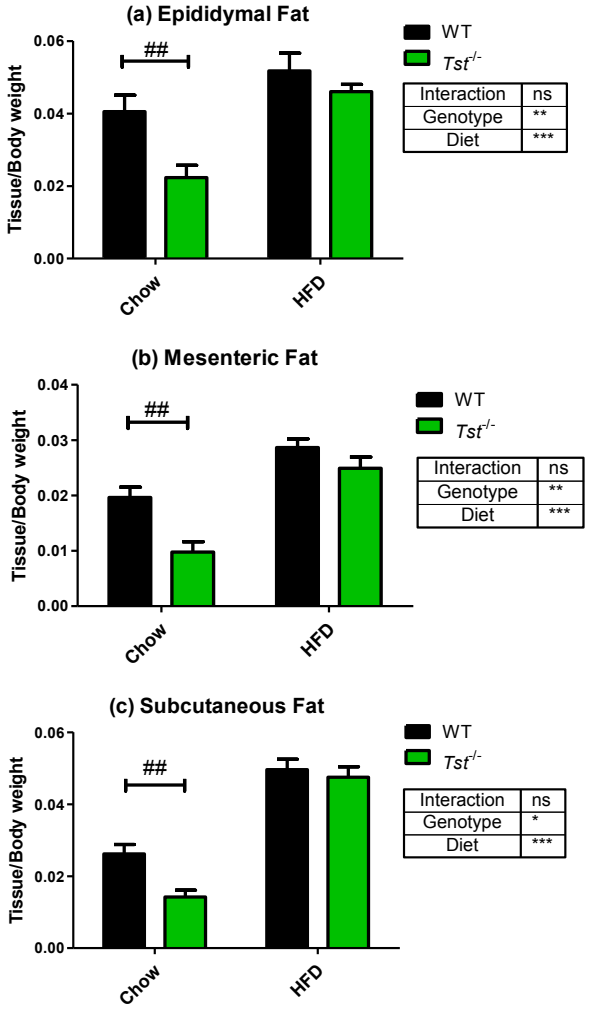

Figure 3.7: White adipose depot weights in Tst$^{-/-}$ and WT mice on chow or HFD for 20 weeks.

*(a) Epididymal, (b) mesenteric and (c) subcutaneous white adipose depots, normalised to body weight at cull. Data are mean ± SEM, analysed by 2-way ANOVA: * P < 0.05, ** P < 0.01, *** P < 0.001, ns = not significant; with Bonferroni post-hoc test comparing between genotypes for each diet: ## P < 0.01; (n = 7-8).*

3.3.2.3 Glucose tolerance was impaired after 18 weeks of HFD in Tst$^{-/-}$ and WT mice, but insulin was lower in in Tst$^{-/-}$ mice.

A glucose tolerance test was carried out on WT and *Tst*$^{-/-}$ mice after 18 weeks of chow or HFD to assess the impact of *Tst* gene knockout. WT mice did not have significantly higher glucose levels on HFD compared to chow at any timepoint. This suggests that the control group were glucose intolerant, and is supported by these mice having a glucose peak of 30mmol/L 30-minutes after glucose administration. There was no significant difference between WT and *Tst*$^{-/-}$ mice, however *Tst*$^{-/-}$ mice had significantly higher glucose on HFD than on chow at 30, 60 and 120 minutes after glucose administration (Figure 3.8a). Overall plasma glucose levels during the GTT measured by area under the curve were increased by HFD in both WT and *Tst*$^{-/-}$ mice, although there was no significant difference between genotypes (Figure 3.8b).

Plasma insulin was measured at each timepoint before and after glucose administration. WT mice on HFD had significantly higher fasting insulin than *Tst*$^{-/-}$ mice on HFD (mean 5.4 vs. 2 ng/ml) (Figure 3.8c). No differences were observed between genotypes on chow diet. HFD led to a significant increase ($P < 0.01$-0.001) in plasma insulin at all timepoints after glucose administration in both WT and *Tst*$^{-/-}$ compared to chow-fed controls (mean, WT: 18 ng/ml; *Tst*$^{-/-}$: 11.3 ng/ml). Overall plasma insulin levels during the GTT measured by area under the curve were increased by HFD in both WT and *Tst*$^{-/-}$ mice, although insulin was significantly lower in *Tst*$^{-/-}$ mice (Figure 3.8d). [Insulin ELISA was carried out by Rhona Aird, Molecular Metabolism Group].

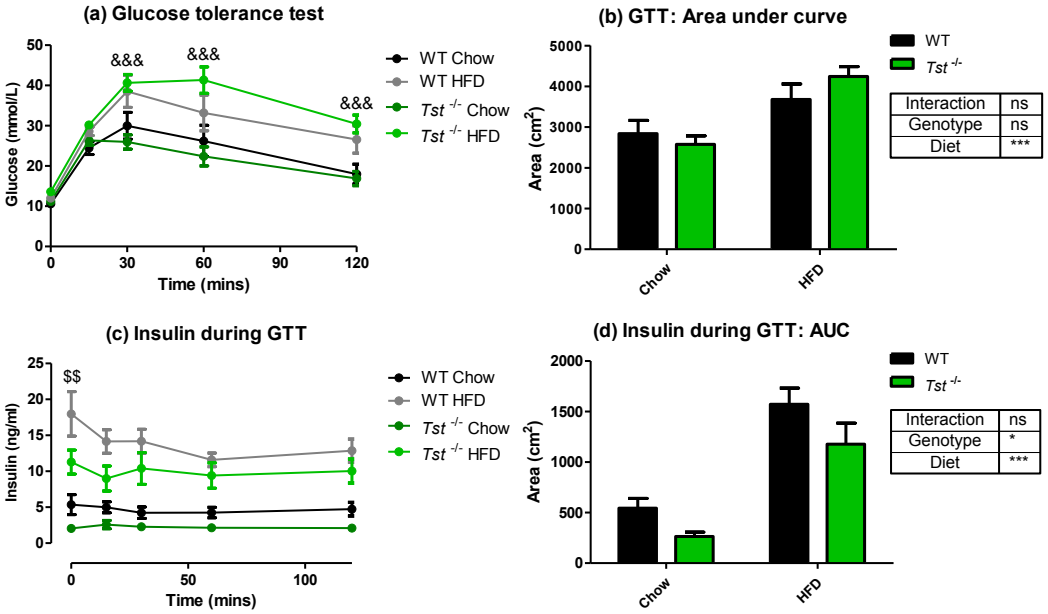

Figure 3.8: Plasma glucose and insulin levels of Tst$^{-/-}$ and WT mice on chow or HFD for 18 weeks after administration of a glucose bolus.

*(a) Plasma glucose levels during a glucose tolerance test (GTT); (b) area under the curve (AUC) of glucose levels during GTT; (c) plasma insulin levels during GTT; (d) AUC of insulin levels during GTT. Data are mean ± SEM, (a) and (c) analysed by 2-way repeated measures ANOVA with Bonferroni post-hoc test comparing each group at each timepoint: Tst$^{-/-}$ chow versus Tst$^{-/-}$ HFD: &&& P < 0.001; WT HFD vs. Tst$^{-/-}$ HFD: $$ P < 0.01; (b) and (d) analysed by 2-way ANOVA: * P < 0.05, *** P < 0.001, ns = not significant (n = 6-8). [Insulin ELISA was carried out by R. Aird, Molecular Metabolism Group].*

3.3.2.4 Insulin tolerance was impaired after 19 weeks of HFD in Tst$^{-/-}$ and WT mice.

An insulin tolerance test was carried out on WT and *Tst*$^{-/-}$ mice after 19 weeks of HFD to assess the impact of *Tst* gene knockout on the responsiveness of glucose levels to insulin. There were no significant differences between WT and *Tst*$^{-/-}$ mice. WT mice had significantly higher glucose levels on HFD compared to chow at only the 15-minute timepoint. *Tst*$^{-/-}$ mice on HFD diet had significantly higher glucose at all timepoints after insulin injection compared to chow-fed *Tst*$^{-/-}$ mice (Figure 3.9a). Overall plasma glucose levels during the ITT measured by area under the curve were increased on HFD in both WT and *Tst*$^{-/-}$ mice, but no significant difference was found between genotypes (Figure 3.9b).

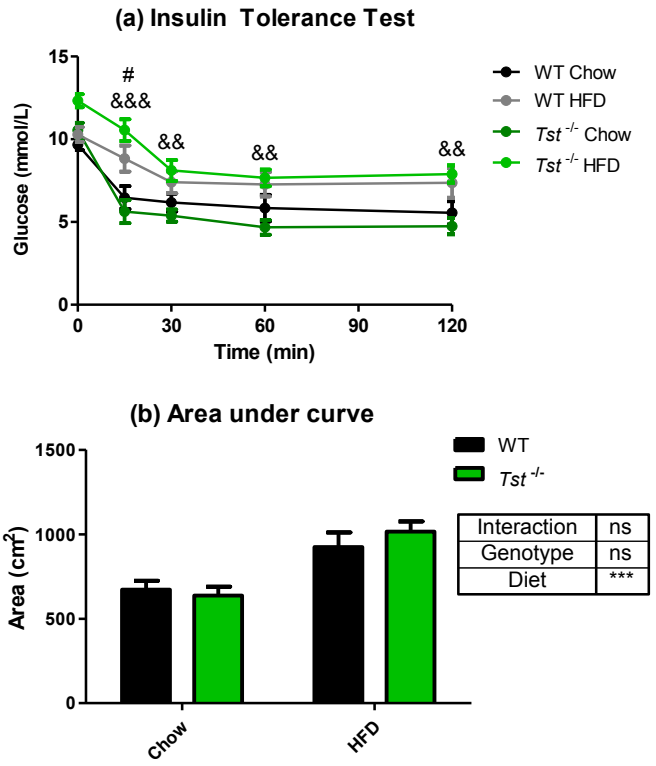

Figure 3.9: Plasma glucose levels of Tst$^{-/-}$ and WT mice on chow or HFD for 19 weeks after administration of an insulin bolus.

*(a) Plasma glucose levels during an insulin tolerance test (ITT); (b) area under the curve (AUC) of glucose levels during GTT. Data are mean ± SEM, (a) analysed by 2-way repeated measures ANOVA with Bonferroni post-hoc test comparing each group at each timepoint: WT chow versus WT HFD: # P < 0.05; Tst$^{-/-}$ chow versus Tst$^{-/-}$ HFD: && P < 0.01, &&& P < 0.001; (b) analysed by 2-way ANOVA: *** P < 0.001, ns = not significant; (n = 7-8).*

3.3.2.5 Plasma adiponectin was reduced in Tst$^{-/-}$ mice on chow diet, and in both Tst$^{-/-}$ and WT mice on HFD for 20 weeks.

Total and high molecular weight (HMW) adiponectin were measured in the plasma of WT and *Tst*$^{-/-}$ mice after 20 weeks of HFD by ELISA. Total and HMW adiponectin were significantly reduced by HFD in WT mice (Figure 3.10a and Figure 3.10b). However, *Tst*$^{-/-}$ mice had lower total and HMW adiponectin compared to WT mice on chow diet. HFD did not cause a further reduction in total or HMW adiponectin in *Tst*$^{-/-}$ mice. HMW as a percentage of total adiponectin showed a similar pattern (Figure 3.10c).

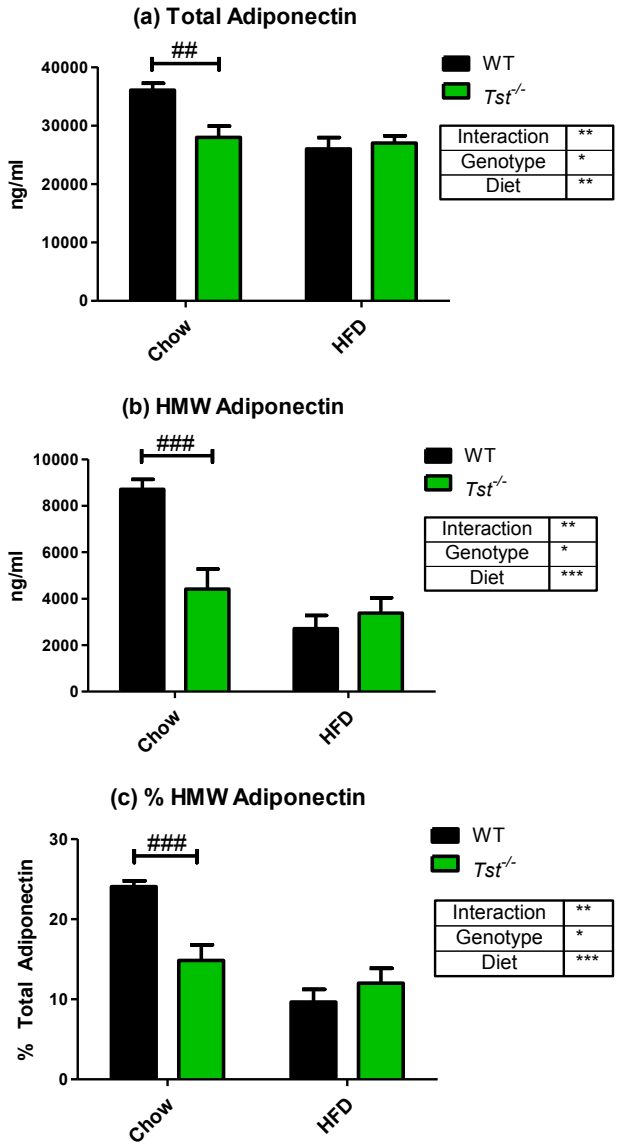

Figure 3.10: Plasma adiponectin levels in Tst$^{-/-}$ and WT mice on chow or HFD for 20 weeks.

*(a) Total adiponectin, (b) high molecular weight (HMW) adiponectin, and (c) HMW as a percentage of total adiponectin. Data are mean ± SEM, analysed by 2-way ANOVA: * P <0.05, ** P <0.01, *** P < 0.001, ns = not significant; with Bonferroni post-hoc test comparing between genotypes for each diet: ## P < 0.01, ### P < 0.001; (n=7-8).*

3.3.2.6 *Gene expression of adiponectin was unchanged in adipose tissue of Tst$^{-/-}$ mice versus WT mice on chow or HFD for 20 weeks.*

Gene expression of adiponectin (*Adipoq*) was measured in mesenteric adipose tissue of WT and *Tst*$^{-/-}$ mice after 20 weeks of HFD. There was no significant effect of *Tst* gene knockout or HFD on *Adipoq* expression in adipose tissue, however there was a trend for a significant reduction in *Tst*$^{-/-}$ mice (P = 0.0763) (Figure 3.11).

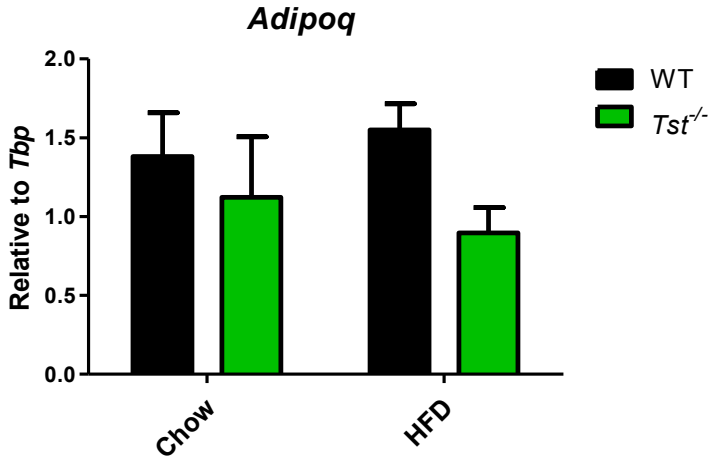

Figure 3.11: Gene expression of adiponectin in mesenteric white adipose tissue of Tst$^{-/-}$ and WT mice on chow or HFD for 20 weeks.

Data are mean ± SEM, analysed by 2-way ANOVA: not significant; (n=4-6).

3.3.2.7 Gene expression of some key antioxidant enzymes was reduced in adipose tissue of Tst$^{-/-}$ versus WT mice on HFD for 20 weeks.

The expression of mitochondrial and cytoplasmic antioxidant enzymes in mesenteric white adipose tissue from *Tst*$^{-/-}$ and WT mice fed HFD or chow for 20 weeks was measured. Expression of many of the nuclear-encoded mitochondrial antioxidant enzymes were reduced in *Tst*$^{-/-}$ mice, particularly when on HFD. Superoxide dismutase 2 (*Sod2*) and peroxiredoxin 3 (*Prx3*) expression was lower in adipose of *Tst*$^{-/-}$ mice. This was largely accounted for by a failure to increase *Sod2* and *Prx3* expression in response to HFD, as seen in the WT mice (Figure 3.12a and Figure 3.12b). Overall expression of glutathione peroxide 1 (*Gpx1*) and thioredoxin 2 (*Txn2*) was lower in *Tst*$^{-/-}$ mice compared to WT (Figure 3.12c and Figure 3.12d). Thioredoxin reductase 2 (*Txnrd2*) and glutathione peroxidase 4 (*Gpx4*) were unchanged by *Tst* gene knockout or HFD (Figure 3.12e and Figure 3.12f). Superoxide dismutase 1 (*Sod1*) was unchanged by *Tst* gene knockout or HFD (Figure 3.12g), however peroxiredoxin 1 (*Prx1*) showed reduced expression in adipose from *Tst*$^{-/-}$ mice, with significant difference observed on HFD by post-hoc comparison (Figure 3.12h).

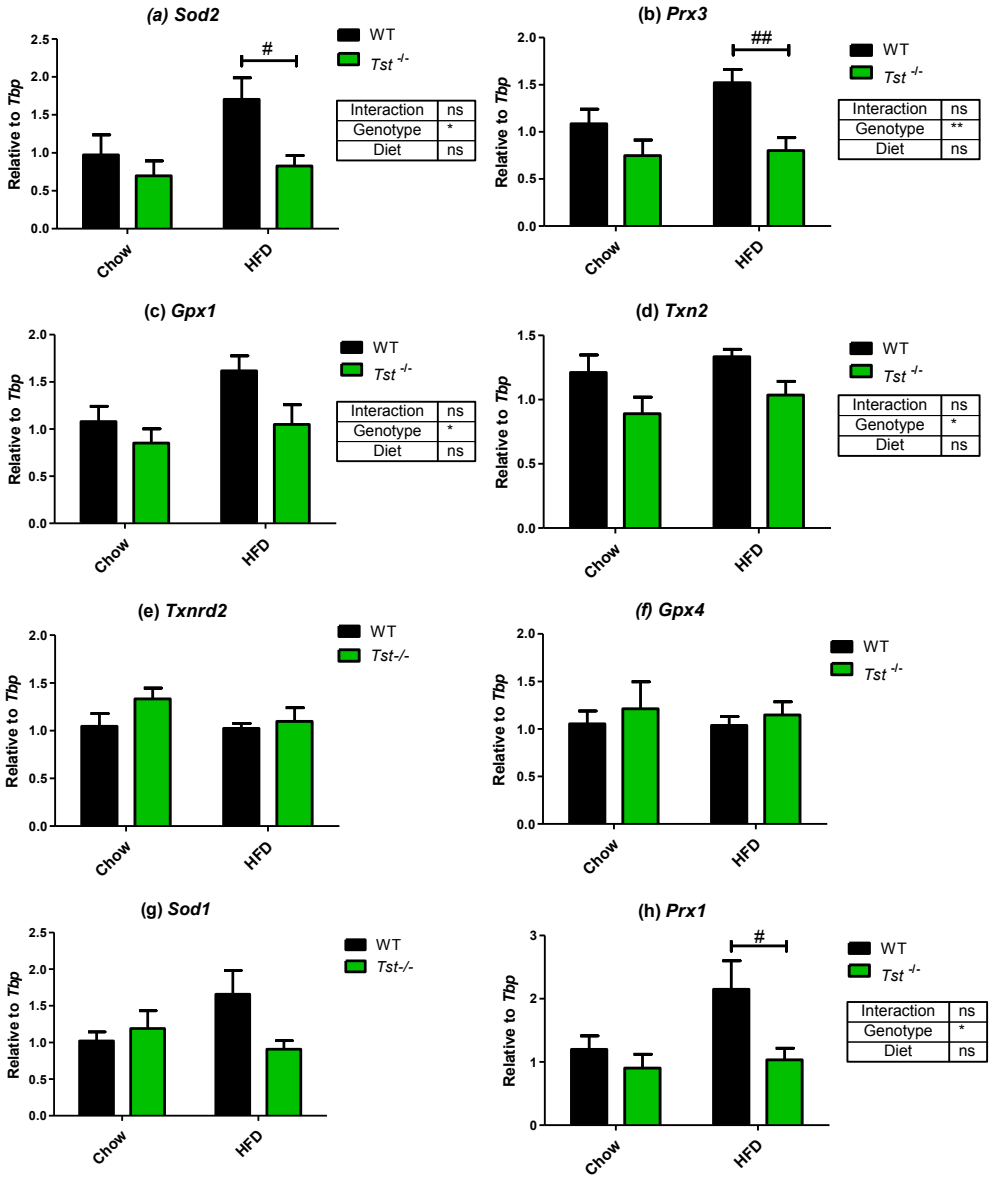

Figure 3.12: Gene expression of key antioxidant enzymes in mesenteric adipose tissue in Tst$^{-/-}$ and WT mice on chow or HFD for 20 weeks.

*(a) Superoxide dismutase 2 (Sod2), (b)peroxiredoxin 3 (Prx3), (c) glutathione peroxidase 1 (Gpx1), (d) thioredoxin 2 (Txn2), (e) thioredoxin reductase 2 (Txnrd2) and (f) glutathione peroxidase 4 (Gpx4), (g) superoxide dismutase 1 (Sod1), and (h) peroxiredoxin 1 (Prx1) mRNA abundance normalised to housekeeping gene Tbp. Data are mean ± SEM, analysed by 2-way ANOVA: * P <0.05, ** P < 0.01, ns = not significant; with Bonferroni post-hoc test comparing between genotypes for each diet: # P < 0.05, ## P < 0.01; (n=4-6).*

NRF2 is a transcription factor that regulates the expression of many antioxidants genes in response to oxidative stress (section 1.2.2.2 on page 23). To assess activation of NRF2-mediated transcription, the expression of two NRF2-target genes was measured. No difference was found in the expression of heme oxygenase 1 (*Hmox1*) or NAD(P)H quinone oxidoreductase 1 (*Nqo1*) in mesenteric adipose tissue of *Tst*$^{-/-}$ mice on chow or HFD (Figure 3.13).

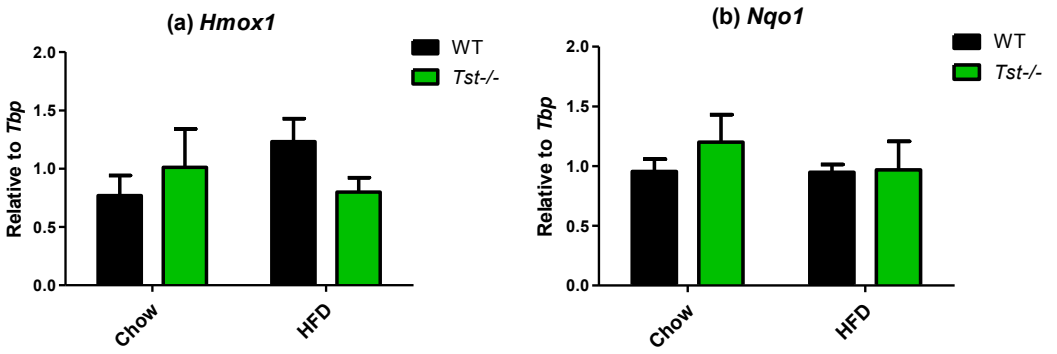

Figure 3.13: Gene expression of NRF2-responsive antioxidant enzymes in mesenteric adipose tissue in Tst$^{-/-}$ vs. WT mice on chow or HFD for 20 weeks.

(a) Heme oxygenase 1 (Hmox1) and (b) NAD(P)H:quinone acceptor oxidoreductase 1 (Nqo1) abundance normalised to housekeeping gene Tbp. Data are mean ± SEM, analysed by 2-way ANOVA: ns = not significant; (n=4-6).

3.3.2.8 *Carbonyl content of adipose tissue was unchanged in Tst$^{-/-}$ versus WT mice on chow or HFD for 20 weeks.*

Carbonylation of proteins is a marker of oxidative stress in adipose tissue of obese mice and humans. Protein lysate from mesenteric white adipose tissue was separated by SDS-PAGE, and an antibody against 4-hydroxynonenal (4-HNE) was used to visualise proteins with carbonyl adducts (Figure 3.14a). Carbonyl content was found to be unchanged in *Tst*$^{-/-}$ mice on chow and HFD (Figure 3.14b).

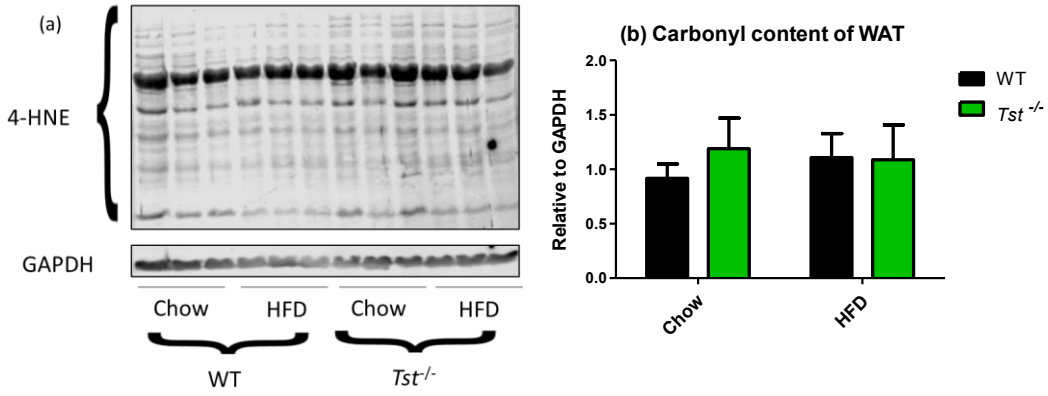

Figure 3.14: Carbonyl content of mesenteric adipose tissue of Tst$^{-/-}$ and WT mice on chow or HFD for 20 weeks.

(a) Representative images of protein lysates separated by SDS-PAGE and blotted with anti-4-HNE and anti-GAPDH antibodies; (b) quantification of intensity of all bands relative to GAPDH control. Data are mean ± SEM, analysed by 2-way ANOVA: not significant (n = 4-6).

3.3.2.9 Immune cell populations in stromal vascular fraction of adipose tissue were not different in Tst$^{-/-}$ versus WT mice on HFD for 20 weeks.

Macrophage number as a percentage of total hematopoietic cell population ($CD45^+$ population) was increased by HFD in both *Tst*$^{-/-}$ and WT mice (Figure 3.15a). However, on chow diet, *Tst*$^{-/-}$ mice had a lower percentage of macrophages than WTs, with post-hoc testing revealing significant reduction in *Tst*$^{-/-}$ mice compared to WT on chow diet (Figure 3.15a). The percentage of hematopoietic cells expressing the pro-inflammatory macrophage marker CD11c was increased by HFD in both *Tst*$^{-/-}$ and WT mice (Figure 3.15b). The percentage of eosinophils was significantly reduced by HFD in both genotypes (Figure 3.15c).

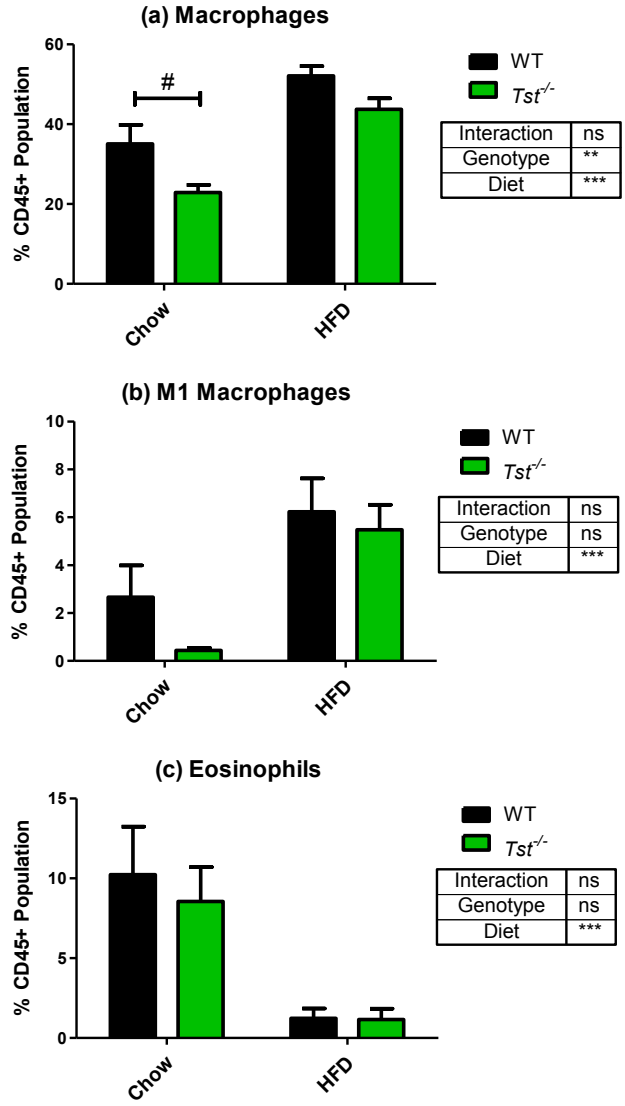

Figure 3.15: Immune cell populations in stromal vascular fraction (SVF) of epididymal adipose tissue in Tst$^{-/-}$ and WT mice on chow or HFD for 20 weeks.

*(a) Macrophages (F4/80$^+$ CD11b$^+$ Ly6C$^-$), (b) M1 macrophages (F4/80$^+$ CD11b$^+$ Ly6C$^-$ CD11c$^+$), and (c) eosinophils (SiglecF$^+$) measured in SVF of epididymal fat by flow cytometry. Results are expressed as percentage of hematopoietic population (CD45$^+$). Data are mean ± SEM, analysed by 2-way ANOVA: ** P > 0.01, *** P < 0.001, ns = not significant; with Bonferroni post-hoc test comparing between genotypes for each diet: # P < 0.05; (n = 6).*

3.3.2.10 Gene expression of pro-inflammatory adipokines was not different in adipose tissue of Tst$^{-/-}$ versus WT mice on HFD for 20 weeks.

Gene expression of pro-inflammatory adipokines was measured in mesenteric fat to assess the impact of *Tst* gene deficiency on adipose tissue inflammatory markers with HFD. Plasminogen activator inhibitor 1 (*Pai1*) was greatly increased by HFD in both WT and *Tst*$^{-/-}$ mice (Figure 3.16a). Monocyte chemotactic protein 1 (*Mcp1*) was also increased by HFD in both genotypes (Figure 3.16b). Tumour necrosis factor α (*Tnfα*) was not significantly different with *Tst* gene deficiency or HFD (Figure 3.16c).

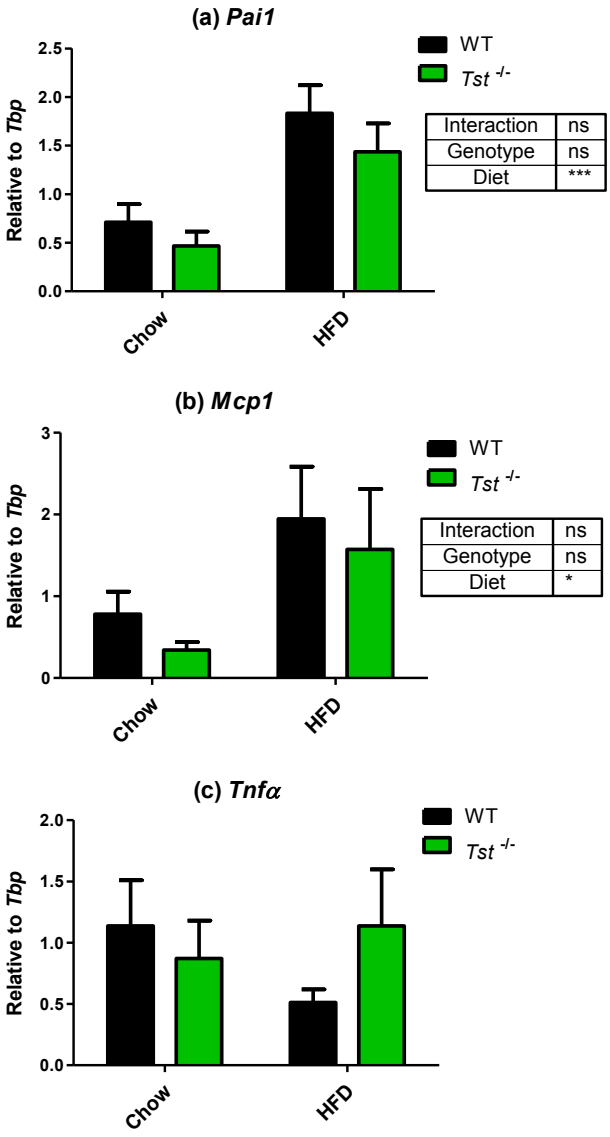

Figure 3.16: Gene expression of pro-inflammatory adipokines in mesenteric adipose tissue of Tst$^{-/-}$ and WT mice on chow or HFD for 20 weeks.

*(a) Plasminogen activator inhibitor 1 (Pai1), (b) monocyte chemotactic protein 1 (Mcp1), and (c) tumour necrosis factor α (Tnfα) abundance normalised to housekeeping gene Tbp. Data are mean ± SEM, analysed by 2-way ANOVA: * P < 0.05, *** P < 0.001, ns = not significant; (n = 4-6).*

3.3.2.11 *Gene expression of an endoplasmic reticulum stress marker was increased in adipose tissue of Tst$^{-/-}$ versus WT mice on chow diet, but unchanged on HFD for 20 weeks.*

To assess activation of the unfolded protein response, the expression of two key genes involved in this process was measured in mesenteric fat of *Tst*$^{-/-}$ after 20 weeks of HFD. Expression of activating transcription factor 4 (*Atf4*) was unchanged by *Tst* gene knockout or HFD (Figure 3.17a). C/EBP-Homologous Protein (*Chop*) was increased in *Tst*$^{-/-}$ mice, with a greater increase observed on chow diet only (Figure 3.17b).

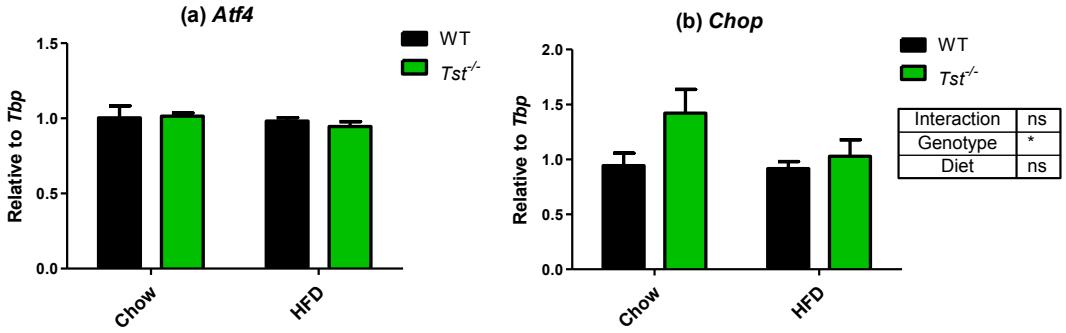

Figure 3.17: Gene expression of endoplasmic reticulum stress markers in mesenteric adipose tissue of Tst$^{-/-}$ and WT mice on chow or HFD for 20 weeks.

*(a) Activating transcription factor 4 (Atf4) and (b) C/EBP-Homologous Protein (Chop) mRNA abundance normalised to housekeeping gene Tbp. Data are mean ± SEM, analysed by 2-way ANOVA: * P < 0.05, ns = not significant; (n=4-6).*

3.3.2.12 *Gene expression of thiosulfate sulfurtransferase was reduced in adipose tissue of WT mice on HFD for 6 weeks, and chow and HFD for 20 weeks.*

Tst mRNA was not detected in $Tst^{-/-}$ mice. After 6 weeks of HFD, *Tst* mRNA levels were greatly reduced in WT mice (Figure 3.18a). However, at the end of the 20-week HFD challenge, *Tst* mRNA levels were unchanged between chow and HFD mice (Figure 3.18b). This was due to already low *Tst* mRNA levels in adipose of WT mice on chow diet for 20 weeks.

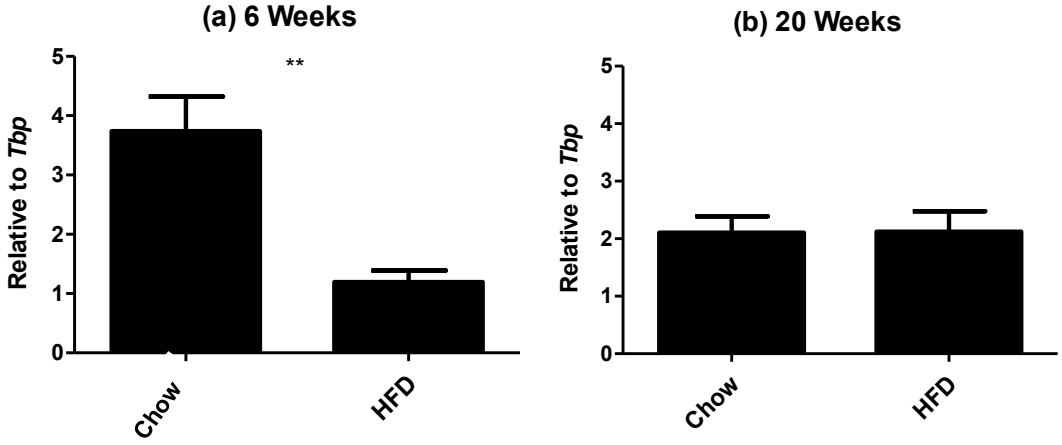

Figure 3.18: Comparison of Tst gene expression in mesenteric adipose tissue in WT mice after (a) 6 weeks and (b) 20 weeks of chow or HFD.

*Tst mRNA abundance normalised to housekeeping gene Tbp. Tst gene expression was undetectable in RNA from $Tst^{-/-}$ mesenteric adipose tissue. Data are mean ± SEM, analysed by Student's t-test: ** P < 0.01; (6 weeks, n=4/5; 20 weeks, (n=4-6).*

3.3.2.13 Gene expression of sulfide production enzymes were reduced in adipose tissue of in Tst$^{-/-}$ versus WT mice on chow or HFD for 20 weeks.

To assess the effect of *Tst* gene knockout and HFD on hydrogen sulfide production, gene expression of the three enzymes responsible for producing sulfide (section 1.3.3.1 on page 48) were measured in mesenteric white adipose tissue. Cystathionine γ lyase (*Cse*) was reduced in *Tst*$^{-/-}$ mice on chow diet only, with no significant difference observed between high fat-fed groups (Figure 3.19a). Cystathionine β synthase (*Cbs*) was reduced in both WT and *Tst*$^{-/-}$ mice fed HFD, however no difference was found between genotypes (Figure 3.19b). Mercaptopyruvate sulfurtransferase (*Mpst*) was reduced in adipose of *Tst*$^{-/-}$ compared to WT mice, however no effect of diet was observed (Figure 3.19c).

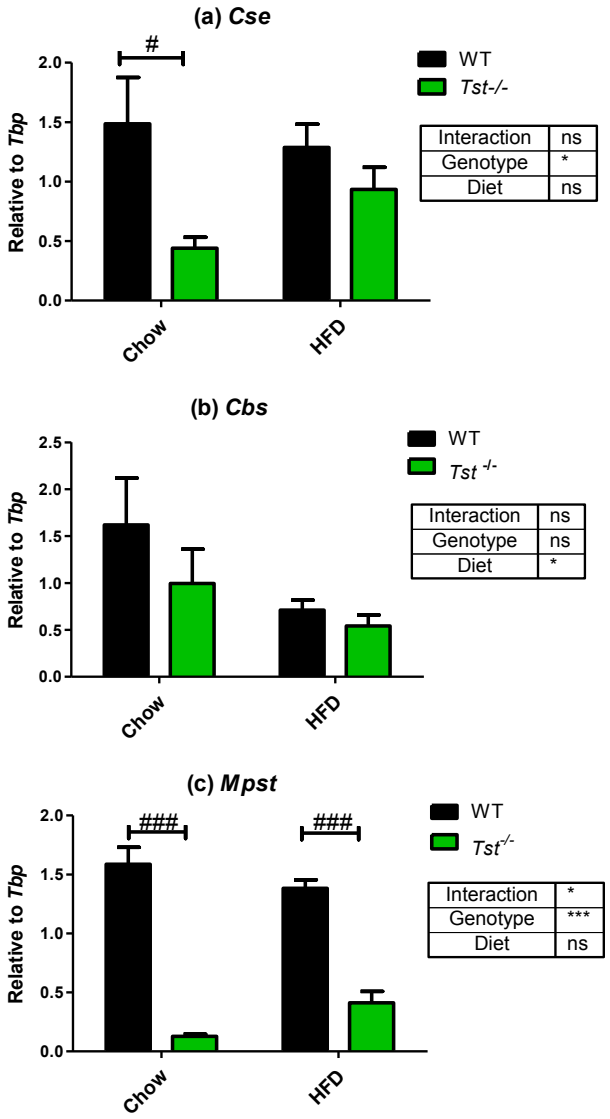

Figure 3.19: Gene expression of H_2S-producing enzymes in mesenteric adipose tissue of $Tst^{-/-}$ and WT mice on chow or HFD for 20 weeks.

*(a) Cystathionine γ lyase (Cse) (b) cystathionine β synthase(Cbs) and (c) mercaptopyruvate sulfurtransferase (Mpst) abundance normalised to housekeeping gene Tbp. Data are mean ± SEM, analysed by 2-way ANOVA: * P <0.05, *** P < 0.001, ns = not significant; with Bonferroni post-hoc test comparing between genotypes for each diet: # P < 0.05, ### P < 0.001; (n=4-6).*

3.3.2.14 *Gene expression of sulfide oxidation enzymes was unchanged in adipose tissue of Tst$^{-/-}$ versus WT mice on chow or HFD for 20 weeks.*

The gene expression of enzymes involved in the oxidation of sulfide was measured. Sulfide-quinone oxidoreductase (*Sqrdl*) and ethylmalonic encephalopathy protein 1 (*Ethe1*) were unchanged by *Tst* gene deficiency or HFD (Figure 3.20).

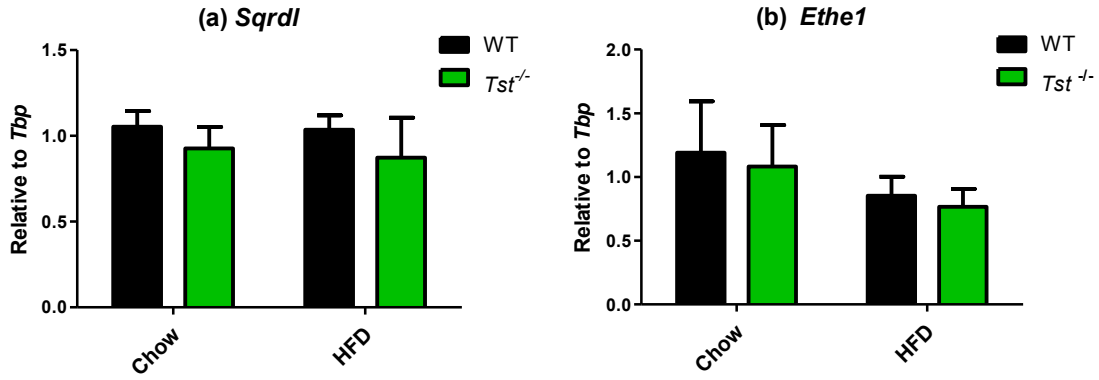

Figure 3.20: Gene expression of sulfide oxidation genes in mesenteric adipose tissue of Tst$^{-/-}$ and WT mice on chow or HFD for 20 weeks.

(a) Sulfide:quinone oxidoreductase (Sqrdl) and (b) ethylmalonic encephalopathy protein 1 (Ethe1) abundance normalised to housekeeping gene Tbp. Data are mean ± SEM, analysed by 2-way ANOVA: not significant; (n=4-6).

3.4 DISCUSSION

Thiosulfate sulfurtransferase, when over-expressed in adipose tissue, was previously found to be protective against metabolic impairment due to exposure to a high fat diet (Morton *et al.* 2016). For this chapter, *Tst* knockout mice were used to test the hypothesis that the absence of this gene would lead to increased adipose oxidative stress and inflammation, and subsequently, a worse metabolic profile after exposure to high fat diet. The findings show that *Tst*$^{-/-}$ mice are potentially more prone to metabolic impairment on high fat diet due to a failure to induce adipose antioxidant genes in response to high fat diet and reduced high molecular weight adiponectin in plasma. However, there was no clear evidence of functional oxidative damage, perhaps due to limitations in the carbonyl measurement method, and no clear evidence for the expected increase in macrophage infiltration and inflammatory cytokine contribution to this phenotype. Indeed, in chow fed *Tst*$^{-/-}$ mice, macrophage infiltration was lower, consistent with reduced fat mass. It is also likely that other factors and organs that are affected by *Tst* gene knockout are important for the overall phenotypic outcome of exposure to high fat diet. Some surprising differences uncovered in older chow-fed *Tst*$^{-/-}$ mice highlighted a previously unobserved interaction of *Tst* gene knockout and age-related fat accumulation which remains to be investigated in future studies.

3.4.1 Metabolic impairment of *Tst*$^{-/-}$ mice on HFD.

The data presented here confirmed previous findings that *Tst*$^{-/-}$ mice are metabolically impaired after exposure to HFD. *Tst*$^{-/-}$ mice on high fat diet for 20 weeks gained a comparable amount of weight to WT mice. This comparable weight gain on HFD was observed in previous experiments with these mice (Morton *et al.* 2016), and was likely due to increased fat mass, as all adipose depots measured increased with HFD in both genotypes. High fat feeding for 6 weeks caused a reduction in *Tst* gene expression in adipose of WT mice, and by 20 weeks, *Tst* expression was reduced in both chow-fed and high fat-fed WT mice. This reduction in *Tst* in adipose may explain the convergence of body weight and fat accumulation in WT and *Tst*$^{-/-}$ groups fed HFD, as the impact of local *Tst* expression was reduced in adipose of WT mice.

A well-characterised effect of high fat feeding on 6J mice is a reduction in plasma concentration of the insulin-sensitising hormone adiponectin due to adipose tissue dysfunction (Furukawa *et al.* 2004; Hosogai *et al.* 2007). While WT mice on HFD showed this expected reduction in total adiponectin and the most biologically active high-molecular weight (HMW) form, adiponectin levels of *Tst*$^{-/-}$ mice were reduced on chow diet, but were resistant to further reduction on HFD. *Tst*$^{-/-}$ mice on chow diet weighed less and had less fat mass than their WT counterparts, and therefore, higher adiponectin levels would be expected (Pannacciulli *et al.* 2003). This unexpected reduction in plasma adiponectin in chow-fed *Tst*$^{-/-}$ mice could be due to unfolded protein response (UPR) activation or oxidative stress. The UPR activation marker C/EBP homologous protein (*Chop*) is implicated in reducing adiponectin expression in adipose tissue (Hosogai *et al.* 2007), and this gene was upregulated in mesenteric adipose tissue of *Tst*$^{-/-}$ mice on chow diet. While this does not confirm full activation of the UPR, increased *Chop* expression could contribute to reduced levels of circulating adiponectin in chow-fed *Tst*$^{-/-}$ mice. Adiponectin expression in adipose tissue is also reduced by excess H_2O_2 and oxidative stress (Furukawa *et al.* 2004), therefore, in adipose tissue from *Tst*$^{-/-}$ mice, lower expression of key antioxidant enzymes such as *Sod2*, *Prx3*, *Txn2* and *Gpx1* could impact adiponectin synthesis and secretion. While adiponectin gene expression in mesenteric adipose tissue was unchanged, there was a trend for lower expression of this gene in adipose of *Tst*$^{-/-}$ mice, and it is possible that its expression in other adipose depots is also impacted by *Tst* gene knockout. As adiponectin is an insulin-sensitising hormone, a reduction in plasma concentration usually leads to reduced insulin sensitivity (Stefan *et al.* 2002), however this was not the case in chow-fed *Tst*$^{-/-}$ mice, which cleared glucose in a manner comparable to WT mice during an insulin tolerance test (ITT).

Despite a similar amount of weight gain, *Tst*$^{-/-}$ mice on HFD for 20 weeks were more susceptible than WT mice to metabolic impairment. A glucose tolerance test (GTT) did not find significant differences between WT and *Tst*$^{-/-}$ mice on HFD. It was revealed however that *Tst*$^{-/-}$ mice had impaired glucose clearance after 20 weeks of HFD compared to chow diet. This impairment in glucose clearance could be due to increased insulin resistance, as the results of the ITT suggest that HFD impairs the

ability of *Tst*$^{-/-}$ mice to clear glucose, however not to a significantly greater degree than in WT mice. A more likely factor affecting glucose clearance may be insulin secretion during the GTT, which was significantly lower in *Tst*$^{-/-}$ mice on HFD compared to WT mice. This failure to increase insulin secretion to compensate for increased plasma glucose indicates progression to diabetes in *Tst*$^{-/-}$ mice on HFD. WT mice on HFD had significantly higher plasma insulin during the GTT than HFD-fed *Tst*$^{-/-}$ mice, indicating a more robust β-cell response to increased glucose than *Tst*$^{-/-}$ mice. Despite HFD-induced insulin resistance in WT mice as observed by ITT, there was no difference in glucose clearance between chow- and HFD-fed WT mice, which likely to be due to compensation by higher insulin secretion. A confounding factor in the metabolic assessment of WT mice was the extensive weight gain in control-fed animals, which may have contributed to glucose intolerance in these mice. Increased weight gain and glucose intolerance without obesogenic diet has been recently observed in C57BL/6N (6N) mice, which were found to gain more weight and have increased plasma glucose during a GTT than 6J mice on a low-fat diet for 18 weeks, (Hull *et al.* 2017). Based on this finding, *Tst*$^{-/-}$ mice were backcrossed to 6J for future experiments to limit any effect of a mixed background containing an unknown and variable amount of genetic information from the 6N sub-strain. Despite the potential cofounding factor of glucose intolerance in control-fed WT mice, *Tst*$^{-/-}$ mice showed metabolic impairment during the GTT by failing to induce insulin secretion. However, to confirm that *Tst*$^{-/-}$ mice were more susceptible to metabolic impairment than WT mice, this experiment must be repeated using a specific low-fat diet to reduce age-related fat accumulation and metabolic impairment in control-fed WT mice.

I have confirmed that *Tst*$^{-/-}$ mice are susceptible to metabolic impairment on HFD. *Tst*$^{-/-}$ mice gained a similar amount of weight and fat mass to WT mice after 20 weeks of HFD, and their ability to clear glucose, as measured by glucose and insulin tolerance tests was impaired by HFD. This agrees with our previously reported findings of glucose intolerance in *Tst*$^{-/-}$ mice after 6 weeks of HFD (Morton *et al.* 2016). An investigation of adipose tissue dysfunction of *Tst*$^{-/-}$ mice was carried out to uncover the physiological basis for the metabolic phenotype of these mice on HFD.

3.4.2 Adipose tissue dysfunction of *Tst*$^{-/-}$ mice on HFD.

An investigation of adipose tissue dysfunction was carried out to uncover the physiological basis of the impaired metabolic phenotype of *Tst*$^{-/-}$ mice on HFD. It was hypothesised that *Tst*$^{-/-}$ mice were more susceptible to oxidative stress and inflammation in adipose tissue. As well as the reduction in plasma adiponectin discussed above, *Tst*$^{-/-}$ mice had lower expression of key antioxidant enzymes in adipose tissue, especially on HFD, without overt changes in a marker of oxidative stress, immune cell infiltration or expression of proinflammatory adipokines.

3.4.2.1 Oxidative stress

Expression of key antioxidant genes in adipose tissue can be altered by high fat feeding (Furukawa *et al.* 2004; Long *et al.* 2013), and overexpression or knockout of some of these key genes have been associated with altered susceptibility to obesity and insulin resistance in mice (Loh *et al.* 2009; Han *et al.* 2016). Key antioxidant enzymes, *Sod2*, *Prx3*, *Txn2*, *Gpx1* and *Prx1*, were lower in mesenteric adipose of *Tst*$^{-/-}$ mice, due to an increase in their expression in adipose of WT mice on HFD that was not matched in *Tst*$^{-/-}$ mice. Some of these results are unexpected as our lab has previously found greatly reduced SOD2 and PRX3 protein in adipose of WT mice after 6 weeks of HFD (Morton *et al.* 2016). As well as this, SOD activity is reduced in adipose of WT mice fed a HFD for 9 weeks (Furukawa *et al.* 2004) and PRX3 protein level is reduced in adipose tissue of obese humans and obese *db/db* mice (Huh *et al.* 2012; Long *et al.* 2013). This could reflect a difference in HFD-mediated induction of antioxidant gene expression between adipose depots, with mesenteric fat used in the current work, but epididymal or subcutaneous used in previous studies. Also, the duration of exposure to HFD could impact these results, with later compensatory antioxidant programmes being switched on in WT mice after 20 weeks of HFD in the current investigation to attempt to limit severe oxidative stress due to hypertrophy. As ROS are essential for adipogenesis (Tormos, Anso, Hamanaka, *et al.* 2011), antioxidant programmes may be not be induced at early stages of obesity to allow for expansion of the tissue by hyperplasia. The lower expression of these antioxidant enzymes in adipose of *Tst*$^{-/-}$ compared to WT mice after 20 weeks of HFD indicates that these mice may have

reduced antioxidant capacity in adipose tissue, and thus be more susceptible to oxidative damage. However, another interpretation of these results could be that antioxidant gene expression fails to increase after HFD, as seen in WT mice, because adipose from *Tst*$^{-/-}$ mice is under less oxidative pressure due to other phenotypic alterations such as an increased concentration of H_2S. This could potentially indicate a failure of the mitohormetic response, in which an oxidative trigger initiates gene expression of stress mechanisms such as antioxidant enzymes, and ultimate strengths the cells ability to deal with further stressors (Ristow and Schmeisser 2014). Future work using adipose-specific *Tst* knockout mice will help to elucidate a full understanding of the cause and consequences of reduced expression of these antioxidant genes.

Expression of a cytosolic and mitochondrial antioxidant enzyme, glutathione peroxidase 1 (*Gpx1*), was also measured in the adipose of *Tst*$^{-/-}$ and WT mice after exposure to HFD. This enzymes reduces H_2O_2 using glutathione as a reducing agent (Brigelius-Flohé and Maiorino 2013), and *Gpx1* knockout protects against diet-induced insulin resistance due to lowered quenching of insulin-stimulated H_2O_2 signalling (Loh *et al.* 2009). Expression of *Gpx1* increased in adipose tissue of WT mice after 20 weeks of HFD, as has been found to occur in 6J mice after 6 weeks of HFD (Matsuzawa-Nagata *et al.* 2008), but was reduced in adipose of *Tst*$^{-/-}$ mice, and failed to increase after 20 weeks of HFD, as in WT mice. Consequently, reduced *Gpx1* expression in adipose tissue of *Tst*$^{-/-}$ mice may be protective against local insulin resistance, and indicates that local adipose insulin resistance may not be the cause of the overall reduction in insulin sensitivity observed during the ITT in *Tst*$^{-/-}$ mice on HFD.

Protein carbonylation is a marker of oxidative stress in adipose tissue caused by addition of reactive lipid aldehydes such as 4-hydroxy-2-nonenal (4-HNE) to protein side chains (Ruskovska and Bernlohr 2013). Carbonylation is increased in adipose tissue of obese humans (Grimsrud *et al.* 2007), and in epididymal, but not subcutaneous adipose of high fat fed 6J mice (Long *et al.* 2013). GPX4 protects against damaging accumulation of reactive lipid aldehyde products including 4-HNE (Katunga *et al.* 2015). *Gpx4* expression was unchanged in adipose of both *Tst*$^{-/-}$ and

WT mice, and there was no difference in carbonylation in mesenteric adipose from *Tst*$^{-/-}$ or WT mice on HFD. This could be due to limitations of the method or the adipose depot in which this marker was measured. Future assessment of oxidative stress will be done using the Oxyblot protein oxidation detection kit which may be more efficient at measuring carbonylation than the 4-HNE antibody used here.

A potential confounding factor in this study is H_2S which can have antioxidant effects at a transcriptional, post-transcriptional and molecular level. *Tst*$^{-/-}$ mice have increased plasma sulfide levels (Morton *et al.* 2016), which may influence adipose tissue oxidative stress through activation of NRF2-mediated transcription (Yang *et al.* 2013), by direct scavenging of 4-HNE (Schreier *et al.* 2010), or through modulating SOD activity or protein (Sun *et al.* 2012). Expression of two NRF2 target genes, *Hmox1* and *Nqo1*, was unchanged in adipose of *Tst*$^{-/-}$ mice, indicating that the increased ambient sulfide concentration did not cause an overt activation of NRF2-mediated transcription in these mice. As no difference was found in carbonyl content between these groups of mice, the increased sulfide levels in *Tst*$^{-/-}$ mice do not appear to have lead to scavenging of 4-HNE, however this must be confirmed with a more effective measurement of carbonylation. H_2S has also been shown to increase expression of SOD2 protein in cardiomyocytes during ischaemia/reperfusion (Sun *et al.* 2012). As discussed previously, *Sod2* mRNA expression was reduced in adipose of *Tst*$^{-/-}$ mice, and while not confirmed at the protein level, this indicates that in this context H_2S does not lead to a transcriptional increase in this antioxidant enzyme. In previous work from our lab, SOD2 protein was increased in adipose of mice with adipose-specific overexpression of *Tst* compared to WT mice on chow diet (Morton *et al.* 2016). Therefore, the reduction in *Sod2* expression in *Tst*$^{-/-}$ mice found here could be a reciprocal phenotype, and further investigation will be required to understand this intriguing link between *Tst* and this major mitochondrial antioxidant enzyme.

It was hypothesised that the metabolic impairment of *Tst*$^{-/-}$ mice was due to increased susceptibility to HFD-induced oxidative stress in adipose tissue. I have confirmed that adipose tissue of *Tst*$^{-/-}$ mice has reduced expression of key antioxidant enzymes potentially causing an increased susceptibility to oxidative damage. No increase was found in carbonylation, which may be due to limitations of the method,

and so the full impact of *Tst* knockout on adipose oxidative stress cannot be confirmed. To address this question, it was decided to assess the *in vitro* response of primary adipocytes lacking or overexpressing TST to an oxidative challenge; work that will be described in Chapter 5.

3.4.2.2 Inflammation

Infiltration of pro-inflammatory macrophages is a key feature of dysfunctional adipose tissue and contributes to insulin resistance (Nguyen *et al.* 2007; Patsouris *et al.* 2008). As well as macrophages, other myeloid cell populations are also altered by HFD, with eosinophils number decreasing after several weeks of HFD (Wu *et al.* 2011). After 6 weeks of HFD, total macrophage content was unchanged in both $Tst^{-/-}$ and WT mice. M1 macrophages, as characterised by expression of the cell surface marker CD11c were increased in both genotypes, indicating a normal response to HFD. However, as no increase in total macrophage content was found, and there was no effect of HFD on eosinophil count, it was concluded that 6 weeks of HFD was not long enough to induce adipose tissue inflammation in this model. Therefore, it was decided to repeat the experiment with a longer duration of high fat feeding to ensure adipose tissue dysfunction in the form of inflammation developed.

After 20 weeks of high fat feeding, $Tst^{-/-}$ mice exhibited features of adipose tissue inflammation, however inflammatory markers were not different compared to WT mice. Immune cell populations were largely unchanged between $Tst^{-/-}$ and WT mice, in particular after HFD. This was unexpected given that $Tst^{-/-}$ mice exhibit an impaired metabolic phenotype, however the increased ambient sulfide levels in these mice (Morton *et al.* 2016) could be exerting anti-inflammatory effects on this tissue, such as suppressing macrophage activation (Zhang, Guo, Wu, *et al.* 2012). H_2S is also known to suppress leukocyte infiltration, and while $Tst^{-/-}$ mice do not have reduced macrophage content, it is possible that this marker of inflammation is comparable to WT, despite increased metabolic impairment, because of the increased sulfide levels in $Tst^{-/-}$ mice (Pan *et al.* 2011). It was hypothesised that $Tst^{-/-}$ mice would be predisposed to increased adipose tissue inflammation leading to metabolic impairment. The evidence presented here shows no difference in adipose tissue

immune cell infiltration in *Tst*$^{-/-}$ mice on HFD, and a similar induction of pro-inflammatory adipokine expression. Therefore, it is unlikely that *Tst* knockout leads to increased inflammation in adipose tissue, but future work with mice lacking *Tst* in adipose only will help to confirm this conclusion.

Investigation of markers of adipose dysfunction in *Tst*$^{-/-}$ mice after high fat feeding found no change in a functional oxidative stress marker or activation of the UPR, as well as unchanged inflammatory responses compared to WT mice. However, some key aspects of adipose tissue function appear to be impaired, including induction of antioxidant gene expression and adiponectin release, and these may contribute to the increased susceptibility to metabolic impairment observed in *Tst*$^{-/-}$ mice after high fat feeding. However, it is likely that the effects of *Tst* gene knockout on tissues other than adipose also contribute to the metabolic impairment observed in these mice on HFD, and whole-body elevated sulfide may also influence adipose tissue dysfunction. Therefore, full interpretation of the contribution of *Tst* in adipose tissue will need further investigation in adipose tissue-specific *Tst* knockout mice, which will help to minimise the contributions of these non-adipose factors.

3.4.3 Impact of increased sulfide on metabolic impairment of *Tst*$^{-/-}$ mice.

As *Tst*$^{-/-}$ mice have a global knockout of the gene and increased plasma sulfide levels, metabolically important organs other than adipose tissue may also influence the phenotype (Morton *et al.* 2016). Work was carried out on these mice by M. Gibbins to characterise the effect of *Tst* knockout on liver function. Evidence was found of increased gluconeogenesis in *Tst*$^{-/-}$ mice, as they produced more glucose in response to a pyruvate bolus after fasting and had increased activity of phosphoenolpyruvate carboxykinase (PEPCK), a key enzyme in the pathway of glucose production (Gibbins, manuscript in preparation). This increase in gluconeogenesis could contribute to the increase in plasma glucose observed in HFD-fed *Tst*$^{-/-}$ mice during the GTT, and may be a result of increased sulfide, which is known to increase PEPCK activity and gluconeogenesis in liver (Zhang *et al.* 2013). Increased sulfide levels may also be responsible for the reduction in plasma insulin in *Tst*$^{-/-}$ mice as observed prior to and

during the GTT, as sulfide is known to inhibit insulin secretion in pancreatic β-cells through activation of K_{ATP} channels and inhibition of calcium channels (Yang, Yang, *et al.* 2005; Tang *et al.* 2013). Therefore, increased plasma sulfide in *Tst*$^{-/-}$ mice may influence the metabolic phenotype beyond the expected detrimental impact of *Tst* knockout in adipose tissue.

3.4.4 Reduced fat mass in *Tst*$^{-/-}$ mice on chow diet.

Some surprising differences were uncovered between chow-fed *Tst*$^{-/-}$ and WT mice that may highlight a previously unobserved effect of *Tst* gene knockout on adipose tissue which may influence susceptibility to metabolic impairment by a mechanism independent of, or in addition to, oxidative stress.

Chow-fed *Tst*$^{-/-}$ mice in the 6-week group weighed less than WT mice, with a similar but non-significant difference observed at 20 weeks. In the 20-week group, all adipose depots measured were smaller in chow-fed *Tst*$^{-/-}$ mice compared to WTs. This finding of reduced body and adipose tissue weight in older *Tst*$^{-/-}$ mice was confirmed in an extra cohort of mice maintained on chow diet until 5 months of age (see appendix, Figure 7.1 and Figure 7.2 on pages 211 and 212) which found them to be significantly lighter and have less white adipose tissue than similarly-aged WT controls. There were no differences in body weight at the start of the feeding regimes, indicating that *Tst* knockout may impact weight gain and fat accumulation with increasing age, an effect that had not previously been observed. It was not possible to measure fat mass longitudinally *in vivo* at the time of these experiments, however a Bruker Minispec LF50 whole body composition analyser will be used on future cohorts of *Tst*$^{-/-}$ mice to investigate the age at which this divergence in fat mass begins.

This reduction in fat mass in older *Tst*$^{-/-}$ mice could be due to the impact of altered sulfide levels on lipid accumulation. We have previously found that SVFs from *Tst*$^{-/-}$ mice accumulate more lipid than WT SVFs when differentiated to adipocytes *in vitro* (Morton *et al.* 2016), and so this finding of reduced fat mass *in vivo* in older mice indicates that *Tst* gene knockout has a more complex effect on fat accumulation than previously thought. The previous finding of increased lipid accumulation in SVFs from *Tst*$^{-/-}$ mice could be due to increased H_2S levels due to impaired sulfide oxidation,

as exposure of 3T3-L1 adipocytes to exogenous H_2S increases activity and expression of PPARγ, and encourages glucose uptake and lipid storage (Cai *et al.* 2016b). However, the current *in vivo* finding in chow-fed *Tst*$^{-/-}$ mice contradicts this evidence, as *Tst*$^{-/-}$ mice have increased plasma sulfide (Morton *et al.* 2016), but reduced fat mass, as well as a trend for reduced SVF expression of *Pparg* (Morton *et al.* 2016). Previous *in vitro* investigation of basal and insulin-stimulated lipogenesis found that both processes were reduced in primary adipocytes from *Tst*$^{-/-}$ mice (Morton *et al.* 2016), which may account for the reduced fat mass in these mice on chow diet. This indicates that adipose from *Tst*$^{-/-}$ mice does not respond as expected to the increased plasma sulfide concentration, and instead may be resistant to lipid accumulation due to downregulation of *Cse* and *Mpst*, and a subsequent reduction in local H_2S production. Pharmacological inhibition of CSE reduced fat mass in mice fed a high fat diet for 4 weeks (Cai *et al.* 2016b). Therefore, a reduction in local H_2S production due to reduced *Cse* expression in *Tst*$^{-/-}$ mice on chow diet and reduced *Mpst* on both chow and HFD may reduce lipid accumulation in adipocytes leading to the overall reduction in fat mass observed in these mice on chow diet. *Cse* expression was not significantly different between *Tst*$^{-/-}$ and WT mice after 20 weeks of HFD, which may explain the lack of difference in fat accumulation between the two genotypes on HFD. Future work to assess the impact of *Tst* knockout on sulfide production and disposal in isolated adipocytes will shed light on the local sulfide environment in adipose tissue of *Tst*$^{-/-}$ mice and allow for a more defined hypothesis on the role of local sulfide signalling in lipid accumulation in adipose tissue of chow-fed mice. Mice lacking the *Tst* gene in adipose tissue only will soon be available to investigate whether this reduced fat mass in chow-fed knockout mice is due to local effects of *Tst* deficiency or a result of increased systemic sulfide.

The reduction in fat mass in *Tst*$^{-/-}$ mice on chow diet may be unrelated to the effects of H_2S on lipid accumulation, and instead be an outcome of increased activation of the unfolded protein response (UPR). *Tst*$^{-/-}$ mice on chow diet had increased expression of C/EBP homologous protein (*Chop*) in mesenteric adipose tissue, although it was not confirmed that this representation activation of the UPR. Forced expression of this UPR mediator was previously found to impair adipogenesis in

differentiating 3T3-L1 adipocytes, and mice lacking this gene gained more weight and fat mass on HFD compared to WT mice (Han *et al.* 2013). An intriguing finding from this paper was that 1-year-old *Chop* knockout mice on chow were heavier and had more fat mass than WTs, which indicates that upregulation of this gene in aged *Tst*$^{-/-}$ mice could be responsible for the reciprocal phenotype of reduced body weight and fat mass observed in *Tst*$^{-/-}$ mice. To understand the cause and implication of UPR activation in *Tst*$^{-/-}$ mice, *in vitro* investigation of the impact of *Tst* gene knockout on *Chop* expression will be carried out in the future in a newly acquired pluripotent stem cell line lacking the *Tst* gene.

Another mechanism by which increased H_2S may influence the metabolic phenotype of the *Tst*$^{-/-}$ mice through its potential role in mediating the beneficial effects of calorie restriction (CR). CR in humans leads to weight loss and improved metabolic parameters (Heilbronn *et al.* 2006), and in rodents, some of the beneficial effects of CR have been shown to be dependant on endogously-produced H_2S (Hine *et al.* 2015). While H_2S has not been directly linked to the metabolic benefits of CR, it has been associated with lifespan extension in fruit flies, yeast and *C. elegans* (Hine *et al.* 2015), therefore it's potential benefit both health and lifespan in the *Tst*$^{-/-}$ mouse must be considered in future studies with this mouse.

The discovery that *Tst*$^{-/-}$ mice on chow diet had reduced weight gain and fat mass, as well as reduced adiponectin without metabolic impairment was unexpected. Further investigation of the cause of this altered phenotype of *Tst*$^{-/-}$ mice on chow diet will be carried out in future to fully elucidate the role of *Tst* in adipose tissue.

3.4.5 Limitations and future work.

The aims of this chapter were to assess the impact of *Tst* gene knockout on the metabolic response to high fat diet, and to investigate adipose tissue dysfunction as the root of this metabolic response. I have confirmed that *Tst*$^{-/-}$ mice are more susceptible than WT mice to metabolic derangement after HFD. I also provided some evidence that this dysfunction is associated with changes in expression of antioxidant enzymes in adipose tissue. I have uncovered altered adipose tissue responses in *Tst*$^{-/-}$ mice on chow diet, particularly in older mice, which were previously unknown, and future

work will focus on understanding the impact of *Tst* gene knockout on sulfide metabolism and mitochondrial function in ageing.

The mice used in this chapter had a global knockout of the *Tst* gene and were on a C57BL/6 background, with a mix of substrains 6J and 6N. This could have caused variability in their metabolic responses to HFD. 6J mice are prone to increased weight gain and metabolic impairment on high fat diet compared to other inbred mouse lines (West *et al.* 1992), and 6N mice have been found to have a similar metabolic response to high fat diet (Podrini *et al.* 2013), although recent work has uncovered differences between the two sub-strains on low fat diet (Hull *et al.* 2017). This genetic heterogeneity could have led to variable results, and so it was decided to backcross the $Tst^{-/-}$ line with 6J mice to minimise any effect of unknown genetic variation in future experiments. These $Tst^{-/-}$ mice on a 6J background were used for experiments in chapter 5. *Tst* is expressed in tissues other than adipose, including hepatocytes and macrophages, as well as endothelial cells, and it is apparent that the lack of *Tst* in these other tissues could also have impacted the response to HFD. A new mouse model is now available which will allow for cre-mediated tissue-specific knockout of *Tst*, however due to delays in its development, it was not available for use during this PhD. In future, this mouse model with adipose-specific knockout of *Tst* will be used to investigate the impact of *Tst* gene knockout on this tissue.

The data from this chapter were challenging to interpret due to unexpected results in the WT groups. WT mice on chow diet gained a large amount of weight during the 20-week experiment and, by the end of the time-period, weighed an average of around 40g and were visibly fat. WT mice on chow also had impaired glucose tolerance, and did not have significantly different plasma glucose to WT mice on HFD at any timepoint after administration of a glucose bolus. Therefore, the use of these mice as a control for diet-induced metabolic impairment was not ideal, as interpretation of the effect of diet was confounded by the deterioration of the mice on chow diet. Future experiments of this diet-induced obesity model will be limited to shorter durations to prevent this unfortunate outcome, and a defined low-fat diet will be used to better maintain a healthy metabolic profile. Another unexpected finding in WT mice was that the expression of several key antioxidant enzymes was increased

by HFD, a result that contradicts certain published literature on this model (Furukawa *et al.* 2004; Huh *et al.* 2012; Long *et al.* 2013; Han *et al.* 2016). This contradiction could be due to type of adipose tissue used for this measurement. Interpretation of the impact of *Tst* gene knockout on antioxidant gene expression must be carried out with this caveat in mind and would benefit from clarification in future experiments with the $Tst^{-/-}$ mouse.

The expression of *Tst* in adipose of WT mice was not stable throughout the duration of both experiments. After 6 weeks of HFD, *Tst* expression had decreased to almost one quarter of the expression in WT mice on chow diet. Older WT mice on chow, that had a degree of fat accumulation and metabolic impairment, also had reduced adipose *Tst* expression, which was not further reduced in the group on HFD for 20 weeks. It had previously been observed that *Tst* mRNA in adipose tissue negatively correlates with fat mass, and that high fat feeding of WT mice causes a reduction in its expression (Morton *et al.* 2016). Therefore, the reduced expression of *Tst* in obese WT mice was expected. However, it was apparent that high fat feeding lead to convergence of body weight, fat mass, and adiponectin levels between WT and $Tst^{-/-}$ mice. The reduction in *Tst* expression in adipose tissue of WT mice could have minimised the differences between the groups, leading to the convergence of these phenotypes.

Because of these limitations, the results presented here cannot definitively support the hypothesis that *Tst* gene knockout leads to impaired metabolic health after a high fat challenge due to increased susceptibility to adipose oxidative stress and inflammation. To address the specific risk of oxidative stress, it was decided to assess the response of primary adipocytes lacking or overexpressing TST *in vitro* to an oxidative challenge, work that will be described in Chapter 5.

Chapter 4 Metabolic characterisation of a new mouse model with human TST expression in adipose tissue

4.1 INTRODUCTION

Overexpression of *Tst* in adipose tissue was previously shown to protect against the metabolic impairment of HFD (Morton *et al.* 2016). The transgenic mouse used in the previous study was no longer available for use during this PhD, however a new model was developed that was hypothesised would have a similar phenotype. The aim of this chapter was to characterise this new mouse model with genetic overexpression of the human TST gene in adipose tissue (Ad-hTST), and to investigate if the increased TST in adipose tissue mediates its protective effects through minimising adipose tissue dysfunction. Unfortunately, this new model failed to recapitulate the phenotype of the Adipoq-*Tst* mouse, raising questions about the impact of genetic differences between the lines.

The previous mouse line in which a protective effect of *Tst* overexpression was first observed was called the Adipoq-*Tst* mouse (Morton *et al.* 2016). These mice had an extra copy of the mouse *Tst* gene under the control of the adiponectin promoter which was inserted randomly in the genome and bred to homozyosity (Figure 4.1a). This led to a 2-fold increase in *Tst* mRNA in adipose tissue. Adipoq-*Tst* mice were protected from weight gain during a high fat challenge and had improved insulin sensitivity compared to wild-type mice. These mice exhibited evidence for increased hepatic fat oxidation and adipocyte lipolysis, as well as maintaining their responsiveness to insulin after HFD, and having increased SOD2 protein and *Prx3* mRNA in adipose tissue. Therefore, it was hypothesised that the increase in antioxidant capability in adipose of Adipoq-*Tst* mice contributed to the improved metabolic phenotype through prevention of local oxidative stress in adipose tissue.

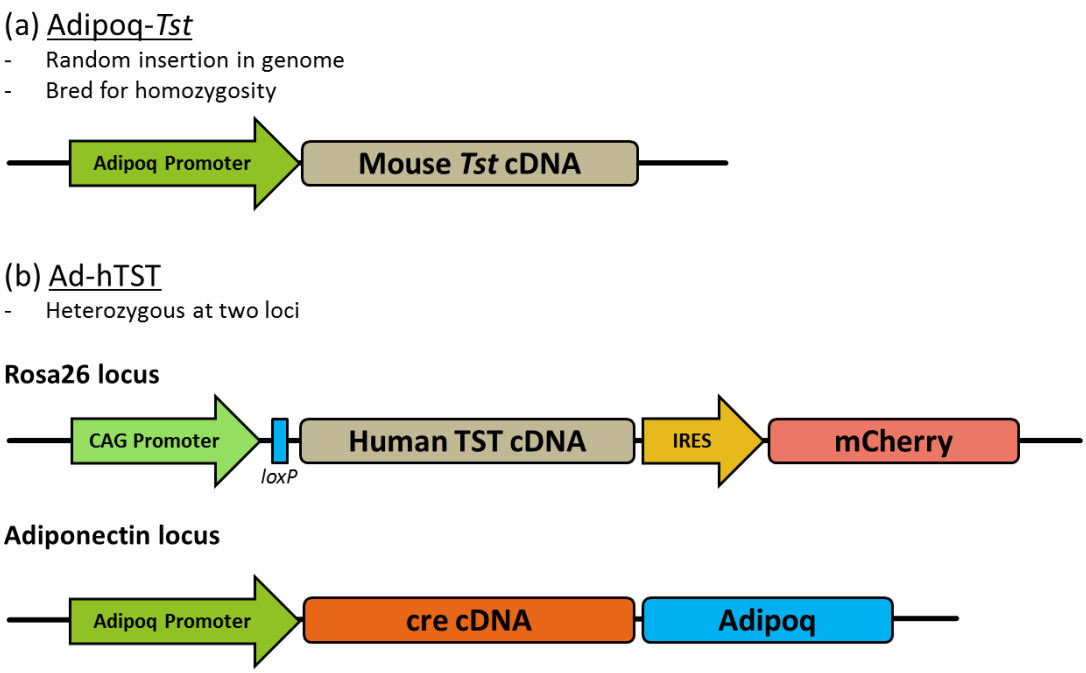

Figure 4.1: Schematic of genetic structure of (a) Adipoq-Tst and (b) Ad-hTST mice.

Adipoq: adiponectin; CAG promoter: adapted from chicken β-actin promoter; loxP: DNA recognition site for cre recombinase; IRES: internal ribosome entry site.

The new mouse model used in this chapter had adipose-specific overexpression of the human TST gene, using cre-*loxP* system to tqarget expression to adipose tissue. This mouse was fully described in paragraph 2.1.1.3 on page 60. The parent mouse ($Rosa26^{LSLhTST}$, Figure 2.1 on page 61) was designed to contain an expression cassette inserted in the constitutively active Rosa26 locus which carried the human TST (hTST) cDNA and mCherry fluorescent reporter gene preceded by a STOP cassette flanked by *loxP* sites (*loxP*-STOP-*loxP*: LSL). To excise the stop region and induce expression of human TST in adipose tissue, homozygous $Rosa26^{LSLhTST}$ mice were bred with heterozygous Adiponectin-cre (Adip-cre) mice, expressing cre recombinase in adipose tissue (Eguchi *et al.* 2011). Excision of the stop cassette allowed for transcription of the TST and mCherry genes, driven by the constitutively active CAG promoter (Figure 4.1b). Cre-positive progeny from this crossing were called Ad-hTST and cre-negative littermates were used as controls and named wild-type-*loxP*-STOP-*loxP* (WT-LSL).

The aim of this chapter was to characterise the new Ad-hTST mouse, including ensuring expression of human TST in adipose only, and assessing the metabolic response to a high fat challenge. Due to time limitations, female mice were used to investigate the pattern of human TST expression in adipose and non-adipose tissues, and male mice were subjected to a high fat exposure for 6 weeks. Metabolic phenotype was assessed by carrying out a glucose tolerance test after 5 weeks of HFD, and by measuring levels of the insulin-sensitising hormone adiponectin. Adipose tissue dysfunction was assessed by looking at expression of antioxidant genes, as well as evaluating immune cell infiltration. This chapter describes the results of these experiments, and discusses potential problems with the new mouse model that may have impacted on these results. Future work to overcome these potential problems is also discussed.

4.1.1 Hypothesis & aims

I hypothesised that thiosulfate sulfurtransferase over-expression in adipose tissue protects against metabolic impairment of a high fat challenge due to increased antioxidant capability.

To test this hypothesis, the aims of this chapter were:

- To characterise TST expression in female Ad-hTST mice.
- To evaluate the metabolic phenotype of Ad-hTST mice after a high fat challenge.
- To assess oxidative stress and inflammation in adipose of Ad-hTST mice after a high fat challenge.

4.2 METHOD

Ad-hTST mice in this chapter were generated by breeding the parent line Rosa26^{LSLhTST} (as described in paragraph 2.1.1.3 on page 60) with Adiponectin-cre (Adip-cre) mice, expressing cre recombinase in adipose tissue (Eguchi *et al.* 2011). Cre-positive mice were presumed to have excision of the stop region in adiponectin-expressing cells (see Figure 2.1 on page 61), and were called Ad-hTST. Excision of the stop cassette and expression of the human TST gene was confirmed using female mice. Cre-negative littermates were used as controls, and were called wild-type-*loxP*-STOP-*loxP* (WT-LSL). These mice were genetically indistinguishable from the parent line Rosa26^{LSLhTST}.

Female Ad-hTST mice and WT-LSL littermates were culled at 8 weeks and tissues harvested to characterise human TST expression and activity in adipose and other tissues. At 8 weeks of age, male Ad-hTST mice and WT-LSL littermates were separated into two groups, one on Surwit D12328 low fat diet (LFD) and the other group on Surwit D12331 high fat, high sucrose diet (HFD; see Table 2.2 on page 63). A glucose tolerance test (GTT) was performed after 5 weeks on experimental diets. At the end of the study period (6 weeks), mice were culled by decapitation, and blood and organs were harvested. Figure 4.2 below shows the timeline of high-fat feeding for male Ad-hTST and control mice.

Due to time constraints and problems with breeding, both the female and male cohorts were carried out in three batches containing between 4 and 16 animals.

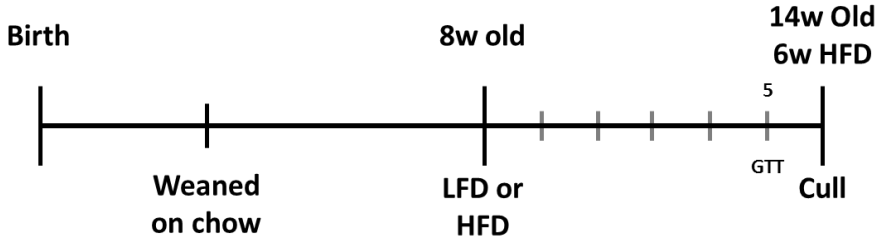

Figure 4.2: Timeline of WT-LSL and male Ad-hTST mice on LFD or HFD for 6 weeks.

Glucose tolerance test (GTT) was carried out after 5 weeks on LFD/HFD.

4.3 RESULTS

4.3.1 Expression of human and mouse TST in adipose and other tissues of female Ad-hTST mice.

4.3.1.1 Expression of human TST mRNA was increased in adipose tissues of Ad-hTST versus WT-LSL female mice.

Adipose depots, including gonadal (female equivalent of epididymal, also called parametrial), mesenteric, subcutaneous and interscapular brown adipose, were excised from 8-week-old female Ad-hTST mice and WT-LSL (LoxP-STOP-LoxP) controls. The abundance of human TST mRNA was measured using a human-specific Taqman® probe. Human TST was undetectable or at very low background levels in all WT-LSL samples (Figure 4.3). Human TST was highly expressed in all adipose depots from Ad-hTST mice, including interscapular brown adipose (Figure 4.3d)

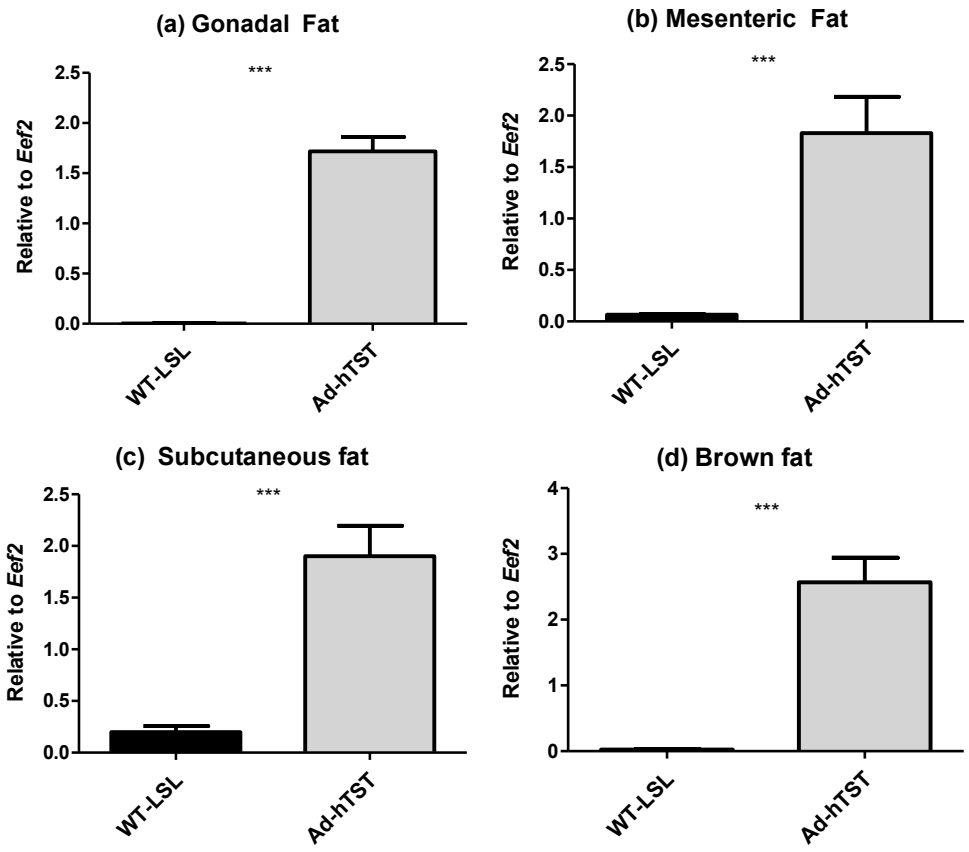

Figure 4.3: Gene expression of human TST in adipose depots of Ad-hTST and WT-LSL female mice at 8 weeks of age.

*Abundance of human TST mRNA in (a) gonadal, (b) mesenteric (c) subcutaneous white adipose and (d) interscapular brown adipose, normalised to housekeeping gene Eef2. Data are mean ± SEM, analysed by Student's t-test: *** P < 0.001; (n=8).*

4.3.1.2 Expression of mouse Tst mRNA was unchanged in adipose tissues of Ad-hTST versus WT-LSL female mice.

The abundance of mouse *Tst* mRNA was assessed in white and brown adipose depots of WT-LSL and Ad-hTST female mice. Expression of the endogenous *Tst* gene was unchanged in adipose depots of Ad-hTST mice (Figure 4.4).

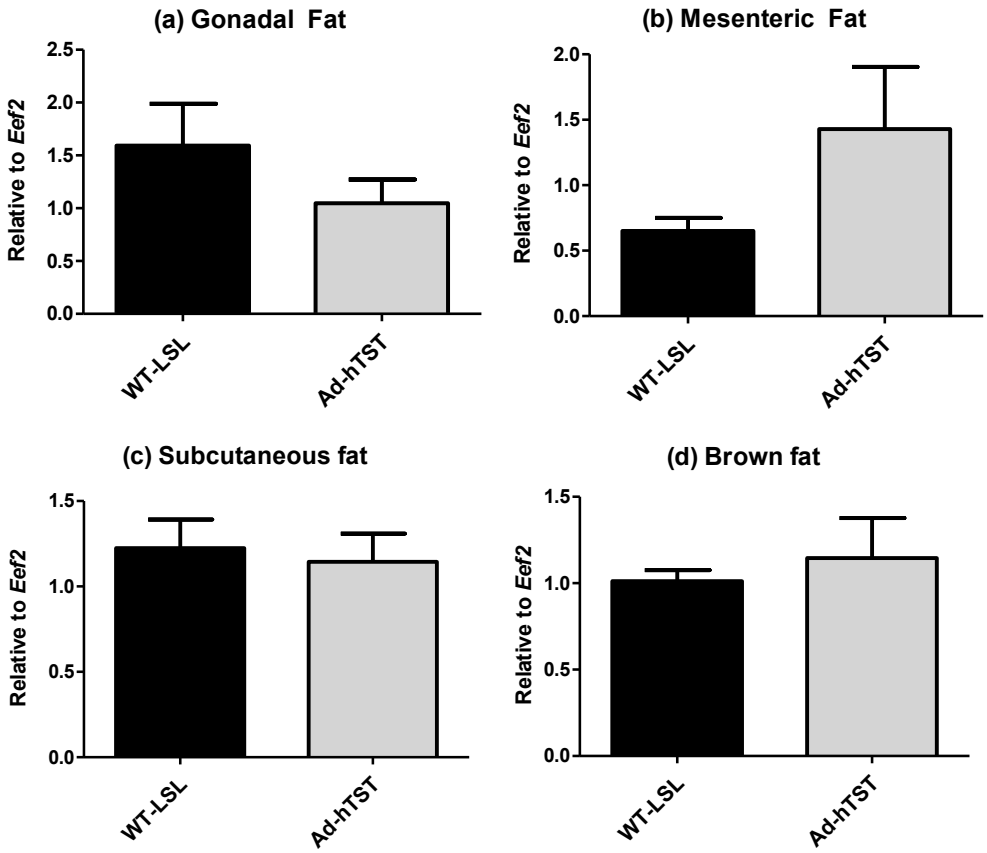

Figure 4.4: Gene expression of mouse* Tst *in adipose depots of Ad-hTST and WT-LSL female mice at 8 weeks old.

Abundance of mouse Tst *mRNA in (a) gonadal, (b) mesenteric (c) subcutaneous white adipose and (d) interscapular brown adipose, normalised to housekeeping gene Eef2. Data are mean ± SEM, analysed by Student's t-test: not significant; (n=8).*

4.3.1.3 Rhodanese activity was increased in adipose tissues of Ad-hTST versus WT-LSL female mice.

Homogenates of gonadal, mesenteric and subcutaneous adipose depots from female Ad-hTST mice were assessed for rhodanese (TST/MPST) activity. Compared to WT-LSL controls, rhodanese activity (expressed per milligram of protein per minute) in gonadal fat was significantly increased by 3.5-fold (Figure 4.5a). In mesenteric fat, rhodanese activity was increased by 2-fold in Ad-hTST mice compared to WT-LSL (Figure 4.5b). Subcutaneous fat of Ad-hTST mice exhibited a 3.3-fold increase in rhodanese activity compared to WT-LSL mice (Figure 4.5c).

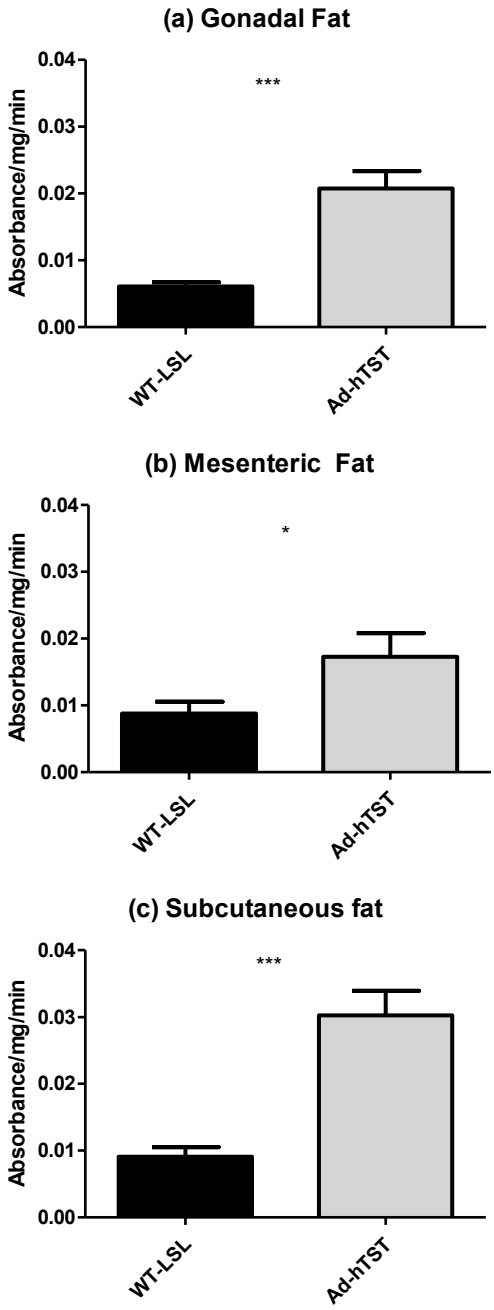

Figure 4.5: Rhodanese activity in homogenates of adipose depots of Ad-hTST and WT-LSL female mice at 8 weeks of age.

*Rhodanese activity per minute in (a) gonadal, (b) mesenteric and (c) subcutaneous adipose depots, normalised to protein concentration. Data are mean ± SEM, analysed by Student's t-test: * P <0.05, *** P < 0.001; (n=5-7).*

4.3.1.4 TST protein was more abundant in adipose tissues of Ad-hTST versus WT-LSL female mice.

TST protein content of gonadal and subcutaneous adipose depots from female Ad-hTST and WT-LSL was measured by Western blot using an antibody with reactivity to both the human and mouse proteins. TST protein was very low or undetectable in WT-LSL samples. Both gonadal and subcutaneous depots from Ad-hTST mice had high TST protein content (Figure 4.6).

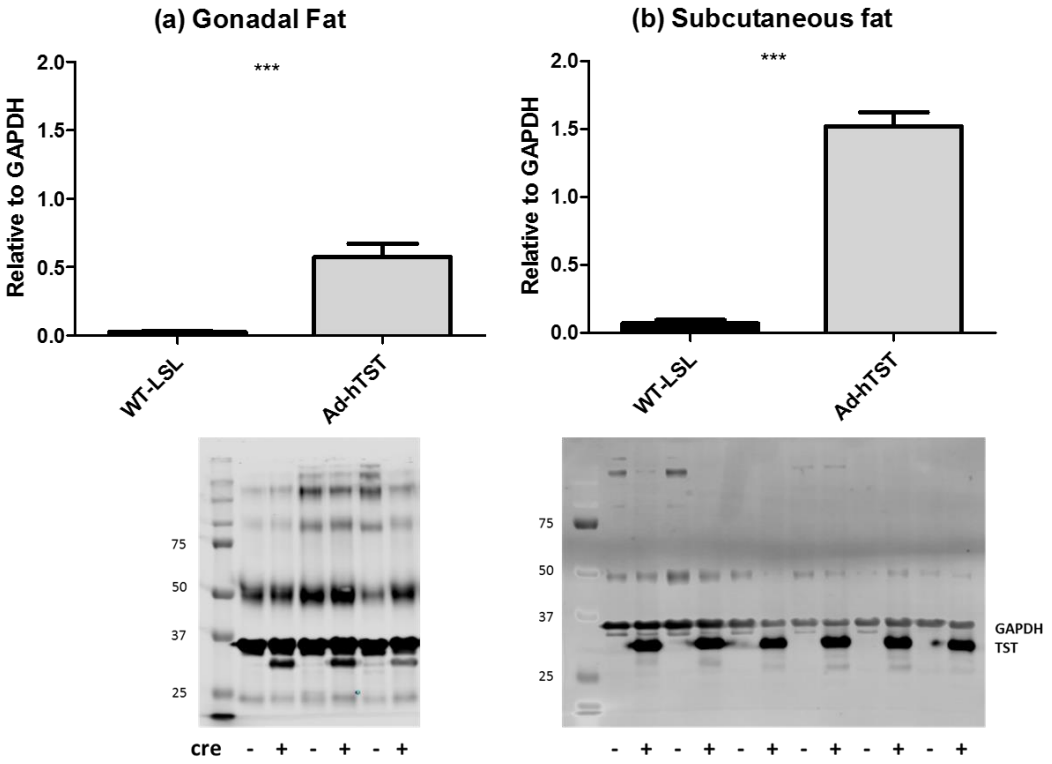

Figure 4.6: TST protein in adipose depots of Ad-hTST and WT-LSL female mice at 8 weeks of age.

*TST protein content, relative to GAPDH endogenous control in (a) gonadal and (b) subcutaneous fat. Representative samples are shown below graphs. Data are mean ± SEM, analysed by Student's t-test: *** P < 0.001; (n=6; except n=4 for (b) WT-LSL due to negative values).*

4.3.1.5 Human TST mRNA was not expressed in non-adipose tissues of Ad-hTST and WT-LSL female mice.

To confirm the tissue specificity of recombination by cre to adipose tissues only, human TST mRNA levels were measured in liver, kidney, spleen, lung and heart of Ad-hTST mice. Gonadal white adipose tissue (WAT) from Ad-hTST mice was used as a positive control and to generate a standard curve. Human TST was undetectable or at low background levels in liver, kidney and spleen (Figure 4.7). Lung and heart tissue had a low, but measurable amount of human TST, however no significant difference was found between Ad-hTST and WT-LSL mice, indicating that this may be due to amplification of a hTST sequence-related transcript in these tissues, giving a false positive.

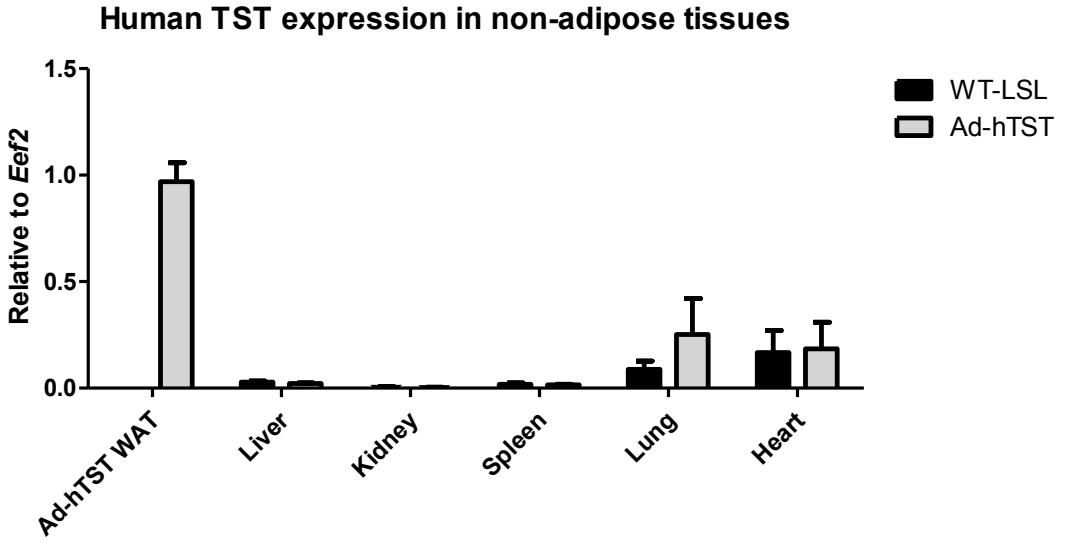

Figure 4.7: Gene expression of human TST in non-adipose tissues of Ad-hTST and WT-LSL female mice at 8 weeks of age.

Abundance of human TST mRNA in gonadal white adipose tissue (WAT), liver, kidney, spleen, lung and heart, normalised to housekeeping gene Eef2. A standard curve for interpolation of relative concentration was created using mRNA from Ad-hTST WAT samples only. Data are mean ± SEM; (n=3).

4.3.1.6 mCherry fluorescence was present in adipose, but not in non-adipose tissues of Ad-hTST female mice.

Adipose and non-adipose tissues of female Ad-hTST and WT-LSL mice were imaged to investigate expression of the red fluorescent marker mCherry. Explants were stained with DAPI to visualise nuclei. Gonadal adipose tissue from Ad-hTST showed red fluorescence in the cytoplasm of adipocytes, but no equivalent red fluorescence was observed in gonadal adipose from WT-LSL mice (Figure 4.8a). Red fluorescence was observed in subcutaneous adipose of Ad-hTST mice, however this was less distinct than in gonadal adipose, potentially due to a high background fluorescence as found in subcutaneous adipose from WT-LSL mice (Figure 4.8b). Explants of liver and quadriceps muscle from Ad-hTST mice showed no red fluorescence and were indistinguishable from WT-LSL tissues (Figure 4.8c and d).

(a) Gonadal fat

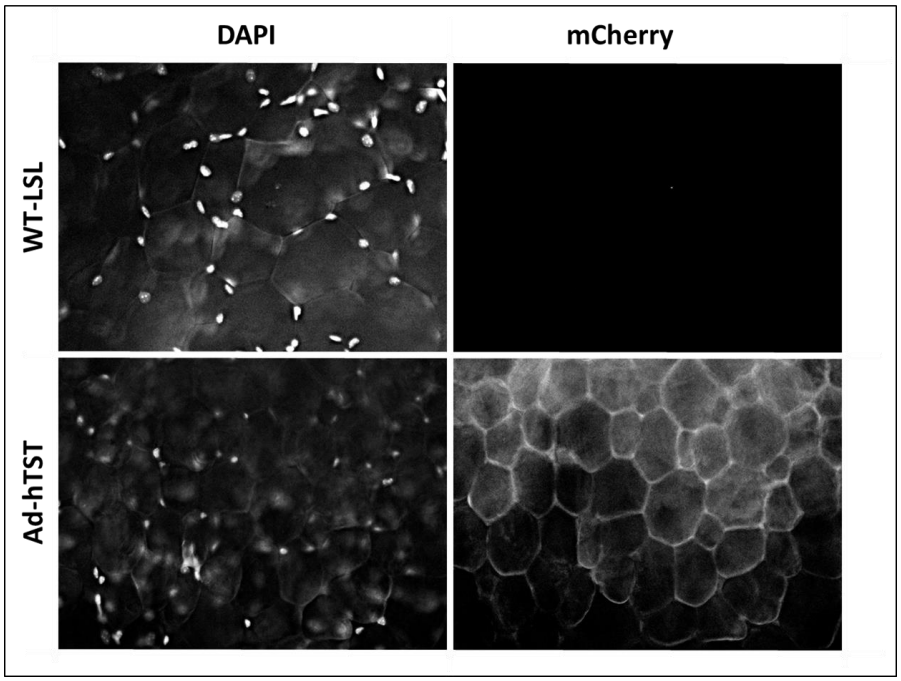

(b) Subcutaneous fat

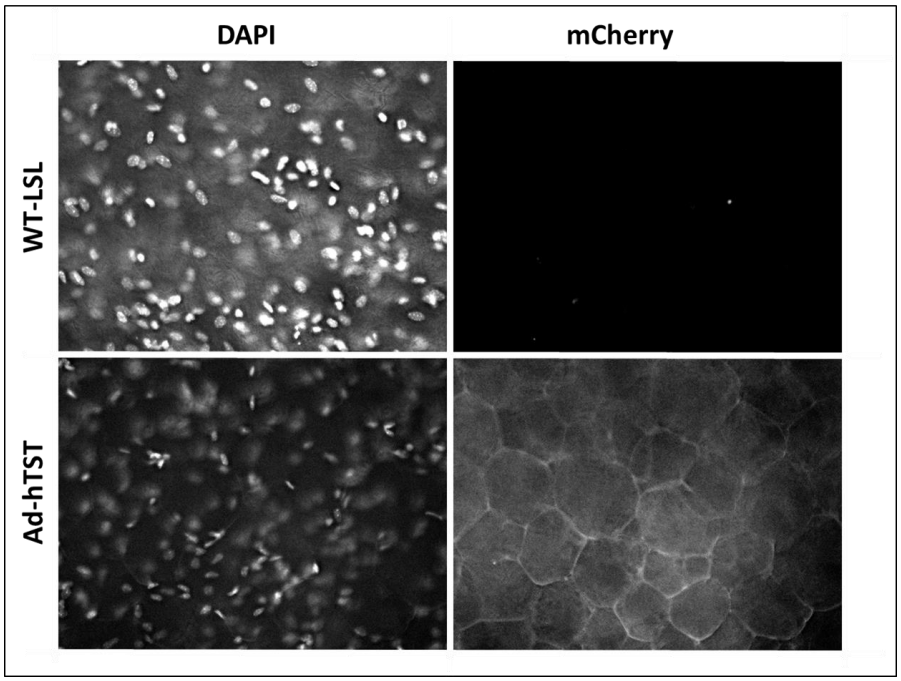

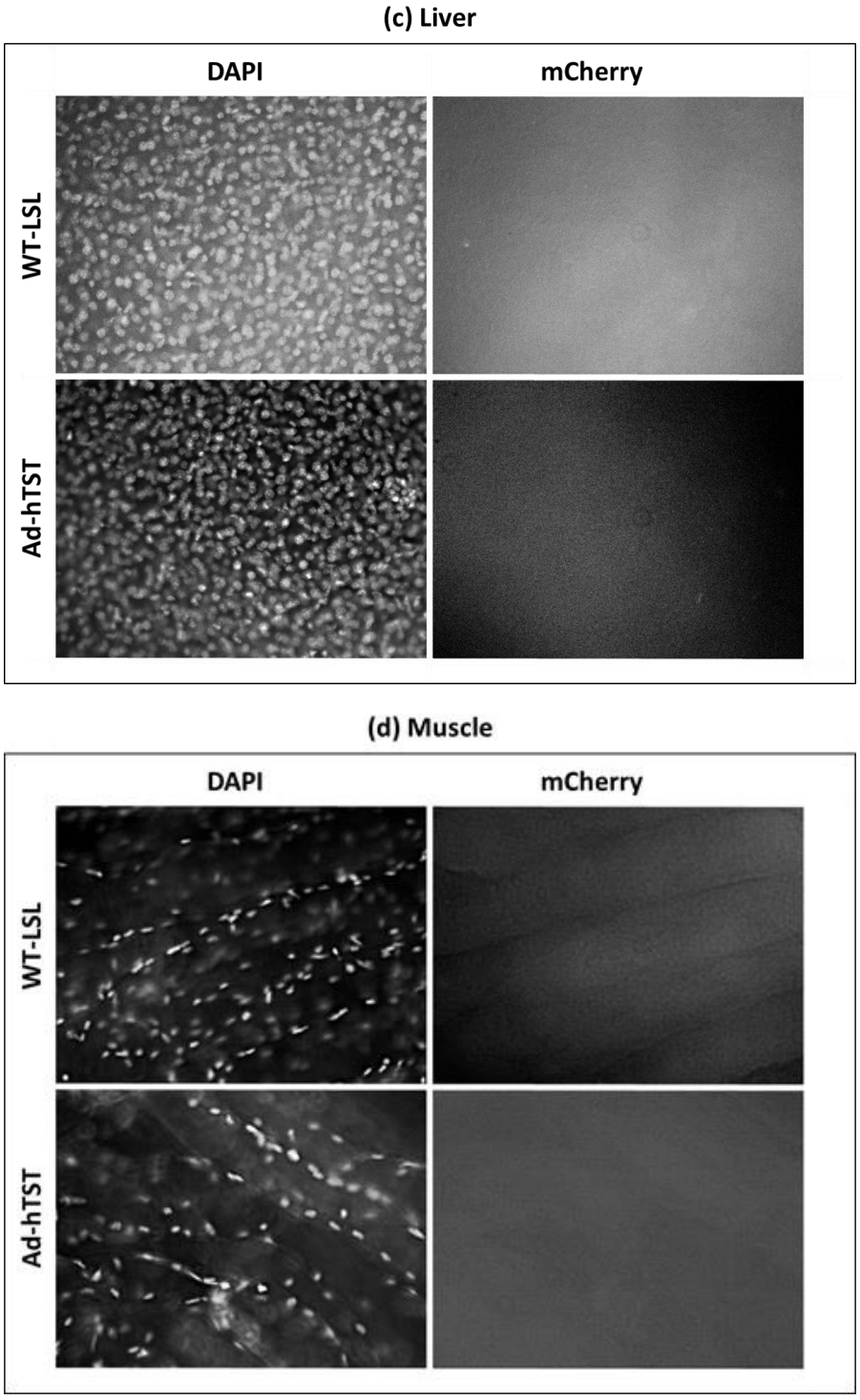

Figure 4.8: mCherry fluorescence in adipose and non-adipose tissues of Ad-hTST and WT-LSL female mice at 8 weeks of age.

DAPI was used to stain nuclei in explants of (a) gonadal fat, (b) subcutaneous fat, (c) liver and (d) quadriceps muscle.

4.3.2 The effects of human TST gene overexpression in adipose on glucose homeostasis and adipose tissue response to high fat diet in Ad-hTST male mice.

4.3.2.1 Body weight was not different in Ad-hTST versus WT-LSL male mice on LFD or HFD for 6 weeks.

Body weights of male Ad-hTST and WT-LSL male mice were measured after 6 weeks of HFD or LFD, and were found to be higher in HFD-fed mice (Figure 4.9a). Mice of both genotypes gained a similar amount of weight on HFD (Figure 4.9b). Ad-hTST and WT-LSL mice on LFD gained very little weight over the 6-week period.

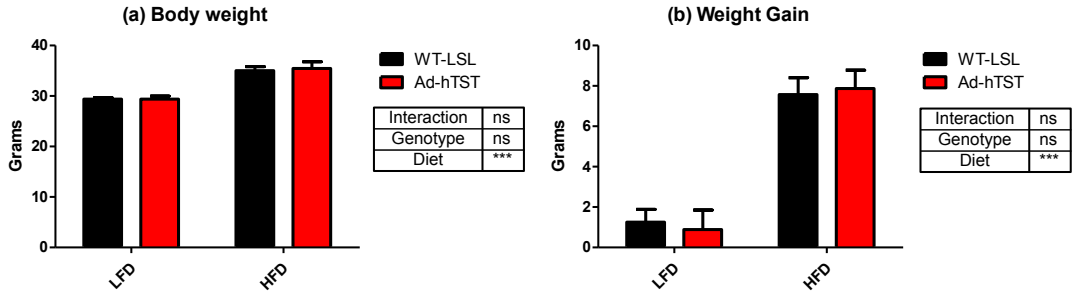

Figure 4.9: Body weight of Ad-hTST and WT-LSL mice on LFD or HFD for 6 weeks.

*(a) Body weight at cull, and (b) weight gain from week 0 to week 6. Data are mean ± SEM, analysed by 2-way ANOVA: *** P < 0.001, ns = not significant; (n = 6-7).*

4.3.2.2 *Body composition was not different in Ad-hTST versus WT-LSL mice on LFD or HFD for 6 weeks.*

To measure changes in body composition *in vivo* during the 6-week feeding period, a Bruker Minispec LF50 whole body composition analyser was used at week 0, week 3 and week 6. After 3 weeks on HFD, both Ad-hTST and WT-LSL mice had significantly increased fat mass, and reduced lean mass as a percentage of total body weight (Figure 4.10). By 6 weeks, fat mass was further increased and lean mass decreased. Ad-hTST mice gained fat mass and lost lean mass at the same rate as WT-LSL mice on HFD.

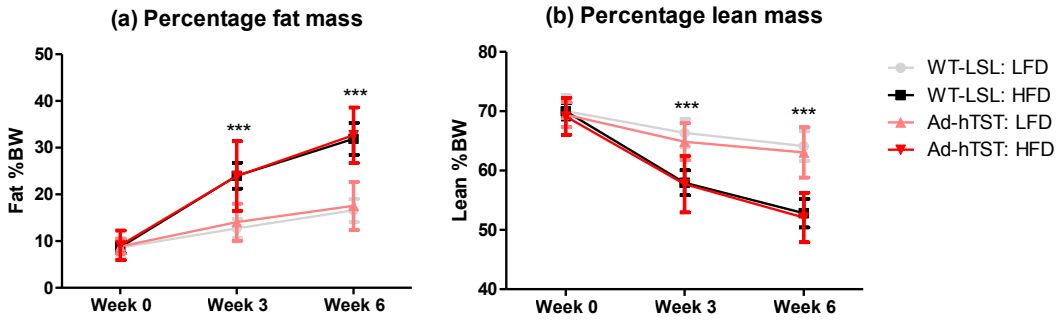

Figure 4.10: Whole body composition of Ad-hTST and WT-LSL mice on LFD or HFD for 6 weeks.

*(a) Fat mass, and (b) lean mass as a percentage of total body weight. Data are mean ± SEM, analysed by 2-way repeated measures ANOVA with Bonferroni post-hoc test comparing each group at each timepoint: LFD vs. HFD for both genotypes: *** P < 0.001; (n = 6-7).*

4.3.2.3 Adipose tissue depots weights were not different in Ad-hTST versus WT-LSL mice on LFD or HFD for 6 weeks.

After 6 weeks on LFD or HFD, mice were culled and three white adipose depots were weighed and normalised to body weight. Epididymal, mesenteric and subcutaneous adipose depots were increased by HFD in both Ad-hTST mice and WT-LSL, with no significant differences between genotypes (Figure 4.11).

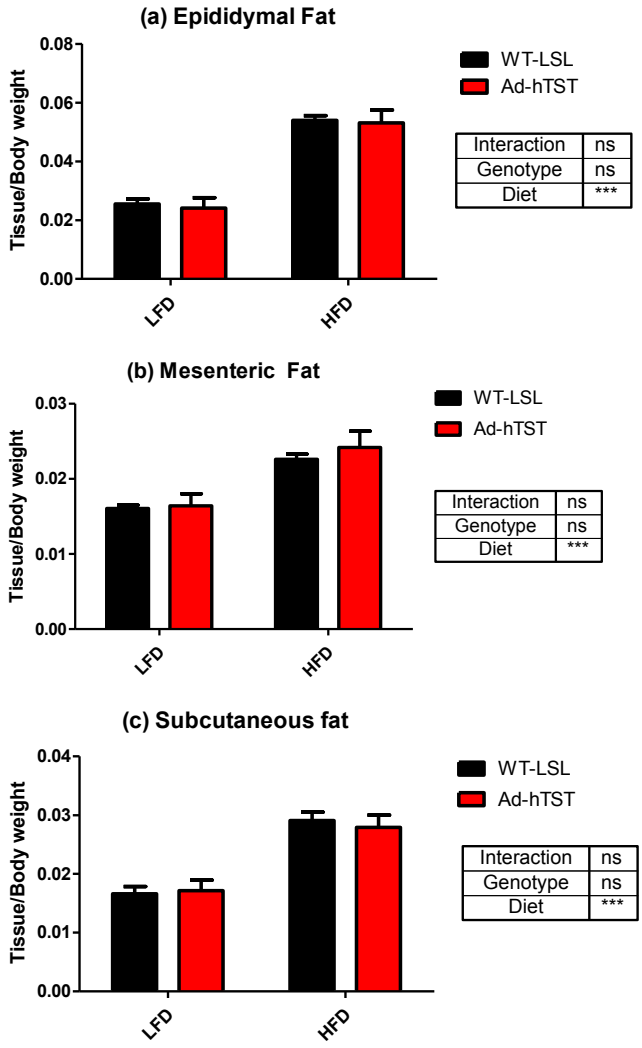

Figure 4.11: White adipose depot weights of Ad-hTST and WT-LSL mice on LFD or HFD for 6 weeks.

*(a) Epididymal, (b) mesenteric, and (c) subcutaneous white adipose depots, normalised to body weight at cull. Data are mean ± SEM, analysed by 2-way ANOVA: *** P < 0.001, ns = not significant; (n = 6-7).*

4.3.2.4 *Food intake and feed efficiency were not different in Ad-hTST versus WT-LSL mice on LFD or HFD for 6 weeks.*

Food intake was measured weekly, and feed efficiency was calculated as grams gained per week per kcal consumed per week. Mice on HFD consumed slightly more kcal per week than those on LFD, however no difference was observed in Ad-hTST mice compared to WT-LSL (Figure 4.12a). Consumption of HFD caused an increase in feed efficiency, with mice of both genotypes gaining a similar amount of weight per kcal consumed (Figure 4.12b).

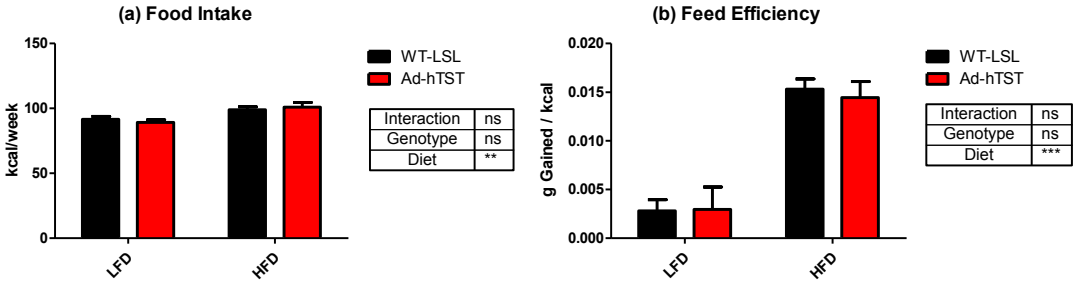

Figure 4.12: Food intake and feed efficiency per week in Ad-hTST and WT-LSL mice on LFD or HFD for 6 weeks.

*(a) Food intake (kcal per week), and (b) feed efficiency (grams gained per kcal consumed). Data are mean ± SEM, analysed by 2-way ANOVA: ** P <0.01, *** P < 0.001, ns = not significant; (n = 6-7).*

4.3.2.5 Glucose tolerance was impaired after 5 weeks of HFD in Ad-hTST and WT-LSL mice.

A glucose tolerance test was carried out on Ad-hTST and WT-LSL mice after 5 weeks of HFD. Comparison of glucose levels between genotypes at each timepoint showed that Ad-hTST mice on LFD had lower glucose than WT-LSL mice on LFD at 15mins post-injection ($P < 0.05$; Figure 4.13a). No differences were observed between genotypes on HFD. Ad-hTST mice had significantly higher glucose on HFD than on LFD at all timepoints after glucose administration (Figure 4.13a). WT-LSL mice had significantly higher glucose on HFD than LFD at later timepoints only (60 and 120 minutes). Overall plasma glucose levels during the GTT measured by area under the curve were increased by HFD in both WT-LSL and Ad-hTST mice, although there was no significant difference between genotypes (Figure 4.13b).

Plasma insulin was measured at each timepoint before and after glucose administration. No differences were observed between Ad-hTST and WT-LSL mice on either diet. Ad-hTST mice had significantly higher fasting insulin (time 0) on HFD than on LFD and at all timepoints after glucose administration (Figure 4.13c). WT-LSL mice had significantly higher insulin on HFD compared to LFD at only 120 minutes post-injection. Overall plasma insulin levels during the GTT measured by area under the curve were increased by HFD in both WT-LSL and Ad-hTST mice, although there was no significant difference between genotypes (Figure 4.13d).

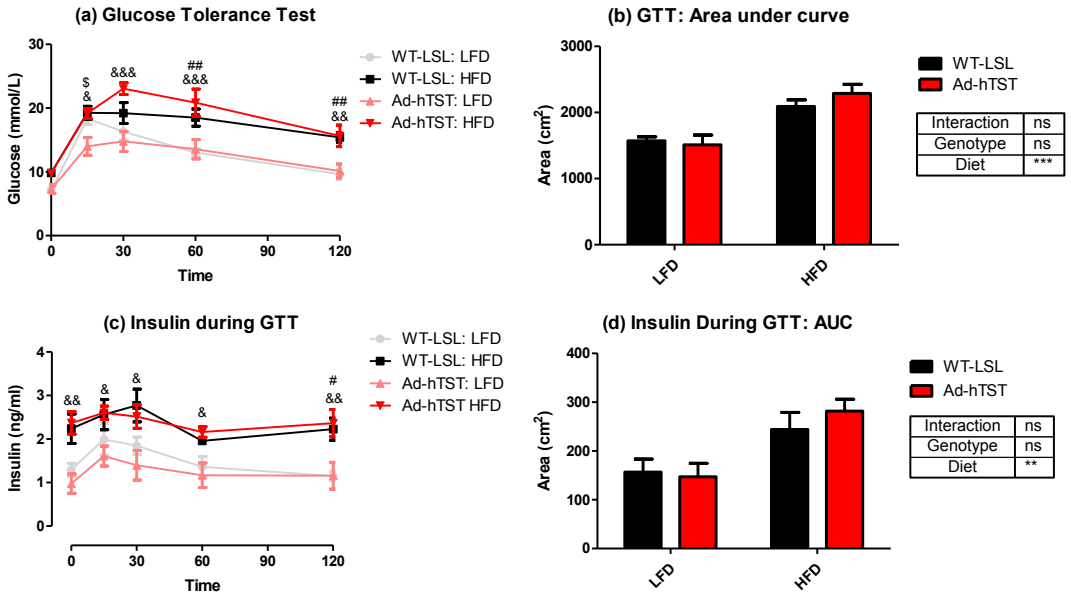

Figure 4.13: Plasma glucose and insulin levels after administration of a glucose bolus to Ad-hTST and WT-LSL mice on LFD or HFD for 5 weeks.

*(a) Plasma glucose levels during a glucose tolerance test (GTT); (b) area under the curve (AUC) of glucose levels during GTT; (c) plasma insulin levels during GTT; (d) AUC of insulin levels during GTT. Data are mean ± SEM; (a) and (c) analysed by 2-way repeated measures ANOVA with Bonferroni post-hoc test comparing each group at each timepoint: LFD WT-LSL vs. Ad-hTST: $ P < 0.05; WT-LSL LFD vs. HFD: # P < 0.05, ## P < 0.01; Ad-hTST LFD vs. HFD: & P < 0.05, && P < 0.01, &&& P < 0.001; (b) and (d) analysed by 2-way ANOVA: ** P <0.01, *** P < 0.001, ns = not significant (n = 6-7).*

4.3.2.6 Total plasma adiponectin was reduced in Ad-hTST versus WT-LSL mice on LFD diet, and total and HMW adiponectin were reduced in both genotypes on HFD for 6 weeks.

Total and high molecular weight (HMW) adiponectin were measured by ELISA in the plasma of WT-LSL and Ad-hTST mice after 6 weeks of HFD. Total adiponectin was significantly reduced in Ad-hTST mice on LFD compared to WT-LSL (Figure 4.14a). High fat feeding caused a reduction in total and HMW adiponectin in both genotypes, but no significant difference was found between genotypes (Figure 4.14b). As a percentage of total adiponectin, HMW was reduced by HFD to the same degree in both Ad-hTST and WT-LSL mice (Figure 4.14c).

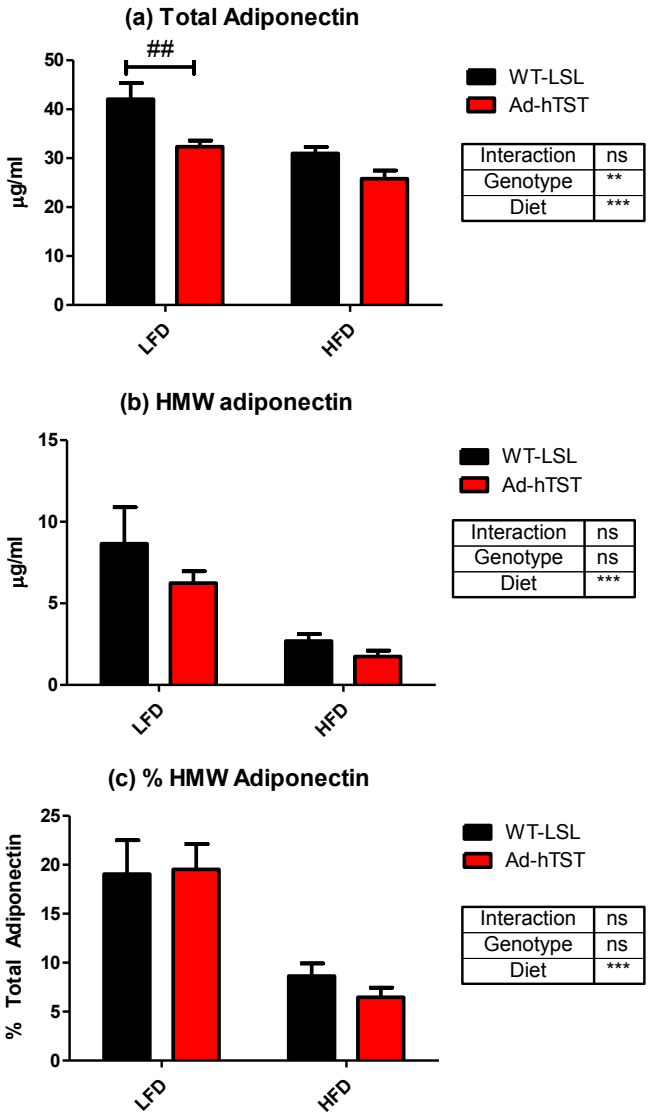

Figure 4.14: Plasma adiponectin levels of Ad-hTST and WT-LSL mice on LFD or HFD for 6 weeks.

*(a) Total adiponectin, (b) high molecular weight (HMW) adiponectin, and (c) HMW as a percentage of total adiponectin. Data are mean ± SEM, analysed by 2-way ANOVA: ** P <0.01, *** P < 0.001, ns = not significant; with Bonferroni post-hoc test comparing between genotypes for each diet: ## P < 0.01; (n=6-7).*

4.3.2.7 Plasma adiponectin was unchanged in Adip-cre versus WT mice.

Adiponectin was measured in the plasma of Adip-cre mice and their corresponding cre-negative wild-type controls (6J) to ascertain if the presence of the Adip-cre gene impacted circulating levels of adiponectin, which could be carried through to Ad-hTST progeny. [Plasma samples for this measurement were provided by Dr. R. Czapiewski, Wellcome Trust Centre for Cell Biology, and the adiponectin ELISA was carried out by Rhona Aird, Molecular Metabolism Group]. Total and HMW adiponectin were unchanged in Adip-cre mice compared to WT mice (Figure 4.15).

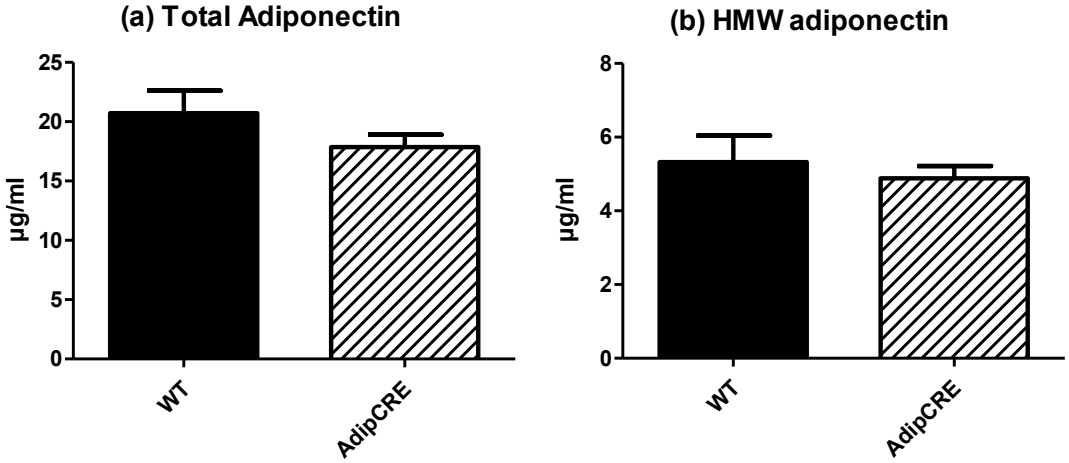

Figure 4.15: Plasma adiponectin levels of Adip-cre and WT (6J) mice.

(a) Total adiponectin and (b) high molecular weight (HMW) adiponectin. Data are mean ± SEM, analysed by Student's t-test: ns = not significant; (n=4-5). [Adiponectin ELISA carried out by R. Aird; samples provided by R. Czapiewski].

4.3.2.8 Gene expression of adiponectin was unchanged in adipose tissue of Ad-hTST versus WT-LSL mice on LFD or HFD for 6 weeks.

Gene expression of adiponectin (*Adipoq*) was measured in epididymal adipose tissue of WT-LSL and Ad-hTST mice after 6 weeks of HFD. There was no significant effect of increased TST expression or HFD on *Adipoq* expression in epididymal fat (Figure 4.16).

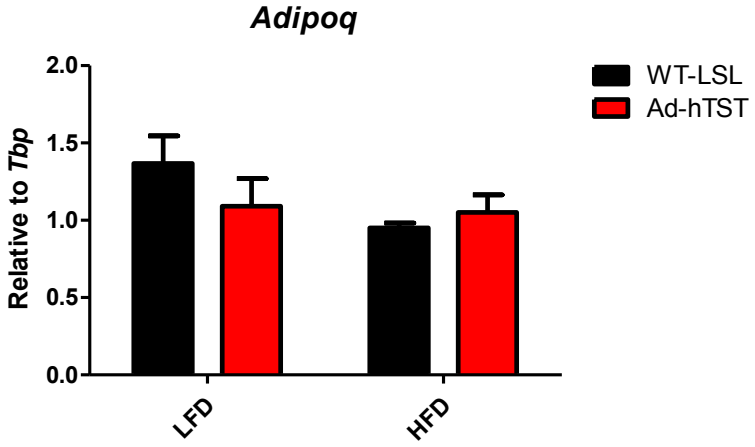

Figure 4.16: Adiponectin gene expression in epididymal white adipose tissue of Ad-hTST and WT-LSL mice on LFD or HFD for 6 weeks.

Data are mean ± SEM, analysed by 2-way ANOVA: not significant; (n=5-7).

4.3.2.9 Gene expression of some key antioxidant enzymes was reduced in adipose tissue of Ad-hTST and WT-LSL mice on HFD for 6 weeks.

The expression of mitochondrial and cytoplasmic antioxidant enzymes was measured in epididymal white adipose tissue from Ad-hTST and WT-LSL mice fed HFD or LFD for 6 weeks. Expression of mitochondrial antioxidant enzymes *Prx3*, *Txn2* and *Gpx4* was reduced in mice fed HFD compared to LFD, but no differences were found in Ad-hTST mice compared to WT-LSL (Figure 4.17). *Sod2*, *Gpx1* and *Txrnd2* were unchanged by increased TST expression or HFD. *Sod1* and *Prx1*, two cytoplasmic antioxidant enzymes were unchanged by increased TST expression or HFD.

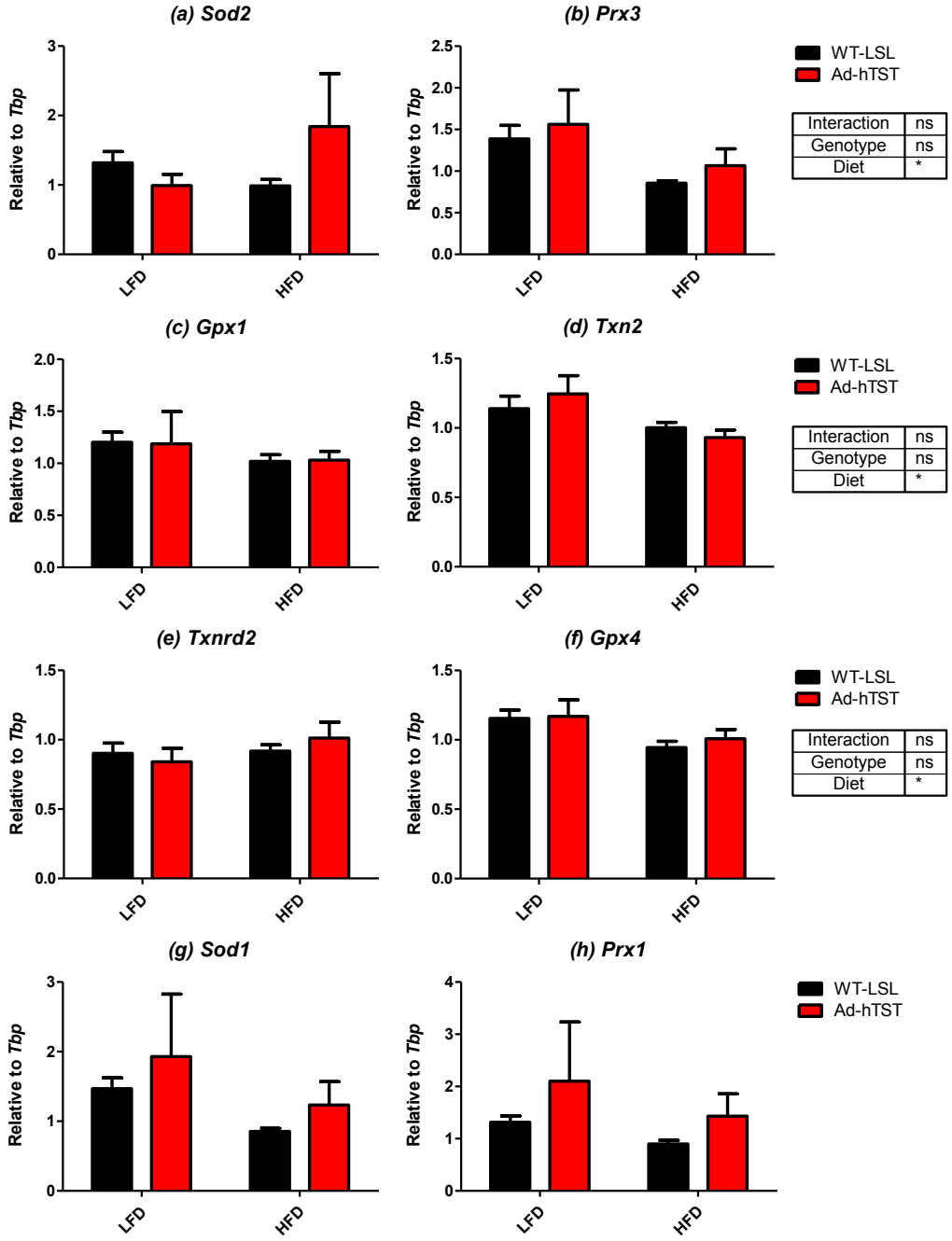

Figure 4.17: Gene expression of key antioxidant enzymes in epididymal adipose tissue of Ad-hTST and WT-LSL mice on LFD or HFD for 6 weeks.

*(a) Superoxide dismutase 2 (Sod2), (b)peroxiredoxin 3 (Prx3), (c) glutathione peroxidase 1 (Gpx1), (d) thioredoxin 2 (Txn2), (e) thioredoxin reductase 2 (Txnrd2), (f) glutathione peroxidase 4 (Gpx4), (g) superoxide dismutase 1 (Sod1), and (h) peroxiredoxin 1 (Prx1) mRNA abundance normalised to housekeeping gene Tbp. Data are mean ± SEM, analysed by 2-way ANOVA: * P <0.05, ns = not significant; (n=5-7).*

To assess activation of NRF2-mediated transcription, the expression of two NRF2-target genes was measured. No difference was found in the expression of *Hmox1* in Ad-hTST mice on LFD or HFD (Figure 4.18a). Expression of *Nqo1* showed a significant interaction between genotype and diet, with lower expression in Ad-hTST mice on LFD compared to WT-LSL, and higher expression in Ad-hTST on HFD (Figure 4.18b).

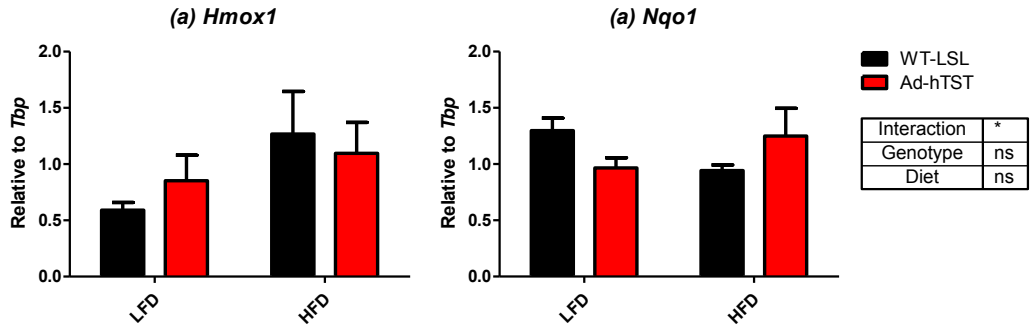

Figure 4.18: Gene expression of NRF2-responsive antioxidant enzymes in epididymal adipose tissue of Ad-hTST and WT mice on LFD or HFD for 6 weeks.

*(a) Heme oxygenase 1 (Hmox1) and (b) NAD(P)H:quinone acceptor oxidoreductase 1 (Nqo1) mRNA abundance normalised to housekeeping gene Tbp. Data are mean ± SEM, analysed by 2-way ANOVA: * P < 0.05, ns = not significant; (n=5-7).*

4.3.2.10 Immune cell populations in stromal vascular fraction of adipose tissue were not different in Ad-hTST versus WT-LSL mice on LFD or HFD for 6 weeks.

Immune cell populations in SVF of epididymal adipose tissue were assessed by flow cytometry. Macrophage number as a percentage of total hematopoietic cell population ($CD45^+$ population) was increased by HFD in both Ad-hTST and WT-LSL mice (Figure 4.19a). The percentage of hematopoietic cells expressing the pro-inflammatory macrophage marker CD11c was also increased by HFD in both genotypes (Figure 4.19b). The percentage of eosinophils was significantly reduced by HFD in adipose from both Ad-hTST and WT mice (Figure 4.19c). There were no differences in immune cell populations between Ad-hTST and WT-LSL mice.

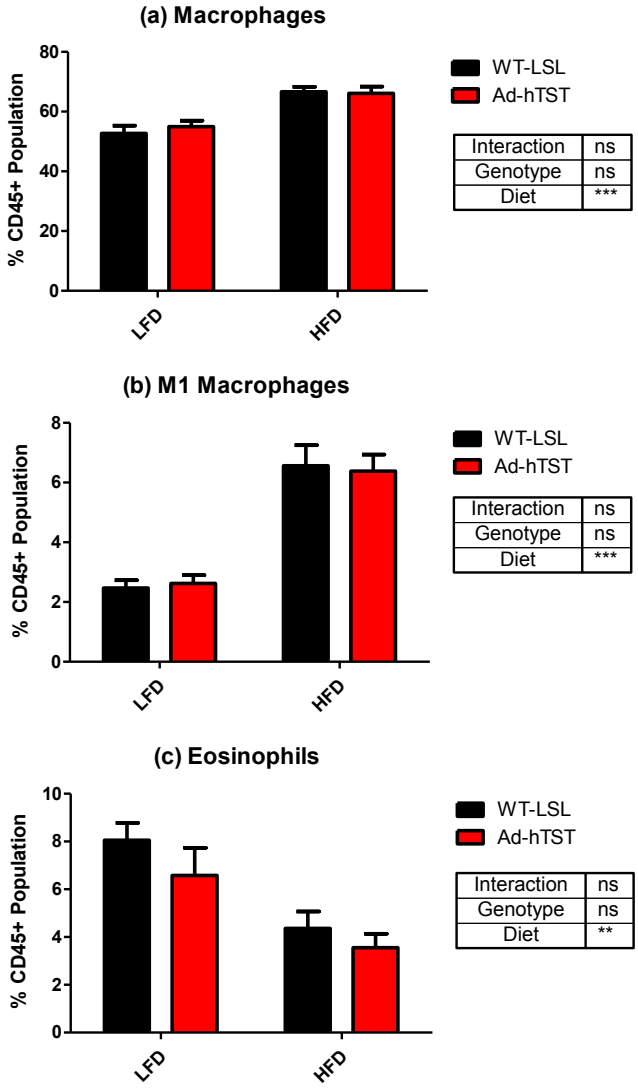

Figure 4.19: Immune cell populations in stromal vascular fraction (SVF) of epididymal adipose tissue of Ad-hTST and WT-LSL mice on LFD or HFD for 6 weeks.

*(a) Macrophages ($F4/80^+$ $CD11b^+$ $Ly6C^-$ $MHCII^+$), (b) M1 macrophages ($F4/80^+$ $CD11b^+$ $Ly6C^-$ $MHCII^+$ $CD11c^+$), and (c) eosinophils ($SiglecF^+$) measured in SVF of epididymal fat by flow cytometry. Results are expressed as percentage of hematopoietic population ($CD45^+$). Data are mean ± SEM, analysed by 2-way ANOVA: ** P < 0.01, *** P < 0.001, ns = not significant: (n = 4-6).*

4.3.2.11 *Gene expression of pro-inflammatory adipokines were not different in adipose tissue of Ad-hTST versus WT-LSL mice on LFD or HFD for 6 weeks.*

Gene expression of pro-inflammatory adipokines was measured in epididymal fat to assess the impact of increased TST expression on adipose tissue inflammatory markers after exposure to HFD. Plasminogen activator inhibitor 1 (*Pai1*) was significantly increased by HFD in both WT-LSL and Ad-hTST mice (Figure 4.20a). Monocyte chemotactic protein 1 (*Mcp1*) was also increased by HFD in both genotypes (Figure 4.20b).

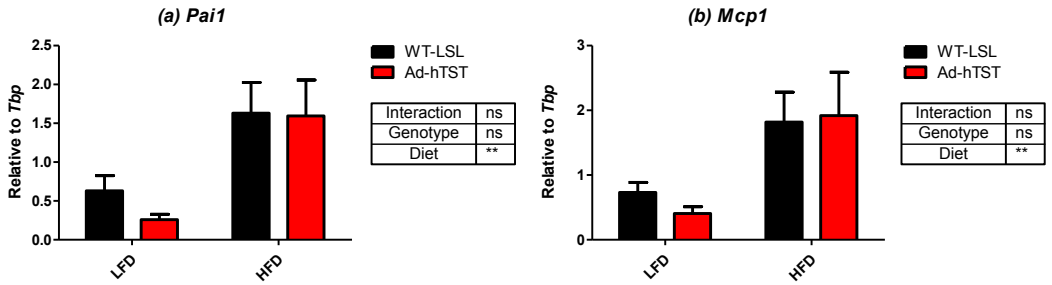

Figure 4.20: Gene expression of pro-inflammatory adipokines in epididymal adipose tissue of Ad-hTST and WT mice on LFD or HFD for 6 weeks.

*(a) Plasminogen activator inhibitor 1 (Pai1), and (b) monocyte chemotactic protein 1 (Mcp1) mRNA abundance normalised to housekeeping gene Tbp. Data are mean ± SEM, analysed by 2-way ANOVA: ** P < 0.01, ns = not significant; (n = 5-7).*

4.3.2.12 *Gene expression of endoplasmic reticulum stress markers were unchanged in adipose tissue of Ad-hTST and WT-LSL mice on LFD or HFD for 6 weeks.*

To assess activation of the unfolded protein response, the expression of two key genes involved in this process was measured in epididymal fat of Ad-hTST mice after 6 weeks of HFD. Expression of activating transcription factor 4 (*Atf4*) and C/EBP-Homologous Protein (*Chop*) was unchanged by increased TST expression or HFD (Figure 4.21).

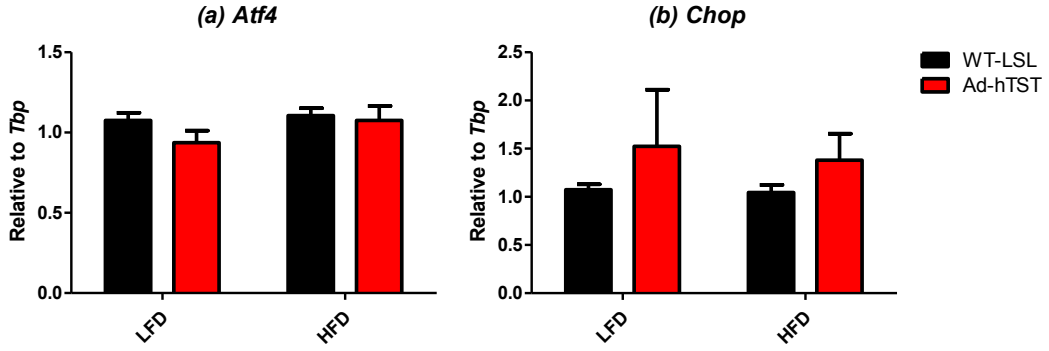

Figure 4.21: Gene expression of endoplasmic reticulum stress markers in epididymal adipose tissue of Ad-hTST and WT mice on LFD or HFD for 6 weeks.

(a) Activating transcription factor 4 (Atf4) and (b) C/EBP-Homologous Protein (Chop) mRNA abundance normalised to housekeeping gene Tbp. Data are mean ± SEM, analysed by 2-way ANOVA: ns = not significant; (n=5-7).

4.3.2.13 Gene expression of mouse Tst was reduced in adipose of Ad-hTST versus WT-LSL mice on LFD diet, and in adipose of both genotypes on HFD for 6 weeks.

Expression of human TST and the endogenous mouse gene was assessed in epididymal adipose tissue of Ad-hTST and WT-LSL mice after 6 weeks of HFD. Human TST was undetectable or very low in all WT-LSL samples, and highly expressed in adipose from Ad-hTST mice, with no change on HFD (Figure 4.22a). Endogenous mouse *Tst* expression was significantly reduced in Ad-hTST on LFD compared to WT-LSL. HFD caused a reduction in *Tst* expression in WT-LSL mice only, leading to a finding of significant interaction between genotype and diet (Figure 4.22b). TST protein content in epididymal adipose tissue was measured by Western blot. No detectable bands were observed for WT-LSL samples, however TST protein content was high in adipose from Ad-hTST mice (Figure 4.22c).

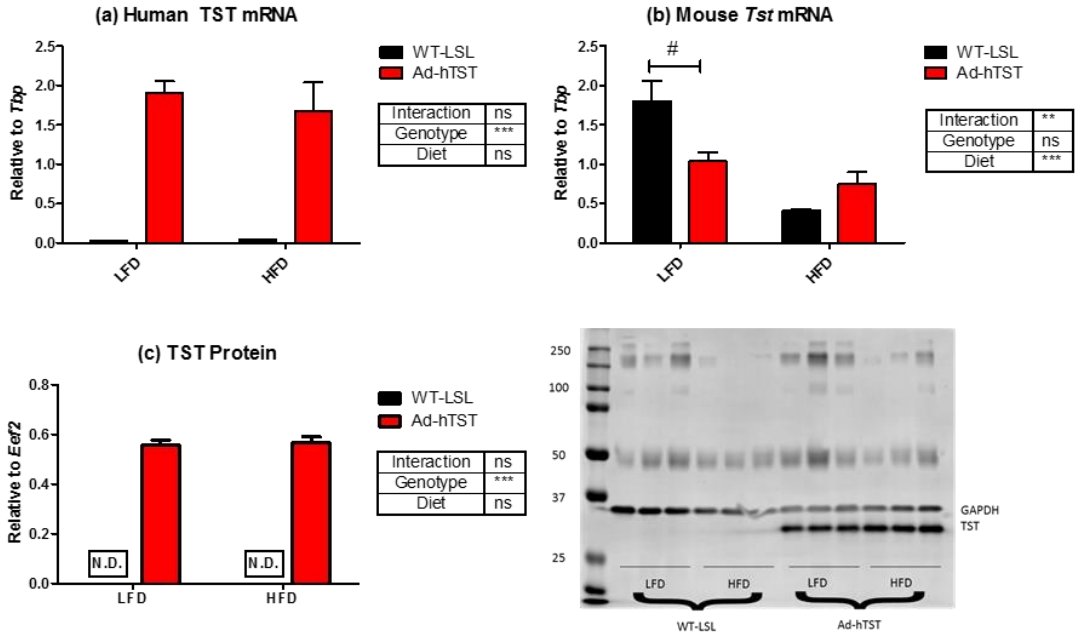

Figure 4.22: TST gene and protein expression in epididymal adipose tissue of Ad-hTST and WT mice on LFD or HFD for 6 weeks.

*Abundance of human TST, and (b) mouse Tst mRNA normalised to housekeeping gene Tbp; (c) TST protein abundance normalised to GAPDH, with representative image of Western blot. Data are mean ± SEM, analysed by 2-way ANOVA: ** P < 0.01, *** P < 0.001, ns = not significant; with Bonferroni post-hoc test comparing between genotypes for each diet: # P < 0.05; (n=5-7; N.D. = not detected).*

4.3.2.14 *Gene expression of H_2S-producing enzymes were not different in adipose tissue of Ad-hTST versus WT-LSL mice on LFD or HFD for 6 weeks.*

Gene expression of two enzymes responsible for producing sulfide were measured in epididymal white adipose tissue. No significant difference was found in expression of cystathionine γ lyase (*Cse*) in adipose of Ad-hTST and WT-LSL mice on LFD or HFD (Figure 4.23a). Mercaptopyruvate sulfurtransferase (*Mpst*) was lower in adipose of mice on HFD, with no significant difference between genotypes (Figure 4.23b).

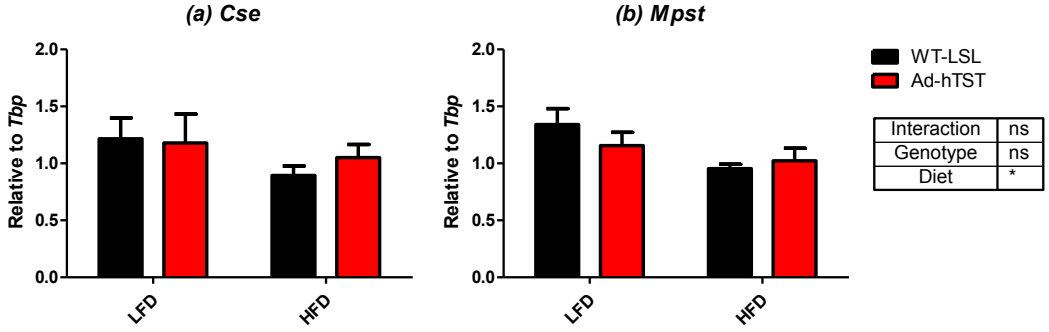

Figure 4.23: Gene expression of H_2S-producing enzymes in epididymal adipose tissue of Ad-hTST and WT-LSL mice on LFD or HFD for 6 weeks.

*(a) Cystathionine γ lyase (Cse), and (b) mercaptopyruvate sulfurtransferase (Mpst) mRNA abundance normalised to housekeeping gene Tbp. Data are mean ± SEM, analysed by 2-way ANOVA: * P <0.05, ns = not significant; (n=5-7).*

4.3.2.15 *Gene expression of H_2S oxidation enzymes were not different in adipose tissue of Ad-hTST versus WT-LSL mice on LFD or HFD for 6 weeks.*

The gene expression of enzymes involved in the oxidation of sulfide was measured. Ethylmalonic encephalopathy protein 1 (*Ethe1*) was unchanged by increased TST expression or HFD (Figure 4.24a). Sulfide-quinone oxidoreductase (*Sqrdl*) was reduced by HFD in both Ad-hTST and WT-LSL mice (Figure 4.24b).

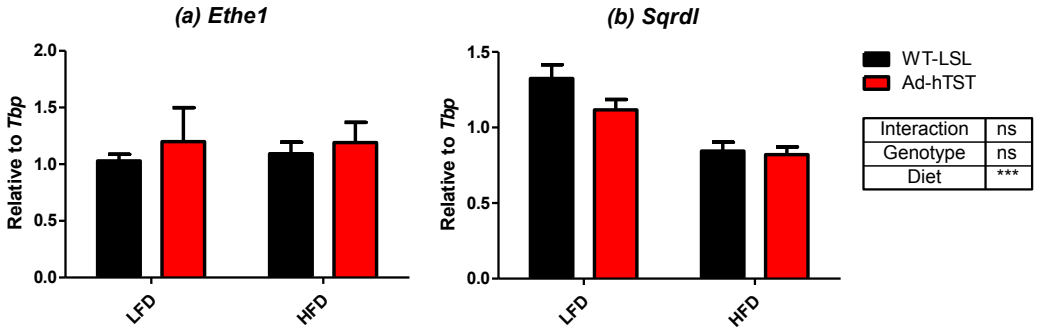

Figure 4.24: Gene expression of sulfide oxidation genes in epididymal adipose tissue of Ad-hTST and WT-LSL mice on LFD or HFD for 6 weeks.

*(a) Ethylmalonic encephalopathy protein 1 (Ethe1), and (b) sulfide:quinone oxidoreductase (Sqrdl) mRNA abundance normalised to housekeeping gene Tbp. Data are mean ± SEM, analysed by 2-way ANOVA: *** P < 0.001, not significant; (n=5-7).*

4.4 DISCUSSION

Thiosulfate sulfurtransferase, when over-expressed in adipose tissue, was previously found to be protective against metabolic impairment due to exposure to a high fat diet (Morton *et al.* 2016). These mice, called Adipoq-*Tst*, expressed the mouse *Tst* gene under the control of the adiponectin promoter which led to a modest 2-fold increase in *Tst* expression in adipose tissue. For this chapter, Ad-hTST mice, with adipose-specific over-expression of the human TST gene, were used to test the hypothesis that protection against metabolic impairment was due to a reduction in HFD-induced adipose tissue dysfunction. The mouse was designed to be used for testing potentially therapeutic compounds with human TST enzyme selectivity in future pre-clinical trials. Surprisingly the findings did not show that Ad-hTST mice were protected against metabolic impairment, and so did not replicate the results from previous work with the similar Adipoq-*Tst* mice. Indeed, high fat-fed Ad-hTST mice were potentially more prone to metabolic impairment, having mildly impaired glucose tolerance and elevated fasting insulin. Also, there was no clear evidence of reduced susceptibility to adipose tissue dysfunction, with antioxidant and endoplasmic reticulum stress gene expression and inflammatory cell populations comparable to controls. The lack of metabolic protection in this new mouse model may be due to differences between the mouse and human TST genes, or could highlight a hormetic effect in which a modest increase in TST expression is protective, as in the old Adipoq-*Tst* mouse, but a higher increase is detrimental.

A new mouse model was characterised for use in this study. 8-week-old female mice expressing cre were used to investigate expression of the human TST transgene and compared to female littermates lacking cre (WT-LSL). To get an accurate measurement of the comparable increase in active TST in adipose from Ad-hTST mice, rhodanese activity was measured and found to be 3.5, 2 and 3.3-fold higher in gonadal, mesenteric and subcutaneous fat respectively. This increase was comparable or greater than the increase in *Tst* mRNA and protein achieved in adipose of Adipoq-*Tst* mice (Morton *et al.* 2016). Human *TST* mRNA was detectable at high levels in adipose depots of Ad-hTST mice, but it was not possible to calculate a "fold increase" due to its absence in adipose of controls. TST protein, detected using an antibody

sensitive to both human and mouse TST, was also greatly increased in adipose from Ad-hTST mice, however levels observed in WT-LSL were low or undetectable in some tissues. This was unexpected as TST protein was previously easily identifiable by Western blot in adipose from wild-type mice (Morton *et al.* 2016). This unexpectedly low measurement of TST protein in WT-LSL mice could indicate a difference in TST protein expression in adipose of female mice, which had previously not been assessed. Alternatively, it could be due to a preference of the currently available antibody for human TST over the mouse protein. However, due to time constraints, it was not possible to further investigate the protein levels of TST in adipose from WT-LSL female mice, and it the evidence was sufficient to confirm that TST was present in adipose of Ad-hTST mice at a greatly increased level.

To confirm specificity of the transgene to adipose tissue, mRNA of human TST was measured and found to be absent in liver, kidney and spleen, and very low in lung and heart. As well as this, mCherry fluorescence, visible in adipose tissues from Ad-hTST mice, was absent in liver and muscle samples. Therefore, it was concluded that expression of the human TST transgene was specific to adipose tissues. Human TST was found to be expressed in brown adipose tissue, indicating that cre-mediated excision of the stop cassette occurred in this tissue. The previous model, Adipoq-*Tst*, did not have overexpression of *Tst* in brown fat (Morton *et al.* 2016), and so this highlights another difference between these models that could account for differences in the metabolic phenotypes. Overexpression of TST in brown fat may impact cold-induced thermogenesis and energy expenditure, and must be taken into account in future investigations with these mice.

4.4.1 Metabolic impairment of Ad-hTST mice on HFD.

It was hypothesised that Ad-hTST mice would be protected against metabolic impairment after exposure to a high fat diet, as overexpression of TST in adipose tissue was protective in Adipoq-*Tst* mice (Morton *et al.* 2016). To test this hypothesis, male Ad-hTST mice and littermates were randomised to receive either a high fat diet (HFD: 58% kcal from fat) or low-fat diet (LFD: 10.5% kcal from fat) for 6 weeks, at which point a significant increase in body weight and adipose tissue dysfunction is normally induced in 6N mice (Podrini *et al.* 2013). This feeding regime led to an increase in body weight and fat mass in WT-LSL mice as expected. However, Ad-hTST mice gained a similar amount of weight, and their increase in fat mass was indistinguishable from controls after 3 and 6 weeks of HFD. There was no effect of human TST overexpression in adipose tissue on food intake or feed efficiency, with both genotypes exhibiting increased feed efficiency on HFD, a well-established effect of HFD on 6J mice (West *et al.* 1992). Therefore, Ad-hTST mice do not appear to be protected from weight gain on HFD, as the previous model, Adipoq-*Tst* was.

Despite a similar amount of weight gain, Ad-hTST mice on HFD for 6 weeks were susceptible to metabolic impairment, potentially more-so than WT-LSL mice, challenging the hypothesis that overexpression of TST in adipose is protective. Glucose tolerance of WT-LSL mice deteriorated slightly with 6 weeks of HFD due to a failure to clear glucose as efficiently at later timepoints as mice on LFD. This duration of exposure to HFD does not always induce glucose intolerance in C57BL/6 mice (Matsuzawa-Nagata *et al.* 2008), or may cause only a minor decline (Fisher-Wellman *et al.* 2016) as observed in WT-LSL mice in the current study. Ad-hTST mice however, showed a more pronounced deterioration on HFD, with significantly higher glucose than LFD-fed Ad-hTST mice at every timepoint after administration of a glucose bolus. Added to this, HFD caused a significant increase in plasma insulin in Ad-hTST mice but not WT-LSL mice, suggesting that insulin resistance was induced more in Ad-hTST mice than WT-LSL mice on HFD. This does not conclusively prove that Ad-hTST mice are more metabolically impaired than controls, as there were no significant differences between the genotypes on HFD. Ad-hTST mice on LFD had a significantly lower glucose level than WT-LSL mice 15 minutes after administration,

indicating that these mice cleared glucose quicker than controls. To fully characterise this slight improvement in glucose tolerance in LFD-fed Ad-hTST, more sensitive assessment of the metabolic phenotype of these mice would be required, such as by hyperinsulinemic-euglycemic clamp. However, for the purposes of this investigation, the data do not support the hypothesis that overexpression of human TST in mouse adipose tissue is protective against metabolic deterioration due to HFD. This may be due to differences in the human and mouse TST protein sequences, which will be discussed below.

Plasma adiponectin levels were also investigated to assess the potential impact of overexpression of TST in adipose tissue on this key insulin-sensitising adipokine. High fat feeding led to a reduction in total and HMW adiponectin in both Ad-hTST and WT-LSL mice, a well-characterised effect of obesity in mice and humans (Hu *et al.* 1996; Ye *et al.* 2007). Overexpression of TST in adipose tissue of Ad-hTST mice did not impact this reduction of adiponectin due to high fat feeding. However, Ad-hTST mice showed a reduction in total adiponectin in plasma on LFD, compared to WT-LSL. Adiponectin can be reduced due to oxidative stress (Furukawa *et al.* 2004), hypoxia and activation of the unfolded protein response in adipose tissue (Chen *et al.* 2006; Hosogai *et al.* 2007). There was no indication that epididymal adipose tissue from LFD-fed Ad-hTST was under oxidative or hypoxic stress, and it also showed no reduction in *Adipoq* mRNA. Therefore, this decrease in plasma adiponectin in Ad-hTST mice remains unexplained. Expression of human TST was not assessed in bone marrow adipose tissue of Ad-hTST mice, which has been shown to be a source of adiponectin under certain circumstances (Cawthorn *et al.* 2014). This should be taken into account in future experiments with these mice. Plasma levels of adiponectin in Ad-hTST mice may also have been impacted by insertion of cre recombinase into the adiponectin locus, as in the parent line Adip-cre (Eguchi *et al.* 2011). Therefore, adiponectin was assessed in the plasma of Adip-cre mice and found to be unchanged, indicating that reduced plasma adiponectin in Ad-hTST mice on LFD was a true effect of TST overexpression in adipose tissue. Despite this intriguing effect, it was apparent that Ad-hTST did not recapitulate the phenotype of Adipoq-*Tst* mice, which had higher plasma HMW adiponectin levels than controls on both chow and high fat diet (Morton

et al. 2016), which could potentially account for the lack of protection against metabolic impairment in Ad-hTST mice.

Based on previous work on Adipoq-*Tst* mice, it was hypothesised that Ad-hTST mice would be protected against metabolic impairment due to high fat feeding. However, the data from this experiment do not support this hypothesis, and indicate that Ad-hTST mice may instead be more prone to glucose intolerance on HFD than controls.

4.4.2 Adipose tissue dysfunction of Ad-hTST mice on HFD.

Previous assessment of the impact of HFD on Adipoq-*Tst* mice indicated that the improved metabolic health of these mice may be due to protection against adipose tissue oxidative stress. Adipoq-*Tst* mice maintained expression of *Prx3* and had higher SOD2 protein levels in adipose than WT mice on HFD. It was hypothesised that Ad-hTST mice would exhibit a similar or greater protection from adipose tissue dysfunction due to oxidative stress. However, Ad-hTST mice failed to show protection against metabolic impairment, and this was reflected in the assessment of adipose tissue dysfunction in these mice, with no apparent improvements compared to controls.

Adipose tissue from Ad-hTST mice did not appear to have increased antioxidant capability, or protection from HFD-induced inflammation. Diet-induced obesity in mice leads to a reduction in expression of key antioxidant enzymes such as *Prx3* (Huh *et al.* 2012) and *Gpx4* (Long *et al.* 2013), as well as reducing gene expression and protein levels of the superoxide dismutase enzymes after longer durations of high fat feeding (Han *et al.* 2016; Morton *et al.* 2016). Ad-hTST were not protected against these reductions in antioxidant enzyme expression, showing a similar reduction to WT-LSL mice in expression of *Prx3*, *Gpx4* and *Txn2*. Therefore, Ad-hTST mice were unlike Adipoq-*Tst* mice, which had higher *Prx3* expression in adipose tissue after HFD, one of the mechanisms suggested for the improvement of metabolic health in these mice (Morton *et al.* 2016). As well as the lack of evidence for protection against oxidative stress in adipose from Ad-hTST mice, inflammatory cell infiltration was also not impacted by overexpression of TST. Macrophage content, including M1 pro-inflammatory macrophages increased with HFD in a similar manner to WT-LSL

mice, a well-characterised effect of high fat feeding (Lumeng *et al.* 2007), and numbers of the beneficial eosinophils were reduced (Wu *et al.* 2011). Expression of pro-inflammatory adipokines, *Pai1* and *Mcp1* were increased by high fat feeding in Ad-hTST and WT-LSL. Expression of two regulators of the UPR, *Chop* and *Atf4*, were also unchanged in adipose tissue of Ad-hTST, however a lack of increase in WT-LSL tissue indicates that the duration of exposure to HFD may not have been sufficient to cause UPR activation (Hosogai *et al.* 2007). Therefore, there was no indication that overexpression of human TST reduced adipose tissue dysfunction through minimising oxidative stress or inflammation, and it is likely that this underscores why Ad-hTST mice did not exhibit protection against metabolic impairment on HFD.

4.4.3 Impact of hydrogen sulfide on adipose tissue in Ad-hTST mice.

It was not possible to assess plasma or tissue sulfide levels in Ad-hTST mice, therefore interpreting the potential impact of sulfide on the phenotype of these mice is challenging. Overexpression of TST did not lead to changes in the expression of sulfide-producing or sulfide oxidation enzymes, however HFD-fed mice had reduced expression of both *Mpst* and *Sqrdl*. These enzymes were previously found to be reduced in liver after high fat feeding (Baiges *et al.* 2010; Peh *et al.* 2014), however their expression in mesenteric adipose tissue was not reduced after HFD in a previous cohort described in this thesis (Figure 3.19 and Figure 3.20 on pages 115 and 116). This could be due to a difference effect of HFD on mesenteric and epididymal adipose tissue, or differences between the WT mice in the previous chapter and WT-LSL mice used here. The reduction in expression of these two enzymes indicates that high fat feeding may impact the production and oxidation of sulfide in adipose of both WT-LSL and Ad-hTST mice.

Overexpression of human TST in adipose tissue has a complex effect on expression of the endogenous mouse *Tst* gene, which could impact the phenotype of these mice on HFD. Male Ad-hTST mice on LFD had a 45% reduction in expression of the endogenous *Tst* gene compared to WT-LSL mice, but were protected from further reduction due to HFD. It was not possible to measure the separate activities of these two homologous enzymes, and it could be possible that the functions do not fully

overlap due to differences in the peptide sequences. Further work will be required to ensure the human TST enzyme can fully substitute for the mouse enzyme, and if it is found that these enzymes function differently, the usefulness of the Ad-hTST mouse and its parent line Rosa26^{LSLhTST} may be called into question.

4.4.4 Limitations and future work.

The aims of this chapter were to characterise human TST gene expression in a new mouse model (Ad-hTST), and assess the impact of this on adipose tissue dysfunction and metabolic impairment due to exposure to high fat diet. I have not confirmed that overexpression of TST in adipose tissue is protective against metabolic impairment, as was observed in a previous model with modest overexpression of the mouse *Tst* gene in adipose tissue. I have not uncovered evidence that overexpression of human TST in adipose tissue of Ad-hTST mice protects against oxidative stress and metabolic impairment. However, the findings presented here are not sufficient to definitively disprove the hypothesis that TST in adipose tissue protects against metabolic impairment due to limitations in our study.

Genetic differences between the new Ad-hTST mouse and the previously described Adipoq-*Tst* mouse may account for the phenotypic differences between these models. Both the gene used and the method of targeting its expression to adipose are different between these two lines, and these features could have influenced the phenotype. The Adipoq-*Tst* mouse was made by random insertion of the mouse *Tst* gene, allowing for seamless integration with the endogenous sulfide oxidation system. The Ad-hTST mouse uses the human TST gene, which produces a TST protein that differs from the mouse protein at twenty-seven residues, potentially causing functional differences despite conservation of the active site (Figure 4.25). A lysine residue (K) at position 219 in the mouse protein is predicted to be a potential site of post-translational acetylation or succinylation (Farriol-Mathis *et al.* 2004; Park *et al.* 2013), whereas the human protein has a glutamate (E) amino acid at this residue with no predicted post-translational modifications. While the impact of this specific change in TST is unknown, alternating lysine and glutamate residues was found to dramatically impact the function of an enzyme in *S. cerevisiae* and a transcriptional regulator in *V.*

cholerae (Blanchard and Karst 1993; Singh *et al.* 2013). It is possible that this change, or any of the twenty-seven altered residues between the human and mouse peptide sequences, could impact protein-protein interactions, substrate preference or other aspects of TST function. Therefore, further characterisation of the human TST protein must be carried out to ensure its activity and function in mouse cells mirrors the activity of the mouse protein.

```
Mouse       MVHQVLYRALVSTKWLAESIRSGRLGPSLRVLDASWYSPGTRQARKEYQERHVPGASFFD   60
Human       MVHQVLYRALVSTKWLAESIRTGKLGPGLRVLDASWYSPGTREARKEYLERHVPGASFFD   60
            **********************:*:***.**************:***** ***********

Mouse       IEECRDTTSPYEMMLPSEAHFGDYVGNLGISNDTHVVVYDGDDLGSFYAPRVWWMFRVFG   120
Human       IEECRDTASPYEMMLPSEAGFAEYVGRLGISNHTHVVVYDGEHLGSFYAPRVWWMFRVFG   120
            *******:*********** *.:***.*****.********:.*****************

Mouse       HRTVSVLNGGFRNWLKEGHPVTSEPSRPEPAVFKATLNLSLLKTYEQVLENLQSKRFQLV   180
Human       HRTVSVLNGGFRNWLKEGHPVTSEPSRPEPAVFKATLDRSLLKTYEQVLENLESKRFQLV   180
            ************************************: *************:*******

Mouse       DSRAQGRYLGTQPEPDIVGLDSGHIRGSVNMPFMDFLTKDGFEKSPEELRAIFQDKKVDL   240
Human       DSRSQGRFLGTEPEPDAVGLDSGHIRGAVNMPFMDFLTEDGFEKGPEELRALFQTKKVDL   240
            ***:***:***:**** **********:**********:*****.******:** *****

Mouse       SQPLIATCRKGVTACHVALAAYLCGKPDVAVYDGSWSEWFRRAPPETRVSQGKSGKA      297
Human       SQPLIATCRKGVTACHVALAAYLCGKPDVAVYDGSWSEWFRRAPPESRVSQGKSEKA      297
            ********************************************:******* **
```

Figure 4.25: Comparison of mouse and human TST protein sequence.

Multiple sequence alignment carried out using Clustal Omega program (online open access tool; Sievers et al. 2014). Asterisk (*) indicates conserved residue; colon (:) indicates change to amino acid with strongly similar properties; period (.) indicates change to amino acid with weakly similar properties; yellow text (position 219) indicates site of potential post-translation modification in mouse protein; red box (position 248) indicates active site cysteine (Farriol-Mathis *et al.* 2004; Park *et al.* 2013).

The cre-*loxP* system, driven by the adiponectin promoter, was used to direct expression of the human TST gene to adipose tissue in Ad-hTST mice. Certain problems associated with the cre-*loxP* system have been identified and may have impacted the efficiency of cre-mediated excision of the STOP cassette in this current study, and thus impacted the phenotype of these mice. The adult Adip-cre mouse is known to have off-target expression of cre in the skin, thyroid gland, salivary gland, testis, uterus and, as found here, in brown adipose tissue, as well as expression in other

tissues during embryonic development (Heffner *et al.* 2012; Blake *et al.* 2017). These off-target effects differentiate Ad-hTST from the Adipoq-*Tst* mouse model, and could influence the phenotype of these mice in unknown ways. In certain cre lines, paternal inheritance of the cre transgene leads to incomplete, mosaic recombination in target tissues (Heffner *et al.* 2012). All Ad-hTST mice were generated by breeding male Adip-cre mice with females containing the floxed transgene, potentially causing incomplete activation of TST expression in adipose tissues, which may explain the relatively modest (2 to 3.5-fold) increase in TST activity in adipose tissues of Ad-hTST mice. Due to mouse availability, it was not possible to use Adip-cre females to generate mice for this study, however it will be essential to compare recombination efficiency of male versus female inheritance of the cre transgene in this line by breeding with a fluorescent reporter line (Klinger *et al.* 2010). Use of this reporter line will also allow for assessment of variation between littermates, another problem associated with the cre-*loxP* system (Heffner *et al.* 2012). In the current study, variability within groups was apparent, especially in the measurement of gene expression. This variability could have been due to the study being carried out with three separate batches of mice, or because mice are on a mixed background of 6N and 6J substrains, but variability from cre expression may also have contributed. The cre-*loxP* system has also been associated with apoptosis in developing embryos due to toxicity caused by cre (Naiche and Papaioannou 2007). To understand the impact of potential cre toxicity in Ad-hTST, Adip-cre littermates should be included as an extra control, but were unfortunately unavailable in this study as the Rosa26^{LSLhTST} parents were homozygous. The contribution of these limitations with the cre-*loxP* system to the phenotype of Ad-hTST mice is unknown, but may account for the phenotypic differences between this model and the previous Adipoq-*Tst* mouse. It will be essential to confirm that efficient expression and activity of cre in adipose tissues has occurred in any future experiments with Ad-hTST mice.

The data presented in this chapter do not support the hypothesis that TST in adipose tissue protects against oxidative stress and adipose tissue dysfunction, and thus helps to maintain metabolic health during exposure to high fat diet. However, the new mouse model discussed here may have inherent problems that were not anticipated

prior to its development and use in this chapter. The human TST protein expressed in adipose tissue of the Ad-hTST mouse may not be functionally comparable to the endogenous mouse protein, and its expression within adipose depots may not be uniform, and could be variable between littermates. These potential problems must be investigated as possible explanations for why Ad-hTST mice do not have the expected phenotype.

Chapter 5 The role of thiosulfate sulfurtransferase in the response to oxidative stress.

5.1 INTRODUCTION

Several pieces of evidence from the literature and from work carried out in this lab suggest a potential role for TST in protecting against oxidative stress. While the results from chapter 3 show that mice lacking *Tst* may be more susceptible to metabolic impairment, it was not possible to show that the phenotype was due to a deteriorating response to oxidative stress. The aim of this chapter was to directly test the hypothesis that TST is involved in ROS breakdown. An inducer of oxidative stress was tested *in vivo*, but was not suitable for use due to the high risk of causing death. Therefore, primary adipocytes and hepatocytes were used to investigate the impact of altered *Tst* expression on ROS breakdown and mitochondrial ROS production *in vitro*.

It was hypothesised that TST may interact with ROS directly, or indirectly by collaboration with antioxidant enzymes. TST can be oxidised by H_2O_2 at its active site cysteine forming a sulfenic acid, which is reversible by thioredoxin, resulting in the oxidation of NADPH and the neutralisation of the attacking H_2O_2 (Nandi *et al.* 2000). This has been observed in a cell-free system, and has not been confirmed in a whole cell. However, previous work from our lab showed that 3T3-L1 adipocytes with si-RNA-mediated knockdown of *Tst* had higher levels of mitochondrial ROS after exposure to H_2O_2 (Morton *et al.* 2016). As well as this *in vitro* evidence, mice with increased *Tst* expression in adipose tissue have increased protein levels of SOD2 and mRNA levels of *Prx3*, two key antioxidant enymes (Morton *et al.* 2016). In chapter 3 of this thesis, mice lacking *Tst* had reduced expression of these and other antioxidant enzymes (see Figure 3.12 on page 105). Another mechanism by which Tst may interact with ROS is through modulation of H_2S, which can act as an antioxidant my directly neutralising ROS or altering the function or transcription of antioxidant enzymes (discussed in paragraph 1.3.3.2 on page 49). While this evidence suggests that TST plays an antioxidant role in cells, it has not been shown directly that altered TST levels lead to altered ROS production or breakdown. One of the aims of this chapter was

therefore to directly test the ability of cells lacking *Tst* – or with overexpression of human TST – to breakdown and produce ROS.

Initially an attempt was undertaken to to induce oxidative stress in vivo using paraquat. Paraquat (chemical name: N,N′-dimethyl-4,4′-bipyridinium dichloride) is a commonly used herbicide, which when ingested in lethal amounts causes respiratory failure with pulmonary oedema, as its primary target organ for toxicity is the lungs (Lock and Wilks 2010). It is used to induce oxidative stress as it undergoes redox cycling *in vivo*. In its reduced form (PQ^{+}), paraquat is oxidised in the presence of oxygen becoming PQ^{2+}, and producing superoxide as a by-product (Figure 5.1). PQ^{2+} is then reduced by NADPH dehydrogenase or similar enzymes using NADPH present in cells, thus recycling the paraquat molecule. Paraquat causes cellular damage by producing an excess of superoxide, which when turned into H_2O_2 by the action of SOD enzymes, overwhelms the antioxidant machinery of the cell resulting in the production of hydroxyl radical and subsequent oxidative damage (Lock and Wilks 2010). Paraquat is commonly used *in vivo* to assess resistance to oxidative stress-induced death when administered at high doses of 50mg/kg or above (Luo *et al.* 2008; Bokov *et al.* 2011). Lower doses are used to assess the impact of oxidative stress on specific body systems such as dopaminergic neurons (McCormack *et al.* 2005) and the lungs (Zheng *et al.* 2015). Therefore, to minimise the risk of death of the mice in this study, it was decided to carry out preliminary investigations to find the lowest dose of paraquat at which oxidative stress would be measurable in adipose tissue.

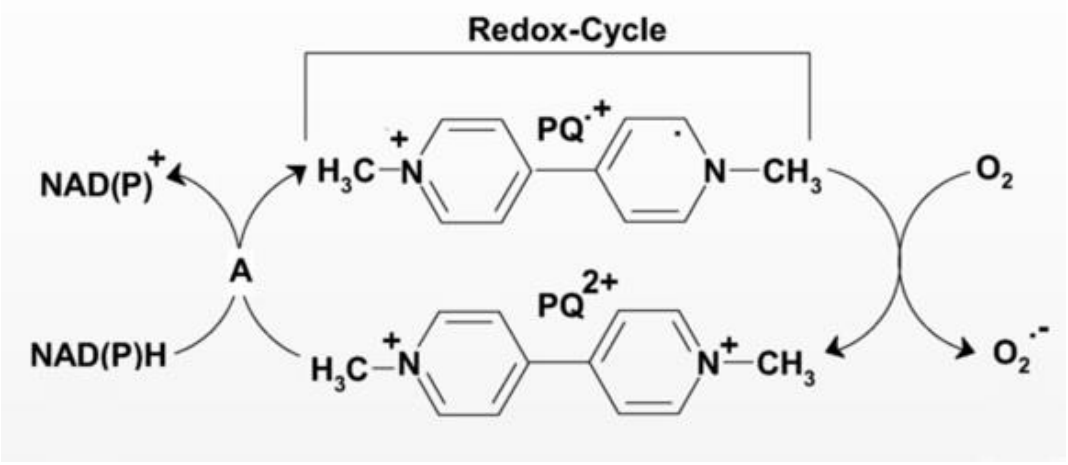

Figure 5.1: Chemical structure and redox cycling mechanism of paraquat dichloride (PQ) in the production of superoxide in vivo.

A: NAPH dehydrogenase or other cellular diaphorase enzyme; $O_2^{\cdot-}$: superoxide ion; (adapted from Dinis-Oliveira *et al.* 2008)*.*

As well as an *in vivo* assessment of the response to oxidative stress in mice with altered *Tst* expression, it was decided to carry out *in vitro* experiments to investigate ROS production and consumption in response to H_2O_2-induced oxidative stress. As TST has been suggested to potentially contribute to the breakdown of H_2O_2 (Nandi *et al.* 2000), an assay was developed to test this in primary adipocytes from *Tst*$^{-/-}$ and Ad-hTST mice. H_2O_2 consumption was assessed by measuring the level of H_2O_2 remaining in the media after a short incubation period. Primary adipocytes from *Tst*$^{-/-}$ mice were also used to test for changes in mitochondrial ROS production in response to exogenous H_2O_2 exoposure. This model of *in vitro* oxidative stress was previously used by our group and others to induce mitochondrial superoxide production which can be measured using the fluorescent MitoSOX™ red mitochondrial superoxide indicator (Huh *et al.* 2012; Morton *et al.* 2016). Unfortunately, primary adipocytes were too fragile for this experiment, and it was difficult to accurately measure fluorescence as they floated outside the range of measurement. Therefore, primary hepatocytes were harvested from *Tst*$^{-/-}$ and WT, and used to investigate the impact of *Tst* loss on mitochondrial ROS production during oxidative stress.

This chapter describes the results of these experiments to uncover a potential role for TST in the breakdown of ROS. It was not possible to use paraquat as an inducer of oxidative stress *in vivo* under the conditions tested here. *In vitro* experiments, while not uncovering major differences in the ability of adipocytes lacking or with extra TST to dispose of H_2O_2, did uncover an unexpected finding in hepatocytes lacking *Tst* that remains to be fully eluidicated in future work.

5.1.1 Hypothesis & Aims

In this chapter, I hypothesised that thiosulfate sulfurtransferase protects against excessive damage during oxidative stress in adipose tissue.

The aims of this chapter were:

- To develop a model of induced oxidative stress in adipose tissue *in vivo*, and assess the outcome in mice with altered *Tst* expression.
- To assess the impact of *Tst* knockout and overexpression in adipocytes on mitochondrial ROS levels and ROS disposal *in vitro*.

5.2 METHOD

5.2.1 Induction of oxidative stress *in vivo* using paraquat

To test the efficacy of paraquat dichloride (PQ) as an inducer of oxidative stress in adipose tissue *in vivo*, PQ (in physiological saline 0.9%) was administered to WT, *Tst*$^{-/-}$ or heterozygous (*Tst*$^{+/-}$) mice by intraperitoneal injection. Three preliminary studies were carried out, with increasing doses and time of exposure. No consistent effects of PQ on markers of oxidative stress in adipose tissue were observed in any of these studies, and so only the results from the study using the highest dose (25mg/kg) are included here. Results from the first and second pilot studies are included in the appendix (page 213). At the end of each study, mice were culled by decapitation and organs were harvested for analysis.

5.2.2 Induction of oxidative stress *in vitro*

5.2.2.1 Primary adipocyte isolation

Male mice between 8 and 12 weeks of age were culled by CO_2, followed by cervical dislocation and epididymal adipose tissue was harvested. This was used to isolate primary adipocytes by collagenase digestion as described on page 76. *Tst*$^{-/-}$ mice and WT (C57BL/6J) mice were used for measurement of H_2O_2 disposal and mitochondrial ROS production. Ad-hTST and WT-LSL mice were used for measurement of H_2O_2 disposal only.

5.2.2.2 Primary hepatocyte isolation

Male mice around 12 weeks of age were culled by CO_2, followed by cervical dislocation, and hepatocytes were isolated according to the protocol described on page 77. Primary hepatocytes were cultured on a 96-well plate and were allowed to settle overnight before experiments were carried out to assess mitochondrial ROS production.

5.3 RESULTS

5.3.1 Paraquat as an inducer of adipose tissue oxidative stress *in vivo*.

5.3.1.1 PQ caused weight loss in heterozygous Tst$^{+/-}$ mice at 24hrs post-injection.

PQ (25mg/kg) or saline was administered to heterozygous *Tst*$^{+/-}$ mice, and after 24hrs, mice were culled and epididymal adipose tissue and lung were collected to assess for effects of PQ, including changes in weight, malondialdehyde content and antioxidant gene expression. PQ-treated mice lost significantly more weight than controls, losing an average of 13% of their starting body weight compared to 4.9% for controls (Figure 5.2).

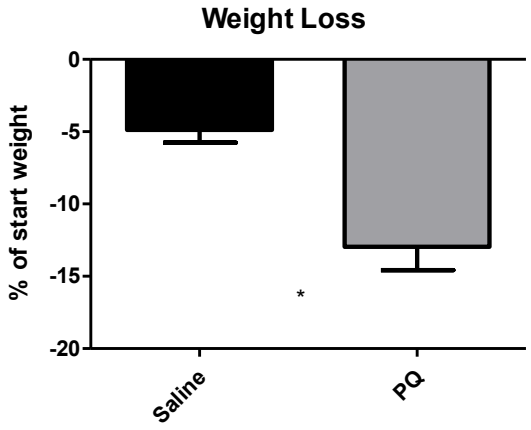

Figure 5.2: Weight loss of Tst$^{+/-}$ mice at 24hrs after administration of PQ (25mg/kg) or saline (0.9%).

*Weight loss expressed as percentage of starting weight. Data are mean ± SEM, analysed by Student's t-test: * P < 0.05; (n=3).*

5.3.1.2 PQ did not alter white adipose tissue weight, malondialdehyde content and antioxidant gene expression at 24hrs post-injection.

The weight of epididymal, mesenteric and subcutaneous white adipose depots were unchanged by exposure to PQ (25mg/kg) for 24hrs (Figure 5.3a). Malondialdehyde (MDA), a product of lipid peroxidation and a marker of oxidative stress, was unchanged in epididymal adipose tissue after PQ treatment (Figure 5.3b). Expression of antioxidant genes *Prx3*, *Gpx1*, *Sod2*, *Txn2*, *Sod1* and *Prx1* in epididymal adipose were unaffected by PQ (Figure 5.3c).

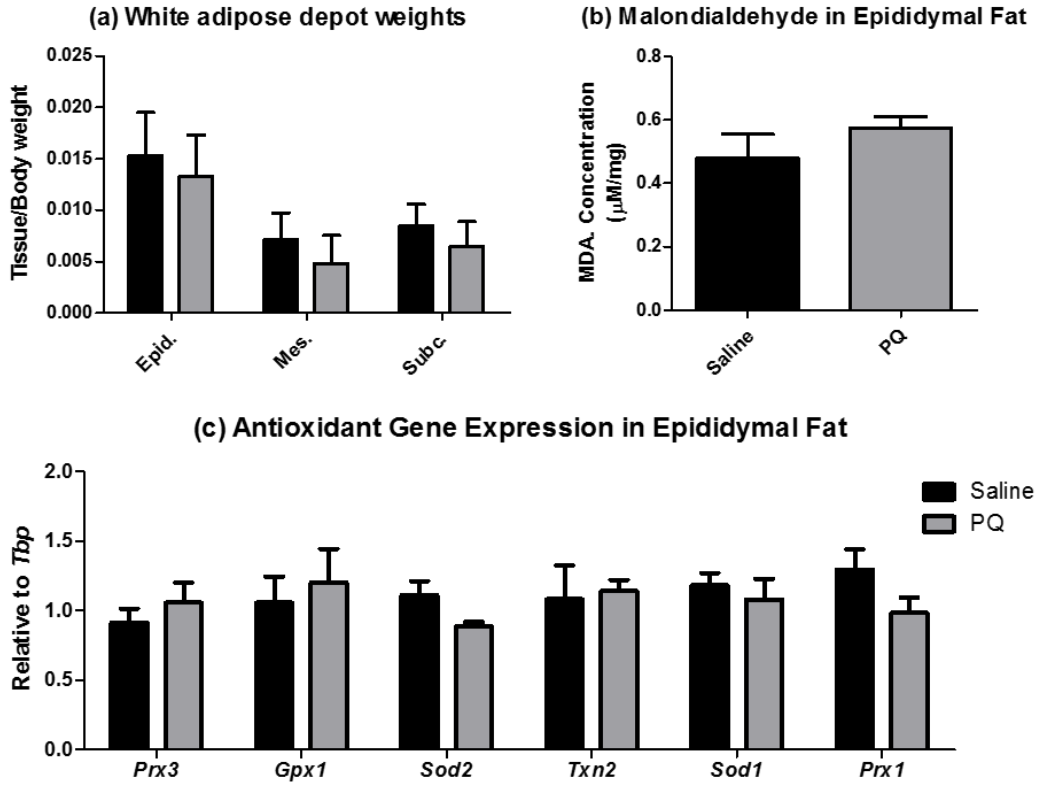

Figure 5.3: White adipose tissue response in Tst$^{+/-}$ mice at 24hrs after administration of PQ (25mg/kg) or saline (0.9%).

(a) White adipose depot weights, (b) malondialdehyde content and (c) mRNA abundance of antioxidant genes normalised to housekeeping gene Tbp in epididymal adipose tissue. Data are mean ± SEM, analysed by Student's t-test: not significant; (n=3).

5.3.1.3 PQ does not alter lung weight or antioxidant gene expression at 24hrs post-injection.

24hr exposure to PQ (25mg/kg) in *Tst*$^{+/-}$ mice did not alter the weight of the lungs compared to saline-treated mice (Figure 5.4a). Expression of antioxidant genes *Prx3*, *Gpx1*, *Sod2*, *Txn2*, *Sod1* and *Prx1* were unchanged in lung tissue of PQ-treated mice (Figure 5.4b).

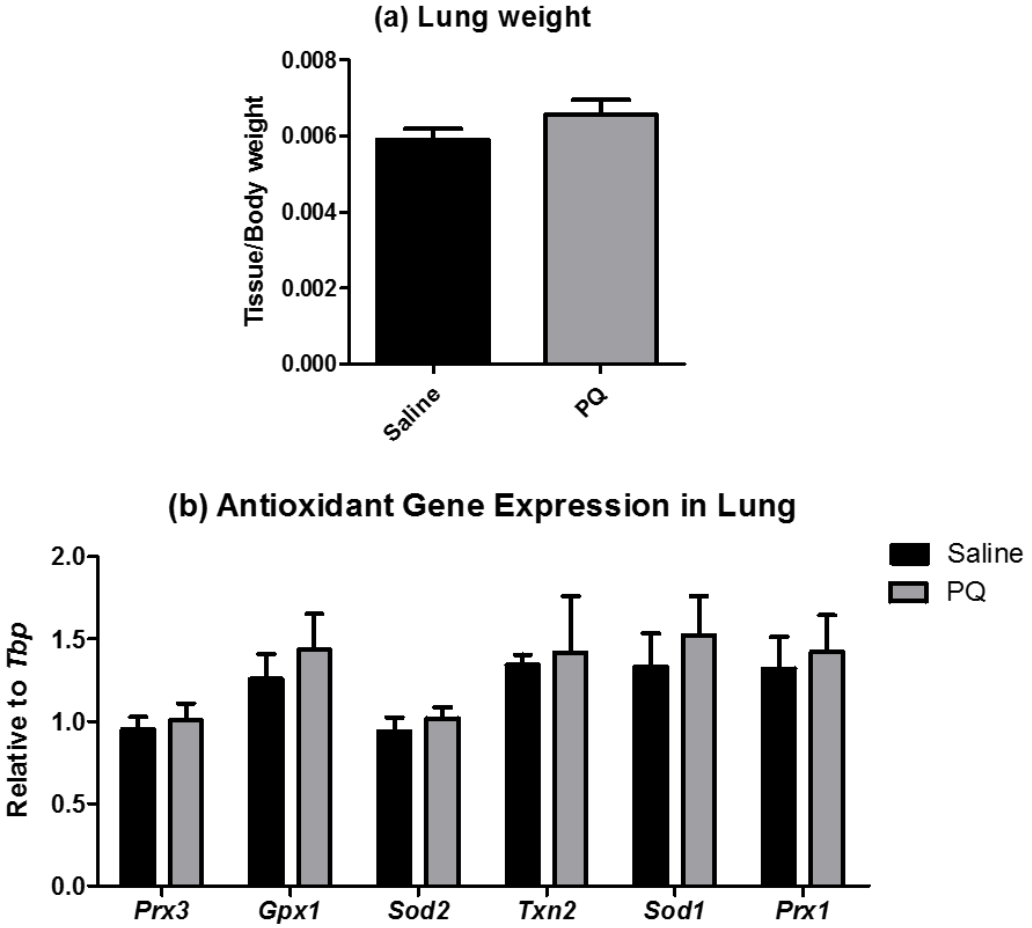

Figure 5.4: Lung response in Tst$^{+/-}$ mice at 24hrs after administration of PQ (25mg/kg) or saline (0.9%).

(a) Lung weight, (b) mRNA abundance of antioxidant genes normalised to housekeeping gene Tbp in lung tissue. Data are mean ± SEM, analysed by Student's t-test: not significant; (n=3).

5.3.2 Consumption of ROS by primary adipocytes from *Tst*$^{-/-}$ and Ad-hTST mice.

5.3.2.1 H_2O_2 consumption is unchanged in primary adipocytes of Tst$^{-/-}$ compared to WT mice.

Primary adipocytes were separated from SVF after collagenase digestion of epididymal adipose tissue of *Tst*$^{-/-}$ and WT mice. Adipocytes from WT and *Tst*$^{-/-}$ mice disposed of H_2O_2 at the same rate, with about 40% of H_2O_2 remaining after 5mins (Figure 5.5).

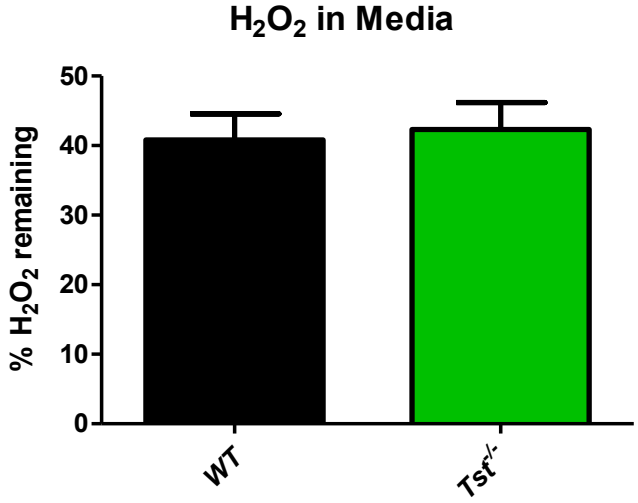

Figure 5.5: Percentage of 100μM H_2O_2 in media after 5mins exposure of primary adipocytes of WT and Tst$^{-/-}$ mice.

Data are mean ± SEM, analysed by Student's t-test: not significant; (WT n=9; Tst$^{-/-}$ n=11).

5.3.2.2 H_2O_2 consumption is unchanged in primary adipocytes of Ad-hTST compared to WT-LSL mice.

H_2O_2 breakdown was also assessed in adipocytes from Ad-hTST mice and their corresponding control line, WT-LSL. There was no significant difference in the amount of H_2O_2 remaining after incubation with adipocytes from WT-LSL or Ad-hTST, with between 24% and 28% of H_2O_2 remaining after 5mins (Figure 5.6).

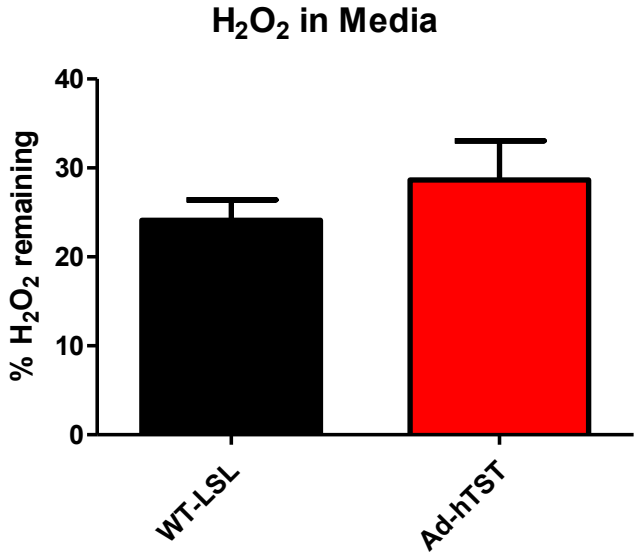

Figure 5.6: Percentage of 100μM H_2O_2 in media after 5mins exposure of primary adipocytes of WT and Ad-hTST mice.

Data are mean ± SEM, analysed by Student's t-test: not significant; (WT-LSL n=9; Ad-hTST n=11).

5.3.3 Mitochondrial superoxide production in primary adipocytes from *Tst*$^{-/-}$ mice.

Primary adipocytes were isolated from epididymal adipose tissue of *Tst*$^{-/-}$ and WT mice by collagenase digestion of the tissue, and incubated in H_2O_2 (0.5%; 163mM) for 2hrs prior to measurement of mitochondrial superoxide using MitoSOX. H_2O_2 caused a similar increase in mitochondrial superoxide in adipocytes from both WT and *Tst*$^{-/-}$ mice (Figure 5.7a). Cell death was assessed by measuring lactate dehydrogenase activity (LDH) in the media following pre-incubation. H_2O_2 led to an increase in LDH activity in the media of both *Tst*$^{-/-}$ and WT samples (Figure 5.7b).

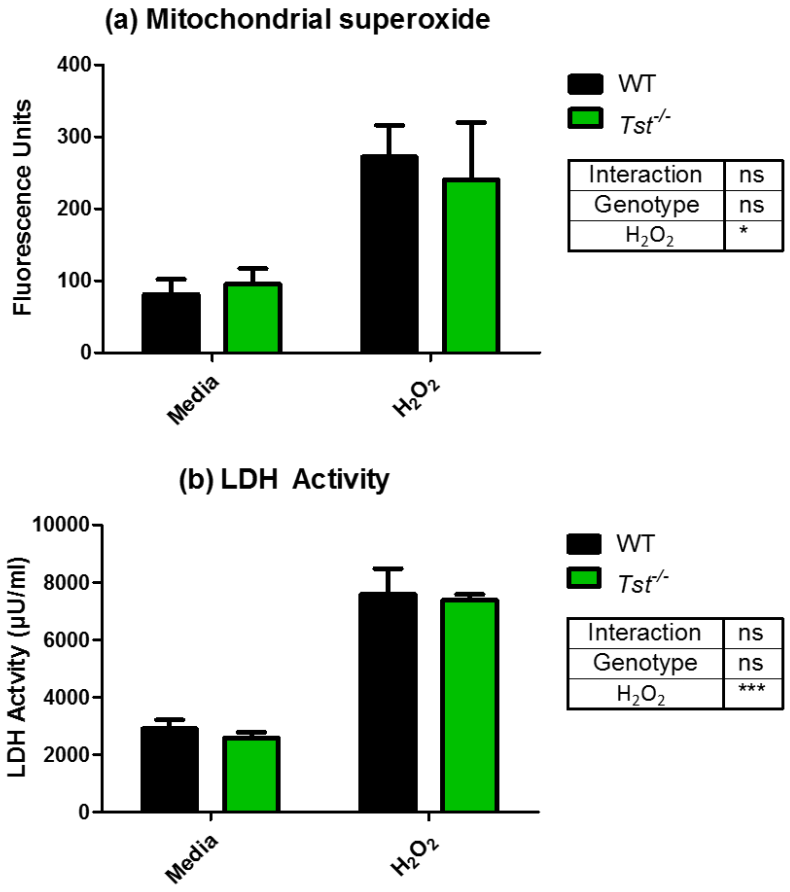

Figure 5.7: Mitochondrial superoxide and LDH activity of primary adipocytes of Tst$^{-/-}$ and WT mice exposed to H_2O_2 (0.5%) for 3hrs.

*(a) Mitochondrial superoxide as fluorescence of MitoSOX dye, and (b) lactate dehydrogenase (LDH) activity in media. Data are mean ± SEM, analysed by 2-way ANOVA: * P <0.05, *** P < 0.001, ns = not significant; (n=2-3).*

Measurement of fluorescence in primary adipocytes was problematic due to technical challenges of working with floating cells. Because of the fragility of adipocytes *in vitro*, many samples were left with too few cells to give an accurate measurement of fluorescence, as the floating cells gathered at the edge of the wells outside of the range of the fluorescent plate reader. Therefore, it was decided to change to adherent cells as a model of *Tst* knockout. SVFs were isolated from adipose of $Tst^{-/-}$ and WT mice, and differentiated into adipocytes, however there was great variability in differentiation efficiency between wells, making them unsuitable for this experiment. Therefore, it was decided to use primary hepatocytes as a model for *Tst* knockout, as the high expression of *Tst* in this cell type would amplify any differences between WT and $Tst^{-/-}$ cells.

5.3.4 Mitochondrial superoxide production in primary hepatocytes from *Tst*$^{-/-}$ mice.

5.3.4.1 Exogenous ROS exposure increases mitochondrial superoxide to a lesser degree in primary hepatocytes of Tst$^{-/-}$ compared to WT mice.

Primary hepatocytes [collected by M. Gibbins, Molecular Metabolism group] from *Tst*$^{-/-}$ and WT mice were exposed to increasing concentrations of H_2O_2 for 2hrs followed by MitoSOX to measure mitochondrial superoxide levels. Hepatocytes from *Tst*$^{-/-}$ mice had lower mitochondrial superoxide than WT hepatocytes, especially at lower concentrations of H_2O_2 (125μM – 1mM) (Figure 5.8a). At higher concentrations of H_2O_2 (2mM and above), *Tst*$^{-/-}$ and WT hepatocytes had similar mitochondrial superoxide levels. No differences were observed in LDH release, an indicator of cell death, between *Tst*$^{-/-}$ and WT hepatocytes, although increasing H_2O_2 concentration lead to increased LDH release (Figure 5.8b).

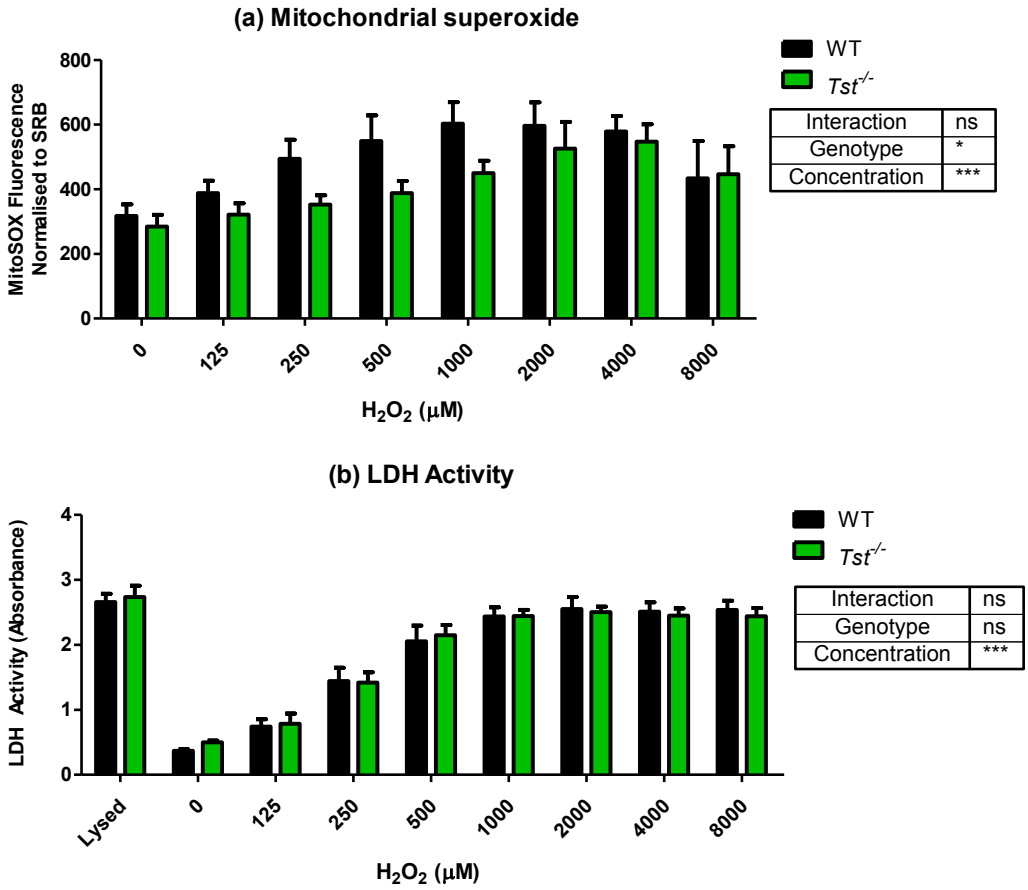

Figure 5.8: Mitochondrial superoxide and LDH activity of primary hepatocytes of $Tst^{-/-}$ and WT mice exposed to H_2O_2 for 2hrs.

*(a) Mitochondrial superoxide as fluorescence of MitoSOX dye, normalised to protein concentration as absorbance of sulforhodamine B (SRB), and (b) lactate dehydrogenase (LDH) activity in media. Data are mean ± SEM, analysed by 2-way ANOVA: * P <0.05, *** P < 0.001, ns = not significant; (n=8). [Hepatocytes collected by M. Gibbins, Molecular Metabolism Group].*

5.3.4.2 Increased mitochondrial superoxide and cell death in response to exogenous ROS is not impacted by pre-incubation of primary hepatocytes of Tst$^{-/-}$ and WT mice with an antioxidant.

Primary hepatocytes were exposed to H_2O_2 (2mM) with or without pre-incubation with the antioxidant N-acetylcysteine (NAC; 1mM). Cells exposed to NAC alone had slightly lower MitoSOX fluorescence than control (* $P < 0.05$), and both groups exposed to H_2O_2 had higher fluorescence than controls (Control vs. H_2O_2: ** $P < 0.01$; NAC vs. NAC + H_2O_2: *** $P < 0.001$). There was no effect of NAC pre-treatment on H_2O_2-related MitoSOX fluorescence (Figure 5.9a). No differences were observed in LDH activity between hepatocytes from *Tst*$^{-/-}$ and WT mice (Figure 5.9b).

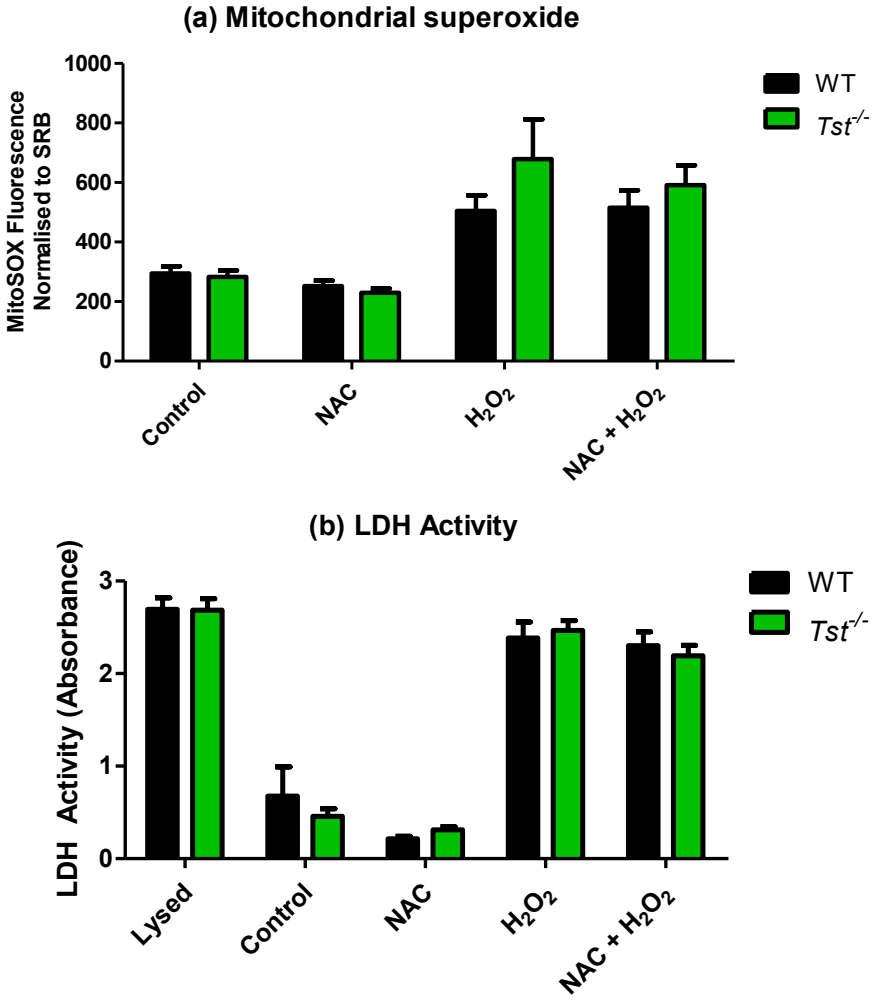

Figure 5.9: Mitochondrial superoxide and LDH activity of primary hepatocytes of $Tst^{-/-}$ and WT mice exposed to H_2O_2 for 2hrs with or without pre-incubation with an antioxidant.

(a) Mitochondrial superoxide as fluorescence of MitoSOX dye, normalised to protein concentration as absorbance of sulforhodamine B (SRB) in hepatocytes pre-incubated in N-acetylcysteine (NAC: 1mM) or media for 1hr, followed by 2hrs in H_2O_2 (2mM) or media; (b) lactate dehydrogenase (LDH) activity in media. Data are mean ± SEM, analysed by 2-way ANOVA comparing genotypes and two treatments: description in text; (n=6). [Hepatocytes collected by M. Gibbins].

5.3.4.3 Increased mitochondrial superoxide and cell death in response to exogenous ROS is not impacted by altered sulfide levels in primary hepatocytes of Tst$^{-/-}$ and WT mice.

To assess the impact of sulfide on hepatocyte responses to exogenous ROS, primary hepatocytes from *Tst*$^{-/-}$ and WT mice were pre-incubated for 1hr with a sulfide donor, disodium sulfide (Na_2S: 200μM) or DL-propargylglycine (PAG: 10mM), an inhibitor of the enzyme that generates H_2S from cystathionine, CSE. As Na_2S dissolves in water, it forms $2Na^+$, $2OH^-$ and H_2S and so sodium hydroxide was used a vehicle control at twice the concentration of Na_2S (400μM). There were no significant differences between *Tst*$^{-/-}$ and WT hepatocytes in their mitochondrial superoxide response after a pre-exposure to increased sulfide or inhibition of CSE activity (Figure 5.10a). In the presence of H_2O_2 (2mM), fluorescence was significantly increased for each condition (*** $P < 0.001$). LDH activity was also increased by treatment with H_2O_2 (*** $P <$ 000.1), although no differences were observed with pre-treatment with Na_2S or PAG, or between *Tst*$^{-/-}$ and WT hepatocytes (Figure 5.10b)

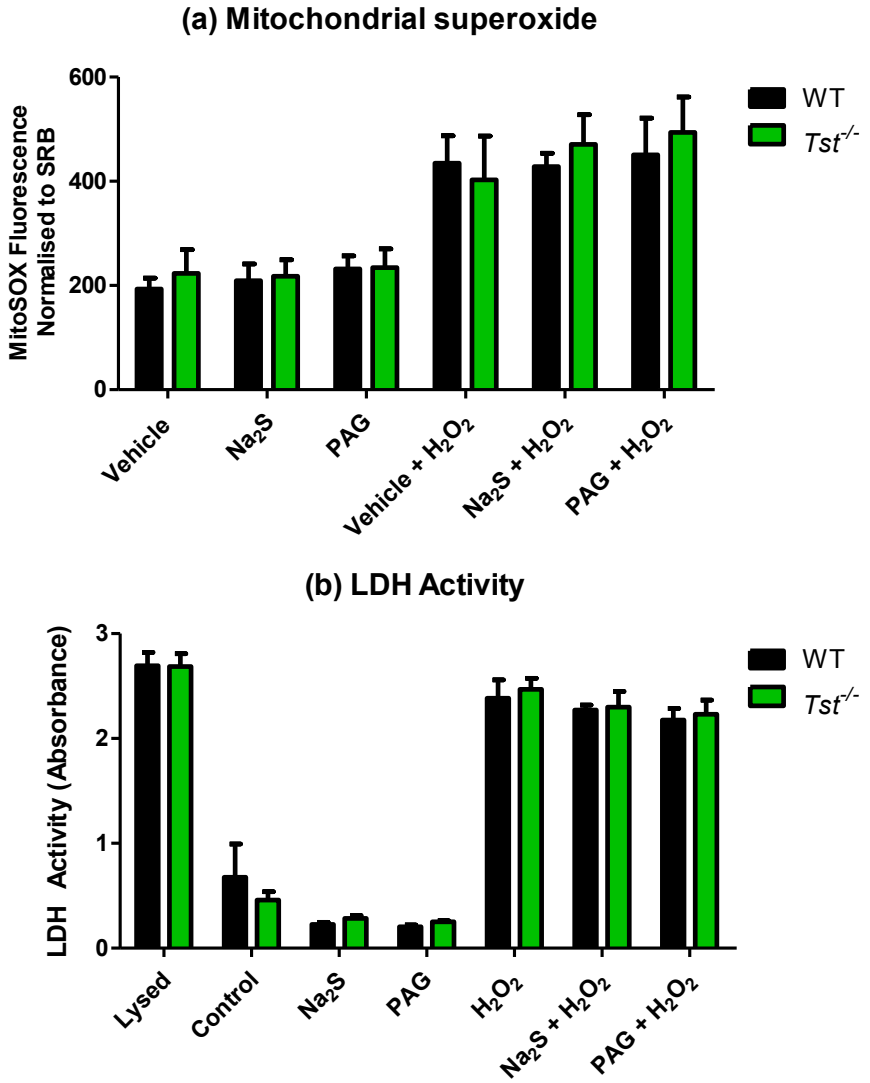

Figure 5.10: Mitochondrial superoxide and LDH activity of primary hepatocytes of $Tst^{-/-}$ and WT mice exposed to H_2O_2 for 2hrs with or without pre-incubation with a sulfide donor or CSE inhibitor.

(a) Mitochondrial superoxide as fluorescence of MitoSOX dye, normalised to protein concentration as absorbance of sulforhodamine B (SRB) in hepatocytes pre-incubated in sodium hydroxide (vehicle: 400μM), sodium disulfide (Na_2S: 200μM) or DL-propargylglycine (PAG: 10mM) for 1hr, followed by 2hrs in H_2O_2 (2mM) or media; (b) lactate dehydrogenase (LDH) activity in media. Data are mean ± SEM, analysed by 2-way ANOVA comparing genotypes and two treatments: description in text; (n=6). [Hepatocytes collected by M. Gibbins].

5.4 DISCUSSION

It was hypothesised that thiosulfate sulfurtransferase has antioxidant capability, and thus protects against adipose dysfunction and subsequent metabolic impairment caused by high fat diet. There is evidence that TST interacts with thioredoxin and may help to neutralise H_2O_2 *in vitro* (Nandi *et al.* 2000), and our lab showed that a reduction in *Tst* expression in 3T3-L1 adipocytes resulted in increased mitochondrial ROS levels (Morton *et al.* 2016). This chapter aimed to directly test the hypothesis that TST is involved in the breakdown of ROS, and thus is protective against cell dysfunction and death due to oxidative stress. To test this hypothesis, both *in vivo* and *in vitro* models of oxidative stress were used. Paraquat dichloride was chosen as an inducer of oxidative stress *in vivo*, but was found to be ineffective at inducing adipose tissue oxidative stress as the highest dose tolerable under these conditions. The ability of primary adipocytes with altered TST levels to consume H_2O_2 *in vitro* was investigated to test the hypothesis that TST aids in the breakdown of ROS, as previously suggested from experiments using a cell-free system (Nandi *et al.* 2000). The response of mitochondria to oxidative stress, and cell death was also assessed in cells lacking *Tst*, to understand if primary adipocytes from $Tst^{-/-}$ mice have increased mitochondrial ROS production, as previously observed in 3T3-L1 adipocytes with si-RNA-mediated knockdown of *Tst* (Morton *et al.* 2016). Primary adipocytes proved to be a challenging model for this investigation, and so primary hepatocytes were employed as a model of high *Tst* expression to investigate further.

5.4.1 Paraquat as a model of oxidative stress *in vivo*

Paraquat dichloride has been used extensively to induce oxidative stress *in vivo* in mice (McCormack *et al.* 2005; Qian *et al.* 2015; Zheng *et al.* 2015). The dose and length of exposure influence the degree of cellular damage and risk of death, with lower doses (10mg/kg) not usually causing death (McCormack *et al.* 2005), but higher doses (50mg/kg and above) or a longer duration of exposure after a lower dose leading to death (Luo *et al.* 2008; Zheng *et al.* 2015). Three cohorts of mice were used to find the correct dose of paraquat and exposure time that would allow for differentiation of susceptibility to oxidative stress in mice with altered *Tst* expression. Optimal

conditions to induce oxidative stress *in vivo* using paraquat were not found based on these three pilot experiments. In consultation with the Named Veterinary Surgeon (NVS) and due to limitations on the severity limit allowed by the conditions of the project licence, it was decided to not pursue the experiment using a higher dose of paraquat. A further increase in paraquat concentration or exposure time could be lethal, as the highest dose used here (25mg/kg) was reported in one study to cause death by 72hrs in all mice treated by intra-gastric route (death rate confirmed by correspondence with author; Zheng et al. 2015).

The results from only one pilot study, in which the highest dose was tested, were included in this chapter for clarity, however the results from the first two pilot studies are including in the appendix (section 7.2 on page 213). In the first pilot experiment, WT and *Tst*$^{-/-}$ mice were treated with increasing doses of paraquat up to a maximum of 10mg/kg for 24 hours, however no consistent differences in weight loss, MDA or antioxidant gene expression in white adipose tissue were found with paraquat treatment or between genotypes. The second experiment was undertaken in WT mice to investigate if exposure for up to 6 days to an increased dose of paraquat (20mg/kg in two injections of 10mg/kg) would lead to increased markers of oxidative stress. This increased exposure time did not result in consistent changes in MDA concentration in adipose or lung, or changes in antioxidant gene expression. These results, and those from the third pilot experiment included in this chapter, indicate that paraquat treatment is not an ideal method of inducing oxidative stress in adipose tissue *in vivo*. At the doses used here, no significant differences other than in body weight were found to allow investigation of the susceptibility of *Tst*$^{-/-}$ mice to oxidative stress in adipose tissue. Paraquat accumulates in the lung due to active transport into alveolar type I and II epithelial cells by an endogenous polyamine carrier system (Dinis-Oliveira et al. 2008). However, no increase in antioxidant gene expression was found in the lung of mice treated with paraquat in this study, indicating that this dose and length of exposure was inadequate to induce oxidative stress in this tissue, despite the clinically significant weight loss. Paraquat has also been found in high concentrations in kidney after exposure *in vivo* as it is mostly excreted by normal glomerular filtration, however it has not been found to accumulate to the same extent in other organs such as brain,

liver or heart (Kurisaki and Hiroko 1974; Rose et al. 1976). Therefore, it is apparent that paraquat is unsuitable for use as an oxidative stress inducer in our investigation into the role of *Tst* in ROS metabolism in adipose tissue. It was subsequently decided to focus on *in vitro* methods to investigate the impact of altered *Tst* expression on the response to oxidative stress.

5.4.2 The role of TST in the response to oxidative stress in adipocytes *in vitro.*

It was hypothesised that overexpression of *Tst* in adipose tissue was protective against metabolic impairment after a high fat diet challenge due to the antioxidant capabilities of TST. To test this hypothesis, primary cells from $Tst^{-/-}$ and Ad-hTST mice were subjected to oxidative stress *in vitro* in the form of excess exogenous H_2O_2. The ability of adipocytes to dispose of ROS was investigated, as was the mitochondrial response to oxidative stress and cellular toxicity. The results described in this chapter do not support the hypothesis that TST protects against cellular damage due to oxidative stress in adipocytes. Due to the technical limitations of using adipocytes *in vitro*, primary hepatocytes were used to investigate the mitochondrial changes and cell death in response to oxidative stress further, highlighting some potential differences in the function of TST in these two cell types.

A role has been suggested for TST in the disposal of H_2O_2 through interaction with thioredoxin (Nandi *et al.* 2000). Peroxiredoxin 3, a key regulator of mitochondrial H_2O_2 levels, requires the presence of thioredoxin 2 for its recycling by reduction (Chae *et al.* 1999), and it is thought that the interaction of TST with thioredoxin may mimic this reaction (Nandi *et al.* 2000). Therefore, the disposal of H_2O_2 by adipocytes lacking and with overexpression of TST was assessed to investigate if TST influences the cellular breakdown of H_2O_2, and if so, to what degree. Under the conditions described in this chapter, there were no apparent differences between adipocytes lacking *Tst* and those overexpressing human TST and their respective controls in their ability to breakdown H_2O_2. This may be because TST does not interact with thioredoxin in an intact cell, as it was suggested to in a cell-free system (Nandi *et al.* 2000), or it may be due to greater activity of other antioxidant systems masking the impact of altered TST,

such as catalase and the glutathione peroxidases, as well as the peroxiredoxins (Gaetani *et al.* 1996). A large difference was observed between the two control lines, with about 40% of H_2O_2 remaining in media of WT cells, but only about 24% remaining in media of WT-LSL cells. This highlights a potential difference between the substrains of mice, as WT and *Tst*$^{-/-}$ mice were on a pure 6J background, but WT-LSL and Ad-hTST were a mix of 6N and 6J substrains. From the current work, it appears unlikely that TST plays a role in the cellular breakdown of H_2O_2. However, the differences observed here in respect to control line, and the possible influence of substrain should be carefully considered when carrying out similar experiments in future.

At a cellular level, it is likely that TST does not impact the breakdown of H_2O_2, however it may exert antioxidant and protective effects within the mitochondria. Exposure of 3T3-L1 adipocytes to H_2O_2 causes an increase in mitochondrial superoxide levels (Huh *et al.* 2012), and si-RNA-mediated knockdown of TST leads to a further increase (Morton *et al.* 2016). Primary adipocytes from *Tst*$^{-/-}$ mice were used to investigate this mitochondrial response to H_2O_2 further, as well as assessing the impact of altered TST on oxidative stress-induced cell death. Results indicated that H_2O_2 induced a significant increase in mitochondrial ROS and cell death in both *Tst*$^{-/-}$ and WT adipocytes. However, adipocytes proved to be a challenging cell model for this experiment as many adipocytes died during the incubation period, leaving too few to get an accurate fluorescence measurement as the floating cells gathered around the edge of wells, mostly outside the range of the measurement of the plate reader. Because of these technical challenges, it was decided to use primary hepatocytes from *Tst*$^{-/-}$ mice to investigate mitochondrial ROS production and cell death in response to oxidative stress, as they are a more robust cell type in culture, and adhere to the plate, making fluorescence measurements more accurate. However, in future this experiment will be repeated with differentiated SVFs grown on coverslips to allow for imaging of MitoSOX fluorescence. Based on the results described in this chapter, it was not possible to definitively discount any effect of *Tst* knockout in adipocytes on cell death and mitochondrial superoxide production in response to oxidative stress.

5.4.3 Primary hepatocytes lacking *Tst* may be protected against oxidative stress

Primary hepatocytes lacking *Tst* proved to be a more successful cell model for the investigation of mitochondrial superoxide levels and cell death in response to exogenous oxidative stress. This more robust cell model was used to establish a basis for the role of TST in the response to oxidative stress that can be applied to future experiments using differentiated SVFs or a new induced pluripotent stem cell line lacking *Tst*. When interpreting the response to oxidative stress in primary hepatocytes, it must be considered that the effect of *Tst* knockout and potential altered sulfide levels could be very different in these cells compared to adipocytes (as discussed in section 1.3.3.4 on page 53).

Based on evidence that TST interacts with thioredoxin in the breakdown of H_2O_2 (Nandi *et al.* 2000), it was hypothesised that hepatocytes lacking *Tst* would be at a higher risk of cell dysfunction and death when subjected to oxidative stress. However, the data presented here suggest that hepatocytes from $Tst^{-/-}$ mice were not more susceptible to cell death than WT hepatocytes, and instead may be protected from the damaging effects of oxidative stress due to reduced mitochondrial superoxide production in response to H_2O_2. Hepatocytes lacking *Tst* had lower mitochondrial superoxide levels than WT when exposed to H_2O_2 concentrations lower than 2mM, suggesting the absence of TST may have an antioxidant effect. One possible explanation for this reduction in mitochondrial superoxide could be altered sulfide levels due to *Tst* gene knockout. *Tst* knockout leads to an increase in ambient sulfide, as was found in plasma of $Tst^{-/-}$ mice (Morton *et al.* 2016). Increased sulfide levels prevented cell death and promoted the activity of antioxidant enzymes such as the superoxide dismutases, catalase and glutathione peroxidases in endothelial cells exposed to a relatively low dose of H_2O_2 (600μM) (Wen *et al.* 2013). However, in the present study a sulfide donor, Na_2S failed to protect against cell death in WT or $Tst^{-/-}$ primary hepatocytes exposed to a higher concentration of H_2O_2 (2mM). Also, PAG, an inhibitor of the sulfide-producing enzyme CSE, did not cause an increase in cell death as would have been expected if sulfide was protective. It is likely that the concentration of H_2O_2 used here (2mM) was too high, as this concentration was above

the point at which both mitochondrial superoxide and cell death plateaued in WT and *Tst*$^{-/-}$ hepatocytes (1/2mM). This reduction in mitochondrial superoxide could also be due to altered mitochondrial number or size, as recent work from our lab has found that mitochondria in liver sections analysed by electron microscopy from *Tst*$^{-/-}$ mice were on average larger than WT mitochondria, although the absolute number of mitochondria was the same [R. Carter, T. Gillingwater & N Morton unpublished]. Larger mitochondria would be expected to hold more fluorescent MitoSOX dye, thus confounding the differences between WT and *Tst*$^{-/-}$ hepatocytes. In future, this experiment should be repeated using a lower dose of H_2O_2 to probe the effect of H_2S on cell viability and mitochondrial superoxide production in hepatocytes in response to oxidative stress, and a control for mitochondrial content, such as a Mitotracker dye, should be incorporated to account for differences in mitochondrial content between genotypes. *Tst* gene knockout in primary hepatocytes appears to reduce mitochondrial superoxide production in response to oxidative stress, without a subsequent reduction in cell death, and future work will focus on elucidating the role of sulfide in this antioxidant effect, and whether it occurs in adipocytes to the same degree.

5.4.4 Limitations and future work.

This chapter aimed to directly test the hypothesis that TST has antioxidant capabilities in adipose tissue. Unfortunately, it was not possible to induce oxidative stress *in vivo* using paraquat without an unacceptable risk of death to the mice, therefore it was not possible to test this hypothesis in mice. Other chemical inducers of oxidative stress such as TCDD (2, 3, 7, 8-tetrachlorodibenzo-*p*-dioxin) or arsenic may be tested in future (Stohs 1990; Flora 1999), and it is likely that these or paraquat may be more effectively targeted to adipose tissue with less systemic damage by direct injection into the epididymal fat pad. Also, oxidative stress in adipose tissue may be induced by adipose-specific genetic ablation of a key antioxidant enzyme such as peroxiredoxin 3 (Huh *et al.* 2012) or overexpression of NOX4 under the control of an adipose-specific promoter. These transgenic mice, when crossed with mice with adipose-specific knockout or overexpression of *Tst* will be a powerful tool to understand the impact of altered *Tst* on adipose oxidative stress.

Using primary cells from *Tst*$^{-/-}$ and Ad-hTST mice, some aspects of the response of these cells to oxidative stress were assessed. Primary adipocytes are a challenging cell type to use *in vitro* as they are not adherent, and are inherently fragile. This led to limitations in my ability to fully characterise the response of these cells to oxidative stress *in vitro*. To successfully and accurately measure mitochondrial superoxide in this cell type, more cells would be needed per reaction, and so isolated adipocytes from separate mice would have to be pooled. This was not possible during this PhD due to constraints with animal numbers, but may be a possibility in future if a larger number of mice are available to repeat this experiment. Alternatively, measurement of MitoSOX fluorescence using flow cytometry instead of a plate reader may be a more efficient method of measuring fluorescence in this cell type (Majka *et al.* 2014). While primary hepatocytes provided a useful backup to investigate mitochondrial superoxide in cells lacking *Tst*, it would be preferable to answer this question using adipocytes due to the clear differences in these cells, including in the effect of sulfide on their activities.

The results presented here do not support the hypothesis that TST protects against cellular damage due to oxidative stress. TST did not impact the ability of adipocytes to consume exogenous H_2O_2. Primary hepatocytes lacking *Tst* had a reduction in mitochondrial superoxide in response to oxidative stress compared to WT hepatocytes, indicating that Tst knockout may partially protect against the damage of exogenous oxidative stress, however this did not lead to a difference in cell death. Future investigations of the role of sulfide in this process, and using models of genetically-induced oxidative stress in adipose tissue will lead to a better understanding of the role of TST in the response to oxidative stress.

Chapter 6 Discussion

The world is in the grips of an obesity epidemic, associated with a rapid increase in the incidence of type two diabetes mellitus and cardiovascular disease (Wormser *et al.* 2011; Zhou *et al.* 2016). The metabolic syndrome is a cluster of associated conditions that represent risk factors for increased morbidity and mortality, and its prevalence is increased in obese and overweight people (Park *et al.* 2003). Pathophysiological changes occur in adipose tissue in obesity, including the development of primary insulin resistance and altered secretion of many adipokines that link obesity with diabetes and cardiovascular disease. In obesity, adipose tissue exhibits oxidative stress due to increased production of ROS (Furukawa *et al.* 2004; Paglialunga *et al.* 2015), as well as chronic inflammation due to infiltration of pro-inflammatory macrophages and increased expression of cytokines (Kanda *et al.* 2006b; Lumeng *et al.* 2007). These detrimental effects reduce the ability of adipose tissue to store excess nutrient as lipid in part due to impaired insulin responsiveness and increased production and secretion of adipokines that drive metabolic dysfunction (Yki-Jarvinen 2002; Furukawa *et al.* 2004; Patsouris *et al.* 2008). Understanding the progression from early adipose tissue dysfunction to metabolic syndrome will lead to the development of new interventions and therapies to prevent and treat the metabolic syndrome and diabetes.

Recent work from our lab showed that elevated TST in adipose tissue was metabolically protective during exposure to high fat diet (HFD) in mice. In response to HFD, Adipoq-*Tst* mice had reduced weight gain, elevated plasma adiponectin and improved glucose tolerance, as well as increased expression of antioxidant enzymes in adipose tissue (Morton *et al.* 2016). Knockdown of TST in 3T3-L1 adipocytes led to increased mitochondrial ROS production after exposure to H_2O_2 (Morton *et al.* 2016), and *in vitro* evidence suggested TST can interact with a key antioxidant enzyme to aid ROS breakdown (Nandi *et al.* 2000). Therefore, it was hypothesised that TST in adipose tissue helps to maintain metabolic health through prevention of excessive local ROS accumulation. To test this hypothesis, two mouse models with altered TST expression in adipose tissue were subjected to HFD, and metabolic impairment and adipose tissue dysfunction was assessed. $Tst^{-/-}$ mice were more prone to glucose

intolerance on HFD, potentially due to reduced expression of antioxidant enzymes in adipose tissue, supporting the hypothesis that TST protects against metabolic impairment by reducing oxidative stress in adipose tissue. However, mice with overexpression of the human *TST* gene in adipose tissue did not have a reciprocal phenotype to the knockout mice, but instead were also potentially more prone to metabolic impairment on HFD than controls. Results from the Ad-hTST mice did not replicate previous findings using a mouse with overexpression of the mouse *Tst* gene in adipose, which was protected against weight gain and glucose intolerance on HFD (Morton *et al.* 2016), and so further characterisation of this new mouse model and the differences between the human and mouse protein sequences and function will be carried out to understand this discrepancy.

To directly test the hypothesis that TST is involved in ROS breakdown, *in vitro* experiments were carried out to investigate the response of primary adipocytes from $Tst^{-/-}$ and Ad-hTST mice to oxidative stress. Adipocytes with altered TST showed no difference in their ability to breakdown H_2O_2, and mitochondrial superoxide production and cell death were unaffected by *Tst* knockout. However, because of the technical challenges of using adipocytes, primary hepatocytes from $Tst^{-/-}$ mice were employed as a more robust cell model to establish a basis for the role of TST in the response to oxidative stress. Hepatocytes from $Tst^{-/-}$ mice were not more susceptible to cell death than WT hepatocytes as was hypothesised, and instead had reduced mitochondrial superoxide production in response to H_2O_2. An increase in sulfide levels due to *Tst* knockout may promote the activity of antioxidant enzymes in hepatocytes, as observed in endothelial cells exposed to H_2O_2 (Wen *et al.* 2013). It remains unclear if this effect occurs in adipocytes, and whether it influences susceptibility to HFD-induced adipose tissue dysfunction, but future work will focus on applying this finding in hepatocytes to adipose tissue.

Adipose tissue dysfunction due to obesity-induced oxidative stress is a key factor in the link between obesity and diabetes (Furukawa *et al.* 2004; Paglialunga *et al.* 2015). The aim of this PhD was to investigate the antioxidant properties of TST in adipose tissue as a potential mechanism by which this mitochondrial enzyme may protect against metabolic impairment in obesity (Morton *et al.* 2016). I have confirmed

that *Tst* knockout increases the risk of metabolic impairment in HFD-fed mice, although it was not possible to confirm that this enzyme plays a direct antioxidant role in the response to oxidative stress. Summaries of the findings from chapters 3, 4 and 5 are found in Table 6.1, Table 6.2 and Table 6.3 below.

Table 6.1: Summary of Results - Chapter 3

Experiment	**Results**
Tst$^{-/-}$ mouse - HFD for 6 weeks	- *Tst*$^{-/-}$ lighter than WT on chow, no difference on HFD. - No difference in epididymal fat weight. - No difference in immune cell populations.
Tst$^{-/-}$ mouse - HFD for 20 weeks	- No difference in body weight on chow or HFD. - *Tst*$^{-/-}$ had less WAT on chow, but not HFD. - Glucose tolerance impaired by HFD in *Tst*$^{-/-}$ and WT. - *Tst*$^{-/-}$ had lower insulin during GTT than WT. - Insulin tolerance impaired by HFD in *Tst*$^{-/-}$ and WT. - *Tst*$^{-/-}$ had reduced adiponectin on chow and HFD, compared to reduction on HFD only for WT. - *Tst*$^{-/-}$ had reduced expression of antioxidant enzymes (*Sod2, Prx3, Prx1, Gpx1, Txn2*) in mesenteric fat. - Carbonyl content of adipose unaffected by HFD. - No differences in immune cell populations. - No differences in pro-inflammatory cytokine expression. - *Tst*$^{-/-}$ on chow had increased *Chop* expression. - *Tst* expression reduced in chow and HFD-fed WT. - *Tst*$^{-/-}$ had reduced *Cse* on chow, and *Mpst* on both diets.

Table 6.2: Summary of Results - Chapter 4

Experiment	**Results**
Female Ad-hTST mice - Human and mouse TST expression	- Human TST mRNA was highly expressed in adipose, but not non-adipose tissues. - Mouse *Tst* mRNA was unchanged in adipose. - Rhodanese activity was increased 2 – 3.5-fold in adipose. - TST protein increased in adipose.
Male Ad-hTST mice - HFD for 6 weeks	- No differences in body weight or adipose weights. - No differences in food intake and feeding efficiency. - No difference in GTT on HFD. - Ad-hTST on LFD had lower glucose at 15min during GTT. - Ad-hTST on LFD had reduced adiponectin. - No differences in expression of antioxidant genes. - No differences in immune cell populations. - No differences in pro-inflammatory cytokine expression. - No differences in UPR markers, H_2S-producing or H_2S-oxidising enzymes.

Table 6.3: Summary of Results - Chapter 5

Experiment	**Results**
PQ exposure *in vivo* in *Tst*$^{+/-}$ - 25mg/kg for 24hrs	- PQ caused weight loss. - No change in adipose weight, malondialdehyde or antioxidant gene expression. - No change in lung weight or antioxidant gene expression.
H_2O_2 disposal in primary adipocytes - *Tst*$^{-/-}$ - Ad-hTST	- No change in H_2O_2 disposal in *Tst*$^{-/-}$ or Ad-hTST adipocytes compared to controls. - H_2O_2 disposal different between control lines (WT vs. WT-LSL).
Tst$^{-/-}$ primary adipocytes - Mitochondrial Superoxide	- Mitochondrial ROS increased by H_2O_2 exposure. - No difference compared to WT. - Technical challenges limited reliability of experiment.
Tst$^{-/-}$ primary hepatocytes - Mitochondrial Superoxide	- Mitochondrial ROS increased by H_2O_2, but to lesser extent in *Tst*$^{-/-}$ hepatocytes. - No effect of antioxidant (NAC), sulfide (Na_2S) or CSE inhibitor (PAG).

6.1 TST AND METABOLIC IMPAIRMENT

Evidence linking TST to metabolic protection was previously provided by investigation of the phenotype of transgenic mice overexpressing *Tst* in adipose tissue under the adiponectin promoter (Morton *et al.* 2016). These mice, in response to high fat diet, had reduced weight gain, elevated plasma adiponectin and improved glucose tolerance, as well increased expression of some antioxidant enzymes in adipose tissue (Morton *et al.* 2016). A full understanding of how TST mediated this protective effect was lacking, and so the *Tst*$^{-/-}$ mouse was developed to examine the impact of *Tst* knockout on the metabolic phenotype, and uncover the basis for the protection offered by TST in Adipoq-*Tst* mice. Despite exhibiting comparable gains in weight and fat mass on HFD, *Tst*$^{-/-}$ mice on HFD had increased plasma glucose with reduced insulin secretion during a glucose tolerance test, highlighting an increased risk of developing diabetes compared to WT mice. *Tst*$^{-/-}$ mice also had reduced expression of antioxidant enzymes in adipose tissue, confirming a reciprocal phenotype to the increased expression observed in adipose of Adipoq-*Tst* mice exposed to HFD (Morton *et al.* 2016). Despite this reduction in antioxidant capabilities, no evidence was found for greatly increased adipose tissue dysfunction compared to WT mice, as a marker of oxidative stress was unchanged, and *Tst*$^{-/-}$ mice did not have significantly greater infiltration of pro-inflammatory macrophages. It is likely that the adipose tissue of *Tst*$^{-/-}$ mice was not more discernibly affected by *Tst* knockout due to the reduction of TST in the adipose of WT mice caused by HFD and prolonged exposure to chow diet which promoted almost comparable fat mass gain, leading to a convergence of the adiposity phenotype. Also, the local deleterious effects of *Tst* knockout on adipose tissue may have been minimised due to the antioxidant and anti-inflammatory effects of H_2S, which was increased in the plasma of *Tst*$^{-/-}$ mice (Whiteman, Li, *et al.* 2010; Xie *et al.* 2014; Cai *et al.* 2016a; Morton *et al.* 2016). While *Tst*$^{-/-}$ mice showed increased metabolic impairment on HFD, as hypothesised, it is likely the phenotype was influenced by sulfide-mediated inhibition of insulin secretion and activation of hepatic gluconeogenesis (Tang *et al.* 2013; Zhang *et al.* 2013). In future, a mouse model with adipose-specific knockout of *Tst* will be available to allow for a more targeted investigation of the effect of *Tst* knockout in adipose tissue on metabolic impairment.

Moreover, a more appropriate defined control diet rather than standard chow may help prevent convergence of body weight gain seen on the HFD WT mice that appeared to confound the comparisons between the diet and genotype effects after prolonged HFD regimens.

A new mouse model with overexpression of the human *TST* gene in adipose tissue was characterised for this thesis. Due to the use of a highly active promoter to drive human *TST* gene expression, the Ad-hTST mouse was expected to have a greater increase in TST compared to the previous model, Adipoq-*Tst*. However, despite increased rhodanese activity in adipose tissue, the Ad-hTST mouse failed to recapitulate the phenotype of the Adipoq-*Tst* mouse, as it was not protected from weight gain and glucose intolerance after a HFD (Morton *et al.* 2016). These results contradict previous findings, and potentially challenge the hypothesis that elevated TST in adipose tissue protects against metabolic impairment. However, the phenotype of Ad-hTST mice also raises questions about the ability of human TST to function in mouse adipose tissue, as no differences were found in any aspect of adipose tissue function compared to WT mice in the experiments conducted in this thesis. Instead of exhibiting protection against metabolic impairment, Ad-hTST mice on HFD showed slightly impaired glucose tolerance, which may have been due to reduced circulating adiponectin, rather than a direct impact of the overexpressed enzyme on oxidative stress in adipose tissue. Ad-hTST mice were heterozygous for adiponectin due to the presence of the cre gene within one adiponectin allele (Eguchi *et al.* 2011), however no difference was found in adiponectin in the plasma of the Adip-cre parents line, and therefore it is likely that this reduction in adiponectin is a true effect of human TST overexpression in adipose depots. While characterisation of the Ad-hTST mouse failed to support the hypothesis that TST in adipose tissue acts to prevent metabolic impairment, it is likely that due to differences between the human and mouse TST protein, this model did not function as expected and may unfortunately be unsuitable for use in future studies.

6.2 TST AND OXIDATIVE STRESS

TST was thought to play a role in ROS breakdown, and thus protect adipose tissue from damage due to oxidative stress during exposure to HFD. As well as evidence that TST interacts with thioredoxin, aiding in the breakdown of H_2O_2 (Nandi *et al.* 2000), we had previously found that 3T3-L1 adipocytes with si-RNA-mediated knockdown of *Tst* produced more mitochondrial ROS in response to exogenous oxidative stress (Morton *et al.* 2016), highlighting a potential mechanism for TST-based metabolic protection. As well as these direct effects of TST, Adipoq-*Tst* mice had increased expression of key antioxidant enzymes in HFD compared to WT mice, and maintained higher expression after exposure to HFD (Morton *et al.* 2016), indicating that indirect transcriptional or post-translational regulation of antioxidant enzymes may also underscore the metabolic protection afforded by increased TST in adipose tissue.

The data presented in this thesis do not support the hypothesis that TST is directly involved in the breakdown of ROS in adipocytes. Primary adipocytes from mice with altered TST expression were used to examine the role of TST in H_2O_2 breakdown, however no difference in the degree of H_2O_2 breakdown was observed with adipocytes lacking *Tst* or with overexpression of human TST. Similarly, primary adipocytes from $Tst^{-/-}$ mice did not have increased mitochondrial superoxide production, or show a higher cell death, as might be expected if TST had antioxidant capabilities. However, a full understanding of the role of TST in adipocytes in response to oxidative stress remains unclear due to technical difficulties which rendered the results of these experiments inconclusive. Because of these difficulties, primary hepatocytes from $Tst^{-/-}$ mice were used as a more robust cell model to investigate the effect of *Tst* knockout on the response to oxidative stress. Unexpectedly, primary hepatocytes lacking *Tst* had reduced production of mitochondrial ROS in response to H_2O_2. This may be a result of increased accumulation of H_2S or other intermediaries due to impaired sulfide oxidation (Libiad *et al.* 2014), as H_2S can reduce the formation of ROS from mitochondria (Xie *et al.* 2014). The mechanism by which *Tst* knockout in hepatocytes influences mitochondrial superoxide remains unknown, however there is potential for this to be harnessed to protect cells from oxidative damage *in vivo*.

6.3 FUTURE WORK

Considerable questions remain to be answered about the impact of TST in adipose tissue, and how it contributes to metabolic health. To fully elucidate the effect of TST on the antioxidant capabilities of adipose, a genetic approach must be undertaken to minimise confounding factors including the effect of diet on TST expression in WT mice, and the potential antioxidant effects of increased plasma sulfide. New mouse and cell models with more precise alterations in *Tst* expression will soon be available, and compounds are under development to allow for more accurate activation of TST than the currently available non-specific substrate, thiosulfate. The function of TST *in vivo* must be fully elucidated before this promising anti-diabetic target can be pursued in a clinical setting.

New mouse models will be available to investigate more aspects of TST function in adipose and other tissues. A line with cre-meditated knockout of *Tst* will be used to produce a mouse with tissue-specific knockout of the gene. It is likely that the phenotype of the $Tst^{-/-}$ mouse used in this thesis is influenced heavily by the effect of *Tst* knockout in the liver, as well as the effects of increased circulating plasma sulfide on the liver and other tissues (Morton *et al.* 2016). An adipose-specific knockout will be used to understand if the impact of *Tst* on metabolic health is selectively due to adipose expression of the gene, as in Adipoq-*Tst* mice (Morton *et al.* 2016), or due to its indirect effect on other tissues through modulation of sulfide. To further question the impact of TST on oxidative stress, a mouse with both *Tst* and *Prx3* knocked out in adipose tissue could be a useful tool, as knockout of this key antioxidant enzyme leads to increased mitochondrial oxidative stress in adipocytes (Huh *et al.* 2012). High fat diet was used to induce oxidative stress in adipose tissue in this thesis, however this led to a reduction in *Tst* expression in adipose of control mice, thus leading to a convergence of phenotype with $Tst^{-/-}$ mice. A genetic approach to oxidative stress induction will avoid this pitfall and allow for better control of the effects of *Tst* knockout in tissues other than adipose.

New cell lines are available to probe the effects of altered *Tst* expression *in vitro*. Induced pluripotent stem cells (iPSCs) with the *Tst* gene knocked out and overexpressed have been developed using CRISPR-mediated gene editing. These cells

can be differentiated into adipocytes (Tashiro *et al.* 2009), and will be useful to fully characterise the phenotype of adipocytes with altered *Tst* expression, including assessing the impact on adipogenic differentiation and function, as well as mitochondrial biogenesis. It will be possible to assess the response to oxidative stress more efficiently in these differentiated iPSCs compared to primary adipocytes, as they are adherent and the cell culture conditions can be manipulated more easily.

It has become increasingly accepted that H_2S is a potent anti-inflammatory factor, despite initial evidence that it played a role in the progression of some inflammatory diseases. The development of new H_2S donor compounds that release H_2S at physiological levels over a sustained period, such as GYY4137 and the mitochondrially-targeted AP39 (Whiteman, Li, *et al.* 2010; Ahmad *et al.* 2016), will allow us to experimentally induce increased sulfide levels, as found in $Tst^{-/-}$ mice, and thus elucidate the varying effects of gene knockout and increased plasma sulfide (Morton *et al.* 2016). H_2S may prove to be a useful target in the fight against metabolic disease, due to its insulin sensitising effects in adipose tissue (Cai *et al.* 2016a), however care must be undertaken if it is to be a useful anti-diabetic target due to the possibility of exacerbating insulin resistance in the liver (Zhang *et al.* 2013), or reducing insulin secretion from β cells (Tang *et al.* 2013). Therefore, the ability to target the sulfide oxidation pathway in a tissue-specific manner may be an important step towards harnessing the potential of H_2S as therapeutic target.

6.4 CONCLUDING REMARKS

In this thesis, I investigated the ability of TST to function as an antioxidant, and thus to help maintain metabolic health. I have found that *Tst* knockout caused metabolic impairment after exposure to HFD, however this was not associated with increased markers of adipose tissue dysfunction, despite a reduction in expression of some antioxidant enzymes. Future work focusing on the impact of sulfide on metabolically active tissues such as the liver and β cells will help to clarify the cause of this metabolic impairment in $Tst^{-/-}$ mice (Tang *et al.* 2013; Zhang *et al.* 2013). I uncovered evidence that TST does not impact ROS breakdown directly in adipocytes, and may not play a role in the response of these cells to oxidative stress, although mice with genetically-induced oxidative stress in adipose tissue should be used to clarify this finding. I also characterised a new mouse model with adipose-specific overexpression of the human *TST* gene, and found that a modest increase in rhodanese activity in adipose depots did not lead to an improved metabolic outcome on HFD, as was hypothesised. It is possible that differences between the human and mouse protein sequences impacted the function of the human enzyme in mouse tissue, and because of this, the Ad-hTST mouse failed to support the hypothesis that TST in adipose tissue helps to maintain metabolic health, as had been previously found with Adipoq-*Tst* mice (Morton *et al.* 2016). The findings presented in this thesis have contributed to a greater understanding of the role of TST in metabolic health, and the development of new mouse and cell models will allow us to identify potential clinical strategies to harness the potential of this enzyme in the treatment or prevention of diabetes.

Chapter 7 Appendix

7.1 BODY WEIGHT AND ADIPOSE TISSUE WEIGHTS OF 5-MONTH-OLD *TST*$^{-/-}$ VERSUS WT MICE ON CHOW DIET.

It was observed in several cohorts that *Tst*$^{-/-}$ mice when maintained past ~5 months old on chow diet may be smaller and have less fat than WT mice. (A trend for smaller body and significantly less fat was observed after 20 weeks of chow diet, page 88 and 89). To confirm this finding, a cohort of mice was maintained on chow diet until 5 months of age. *Tst*$^{-/-}$ mice weighed significantly less than WT mice after this period (Figure 7.1).

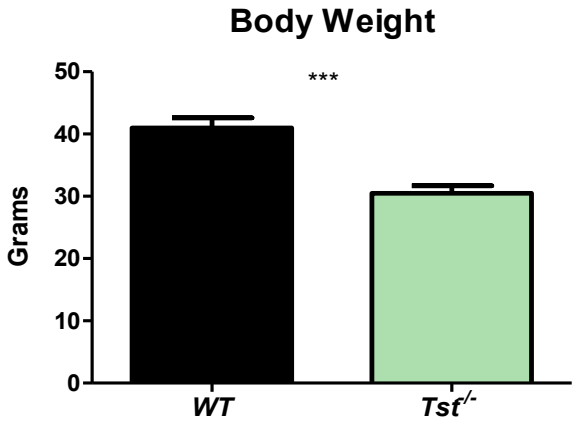

Figure 7.1: Body weight of at 5 months old Tst$^{-/-}$ and WT mice on chow diet.

*Data are mean ± SEM, analysed by Student's t-test: *** P < 0.001; (n = 6).*

Three white adipose depots were weighed in 5-month-old *Tst*$^{-/-}$ and WT mice at cull and normalised to body weight. All three depots – (a) epididymal, (b) mesenteric and (c) subcutaneous – were significantly lighter relative to body weight in *Tst*$^{-/-}$ compared to WT mice (Figure 7.2).

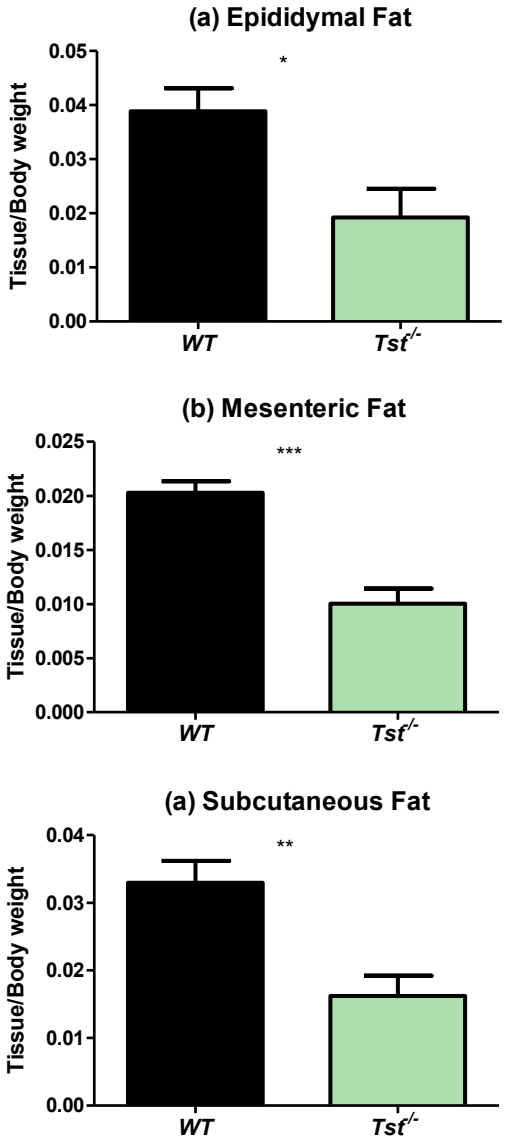

Figure 7.2: White adipose depot weights in 5-month-old Tst$^{-/-}$ versus WT mice on chow diet.

*(a) Epididymal, (b) mesenteric and (c) subcutaneous white adipose depots, normalised to body weight at cull. Data are mean ± SEM, analysed by Student's t-test: * P < 0.05, ** P < 0.01, *** P < 0.001; (n = 5).*

7.2 PARAQUAT PILOT RESULTS

7.2.1 Treatment of *Tst*$^{-/-}$ and WT mice with 1, 5 or 10mg/kg paraquat for 24hrs.

Paraquat (PQ; 1, 5 or 10mg/kg) or saline (0.9%) was administered to WT and *Tst*$^{-/-}$ mice by IP injection. After 24hrs, mice were culled and adipose tissue harvested for investigation of markers of oxidative stress. All mice lost weight after 24hrs, with PQ-treated mice appearing to lose more than saline-treated (not significant potentially to small sample size) (Figure 7.3a). Malondialdehyde did not measurably consistently in mesenteric adipose tissue with PQ treatment in WT or *Tst*$^{-/-}$ mice (Figure 7.3b). Expression of antioxidant genes *Prx3*, *Gpx1* in epididymal adipose were unaffected by PQ (Figure 7.4). Expression of *Txn2*, *Sod2*, *Sod1* and *Prx1* was reduced in adipose of *Tst*$^{-/-}$ mice compared to WT after exposure to 1mg/kg of PQ (Figure 7.4).

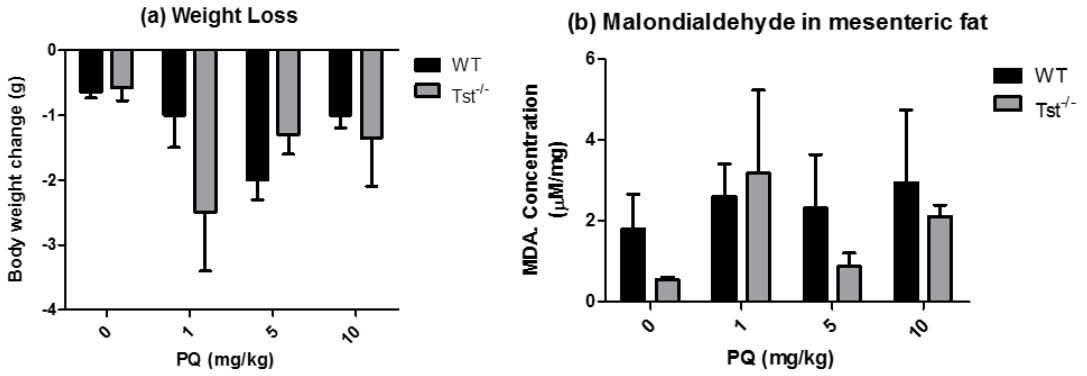

Figure 7.3: Weight and adipose malondialdehyde content of Tst$^{-/-}$ and WT mice treated with 1, 5 or 10mg/kg paraquat or saline (0.9%) for 24hrs.

(a) Weight loss, and (b) malondialdehyde in mesenteric adipose tissue. Data are mean ± SEM, analysed by Student's t-test: not significant; (n=4/5 saline; n=2 PQ-treated).

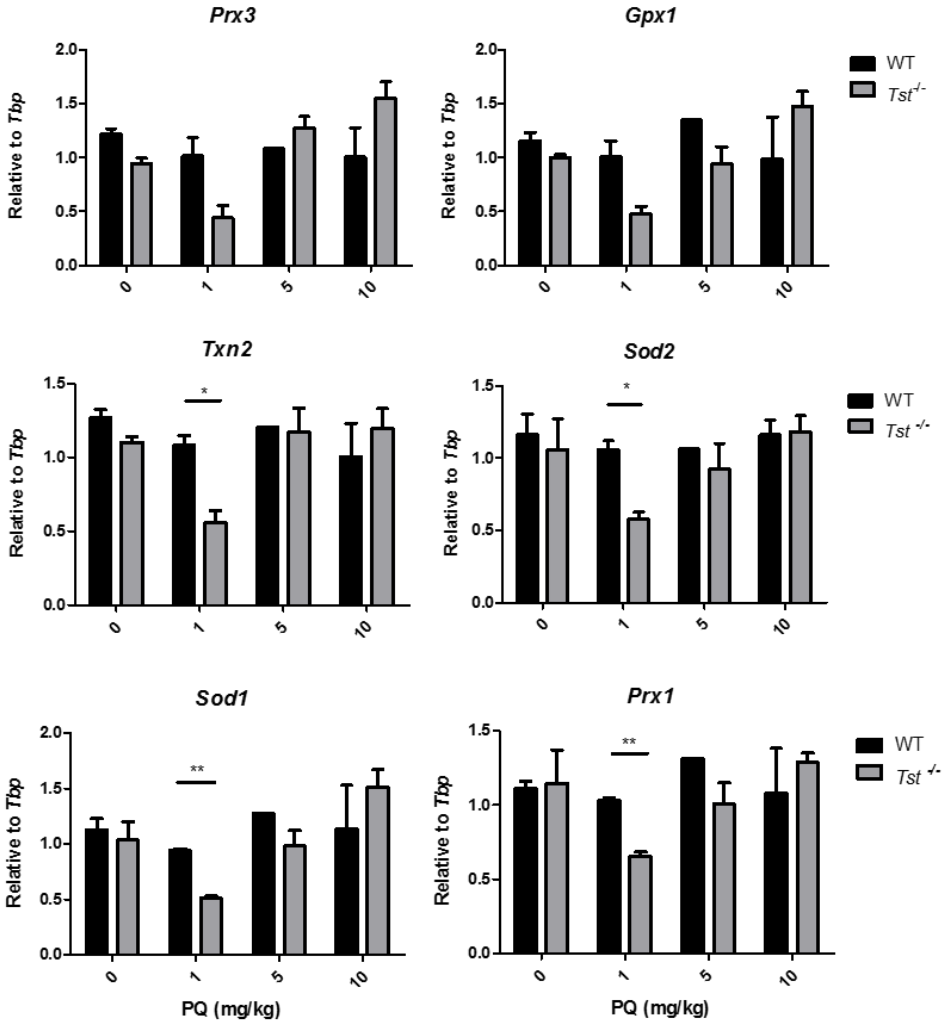

Figure 7.4: Antioxidant gene expression in epididymal adipose tissue of Tst$^{-/-}$ and WT mice treated with 1, 5 or 10mg/kg paraquat or saline (0.9%) for 24hrs.

*mRNA abundance of antioxidant genes normalised to housekeeping gene Tbp in epididymal adipose tissue. Data are mean ± SEM, analysed by Student's t-test: * P < 0.05, ** P < 0.01; (n=4/5 saline; n=2 PQ-treated).*

7.2.2 Treatment of WT mice with 20mg/kg paraquat for 2, 3 or 6 days.

PQ (20mg/kg in two doses of 10mg/kg on day -1 and day 0) or saline (0.9%) was administered to WT mice by IP injection (timeline shown in Figure 7.5). Mice were culled at two, three or six days after the second injection, and adipose and lung tissue harvested for investigation of markers of oxidative stress and lung fibrosis. There was no effect of PQ treatment on body weight at any time point (Figure 7.6a). PQ did not cause an increased in malondialdehyde content of mesenteric fat (Figure 7.6b) at any time point, and expression of antioxidant enzymes was unaffected by PQ (Figure 7.6c).

Exposure to PQ (20mg/kg) for 2, 3 or 6 days in WT mice did not alter the weight of the lungs compared to saline-treated mice (Figure 7.7a). Malondialdehyde in lung was unexpectedly higher in saline-treated mice at 2 days compared to PQ-treated mice at any time point (Figure 7.7b). This may be due to variability in the small sample. Expression of fibrosis genes alpha smooth muscle actin (*αSMA*) and collagen type 1 alpha1 (*Cola1a*) were unaffected by PQ at all time points (Figure 7.7c).

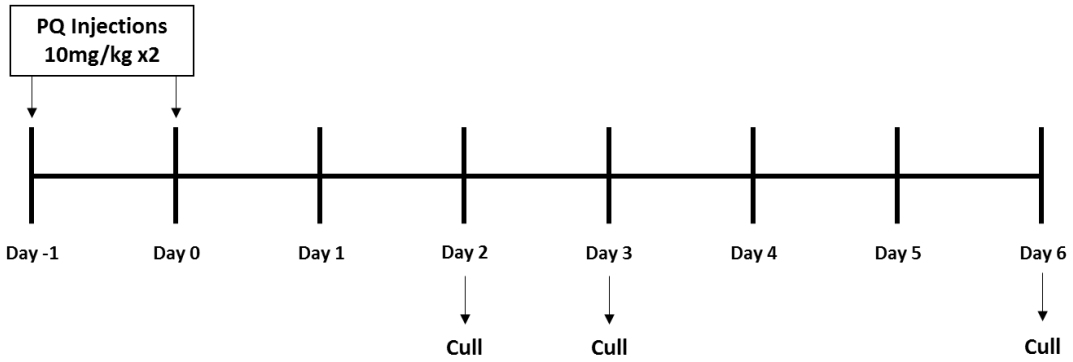

Figure 7.5: Timeline of WT mice exposed to paraquat for 2, 3 or 6 days.

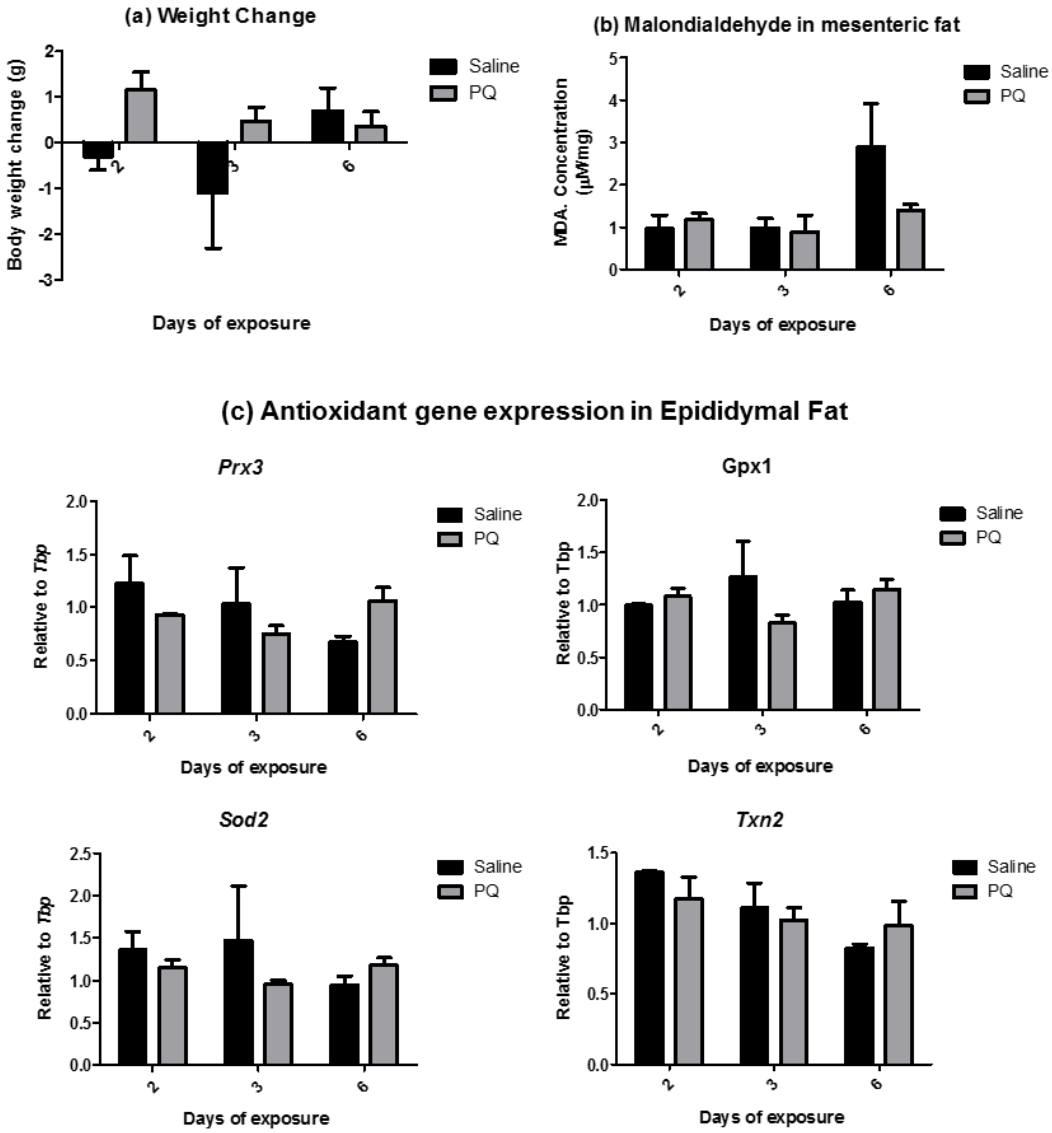

Figure 7.6: Weight and adipose response of WT mice 2, 3 or 6 days after administration of PQ (20mg/kg) or saline (0.9%).

(a) Change in body weight, (b) malondialdehyde content in mesenteric fat, and (c) mRNA abundance of antioxidant genes normalised to housekeeping gene Tbp in epididymal fat. Data are mean ± SEM, analysed by Student's t-test: not significant; (n=2/3, saline/PQ).

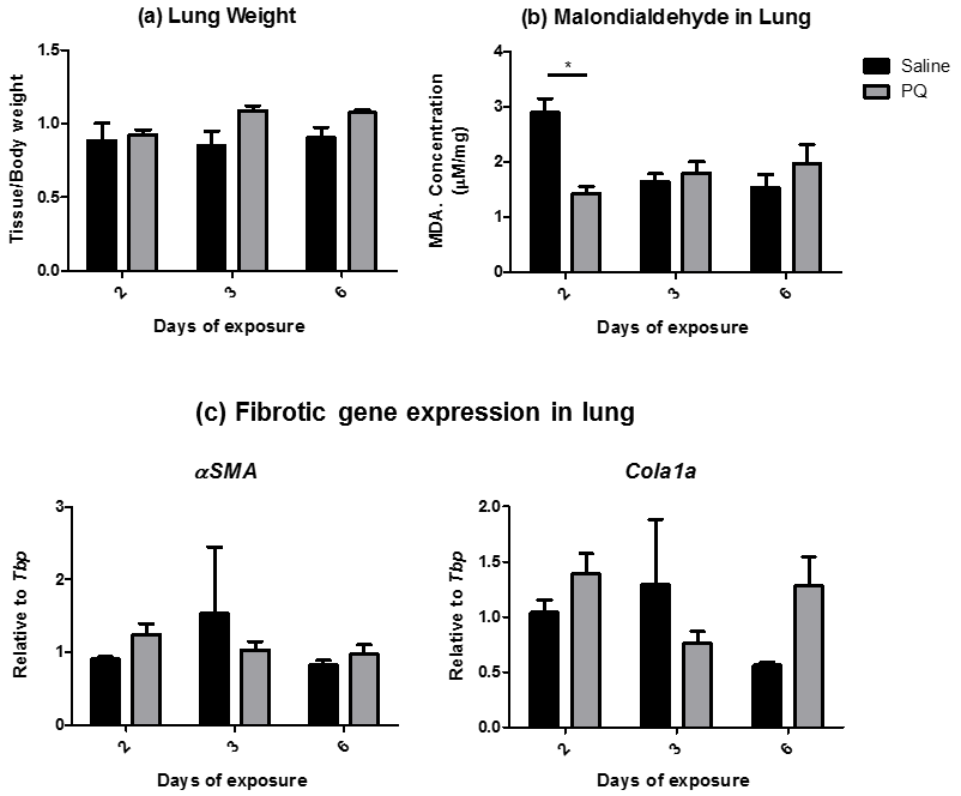

Figure 7.7: Lung response in WT mice 2, 3 or 6 days after administration of PQ (20mg/kg) or saline (0.9%).

*(a) Lung weight, (b) malondialdehyde content, and (c) mRNA abundance of fibrosis genes normalised to housekeeping gene Tbp in lung tissue. Data are mean ± SEM, analysed by Student's t-test: * P < 0.05; (n=2/3, saline/PQ).*

7.3 ABBREVIATIONS AND MANUFACTURER'S DETAILS

Table 7.1: Abbreviations and meanings

Abbreviation	Meaning
%	Percent
µg	Microgram
µl	Microlitre
4-HNE	4-hydroxy-2-nonenal
6J	C57BL/6J
6N	C57BL/6N
ANOVA	2-way analysis of variance
APS	Ammonium Persulfate
ATMs	Adipose tissue macrophages
ATP	Adenosine triphosphate
AUC	Area under curve
BAT	Brown adipose tissue
BMI	Body mass index
BSA	Bovine serum albumin
CLS	Crown-like structures
CO_2	Carbon Dioxide
CRISPR	Clusted regularly interspaced short palindromic repeats
CTRP	C1q/TNF-related protein
DAPI	4',6-diamidino-2-phenylindole
DMEM	Dulbecco's Modified Eagle Medium
DNA	Deoxyribonucleaic acid
ECM	Extracellular matrix
EDTA	Ethylenediaminetetraacetic Acid
EGTA	Ethylene glycol-bis(2-aminoethylether)-N,N,N′,N′-tetraacetic acid
ELISA	Enzyme-linked immunosorbent assay
ER	Endoplasmic reticulum
FADH	Flavin adenine dinucleotide
FSC-A	Forward scatter area
FSC-H	Forward scatter height
g	Relative centrifugal force (AKA. RCF)
GSH	Glutathione
GSH	Glutathione persulfide
GTT	Glucose tolerance test
GWAS	Genome-wide associated study
H_2S	Hydrogen sulfide

Abbreviation	Meaning
H_2O_2	Hydrogen peroxide
HBSS	Hank's balanced salt solution
HFD	High fat diet
HMW	High molecular weight
hr(s)	Hour(s)
HUVEC	Human umbilical vein endothelial cells
IBD	Inflammatory bowel disease
ILC2	Innate lymphoid type 2 cells
iNKT	Invariant-chain natural killer T cells
IP	Intrapertioneal
iPSC	Induced pluripotent stem cell
IRES	Internal ribosome entry site
ITT	Insulin tolerance test
K_{ATP}	ATP-sensitive postassium channel
kcal	Kilocalories
KEAP1	Kelch-Like ECH Associated Protein 1
kg	Kilogram
LDH	Lactate dehydrogenase
LDM	Liver digestion media
LFD	Low fat diet
LPM	Liver perfusion media
M	Molar
mA	Milliamp
MDA	Malondialdehyde
mg	Milligram
min(s)	Minute(s)
ml	Millilitre
mM	Millimolar
MPST	3-mercaptopyruvate sulfurtransferase
Na_2S	Disodium sulfide
NAC	N-acetylcysteine
NADH	Nicotinamide adenine dinucleotide
NADPH	Nicotinamide adenine dinucleotide phosphate
NaHS	Sodium hydrosulfide
NK	Natural killer cells
nm	Nanometre
NSAID	Non-steroidal anti-inflammatory drug
NOX	NADPH oxidases

Abbreviation	Meaning
NRF2	Nuclear factor (erythroid-derived 2)-like 2
^{o}C	Degrees Celcius
oxLDL	Oxidised low density lipoprotein
PAG	DL-propargylglycine
PAGE	Polyacrylamide gel electrophoresis
PBS	Phosphate buffered saline
PolyA	Polyadenosine coding sequence
PPP	Pyridoxal 5' phosphate
PQ	Paraquat dichoride / N,N′-dimethyl-4,4′-bipyridinium dichloride
RAS	Renin-angiotensin system
RNA	Ribonucleic acid
ROS	Reactive oxygen species
rpm	Revolutions per minute
RT	Room tempterature (21oC)
RT-PCR	Real-time quantitative polymerase chain reaction
s	Seconds
SDS	Sodium dodecyl sulfate
SEM	Standard error of the mean
siRNA	Small-interfering RNA
SNPs	Single nucleotide polymorphisms
SRB	Dulforhodamine B
SSC-A	Side scatter area
SVF	Stromal vascular fraction
TBARS	Thiobarbituric acid reactive substances
TBS (-T)	Tris-buffered saline (with Tween)
TCDD	2, 3, 7, 8-tetrachlorodibenzo-*p*-dioxin
TD-NMR	Time domain nuclear magnetic resonance relaxometry
TEMED	N,N,N′,N′-Tetramethylethylenediamine
Treg	Regulatory T cells
TST	Thiosulfate sulfurtransferase (protein)
TST	Thiosulfate sulfurtransferase (human gene)
Tst	Thiosulfate sulfurtransferase (mouse gene)
UPR	Unfolded protein response
WAT	White adipose tissue
WT	wild-type
µM	Micromolar

Table 7.2: Manufacturer's Details

Item	Manufacturer	Address
AC1000 Improved Neubauer haemocytometer	Hawksley	Lancing, UK
100% Acetic acid	Sigma-Aldrich	Dorset, UK
100% Trichloroacetic acid	Sigma-Aldrich	Dorset, UK
384-well white lightcycler plate	Sarstedt	Nümbrecht, Germany
3-Isobutyl-1-methylxanthine (IBMX)	Sigma-Aldrich	Dorset, UK
3T3-L1 cells	American Type Culture Collection	Middlesex, UK
96-well plate, black	Greiner Bio-One	Gloucestershire, UK
96-well plate, black, clear-bottom, cell culture-treated	Corning®	Flintshire, UK
96-well plate, cell culture-treated	Corning® Costar®	Flintshire, UK
96-well plate, V-bottom	Greiner Bio-One	Gloucestershire, UK
Advanced Bench pH Meter 3510	Jenway	Staffordshire, UK
Amersham hybond P 0.45 PVDF Membrane	GE Healthcare	Little Chalfont Bucks, UK
Ammonium persulfate	Sigma-Aldrich	Dorset, UK
Anti-4-hydroxynonenal antibody (rabbit, polyclonal, CAT #: ab46545)	Abcam	Cambridge, UK
Anti-GAPDH antibody (mouse monocloncal, CAT #: 1001-500UG)	Calbiochem (Merck Millipore Ltd)	Watford, UK
Anti-mouse CD11b PerCP Cy5.5 (CAT #: 45-0112-85)	eBioscience	Altrincham, UK
Anti-mouse CD11c Biotin (CAT #: 13-0114-85)	eBioscience	Altrincham, UK
Anti-mouse CD11c Pacific Blue (CAT #:117321)	Biolegend	CA,USA
Anti-mouse CD16/CD32 antibody (CAT #: 11-0161-85)	eBioscience	Altrincham, UK
Anti-mouse CD206 APC (CAT #:141707)	Biolegend	CA,USA
Anti-mouse CD45 FITC (CAT #: 11-0454-85)	eBioscience	Altrincham, UK

Item	Manufacturer	Address
Anti-mouse CD45 Pacific Blue (CAT #: 48-0451-82)	eBioscience	Altrincham, UK
Anti-mouse F4/80 FITC (CAT #:11-4801-81)	eBioscience	Altrincham, UK
Anti-mouse F4/80 PE Cy7 (CAT #: 25-4801-82)	eBioscience	Altrincham, UK
Anti-mouse Gr1 APC Cy7 (CAT #:108424)	Biolegend	CA,USA
Anti-mouse Ly6C AlexaFlour700 (CAT #:128024)	Biolegend	CA,USA
Anti-mouse Ly6C APC (CAT #: 17-5932-80)	eBioscience	Altrincham, UK
Anti-mouse MHCII APC efluor780 (CAT #:47-5321-82)	eBioscience	Altrincham, UK
Anti-mouse SiglecF PE (CAT #: 552126)	BD Biosciences	Wokingham, UK
Anti-TST antibody (rabbit, polyclonal, CAT #: 16311-1-AP)	Proteintech	Manchester, UK
BD FACSDiva™ software	BD Biosciences	Wokingham, UK
BD LSRfortessa™ cell analyser	BD Biosciences	Wokingham, UK
BD Micro-Fine™ Insulin syringes (0.3ml)	BD Biosciences	Wokingham, UK
Bijoux, Sterile, 7ml	Greiner Bio-One	Gloucestershire, UK
Bovine serum albumin (BSA)	Sigma-Aldrich	Dorset, UK
Bruker minispec LF90II	Bruker UK Ltd.	Coventry, UK
Calcium chloride	Sigma-Aldrich	Dorset, UK
Cell strainer, 100µm, 40µm	Fisher Scientific	Loughborough, UK
Cellstar® centrifuge tubes, 50ml	Greiner Bio-One	Gloucestershire, UK
Centrifuge 5415R	Eppendorf	Stevenage, UK
Chloroform	Fisher Scientific	Loughborough, UK
Collagen	Sigma-Aldrich	Dorset, UK
Collagenase, Type 1	Worthington Biochemical Corp.	New Jersey, USA
cOmplete ULTRA Tablet (mini)	Roche LifeScience	Burgess Hill, UK
DAPI, 4',6-diamidino-2-phenylindole dehydrochloride	ThermoFisher Scientific	Paisley, UK
Dexamethasone	Sigma-Aldrich	Dorset, UK

Item	Manufacturer	Address
DC™ Protein Assay	Bio-Rad Laboratories Ltd	Hertfordshire, UK
Disodium hydrogen phosphate	Sigma-Aldrich	Dorset, UK
Dulbecco's Modified Eagle Medium powder	Gibco™	Paisley, UK
Dulbecco's Modified Eagle Medium with high glucose (DMEM)	Gibco™	Paisley, UK
Dulbecco's Modified Eagle Medium with low glucose (DMEM)	Gibco™	Paisley, UK
Ethanol Absolute	VMR Chemicals	Lutterworth, UK
Ethylene glycol-bis(2-aminoethylether)-N,N,N′,N′-tetraacetic acid (EGTA)	Sigma-Aldrich	Dorset, UK
Ethylenediaminetetraacetic Acid (EDTA)	Sigma-Aldrich	Dorset, UK
Flow cytometry tubes	Gibco™	Paisley, UK
FlowJo™ software	FlowJo, LLC	Ashland, OR, USA
Fluorimetric Hydrogen Peroxide Assay Kit	Sigma-Aldrich	Dorset, UK
Fluoromount™ Aqueous Mounting Medium	Sigma-Aldrich	Dorset, UK
Glucose	Sigma-Aldrich	Dorset, UK
Glutamine	Gibco™	Paisley, UK
Glycine	Sigma-Aldrich	Dorset, UK
GraphPad Prism 5 software	Prism	CA, USA
Hamamatsu Orca II CCD camera	Hamamatsu Photonics UK Ltd.	Hertfordshire, UK
Hank's balanced salt solution (HBSS)	Gibco™	Paisley, UK
HEPES	Sigma-Aldrich	Dorset, UK
Heracell™ Incubator 5% CO_2, 37°C	ThermoFisher Scientific	Paisley, UK
Heraeus Megafuge 40R plate centrifuge	ThermoFisher Scientific	Paisley, UK
Humulin® U-100, human insulin	Eli Lilly	Hampshire, UK
HyClone™ foetal bovine serum, heat inactivated (South American Origin)	GE Healthcare	Little Chalfont Bucks, UK
Hydrochloric acid	Sigma-Aldrich	Dorset, UK
Hydrogen peroxide	Sigma-Aldrich	Dorset, UK
Image Studio™ Lite software	LI-COR Biosciences	Cambridge, UK
Infinite® M1000 PRO microplate reader	TECAN	Reading, UK
Insulin	Sigma-Aldrich	Dorset, UK

Item	Manufacturer	Address
IRDye® 680RD Donkey Anti-Mouse	LI-COR Biosciences	Cambridge, UK
IRDye® 800RD Goat Anti-Rabbit	LI-COR Biosciences	Cambridge, UK
Iron (III) nitrate	Sigma-Aldrich	Dorset, UK
Isopropanol	VMR Chemicals	Lutterworth, UK
LI-COR Odyssey scanner	LI-COR Biosciences	Cambridge, UK
Lightcyler® 480	Roche Applied Science	Burgess Hill, UK
Low fat corn starch diet (D12328)	Research Diets Inc.	New Brunswick, NJ, USA
Magnesium sulfate heptahydrate	Sigma-Aldrich	Dorset, UK
Methanol	Fisher Scientific	Loughborough, UK
Microcentrifuge tubes, DNase/RNase-free, 0.5ml	Greiner Bio-One	Gloucestershire, UK
Microcentrifuge tubes, DNase/RNase-free, 1.5ml	Greiner Bio-One	Gloucestershire, UK
Microcentrifuge tubes, DNase/RNase-free, 2ml	Eppendorf	Stevenage, UK
Microscope Slides Plain 1.0-1.2mm 76x26mm	Scientific laboratory supplies Ltd.	Lanarkshire, UK
Microvette CB 300 tubes	Sarstedt	Nümbrecht, Germany
Millex® Syringe Filter Units, sterile, 33mm	Merck Millipore Ltd	Watford, UK
Milli-Q® Integral Water Purification System	Merck Millipore Ltd	Watford, UK
Mini-PROTEAN Tetra gel electrophoresis and transfer system	Bio-Rad Laboratories Ltd	Hertfordshire, UK
MitoSOX™ Red Mitochondrial Superoxide Indicator	Life Technologies	Carlsbad, CA, USA
Mixer Mill MM301 homogeniser	Retsch™	Haan, Germany
Mouse HMW & Total Adiponectin ELISA	Alpco	Salem, NH, USA
N,N,N′,N′-Tetramethylethylenediamine	Sigma-Aldrich	Dorset, UK
NanoDrop ND-1000	ThermoFisher Scientific	Wilmington, USA
Newborn calf serum (NBCS)	Gibco™	Paisley, UK
Nitric acid	Sigma-Aldrich	Dorset, UK
Normal mouse serum	ThermoFisher Scientific	Wilmington, USA

Item	Manufacturer	Address
Normal rat serum	ThermoFisher Scientific	Wilmington, USA
Nylon mesh, 500µM aperture	Plastok	Merseyside, UK
Odyssey imaging system and software	LI-COR Biosciences	Cambridge, UK
Olympus AX-70 Provis microscope	Olympus	Center Valley, PA, USA
OneTough Ultra® Glucometer and test strips	LifeScan	Tunbridge Wells, UK
Optically clear sealing tape for lightcycler plate	Sarstedt	Nümbrecht, Germany
OxiSelect TBARS Assay Kit	Cell Biolabs	
Paraformaldehyde (38%)	Sigma-Aldrich	Dorset, UK
Paraquat dichloride	Sigma-Aldrich	Dorset, UK
Penicillin/streptomycin (P/S)	Gibco™	Paisley, UK
Percoll	Gibco™	Paisley, UK
PerfeCTa® Fastmix II	Quanta Bioscience	MD, USA
Phosphate buffered saline (PBS)	Sigma-Aldrich	Dorset, UK
Pierce™ LDH Cytotoxicity assay kit	ThermoFisher Scientific	Paisley, UK
Pipette tips, DNase/RNase-free, 1000/200/20/10µl	Greiner Bio-One	Gloucestershire, UK
Potassium chloride	Sigma-Aldrich	Dorset, UK
Potassium cyanide	Sigma-Aldrich	Dorset, UK
Potassium phosphate	Sigma-Aldrich	Dorset, UK
PowerPac™ Basic Power Supply	Bio-Rad Laboratories Ltd	Hertfordshire, UK
Precision Plus Protein Dual Colour Standards	Bio-Rad Laboratories Ltd	Hertfordshire, UK
ProtoFLOWgel (37:5:2)	Flowgen Biosciences Ltd	Nottingham, UK
QIAzol lysis reagent	Qiagen	West Sussex, UK
QuantiTect Reverse Transcription Kit	Qiagen	West Sussex, UK
RM1 standard chow diet	Special Diet Services	Essex, UK
Rosiglitazone	Sigma-Aldrich	Dorset, UK
RNAase/DNAase-free water	Gibco™	Paisley, UK
Skimmed milk powder	Marvel	
Sodium bicarbonate	Sigma-Aldrich	Dorset, UK

Item	Manufacturer	Address
SLS Coverslips 20x20mm	Scientific laboratory supplies Ltd.	Lanarkshire, UK
Sodium chloride	Sigma-Aldrich	Dorset, UK
Sodium dihydrogen phosphate	Sigma-Aldrich	Dorset, UK
Sodium dodecyl sulfate	Sigma-Aldrich	Dorset, UK
Sodium fluoride	Sigma-Aldrich	Dorset, UK
Sodium orthovanadate	Sigma-Aldrich	Dorset, UK
Sodium thiosulfate	Sigma-Aldrich	Dorset, UK
Stainless steel grinding balls	Retsch™	Haan, Germany
Strepatvidin PE Cy7 (CAT #: 25-4317-82)	eBioscience	Altrincham, UK
Sucrose	Sigma-Aldrich	Dorset, UK
Surwit high fat diet (D12331)	Research Diets Inc.	New Brunswick, NJ, USA
TaqMan® Real-Time PCR assay probes	Applied Biosystems	Carlsbad, CA, USA
Thiobarbituric acid reactive substances (TBARS) assay kit	Cayman Chemical	Ann Arbor, MI, USA
Tris base	Sigma-Aldrich	Dorset, UK
Triton X-100	Sigma-Aldrich	Dorset, UK
Tween	Sigma-Aldrich	Dorset, UK
Ultra pure ProtoFLOWgel 30% Acrylamide/ Bis Acrylamide	Flowgen Bioscience	Nottingham, UK
Ultra Sensitive Mouse Insulin ELISA kit	Crystal Chem	Downers Grove, IL, USA
Western Blotting Filter Paper, 8 cm x 10.5 cm	ThermoFisher Scientific	Paisley, UK
β-glycerophosphate	Sigma-Aldrich	Dorset, UK
β-mercaptoethanol	Sigma-Aldrich	Dorset, UK

References

- Abe, Kimura (1996) 'The possible role of hydrogen sulfide as an endogenous neuromodulator', The Journal of neuroscience, 76(3), 1–6.
- Ahmad, Olah, Szczesny, Wood, Whiteman, Szabo (2016) 'AP39, a mitochondrially- targeted hydrogen sulfide donor, exerts protective effects in renal epithelial cells subjected to oxidative stress in vitro and in acute renal injury in vivo', Shock, 45(1), 88–97.
- Al-Magableh, Kemp-Harper, Ng, Miller, Hart (2014) 'Hydrogen sulfide protects endothelial nitric oxide function under conditions of acute oxidative stress in vitro.', Naunyn-Schmiedeberg's Archives of Pharmacology, 387(1), 67–74.
- Alberti, Gilardini, Girola, Moro, Cavagnini, Invitti (2007) 'Adiponectin receptors gene expression in lymphocytes of obese and anorexic patients', Diabetes, Obesity and Metabolism, 9(3), 344–349.
- Alessi, Peiretti, Henry, Nalbone, Juhan-Vague (1997) 'Production of Plasminogen Activator Inhibitor 1 by Human Adipose Tissue.', Diabetes, 46(May), 860–867.
- Andruski, McCafferty, Ignacy, Millen, McDougall (2008) 'Leukocyte trafficking and pain behavioral responses to a hydrogen sulfide donor in acute monoarthritis.', American journal of physiology. Regulatory, integrative and comparative physiology, 295(3), R814–R820.
- Arijs, Vanhove, Rutgeerts, Schuit, Verbeke, De Preter (2013) 'Decreased mucosal sulfide detoxification capacity in patients with Crohn's disease.', Inflammatory bowel diseases, 19(5), E70-2.
- Arner, Mejhert, Kulyté, Balwierz, Pachkov, Cormont, Lorente-Cebrián, Ehrlund, Laurencikiene, Hedén, Dahlman-Wright, Tanti, Hayashizaki, Rydén, Dahlman, Van Nimwegen, Daub, Arner (2012) 'Adipose tissue MicroRNAs as regulators of CCL2 production in human obesity', Diabetes, 61(8), 1986–1993.
- Ayala, Munoz, Arguelles (2014) 'Lipid peroxidation: Production, metabolism, and signaling mechanisms of malondialdehyde and 4-hydroxy-2-nonenal', Oxidative Medicine and Cellular Longevity, (Epub), 360438.
- Baiges, Palmfeldt, Bladé, Gregersen, Arola (2010) 'Lipogenesis is decreased by grape seed proanthocyanidins according to liver proteomics of rats fed a high fat diet.', Molecular & cellular proteomics: MCP, 9(7), 1499–513.
- Ball, Reiffel, Chintalapani, Kim, Spector, King (2013) 'Hydrogen Sulfide Reduces Neutrophil Recruitment in Hind-Limb Ischemia-Reperfusion Injury in an L-Selectin and ADAM-17-Dependent Manner.', Plastic and reconstructive surgery, 131(3), 487–97.
- Baskin, Horowitz, Nealley (1992) 'The Antidotal Action of Sodium Nitrite and Sodium Thiosulfate Against Cyanide Poisoning', J Clin Pharmacol, 32, 368–375.
- Bennett, Solar, Yuan, Mathias, Thomas, Matthews (1996) 'A role for leptin and its cognate receptor in hematopoiesis', Current Biology, 6(9), 1170–1180.
- Berg, Combs, Du, Brownlee, Scherer (2001) 'The adipocyte-secreted protein Acrp30 enhances hepatic insulin action.', Nature medicine, 7(8), 947–53.
- Berner, Lyngstadaas, Spahr, Monjo, Thommesen, Drevon, Syversen, Reseland (2004) 'Adiponectin and its receptors are expressed in bone-forming cells', Bone, 35(4), 842–849.
- Berti, Gammeltoft (1999) 'Leptin stimulates glucose uptake in C2C12 muscle cells by activation of ERK2', Molecular and Cellular Endocrinology, 157(1–2), 121–130.
- Bhatia, Sidhapuriwala, Moochhala, Moore (2005) 'Hydrogen sulphide is a mediator of carrageenan-induced hindpaw oedema in the rat.', British journal of pharmacology, 145(2), 141–4.
- Billaut-Laden, Allorge, Crunelle-Thibaut, Rat, Cauffiez, Chevalier, Houdret, Lo-Guidice, Broly (2006) 'Evidence for a functional genetic polymorphism of the human thiosulfate sulfurtransferase (Rhodanese), a cyanide and H2S detoxification enzyme', Toxicology, 225(1), 1–11.
- Blake, Eppig, Kadin, Richardson, Smith, Bult, Anagnostopoulos, Baldarelli, Beal, Bello, Blodgett, Butler, Corbani, Dene, Drabkin, Forthofer, Giannatto, Hale, Hill, Hutchins, Knowlton, Lavertu, Law, Lewis, Lopez, Maghini, Perry, McAndrews, Miers, Montenko, Ni, Onda, Recla, Reed, Richards-Smith, Sitnikov, Tomczuk, Wilming, Zhu (2017) 'Mouse Genome Database (MGD)-2017: Community knowledge resource for the laboratory mouse', Nucleic Acids Research, 45(D1), D723–D729.
- Blanchard, Karst (1993) 'Characterization of a lysine-to-glutamic acid mutation in a conservative sequence of farnesyl diphosphate synthase from Saccharomyces cerevisiae', Gene, 125(2), 185–189.
- Blanchette-Mackie, Dwyer, Barber, Coxey, Takeda, Rondinone, Theodorakis, Greenberg, Londos (1995) 'Perilipin is located on the surface layer of intracellular lipid droplets in adipocytes.', Journal of lipid research, 36(6), 1211–1226.
- Blüher, Fasshauer, Kralisch, Schön, Krohn, Paschke (2005) 'Regulation of adiponectin receptor R1 and R2 gene expression in adipocytes of C57BL/6 mice', Biochemical and Biophysical Research Communications, 329(3), 1127–1132.

- Bokov, Garg, Ikeno, Thakur, Musi, DeFronzo, Zhang, Erickson, Gelfond, Hubbard, Adamo, Richardson (2011) 'Does reduced IGF-1R signaling in igf1r +/- mice alter aging?', PLoS ONE, 6(11).
- Bolic, Mijuskovic, Popovic-Bijelic, Nikolic-Kokic, Spasic, Blagojevic, Spasic, Spasojevic (2015) 'Reactions of superoxide dismutases with HS-/H2S and superoxide radical anion: An in vitro EPR study', Nitric Oxide, 51, 19–23.
- Bonomi, Pagani, Cerletti, Cannella (1977) 'Rhodanese-•Med iated Sulfur Transfer to Succinate Dehydrogenase', European Journal of Biochemistry, 72, 17–24.
- Borch, Nyegaard, Hansen, Mathiesen, Njølstad, Wilsgaard, Brækkan (2011) 'Joint effects of obesity and body height on the risk of venous thromboembolism: the Tromsø Study.', Arteriosclerosis, thrombosis, and vascular biology, 31, 1439–1444.
- Bordo, Bork (2002) 'The rhodanese/Cdc25 phosphatase superfamily', EMBO reports, 3(8), 741–746.
- Boustany, Bharadwaj, Daugherty, Brown, Randall, Cassis (2004) 'Activation of the systemic and adipose renin-angiotensin system in rats with diet-induced obesity and hypertension', Am J Physiol Regul Integr Comp Physiol, 287(4), R943-9.
- Bozaoglu, Segal, Shields, Cummings, Curran, Comuzzie, Mahaney, Rainwater, Vandeberg, MacCluer, Collier, Blangero, Walder, Jowett (2009) 'Chemerin is associated with metabolic syndrome phenotypes in a Mexican-American population', Journal of Clinical Endocrinology and Metabolism, 94(8), 3085–3088.
- Brestoff, Kim, Saenz, Stine, Monticelli, Sonnenberg, Thome, Farber, Lutfy, Seale, Artis (2015) 'Group 2 innate lymphoid cells promote beiging of white adipose tissue and limit obesity', Nature, 519(7542), 242–246.
- Brigelius-Flohé, Maiorino (2013) 'Glutathione peroxidases', Biochimica et Biophysica Acta - General Subjects, 1830(5), 3289–3303.
- Cadet, Delatour, Douki, Gasparutto, Pouget, Ravanat, Sauvaigo (1999) 'Hydroxyl radicals and DNA base damage', Mutation Research - Fundamental and Molecular Mechanisms of Mutagenesis, 424(1–2), 9–21.
- Cai, Shi, Wang, Fan, Feng, Lin, Yang, Cui, Tang, Xu, Geng (2016a) 'Cystathionine γ lyase–hydrogen sulfide increases peroxisome proliferator-activated receptor γ activity by sulfhydration at C139 site thereby promoting glucose uptake and lipid storage in adipocytes', BBA - Molecular and Cell Biology of Lipids, 1861, 419–429.
- Cai, Shi, Wang, Fan, Feng, Lin, Yang, Cui, Tang, Xu, Geng (2016b) 'Cystathionine γ lyase–hydrogen sulfide increases peroxisome proliferator-activated receptor γ activity by sulfhydration at C139 site thereby promoting glucose uptake and lipid storage in adipocytes', Biochimica et Biophysica Acta (BBA) - Molecular and Cell Biology of Lipids, 1861(5), 419–429.
- Caldefie-Chezet, Poulin, Vasson (2003) 'Leptin regulates functional capacities of polymorphonuclear neutrophils.', Free radical research, 37(8), 809–814.
- Calvert, Jha, Gundewar, Elrod, Ramachandran, Pattillo, Kevil, Lefer (2009) 'Hydrogen sulfide mediates cardioprotection through Nrf2 signaling.', Circulation research, 105(4), 365–74.
- Carrière, Carmona, Fernandez, Rigoulet, Wenger, Pénicaud, Casteilla (2004) 'Mitochondrial reactive oxygen species control the transcription factor CHOP-10/GADD153 and adipocyte differentiation: A mechanism for hypoxia-dependent effect', Journal of Biological Chemistry, 279(39), 40462–40469.
- Carrière, Fernandez, Rigoulet, Pénicaud, Casteilla (2003) 'Inhibition of preadipocyte proliferation by mitochondrial reactive oxygen species', FEBS Letters, 550(1–3), 163–167.
- Cawthorn, Scheller, Learman, Parlee, Simon, Mori, Ning, Bree, Schell, Broome, Soliman, DelProposto, Lumeng, Mitra, Pandit, Gallagher, Miller, Krishnan, Hui, Bredella, Fazeli, Klibanski, Horowitz, Rosen, MacDougald (2014) 'Bone marrow adipose tissue is an endocrine organ that contributes to increased circulating adiponectin during caloric restriction.', Cell metabolism, 20(2), 368–75.
- Chae, Kim, Kang, Rhee (1999) 'Characterization of three isoforms of mammalian peroxiredoxin that reduce peroxides in the presence of thioredoxin', Diabetes Research and Clinical Practice, 45(2–3), 101–112.
- Chan, Rimm, Colditz, Stampfer, Willett (1994) 'Obesity, fat distribution, and weight gain as risk factors for clinical diabetes in men', Diabetes Care, 17(9), 961–969.
- Chehab, Lim, Lu (1996) 'Correction of the sterility defect in homozygous obese female mice by treatment with the human recombinant leptin', Nature genetics, 12(3), 318–320.
- Chen, Lam, Wang, Wu, Lam, Shen, Wong, Hoo, Zhang, Xu (2006) 'Hypoxia dysregulates the production of adiponectin and plasminogen activator inhibitor-1 independent of reactive oxygen species in adipocytes', Biochemical and Biophysical Research Communications, 341(2), 549–556.
- Chen, Wei, Wang, Cui, Zhao, Zhu, Zhu, Guo, Yu (2009) 'Identification of signaling pathways involved in aberrant production of adipokines in adipocytes undergoing oxidative stress.', Archives of medical research, 40(4), 241–8.
- Chinetti, Zawadski, Fruchart, Staels (2004) 'Expression of adiponectin receptors in human macrophages and regulation by agonists of the nuclear receptors PPAR??, PPAR??, and LXR', Biochemical and Biophysical Research Communications, 314(1), 151–158.

- Cinti, Mitchell, Barbatelli, Murano, Ceresi, Faloia, Wang, Fortier, Greenberg, Obin (2005) 'Adipocyte death defines macrophage localization and function in adipose tissue of obese mice and humans.', Journal of lipid research, 46(11), 2347–2355.
- Coelho, Oliveira, Fernandes (2013) 'Biochemistry of adipose tissue: an endocrine organ.', Archives of medical science : AMS, 9(2), 191–200.
- Considine, Sinha, Heiman, Kriauciunas, Stephens, Nyce, Ohannesian, Marco, McKee, Bauer, Caro (1996) 'Serum immunoreactive-leptin concentrations in normal-weight and obese humans.', The New England journal of medicine, 334(5), 292–295.
- Costa, Pecci, Pensa, Cannella (1977) 'Hydrogen peroxide involvement in the rhodanese inactivation by dithiothreitol', Biochemical and biophysical research communications, 78(2), 596–603.
- Curtis, Grimsrud, Wright (2010) 'Downregulation of adipose glutathione S-transferase A4 leads to increased protein carbonylation, oxidative stress, and mitochondrial dysfunction', Diabetes, 59, 1132–1142.
- Demozay, Mas, Rocchi, Obberghen (2008) 'FALDH reverses the deleterious action of oxidative stress induced by lipid peroxidation product 4-hydroxynonenal on insulin signaling in 3T3-L1 adipocytes', Diabetes, 57, 1216–1226.
- Díaz-Ruiz, Guzmán-Ruiz, Moreno, García-Rios, Delgado-Casado, Membrives, Túnez, El Bekay, Fernández-Real, Tovar, Diéguez, Tinahones, Vázquez-Martínez, López-Miranda, Malagón (2015) 'Proteasome Dysfunction Associated to Oxidative Stress and Proteotoxicity in Adipocytes Compromises Insulin Sensitivity in Human Obesity.', Antioxidants & redox signaling, 23(7), 597–612.
- Diaz, Herzig, Vegiopoulos (2014) 'Thermogenic adipocytes: From cells to physiology and medicine', Metabolism: Clinical and Experimental, 63(10), 1238–1249.
- Dina, Meyre, Gallina, Durand, Körner, Jacobson, Carlsson, Kiess, Vatin, Lecoeur, Delplanque, Vaillant, Pattou, Ruiz, Weill, Levy-Marchal, Horber, Potoczna, Hercberg, Le Stunff, Bougnères, Kovacs, Marre, Balkau, Cauchi, Chèvre, Froguel (2007) 'Variation in FTO contributes to childhood obesity and severe adult obesity.', Nature genetics, 39(6), 724–6.
- Ding, Qin, He, Francis-David, Hou, Liu, Ricks, Yang (2007) 'Adiponectin and its receptors are expressed in adult ventricular cardiomyocytes and upregulated by activation of peroxisome proliferator-activated receptor ??', Journal of Molecular and Cellular Cardiology, 43(1), 73–84.
- Dinis-Oliveira, Duarte, Sánchez-Navarro, Remião, Bastos, Carvalho (2008) 'Paraquat poisonings: mechanisms of lung toxicity, clinical features, and treatment.', Critical reviews in toxicology, 38(1), 13–71.
- Dryden, Pickavance, Frankish, Williams (1995) 'Increased neuropeptide Y secretion in the hypothalamic paraventricular nucleus of obese (fa/fa) Zucker rats', Brain Research, 690(2), 185–188.
- Ducy, Amling, Takeda, Priemel, Schilling, Beil, Shen, Vinson, Rueger, Karsenty (2000) 'Leptin inhibits bone formation through a hypothalamic relay: a central control of bone mass.', Cell, 100(2), 197–207.
- Eggo, Warrack, Ramasamy, Langman, Singh (2008) 'Is thiosulfate sulfurtransferase the colonic sulfide oxidase?', Digestive diseases and sciences, 53(3), 862.
- Eguchi, Wang, Yu, Kershaw, Chiu, Dushay, Estall, Klein, Maratos-Flier, Rosen (2011) 'Transcriptional control of adipose lipid handling by IRF4', Cell Metabolism, 13(3), 249–259.
- Ekundi-Valentim, Santos, Camargo, Denadai-Souza, Teixeira, Zanoni, Grant, Wallace, Muscará, Costa (2010) 'Differing effects of exogenous and endogenous hydrogen sulphide in carrageenan-induced knee joint synovitis in the rat.', British journal of pharmacology, 159(7), 1463–1474.
- Elgazar-Carmon, Rudich, Hadad, Levy (2008) 'Neutrophils transiently infiltrate intra-abdominal fat early in the course of high-fat feeding.', Journal of lipid research, 49(9), 1894–903.
- Ernst, Issa, Goralski, Sinal (2010) 'Chemerin exacerbates glucose intolerance in mouse models of obesity and diabetes', Endocrinology, 151(5), 1998–2007.
- Fain, Madan, Hiler, Cheema, Bahouth (2004) 'Comparison of the release of adipokines by adipose tissue, adipose tissue matrix, and adipocytes from visceral and subcutaneous abdominal adipose tissues of obese humans', Endocrinology, 145(5), 2273–2282.
- Farooqi, Jebb, Langmack, Lawrence, Cheetham, Prentice, Hughes, McCamish, O'Rahilly (1999) 'Effects of Recombinant Leptin Therapy in a Child with Congenital Leptin Deficiency', New England Journal of Medicine, 341(12), 879–884.
- Farriol-Mathis, Garavelli, Boeckmann, Duvaud, Gasteiger, Gateau, Veuthey, Bairoch (2004) 'Annotation of post-translational modifications in the Swiss-Prot knowledge base', Proteomics, 4(6), 1537–1550.
- Feng, Chen, Zhao, Tang, Jiang, Geng (2009) 'Hydrogen sulfide from adipose tissue is a novel insulin resistance regulator.', Biochemical and biophysical research communications, 380(1), 153–9.
- Feuerer, Herrero, Cipolletta, Naaz, Wong, Nayer, Lee, Goldfine, Benoist, Shoelson, Mathis (2009) 'Lean, but not obese, fat is enriched for a unique population of regulatory T cells that affect metabolic parameters', Nature Medicinee, 15(8), 930–939.
- Fiorucci, Antonelli, Distrutti, Rizzo, Mencarelli, Orlandi, Zanardo, Renga, Di Sante, Morelli, Cirino, Wallace (2005) 'Inhibition of hydrogen sulfide generation contributes to gastric injury caused by anti-inflammatory nonsteroidal drugs.', Gastroenterology, 129(4), 1210–24.

- Fiorucci, Orlandi, Mencarelli, Caliendo, Santagada, Distrutti, Santucci, Cirino, Wallace (2007) 'Enhanced activity of a hydrogen sulphide-releasing derivative of mesalamine (ATB-429) in a mouse model of colitis.', British journal of pharmacology, 150(8), 996–1002.
- Fisher-Wellman, Ryan, Smith, Gilliam, Lin, Reese, Torres, Neufer (2016) 'A direct comparison of metabolic responses to high-fat diet in C57BL/6J and C57BL/6NJ mice', Diabetes, 65(11), 3249–3261.
- Flora (1999) 'Arsenic-induced oxidative stress and its reversibility following combined administration of n-acetylcysteine and meso 2, 3--dimercaptosuccinic acid in rats', Clinical and experimental pharmacology and physiology, 26(11), 865–869.
- Frayling, Timpson, Weedon, Freathy, Lindgren, Perry, Katherine, Lango, Rayner, Shields, Harries, Barrett, Ellard, Groves, Knight, Patch, Ness, Ebrahim, Lawlor, Ring, Ben-shlomo, Jarvelin, Sovio, Bennett, Melzer, Loos, Barroso, Wareham, Karpe, Owen, Cardon, Walker, Hitman, Colin, Doney, Morris, Smith, Wellcome, Case, Consortium, Hattersley, Mccarthy (2007) 'A Common Variant in the FTO Gene Is Associated with Body Mass Index and Predisposes to Childhood and Adult Obesity', Science, 316(5826), 889–894.
- Frederich, Hamann, Anderson, Lollmann, Lowell, Flier (1995) 'Leptin Levels Reflect Body Lipid Content in Mice: Evidence for Diet-Induced Resistance To Leptin Action', Nature Medicine, 1(12), 1311–1314.
- Friedman, Halaas (1998) 'Leptin and the regulation of body weight in mammals.', Nature, 395, 763–770.
- Frohnert, Long, Hahn, Bernlohr (2014) 'Glutathionylated lipid aldehydes are products of adipocyte oxidative stress and activators of macrophage inflammation.', Diabetes, 63(1), 89–100.
- Fu, Luo, Klein, Garvey (2005) 'Adiponectin promotes adipocyte differentiation, insulin sensitivity, and lipid accumulation.', Journal of lipid research, 46(7), 1369–1379.
- Furne, Saeed, Levitt (2008) 'Whole tissue hydrogen sulfide concentrations are orders of magnitude lower than presently accepted values.', American journal of physiology. Regulatory, integrative and comparative physiology, 295(5), R1479-85.
- Furukawa, Fujita, Shimabukuro, Iwaki, Yamada, Nakajima, Nakayama, Makishima, Matsuda, Shimomura (2004) 'Increased oxidative stress in obesity and its impact on metabolic syndrome', Journal of Clinical Investigation, 114(12), 1752–1781.
- Gabay, Dreyer, Pellegrinelli, Chicheportiche, Meier (2001) 'Leptin directly induces the secretion of interleukin 1 receptor antagonist in human monocytes', Journal of Clinical Endocrinology and Metabolism, 86(2), 783–791.
- Gaetani, Ferraris, Rolfo, Mangerini, Arena, Kirkman (1996) 'Predominant role of catalase in the disposal of hydrogen peroxide within human erythrocytes.', Blood, 87(4), 1595–1599.
- Gao, Madi, Ding, Fok, Steele, Ford, Hunter, Bing (2014) 'Interleukin-1β mediates macrophage-induced impairment of insulin signaling in human primary adipocytes.', American journal of physiology. Endocrinology and metabolism, 307(3), E289-304.
- Geng, Cai, Liao, Zheng, Zeng, Fan, Gong, Yang, Cui, Tang, Xu (2013) 'Increase or decrease hydrogen sulfide exert opposite lipolysis, but reduce global insulin resistance in high fatty diet induced obese mice.', PloS one, 8(9), e73892.
- Gieseg, Simpson, Charlton, Duncan, Dean (1993) 'Protein-bound 3,4-dihydroxyphenylalanine is a major reductant formed during hydroxyl radical damage to proteins.', Biochemistry, 32(18), 4780–6.
- Ginhoux, Schultze, Murray, Ochando, Biswas (2015) 'New insights into the multidimensional concept of macrophage ontogeny, activation and function.', Nature immunology, 17(1), 34–40.
- Di Girolamo, Skinner Jr., Hanley, Sachs (1971) 'Relationship of adipose tissue blood flow to fat cell size and number', Am J Physiol, 220(4), 932–937.
- Goralski, McCarthy, Hanniman, Zabel, Butcher, Parlee, Muruganandan, Sinal (2007) 'Chemerin, a novel adipokine that regulates adipogenesis and adipocyte metabolism', Journal of Biological Chemistry, 282(38), 28175–28188.
- Goubern, Andriamihaja, Nübel (2007) 'Sulfide, the first inorganic substrate for human cells', The FASEB Journal, 21(8), 1699–1706.
- Gregor, Hotamisligil (2007) 'Adipocyte stress: the endoplasmic reticulum and metabolic disease.', Journal of lipid research, 48(9), 1905–14.
- Gregor, Hotamisligil (2011) 'Inflammatory mechanisms in obesity.', Annual review of immunology, 29, 415–45.
- Grimsrud, Picklo, Griffin, Bernlohr (2007) 'Carbonylation of adipose proteins in obesity and insulin resistance: identification of adipocyte fatty acid-binding protein as a cellular target of 4-hydroxynonenal.', Molecular & cellular proteomics, 6, 624–37.
- Grundy (2016) 'Metabolic syndrome update', Trends in Cardiovascular Medicine, 26(4), 364–373.
- Gupta, Kruger (2011) 'Cystathionine beta-synthase deficiency causes fat loss in mice', PLoS ONE, 6(11).
- Halberg, Khan, Trujillo, Wernstedt-Asterholm, Attie, Sherwani, Wang, Landskroner-Eiger, Dineen, Magalang, Brekken, Scherer (2009) 'Hypoxia-Inducible Factor 1 Induces Fibrosis and Insulin Resistance in White Adipose Tissue', Mol Cell Biol., 29(16), 4467–4483.

- Han, Buffolo, Pires, Pei, Scherer, Boudina (2016) 'Adipocyte-Specific Deletion of Manganese Superoxide Dismutase Protects from Diet-Induced Obesity Via Increased Mitochondrial Uncoupling and Biogenesis.', Diabetes, 65(September), db160283.
- Han, Murthy, Wood, Song, Wang, Sun, Malhi, Kaufman (2013) 'ER stress signalling through eIF2a and CHOP, but not IRE1a, attenuates adipogenesis in mice', Diabetologia, 56(4), 911–924.
- Han, Umemoto, Omer, Den Hartigh, Chiba, LeBoeuf, Buller, Sweet, Pennathur, Abel, Chait (2012) 'NADPH oxidase-derived reactive oxygen species increases expression of monocyte chemotactic factor genes in cultured adipocytes', Journal of Biological Chemistry, 287(13), 10379–10393.
- Harding, Zhang, Zeng, Novoa, Lu, Calfon, Sadri, Yun, Popko, Paules, Stojdl, Bell, Hettmann, Leiden, Ron (2003) 'An integrated stress response regulates amino acid metabolism and resistance to oxidative stress', Molecular Cell, 11(3), 619–633.
- Harvey, Thimmulappa, Singh, Blake, Ling, Wakabayashi, Fujii, Myers, Biswal (2009) 'Nrf2-regulated glutathione recycling independent of biosynthesis is critical for cell survival during oxidative stress', Free Radical Biology and Medicine, 46(4), 443–453.
- Heffner, Herbert Pratt, Babiuk, Sharma, Rockwood, Donahue, Eppig, Murray (2012) 'Supporting conditional mouse mutagenesis with a comprehensive cre characterization resource', Nature Communications, 3, 1218.
- Henne, König, Triulzi, Baroni, Forlani, Scheibe, Papenbrock (2015) 'Sulfurtransferase and thioredoxin specifically interact as demonstrated by bimolecular fluorescence complementation analysis and biochemical tests', FEBS Open Bio, 5, 832–843.
- Hildebrandt, Grieshaber (2008) 'Three enzymatic activities catalyze the oxidation of sulfide to thiosulfate in mammalian and invertebrate mitochondria.', The FEBS journal, 275(13), 3352–61.
- Hiramatsu-Ito, Shibata, Ohashi, Uemura, Kanemura, Kambara, Enomoto, Yuasa, Matsuo, Ito, Hayakawa, Ogawa, Otaka, Kihara, Murohara, Ouchi (2016) 'Omentin attenuates atherosclerotic lesion formation in Apolipoprotein E-deficient mice', Cardiovascular Research, 110(1), 107–117.
- Horvat, Bünger, Falconer, Mackay, Law, Bulfield, Keightley (2000) 'Mapping of obesity QTLs in a cross between mouse lines divergently selected on fat content.', Mammalian genome : official journal of the International Mammalian Genome Society, 11(1), 2–7.
- Hosogai, Fukuhara, Oshima, Miyata, Tanaka, Segawa, Furukawa, Tochino, Komuro, Matsuda, Shimomura (2007) 'Adipose tissue hypoxia in obesity and its impact on adipocytokine dysregulation', Diabetes, 56(4), 901–911.
- Hosoki, Matsuki, Kimura (1997) 'The Possible Role of Hydrogen Sulfide as an Endogenous Smooth Muscle Relaxant in Synergy with Nitric Oxide ☆', Biochemical & Biophysical Research Communications, 237(3), 527–531.
- Hotamisligil, Murray, Choy, Spiegelman (1994) 'Tumor necrosis factor alpha inhibits signaling from the insulin receptor.', Proceedings of the National Academy of Sciences of the United States of America, 91(11), 4854–8.
- Hotamisligil, Shargill, Spiegelman (1993) 'Adipose expression of tumor necrosis factor-alpha: direct role in obesity-linked insulin resistance', Science, 259(5091), 87–91.
- Hu, Liang, Spiegelman (1996) 'AdipoQ is a novel adipose-specific gene dysregulated in obesity', Journal of Biological Chemistry, 271, 10697–10703.
- Huh, Kim, Jeong, Park, Kim, Huh, Kim, Woo, Rhee, Lee, Ha (2012) 'Peroxiredoxin 3 is a key molecule regulating adipocyte oxidative stress, mitochondrial biogenesis, and adipokine expression.', Antioxidants & redox signaling, 16(3), 229–43.
- Hull, Willard, Struck, Barrow, Brar, Andrikopoulos, Zraika (2017) 'High fat feeding unmasks variable insulin responses in male C57BL/6 mouse substrains', Journal of Endocrinology, 233(1), 53–64.
- Huszar, Lynch, Fairchild-Huntress, Dunmore, Fang, Berkemeier, Gu, Kesterson, Boston, Cone, Smith, Campfield, Burn, Lee (1997) 'Targeted Disruption of the Melanocortin-4 Receptor Results in Obesity in Mice', Cell, 88(1), 131–141.
- Ingalls, Dickie, Snell (1950) 'Obese, a new mutation in the house mouse', Journal of Heredity, 41(12), 315–317.
- James, Collins, Logan, Murphy (2012) 'Mitochondrial oxidative stress and the metabolic syndrome.', Trends in endocrinology and metabolism, 23(9), 429–34.
- Jun-ichi, Satoshi, Kimi, Fumi, Akira, Kiyoshi, Ken-ichi (1989) 'Expression vector system based on the chicken β-actin promoter directs efficient production of interleukin-5', Gene, 79(2), 269–277.
- Kabon, Nagele, Reddy, Eagon, Fleshman, Sessler, Kurz (2004) 'Obesity decreases perioperative tissue oxygenation.', Anesthesiology, 100(2), 274–80.
- Kamei, Tobe, Suzuki, Ohsugi, Watanabe, Kubota, Ohtsuka-Kowatari, Kumagai, Sakamoto, Kobayashi, Yamauchi, Ueki, Oishi, Nishimura, Manabe, Hashimoto, Ohnishi, Ogata, Tokuyama, Tsunoda, Ide, Murakami, Nagai, Kadowaki (2006) 'Overexpression of monocyte chemoattractant protein-1 in adipose

tissues causes macrophage recruitment and insulin resistance', Journal of Biological Chemistry, 281(36), 26602–26614.

- Kanda, Tateya, Tamori, Kotani, Hiasa, Kitazawa, Kitazawa, Miyachi, Maeda, Egashira, Kasuga (2006a) 'MCP-1 contributes to macrophage infiltration into adipose tissue, insulin resistance, and hepatic steatosis in obesity', Journal of Clinical Investigation, 116(6), 1494–1505.
- Kanda, Tateya, Tamori, Kotani, Hiasa, Kitazawa, Kitazawa, Miyachi, Maeda, Egashira, Kasuga (2006b) 'MCP-1 contributes to macrophage infiltration into adipose tissue, insulin resistance, and hepatic steatosis in obesity.', Journal of Clinical Investigation, 116(6), 1494–1505.
- Kaneko, Kimura, Taniguchi, Souma, Kojima, Kimura, Kimura, Niki (2009) 'Glucose-induced production of hydrogen sulfide may protect the pancreatic beta-cells from apoptotic cell death by high glucose', FEBS Letters, 583(2), 377–382.
- Katunga, Gudimella, Efird, Abernathy, Mattox, Beatty, Darden, Thayne, Alwair, Kypson, Virag, Anderson (2015) 'Obesity in a model of gpx4 haploinsufficiency uncovers a causal role for lipid-derived aldehydes in human metabolic disease and cardiomyopathy', Molecular Metabolism, 4(6), 493–506.
- Khan, Muise, Iyengar, Wang, Chandalia, Abate, Zhang, Bonaldo, Chua, Scherer (2009) 'Metabolic dysregulation and adipose tissue fibrosis: role of collagen VI.', Molecular and cellular biology, 29(6), 1575–1591.
- Kharroubi, Rasschaert, Eizirik, Cnop (2003) 'Expression of adiponectin receptors in pancreatic β cells', Biochemical and Biophysical Research Communications, 312(4), 1118–1122.
- Kiguchi, Maeda, Kobayashi, Fukazawa, Kishioka (2009) 'Leptin enhances CC-chemokine ligand expression in cultured murine macrophage', Biochemical and Biophysical Research Communications, 384(3), 311–315.
- Van Der Klaauw, Farooqi (2015) 'The Hunger Genes: Pathways to Obesity', Cell, 161, 119–132.
- Klinger, Chmura, Killeen (2010) 'Reporter alleles that inform on differences in Cre recombinase expression', J Immunol, 184(11), 6170–6176.
- Klover, Clementi, Mooney (2005) 'Interleukin-6 depletion selectively improves hepatic insulin action in obesity', Endocrinology, 146(8), 3417–3427.
- Koh, Park, Park, Jeon, Ryu, Kim, Kim, Kim, Kim, Park, Youn, Lee (2007) 'Essential role of mitochondrial function in adiponectin synthesis in adipocytes', Diabetes, 56, 2973–2981.
- Komura, Maeda, Mori, Kihara, Nakatsuji, Hirata, Tochino, Funahashi, Shimomura (2013) 'Adiponectin Protein Exists in Aortic Endothelial Cells', PLoS ONE, 8(8), 1–5.
- Konstantinides, Schäfer, Koschnick, Loskutoff (2001) 'Leptin-dependent platelet aggregation and arterial thrombosis suggests a mechanism for atherothrombotic disease in obesity', Journal of Clinical Investigation, 108(10), 1533–1540.
- Koppaka, Kehlenbrink, Carey, Li, Sanchez, Lee, Lee, Chen, Carrasco, Kishore, Zhang, Hawkins (2013) 'Reduced adipose tissue macrophage content is associated with improved insulin sensitivity in thiazolidinedione-treated diabetic humans', Diabetes, 62(6), 1843–1854.
- Kotnik, Fischer-Posovszky, Wabitsch (2011) 'RBP4: A controversial adipokine', European Journal of Endocrinology, 165(5), 703–711.
- Koumenis, Naczki, Koritzinsky, Rastani, Diehl, Sonenberg, Koromilas, Wouters (2002) 'Regulation of protein synthesis by hypoxia via activation of the endoplasmic reticulum kinase PERK and phosphorylation of the translation initiation factor eIF2alpha.', Molecular and cellular biology, 22(21), 7405–16.
- Kraakman, Kammoun, Allen, Deswaerte, Henstridge, Estevez, Matthews, Neill, White, Murphy, Peijs, Yang, Risis, Bruce, Du, Bobik, Lee-Young, Kingwell, Vasanthakumar, Shi, Kallies, Lancaster, Rose-John, Febbraio (2015) 'Blocking IL-6 trans-signaling prevents high-fat diet-induced adipose tissue macrophage recruitment but does not improve insulin resistance', Cell Metabolism, 21(3), 403–416.
- Krueger, Koch, Jühling, Tepel, Scholze (2010) 'Low expression of thiosulfate sulfurtransferase (rhodanese) predicts mortality in hemodialysis patients', Clinical Biochemistry, 43(1–2), 95–101.
- Kubota, Yano, Kubota, Yamauchi, Itoh, Kumagai, Kozono, Takamoto, Okamoto, Shiuchi, Suzuki, Satoh, Tsuchida, Moroi, Sugi, Noda, Ebinuma, Ueta, Kondo, Araki, Ezaki, Nagai, Tobe, Terauchi, Ueki, Minokoshi, Kadowaki (2007) 'Adiponectin Stimulates AMP-Activated Protein Kinase in the Hypothalamus and Increases Food Intake', Cell Metabolism, 6(1), 55–68.
- Künnecke, Verry, Bénardeau, von Kienlin (2004) 'Quantitative body composition analysis in awake mice and rats by magnetic resonance relaxometry.', Obesity research, 12(10), 1604–1615.
- Kurisaki, Hiroko (1974) 'Tissue distribution of paraquat and diquat after oral administration in rats', Forensic Science International, 14, 165–170.
- Landin, Stigendal, Eriksson, Krotkiewski, Risberg, Tengborn, Smith (1990) 'Abdominal obesity is associated with an impaired fibrinolytic activity and elevated plasminogen activator inhibitor-1', Metabolism, 39(10), 1044–1048.
- Lee, Kim, Choi, Kim, Yasue, Son, Masuzaki, Park, Kim (2008) 'Dysregulation of adipose glutathione peroxidase 3 in obesity contributes to local and systemic oxidative stress.', Molecular endocrinology, 22(9), 2176–2189.

- Lee, Petkova, Granneman (2013) 'Identification of an adipogenic niche for adipose tissue remodeling and restoration', Cell Metabolism, 18(3), 355–367.
- Leschelle, Goubern, Andriamihaja, Blottière, Couplan, Gonzalez-Barroso, Petit, Pagniez, Chaumontet, Mignotte, Bouillaud, Blachier (2005) 'Adaptative metabolic response of human colonic epithelial cells to the adverse effects of the luminal compound sulfide.', Biochimica et biophysica acta, 1725(2), 201–212.
- Li, Rose, Moore (2011) 'Hydrogen sulfide and cell signaling.', Annual review of pharmacology and toxicology, 51, 169–87.
- Li, Salto-Tellez, Tan, Whiteman, Moore (2009) 'GYY4137, a novel hydrogen sulfide-releasing molecule, protects against endotoxic shock in the rat.', Free radical biology & medicine, 47(1), 103–13.
- Li, Whiteman, Guan, Neo, Cheng, Lee, Zhao, Baskar, Tan, Moore (2008) 'Characterization of a novel, water-soluble hydrogen sulfide-releasing molecule (GYY4137): new insights into the biology of hydrogen sulfide.', Circulation, 117(18), 2351–60.
- Libiad, Sriraman, Banerjee (2015) 'Polymorphic variants of human rhodanese exhibit differences in thermal stability and sulfur transfer kinetics', Journal of Biological Chemistry, 290(39), 23579–23588.
- Libiad, Yadav, Vitvitsky, Martinov, Banerjee (2014) 'Organization of the human mitochondrial hydrogen sulfide oxidation pathway', Journal of Biological Chemistry, 289(45), 30901–30910.
- Ljungvall, Zimmerman (2012) 'Bigger bodies: Long-term trends and disparities in obesity and body-mass index among U.S. adults, 1960–2008', Social Science & Medicine, 75(1), 109–119.
- Lock, Wilks (2010) 'Paraquat', Hayes' Handbook of Pesticide Toxicology, 1771–1827.
- Locke, Kahali, Berndt, Justice, Pers, Day, Powell, Vedantam, Buchkovich, Yang, Croteau-Chonka, Esko, Fall, Ferreira, Gustafsson, Kutalik, Speliotes, et al. (2015) 'Genetic studies of body mass index yield new insights for obesity biology', Nature, 518(7538), 197–206.
- Loh, Deng, Fukushima, Cai, Boivin, Galic, Bruce, Shields, Skiba, Ooms, Stepto, Wu, Mitchell, Tonks, Watt, Febbraio, Crack, Andrikopoulos, Tiganis (2009) 'Reactive oxygen species enhance insulin sensitivity.', Cell metabolism, 10(4), 260–72.
- Long, Olson, Bernlohr (2013) 'High-fat diet induces changes in adipose tissue trans-4-oxo-2-nonenal and trans-4-hydroxy-2-nonenal levels in a depot-specific manner.', Free radical biology & medicine, 63, 390–8.
- Lord, Matarese, Howard, Baker, Bloom, Lechler (1998) 'Leptin modulates the T-cell immune response and reverses starvation-induced immunosuppression.', Nature, 394(6696), 897–901.
- Lu, Holmgren (2014) 'The thioredoxin antioxidant system.', Free radical biology & medicine, 66, 75–87.
- Lumeng, Bodzin, Saltiel (2007) 'Obesity induces a phenotypic switch in adipose tissue macrophage polarization', Journal of Clinical Investigation, 117(1), 175–184.
- Luo, Cao, Li, He (2008) 'Adipose tissue-specific PPARgamma deficiency increases resistance to oxidative stress.', Experimental gerontology, 43(3), 154–63.
- Lynch (2014) 'Adipose invariant natural killer T cells', Immunology, 142(3), 337–346.
- Lynch, Nowak, Varghese, Clark, Hogan, Toxavidis, Balk, O'Shea, O'Farrelly, Exley (2012) 'Adipose tissue invariant NKT cells protect against diet-induced obesity and metabolic disorder through regulatory cytokine production.', Immunity, 37(3), 574–87.
- Macfarlane, Gibson, Cummings (1992) 'Comparison of fermentation reactions in different regions of the human colon', Journal of Applied Bacteriology, 72(1), 57–64.
- Mahadev, Motoshima, Wu, Ruddy, Arnold, Cheng, Lambeth, Goldstein, Lambeth (2004) 'The NAD (P) H Oxidase Homolog Nox4 Modulates Insulin-Stimulated Generation of H 2 O 2 and Plays an Integral Role in Insulin Signal Transduction', Molecular and cellular biology, 24(5), 1844–1854.
- Majka, Miller, Helm, Acosta, Childs, Kong, Klemm (2014) Analysis and Isolation of Adipocytes by Flow Cytometry, 1st ed, Methods in Enzymology, Elsevier Inc.
- Malik, Willett, Hu, Malik, Willett, Hu (2012) 'Global obesity: trends, risk factors and policy implications', Nature Reviews Endocrinology, 9, 13–27.
- Mani, Yang, Wang (2011) 'A critical life-supporting role for cystathionine γ-lyase in the absence of dietary cysteine supply.', Free radical biology & medicine, 50(10), 1280–7.
- Manna, Jain (2011) 'Hydrogen sulfide and L-cysteine increase phosphatidylinositol 3,4,5-trisphosphate (PIP3) and glucose utilization by inhibiting phosphatase and tensin homolog (PTEN) protein and activating phosphoinositide 3-kinase (PI3K)/serine/threonine protein kinase (A', Journal of Biological Chemistry, 286(46), 39848–39859.
- Marí, Morales, Colell, Garcia-Ruiz, Fernandes-Checa (2009) 'Mitochondrial glutathione, a key survival antioxidant', Antioxidants & redox signaling, 11(11), 2685–2700.
- Matsuzawa-Nagata, Takamura, Ando, Nakamura, Kurita, Misu, Ota, Yokoyama, Honda, Miyamoto, Kaneko (2008) 'Increased oxidative stress precedes the onset of high-fat diet-induced insulin resistance and obesity.', Metabolism: clinical and experimental, 57(8), 1071–7.

- Matthews, Allen, Risis, Chan, Henstridge, Watson, Zaffino, Babb, Boon, Meikle, Jowett, Watt, Jansson, Bruce, Febbraio (2010) 'Interleukin-6-deficient mice develop hepatic inflammation and systemic insulin resistance', Diabetologia, 53(11), 2431–2441.
- McCormack, Atienza, Johnston, Andersen, Vu, Di Monte (2005) 'Role of oxidative stress in paraquat-induced dopaminergic cell degeneration', Journal of Neurochemistry, 93(4), 1030–1037.
- McGill, Schneider, Arfken, Lucore, Sobel (1994) 'Factors responsible for impaired fibrinolysis in obese subjects and NIDDM patients', Diabetes, 43(1), 104–109.
- Mellouk, Hachimi Idrissi, Louchami, Hupkens, Malaisse, Ait Yahia, Sener (2011) 'The metabolic syndrome of fructose-fed rats: effects of long-chain polyunsaturated ω3 and ω6 fatty acids. I. Intraperitoneal glucose tolerance test.', International journal of molecular medicine, 28(6), 1087–92.
- Mellouk, Sener, Ait Yahia, Malaisse (2012) 'The metabolic syndrome of fructose-fed rats: effects of long-chain polyunsaturated ω3 and ω6 fatty acids. VII. Oxidative stress.', Molecular medicine reports, 6(6), 1409–12.
- Molofsky, Nussbaum, Liang, Van Dyken, Cheng, Mohapatra, Chawla, Locksley (2013) 'Innate lymphoid type 2 cells sustain visceral adipose tissue eosinophils and alternatively activated macrophages', Journal of experiemental medicine, 210(3), 535–549.
- Montague, Farooqi, Whitehead, Soos, Rau, Wareham, Sewter, Digby, Mohammed, Hurst, Cheetham, Earley, Barnett, Prins, O'Rahilly (1997) 'Congenital leptin deficiency is associated with severe early-onset obesity in humans.', Nature, 387(6636), 903–908.
- Moraes-Vieira, Yore, Dwyer, Syed, Aryal, Kahn (2014) 'RBP4 activates antigen-presenting cells, leading to adipose tissue inflammation and systemic insulin resistance', Cell Metabolism, 19(3), 512–526.
- Morton, Beltram, Carter, Michailidou, Gorjanc, McFadden, Barrios-Llerena, Rodriguez-Cuenca, Gibbins, Aird, Moreno-Navarrete, Munger, Svenson, Gastaldello, Ramage, Naredo, Zeyda, Wang, Howie, Saari, Sipilä, Stulnig, Gudnason, Kenyon, Seckl, Walker, Webster, Dunbar, Churchill, Vidal-Puig, Fernandez-Real, Emilsson, Horvat (2016) 'Genetic identification of thiosulfate sulfurtransferase as an adipocyte-expressed antidiabetic target in mice selected for leanness', Nature Medicine, (April).
- Muellner, Schreier, Laggner, Hermann, Esterbauer, Exner, Gmeiner, Kapiotis (2009) 'Hydrogen sulfide destroys lipid hydroperoxides in oxidized LDL.', The Biochemical journal, 420(2), 277–81.
- Murano, Barbatelli, Parisani, Latini, Muzzonigro, Castellucci, Cinti (2008) 'Dead adipocytes, detected as crown-like structures, are prevalent in visceral fat depots of genetically obese mice.', Journal of lipid research, 49(7), 1562–1568.
- Murphy (2009) 'How mitochondria produce reactive oxygen species.', The Biochemical journal, 417(1), 1–13.
- Nagahara, Katayama (2005) 'Post-translational regulation of mercaptopyruvate sulfurtransferase via a low redox potential cysteine-sulfenate in the maintenance of redox homeostasis', Journal of Biological Chemistry, 280(41), 34569–34576.
- Nagahara, Okazaki, Nishino (1995) 'Cytosolic Mercaptopyruvate Sulfurtransferase Is Evolutionarily Related to Mitochondrial Rhodanese', Journal of Biological Chemistry, 270(27), 16230–16235.
- Nagareddy, Kraakman, Masters, Stirzaker, Gorman, Grant, Dragoljevic, Hong, Abdel-Latif, Smyth, Choi, Korner, Bornfeldt, Fisher, Dixit, Tall, Goldberg, Murphy (2014) 'Adipose tissue macrophages promote myelopoiesis and monocytosis in obesity', Cell Metabolism, 19(5), 821–835.
- Naiche, Papaioannou (2007) 'Cre activity causes widespread apoptosis and lethal anemia during embryonic development', Genesis, 45, 786–775.
- Nakajima, Taki, Wang, Ono, Matsumoto, Oghiso, Tanaka, Ichinohe, Nakamura, Tanaka, Nenoi (2008) 'Induction of rhodanese, a detoxification enzyme, in livers from mice after long-term irradiation with low-dose-rate gamma-rays.', Journal of radiation research, 49(6), 661–666.
- Nakamura, Sano, Fuster, Kikuchi, Shimizu, Ohshima, Katanasaka, Ouchi, Walsh (2016) 'Secreted frizzled-related protein 5 diminishes cardiac inflammation and protects the heart from ischemia/reperfusion injury', Journal of Biological Chemistry, 291(6), 2566–2575.
- Nakatsuji, Kishida, Sekimoto, Komura, Kihara, Funahashi, Shimomura (2014) 'Accumulation of adiponectin in inflamed adipose tissues of obese mice.', Metabolism: clinical and experimental, 63(4), 542–53.
- Nandi, Horowitz, Westley (2000) 'Rhodanese as a thioredoxin oxidase.', The International Journal of Biochemistry & Cell Biology, 32(4), 465–73.
- Neumeier, Weigert, Schäffler, Weiss, Kirchner, Laberer, Schölmerich, Buechler (2005) 'Regulation of adiponectin receptor 1 in human hepatocytes by agonists of nuclear receptors', Biochemical and Biophysical Research Communications, 334(3), 924–929.
- Ng, Fleming, Robinson, Thomson, Graetz, Margono, Mullany, Biryukov, Abbafati, Abera, Abraham, Abu-Rmeileh, Achoki, Albuhairan, Alemu, Alfonso, Gakidou, et al. (2014) 'Global, regional, and national prevalence of overweight and obesity in children and adults during 1980-2013: A systematic analysis for the Global Burden of Disease Study 2013', The Lancet, 384(9945), 766–781.

- Nguyen, Favelyukis, Nguyen, Reichart, Scott, Jenn, Liu-Bryan, Glass, Neels, Olefsky (2007) 'A subpopulation of macrophages infiltrates hypertrophic adipose tissue and is activated by free fatty acids via toll-like receptors 2 and 4 and JNK-dependent pathways', Journal of Biological Chemistry, 282(48), 35279–35292.
- Nguyen, Satoh, Favelyukis, Babendure, Imamura, Sbodio, Zalevsky, Dahiyat, Chi, Olefsky (2005) 'JNK and tumor necrosis factor-α mediate free fatty acid-induced insulin resistance in 3T3-L1 adipocytes', Journal of Biological Chemistry, 280(42), 35361–35371.
- Nicholls, Kim (1982) 'Sulphide as an inhibitor and electron donor for the cytochrome c oxidase system', Canadian journal of biochemistry, 60(6), 613–623.
- Nishimura, Manabe, Nagasaki, Eto, Yamashita, Ohsugi, Otsu, Hara, Ueki, Sugiura, Yoshimura, Kadowaki, Nagai (2009) 'CD8+ effector T cells contribute to macrophage recruitment and adipose tissue inflammation in obesity', Nat Med, 15(8), 914–920.
- O'Rourke, Grønning, Yeaman, Shepherd (2002) 'Glucose-dependent regulation of cholesterol ester metabolism in macrophages by insulin and leptin', Journal of Biological Chemistry, 277(45), 42557–42562.
- Ohashi, Parker, Ouchi, Higuchi, Vita, Gokce, Pedersen, Kalthoff, Tullin, Sams, Summer, Walsh (2010) 'Adiponectin promotes macrophage polarization toward an anti-inflammatory phenotype', Journal of Biological Chemistry, 285(9), 6153–6160.
- Ohashi, Shibata, Murohara, Ouchi (2014) 'Role of anti-inflammatory adipokines in obesity-related diseases', Trends in Endocrinology and Metabolism, 25(7), 348–355.
- Okamoto, Folco, Minami, Wara, Feinberg, Sukhova, Colvin, Kihara, Funahashi, Luster, Libby (2008) 'Adiponectin inhibits the production of CXC receptor 3 chemokine ligands in macrophages and reduces T-lymphocyte recruitment in atherogenesis', Circulation Research, 102(2), 218–225.
- Okamoto, Kihara, Ouchi, Nishida, Arita, Kumada, Ohashi, Sakai, Shimomura, Kobayashi, Terasaka, Inaba, Funahashi, Matsuzawa (2002) 'Adiponectin reduces atherosclerosis in apolipoprotein E-deficient mice', Circulation, 106(22), 2767–2770.
- Okamoto, Yamaoka, Takei, Ando, Taniguchi, Ishii, Tohya, Ishizaki, Niki, Kimura (2013) 'Endogenous hydrogen sulfide protects pancreatic beta-cells from a high-fat diet-induced glucotoxicity and prevents the development of type 2 diabetes.', Biochemical and biophysical research communications, 442(3–4), 227–33.
- Okuno, Matsuda, Kobayashi, Morita, Suzuki, Fukuhara, Komuro, Shimabukuro, Shimomura (2008) 'Adipose expression of catalase is regulated via a novel remote PPARy-responsive region', Biochemical and Biophysical Research Communications, 366(3), 698–704.
- Ouchi, Higuchi, Ohashi, Oshima, Gokce, Shibata, Akasaki, Shimono, Walsh (2010) 'Sfrp5 is an anti-inflammatory adipokine that modulates metabolic dysfunction in obesity', Science, 329(5990), 454–457.
- Ouchi, Kihara, Arita, Nishida (2001) 'Adipocyte-derived plasma protein, adiponectin, suppresses lipid accumulation and class A scavenger receptor expression in human monocyte-derived macrophages', Circulation, 103, 1057–1063.
- Ouchi, Kihara, Arita, Okamoto, Maeda, Kuriyama, Hotta, Nishida, Takahashi, Muraguchi, Ohmoto, Nakamura, Yamashita, Funahashi, Matsuz (2000) 'Adiponectin, an adipocyte-derived plasma protein, inhibits endothelial NF-kB signaling through a cAMP-dependent pathway', Circulation, 102, 1296–1301.
- Özcan, Cao, Yilmaz, Lee (2004) 'Endoplasmic reticulum stress links obesity, insulin action, and type 2 diabetes', Science, 306(October), 457–461.
- Pagani, Cannella, Cerletti, Pecci (1975) 'Restoration of the reconstitutive capacity of succinate dehydrogenase by rhodanese', FEBS Letters, 51(1), 112–115.
- Pagani, Galante (1983) 'Interaction of rhodanese with mitochondrial NADH dehydrogenase', Biochimica et Biophysica Acta, 742, 278–284.
- Paglialunga, Ludzki, Root-McCaig, Holloway (2015) 'In adipose tissue, increased mitochondrial emission of reactive oxygen species is important for short-term high-fat diet-induced insulin resistance in mice', Diabetologia, 1071–1080.
- Pan, Liu, Gong, Wu, Zhu (2011) 'Hydrogen sulfide attenuated tumor necrosis factor a-induced inflammatory signaling and dysfunction in vascular endothelial cells', PLoS ONE, 6(5).
- Pan, Wang, Liu, Yu, Zhang, Chen, Wang, Guan (2014) 'Involvement of CSE/ H2S in high glucose induced aberrant secretion of adipokines in 3T3-L1 adipocytes', Lipids Health Dis, 13, 155.
- Pannacciulli, Vettor, Milan, Granzotto, Catucci, Federspil, De Giacomo, Giorgino, De Pergola (2003) 'Anorexia nervosa is characterized by increased adiponectin plasma levels and reduced nonoxidative glucose metabolism', Journal of Clinical Endocrinology and Metabolism, 88(4), 1748–1752.
- Papapetropoulos, Pyriochou, Altaany, Yang, Marazioti, Zhou, Jeschke, Branski, Herndon, Wang, Szabó (2009) 'Hydrogen sulfide is an endogenous stimulator of angiogenesis.', Proceedings of the National Academy of Sciences of the United States of America, 106(51), 21972–21977.
- Park, Chen, Tishkoff, Peng, Tan, Dai, Xie, Zhang, Zwaans, Skinner, Lombard, Zhao (2013) 'SIRT5-Mediated Lysine Desuccinylation Impacts Diverse Metabolic Pathways', Molecular Cell, 50(6), 919–930.

- Park, Zhu, Palaniappan, Heshka, Carnethon, Heymsfield (2003) 'The metabolic syndrome: prevalence and associated risk factor findings in the US popu- lation from the Third National Health and Nutrition Examination Survey', Arch Intern Med, 163(1), 427–436.
- Patsouris, Li, Thapar, Chapman, Olefsky, Neels (2008) 'Ablation of CD11c-positive cells normalizes insulin sensitivity in obese insulin resistant animals.', Cell metabolism, 8(4), 301–9.
- Peh, Anwar, Ng, Atan, Kumar, Moore (2014) 'Effect of feeding a high fat diet on hydrogen sulfide (H2S) metabolism in the mouse.', Nitric oxide: biology and chemistry / official journal of the Nitric Oxide Society, 41, 138–145.
- Pesce, Ramalingam, Mentink-Kane, Wilson, Kasmi, Smith, Thompson, Cheever, Murray, Wynn (2009) 'Arginase-1-expressing macrophages suppress Th2 cytokine-driven inflammation and fibrosis', PLoS Pathogens, 5(4).
- Picton, Eggo, Merrill, Langman, Singh (2002) 'Mucosal protection against sulphide: importance of the enzyme rhodanese', Gut, 50, 201–206.
- Podrini, Cambridge, Lelliott, Carragher, Estabel, Gerdin, Karp, Scudamore, Ramirez-Solis, White (2013) 'High-fat feeding rapidly induces obesity and lipid derangements in C57BL/6N mice', Mammalian Genome, 24(5–6), 240–251.
- Pradhan, Manson, Rifai, Buring, Ridker (2001) 'C-reactive protein, interleukin 6, and risk of developing type 2 diabetes mellitus.', Jama, 286(3), 327–34.
- De Preter, Arijs, Windey, Vanhove, Vermeire, Schuit, Rutgeerts, Verbeke (2012) 'Decreased mucosal sulfide detoxification is related to an impaired butyrate oxidation in ulcerative colitis', Inflammatory Bowel Diseases, 18(12), 2371–2380.
- Qatanani, Szwergold, Greaves, Ahima, Lazar (2009) 'Macrophage-derived human resistin exacerbates adipose tissue inflammation and insulin resistance in mice', The journal of clinical investigation, 119(3), 531–539.
- Qian, Liu, Chen, Lu, Zhu (2015) 'Increased toll-like receptor 9 expression is associated with the severity of paraquat-induced lung injury in mice', Human and Experimental Toxicology, Epub.
- Quinlan, Perevoshchikova, Hey-Mogensen, Orr, Brand (2013) 'Sites of reactive oxygen species generation by mitochondria oxidizing different substrates.', Redox biology, 1(1), 304–12.
- Quintana-Cabrera, Bolaños (2013) 'Glutathione and γ-glutamylcysteine in the antioxidant and survival functions of mitochondria.', Biochemical Society transactions, 41(1), 106–10.
- Rafail, Ritis, Schaefer, Kourtzelis, Speletas, Doumas, Giaglis, Kambas, Konstantinides, Kartalis (2008) 'Leptin induces the expression of functional tissue factor in human neutrophils and peripheral blood mononuclear cells through JAK2-dependent mechanisms and TNF?? involvement', Thrombosis Research, 122(3), 366–375.
- Renehan, Tyson, Egger, Heller, Zwahlen (2008) 'Body-mass index and incidence of cancer: a systematic review and meta-analysis of prospective observational studies.', Lancet, 371, 569–78.
- Rose, Lock, Smith, Wyatt (1976) 'Paraquat accumulation: tissue and species specificity', Biochemical Pharmacology, 25(4), 419–423.
- Rosen, Spiegelman (2014) 'What we talk about when we talk about fat.', Cell, 156(1–2), 20–44.
- Rossoni, Manfredi, Tazzari, Sparatore, Trivulzio, Del Soldato, Berti (2010) 'Activity of a new hydrogen sulfide-releasing aspirin (ACS14) on pathological cardiovascular alterations induced by glutathione depletion in rats', European Journal of Pharmacology, 648(1–3), 139–145.
- Rudich, Kozlovsky (1997) 'Oxidant stress reduces insulin responsiveness in 3T3-L1 adipocytes', American Journal of …, 272, E935–40.
- Rudich, Tirosh, Potashink, Hemi, Kanety, Bashan (1998) 'Prolonged oxidative stress impairs insulin-induced GLUT4 translocation in 3T3-L1 adipocytes.', Diabetes., 47(October), 1562–1569.
- Ruskovska, Bernlohr (2013) 'Oxidative stress and protein carbonylation in adipose tissue - Implications for insulin resistance and diabetes mellitus.', Journal of proteomics.
- Sacks, Symonds (2013) 'Anatomical locations of human brown adipose tissue: Functional relevance and implications in obesity and type 2 diabetes', Diabetes, 62(6), 1783–1790.
- Samad, Pandey, Loskutoff (1998) 'Tissue factor gene expression in the adipose tissues of obese mice.', Proceedings of the National Academy of Sciences of the United States of America, 95(13), 7591–7596.
- Samad, Uysal, Wiesbrock, Pandey, Hotamisligil, Loskutoff (1999) 'Tumor necrosis factor alpha is a key component in the obesity-linked elevation of plasminogen activator inhibitor 1.', Proceedings of the National Academy of Sciences of the United States of America, 96(12), 6902–7.
- Satoh, Ogawa, Katsuura, Hayase, Tsuji, Imagawa, Yoshimasa, Nishi, Hosoda, Nakao (1997) 'The arcuate nucleus as a primary site of satiety effect of leptin in rats', Neuroscience Letters, 224(3), 149–152.
- Savage, Sewter, Klenk, Segal, Vidal-Puig, Considine, O'Rahilly (2001) 'Resistin / Fizz3 Expression in Relation to Obesity and Peroxisome Proliferator - Activated Receptor-?? Action in Humans', Diabetes, 50(10), 2199–2202.

- Scherer, Williams, Fogliano, Baldini, Lodish (1995) 'A novel serum protein similar to C1q, produced exclusively in adipocytes', Journal of Biological Chemistry, 270(45), 26746–26749.
- Schreier, Muellner, Steinkellner, Hermann, Esterbauer, Exner, Gmeiner, Kapiotis, Laggner (2010) 'Hydrogen sulfide scavenges the cytotoxic lipid oxidation product 4-HNE.', Neurotoxicity research, 17(3), 249–56.
- Schröder, Wandzioch, Helmcke, Brandes (2009) 'Nox4 acts as a switch between differentiation and proliferation in preadipocytes', Arteriosclerosis, Thrombosis, and Vascular Biology, 29(2), 239–245.
- Sell, Dietze-Schroeder, Kaiser, Eckel (2006) 'Monocyte chemotactic protein-1 is a potential player in the negative cross-talk between adipose tissue and skeletal muscle', Endocrinology, 147(5), 2458–2467.
- Seuring, Archangelidi, Suhrcke (2015) 'The Economic Costs of Type 2 Diabetes: A Global Systematic Review', PharmacoEconomics, 33(8), 811–831.
- Sharma, Das, Mondal, Hackney, Chu, Kern, Rasouli, Spencer, Yao-Borengasser, Elbein (2008) 'Endoplasmic reticulum stress markers are associated with obesity in nondiabetic subjects', The Journal of clinical endocrinology and metabolism, 93(11), 4532–4541.
- Shibuya, Tanaka, Yoshida, Ogasawara, Togawa, Ishii, Kimura (2009) '3-Mercaptopyruvate sulfurtransferase produces hydrogen sulfide and bound sulfane sulfur in the brain.', Antioxidants & redox signaling, 11(4), 703–14.
- Shungin, Winkler, Croteau-Chonka, Ferreira, Locke, Magi, Strawbridge, Pers, Fischer, Justice, Workalemahu, Wu, Buchkovich, Heard-Costa, Roman, Drong, Mohlke, et al. (2015) 'New genetic loci link adipose and insulin biology to body fat distribution.', Nature, 518(7538), 187–196.
- Sidhapuriwala, Li, Sparatore, Bhatia, Moore (2007) 'Effect of S-diclofenac, a novel hydrogen sulfide releasing derivative, on carrageenan-induced hindpaw oedema formation in the rat', European Journal of Pharmacology, 569(1–2), 149–154.
- Sierra-Honigmann, Nath, Murakami, García-Cardeña, Papapetropoulos, Sessa, Madge, Schechner, Schwabb, Polverini, Flores-Riveros (1998) 'Biological action of leptin as an angiogenic factor.', Science, 281(5383), 1683–1686.
- Sies (2014) 'Role of metabolic H2O2 generation: Redox signaling and oxidative stress', Journal of Biological Chemistry, 289(13), 8735–8741.
- Sievers, Wilm, Dineen, Gibson, Karplus, Li, Lopez, McWilliam, Remmert, Soding, Thompson, Higgins (2014) 'Fast, scalable generation of high-quality protein multiple sequence alignments using Clustal Omega', Molecular Systems Biology, 7(1), 539–539.
- Silventoinen, Magnusson, Tynelius, Kaprio, Rasmussen (2008) 'Heritability of body size and muscle strength in young adulthood: A study of one million Swedish men', Genetic Epidemiology, 32(4), 341–349.
- Singh, Rathore, Singh, Peddada, Ashish, Raychaudhuri (2013) 'Substitution of Glutamate Residue by Lysine in the Dimerization Domain Affects DNA Binding Ability of HapR by Inducing Structural Deformity in the DNA Binding Domain', PLoS ONE, 8(10).
- Skehan, Storeng, Scudiero, Monks, Mcmahon, Vistica, Warren, Bokesch, Kenney, Boyd (1990) 'New colorimetric cytotoxicity assay for anticancer-drug screening', Journal of the National Cancer Institute, 82(13), 1107–1112.
- Smirnov, Comte, Mager-Heckel, Addis, Krasheninnikov, Martin, Entelis, Tarassov (2010) 'Mitochondrial enzyme rhodanese is essential for 5 S ribosomal RNA import into human mitochondria.', The Journal of biological chemistry, 285(40), 30792–803.
- De Souza Batista, Yang, Lee, Glynn, Yu, Pray, Ndubuizu, Patil, Schwartz, Kligman, Fried, Gong, Shuldiner, Pollin, McLenithan (2007) 'Omentin plasma levels and gene expression are decreased in obesity', Diabetes, 56(6), 1655–1661.
- Staiger, Kaltenbach, Staiger, Stefan, Fritsche, Guirguis, Péterfi, Weisser, Machicao, Stumvoll, Häring (2004) 'Expression of adiponectin receptor mRNA in human skeletal muscle cells is related to in vivo parameters of glucose and lipid metabolism', Diabetes, 53(9), 2195–2201.
- Stefan, Vozarova, Funahashi, Weyer, Lindsay (2002) 'Plasma adiponectin concentration is associated with skeletal muscle insulin receptor tyrosine phosphorylation, and low plasma concentration precedes a decrease in whole-body insulin sensitivity in humans.', Diabetes, 50(June).
- Steppan, Bailey, Bhat, Brown, Banerjee, Wright, Patel, Ahima, Lazar (2001) 'The hormone resistin links obesity to diabetes', Nature, 409(6818), 307–312.
- Stohs (1990) 'Oxidative Stress Induced By TCDD', Free Radical Biology & Medicine1, 9, 79–90.
- Sun, Liu, Chen, Zhu (2012) 'Hydrogen sulfide decreases the levels of ROS by inhibiting mitochondrial complex IV and increasing SOD activities in cardiomyocytes under ischemia/reperfusion', Biochemical and Biophysical Research Communications, 421(2), 164–169.
- Surwit, Feinglos, Rodin, Sutherland, Petro, Opara, Kuhn, Rebuffe-Scribe (1995) 'Differential effects of fat and sucrose on the development of obesity and diabetes in C57BL/6J and A/J mice.', Metabolism, 44(5), 645–651.

- Szczesny, Módis, Yanagi, Coletta, Le Trionnaire, Perry, Wood, Whiteman, Szabo (2014) 'AP39, a novel mitochondria-targeted hydrogen sulfide donor, stimulates cellular bioenergetics, exerts cytoprotective effects and protects against the loss of mitochondrial DNA integrity in oxidatively stressed endothelial cells in vitro', Nitric Oxide - Biology and Chemistry, 41, 120–130.
- Talukdar, Oh, Bandyopadhyay, Li, Xu, McNelis, Lu, Li, Yan, Zhu, Ofrecio, Lin, Brenner, Olefsky (2012) 'Neutrophils mediate insulin resistance in mice fed a high-fat diet through secreted elastase.', Nature medicine, 18(9), 1407–12.
- Tang, Zhang, Yang, Wu, Wang (2013) 'Hydrogen sulfide-induced inhibition of L-type Ca2+ channels and insulin secretion in mouse pancreatic beta cells', Diabetologia, 56(3), 533–541.
- Taniguchi, Kang, Kimura, Niki (2011) 'Hydrogen sulphide protects mouse pancreatic B-cells from cell death induced by oxidative stress, but not by endoplasmic reticulum stress', British Journal of Pharmacology, 162(5), 1171–1178.
- Tartaglia, Dembski, Weng, Deng, Culpepper, Devos, Richards, Campfield, Clark, Deeds, Muir, Sanker, Moriarty, Moore, Smutko, Mays, Wool, Monroe, Tepper (1995) 'Identification and expression cloning of a leptin receptor, OB-R', Cell, 83(7), 1263–1271.
- Tashiro, Inamura, Kawabata, Sakurai, Yamanishi, Hayakawa, Mizuguchi (2009) 'Efficient adipocyte and osteoblast differentiation from mouse induced pluripotent stem cells by adenoviral transduction', Stem Cells, 27(8), 1802–1811.
- Tchernof, Després (2013) 'Pathophysiology of human visceral obesity: an update.', Physiological reviews, 93(1), 359–404.
- Tiranti, Viscomi, Hildebrandt, Di Meo, Mineri, Tiveron, Levitt, Prelle, Fagiolari, Rimoldi, Zeviani (2009) 'Loss of ETHE1, a mitochondrial dioxygenase, causes fatal sulfide toxicity in ethylmalonic encephalopathy.', Nature medicine, 15(2), 200–5.
- Tormos, Anso, Hamanaka (2011) 'Mitochondrial complex III ROS regulate adipocyte differentiation', Cell metabolism, 14(4), 537–544.
- Tormos, Anso, Hamanaka, Eisenbart, Joseph, Kalyanaraman, Chandel (2011) 'Mitochondrial complex III ROS regulate adipocyte differentiation.', Cell metabolism, 14(4), 537–44.
- Tsai, Peh, Feng, Dymock, Moore (2015) 'Hydrogen Sulfide Promotes Adipogenesis in 3T3L1 Cells', Plos One, 10(3), e0119511.
- Vega, Adams-Huet, Peshock, Willett, Shah, Grundy (2006) 'Influence of body fat content and distribution on variation in metabolic risk', Journal of Clinical Endocrinology and Metabolism, 91(11), 4459–4466.
- Velmurugan, Huang, Sun, Candela, Jaiswal, Beaman, Yamashita, Prakriya, White (2015) 'Depletion of H2S during obesity enhances store-operated Ca2+ entry in adipose tissue macrophages to increase cytokine production', Science Signaling, 8(407), ra128-ra128.
- Vitvitsky, Yadav, Kurthen, Banerjee (2015) 'Sulfide oxidation by a noncanonical pathway in red blood cells generates thiosulfate and polysulfides', Journal of Biological Chemistry, 290(13), 8310–8320.
- Vomhof-Dekrey, Picklo (2012) 'The Nrf2-antioxidant response element pathway: a target for regulating energy metabolism.', The Journal of nutritional biochemistry, 23(10), 1201–6.
- Wallace, Caliendo, Santagada, Cirino, Fiorucci (2007) 'Gastrointestinal Safety and Anti-Inflammatory Effects of a Hydrogen Sulfide-Releasing Diclofenac Derivative in the Rat', Gastroenterology, 132(1), 261–271.
- Wang, Zhao, Jin, Wei, Li, Bu, Tang, Ren, Tang, Du (2009) 'Role of hydrogen sulfide in the development of atherosclerotic lesions in apolipoprotein e knockout mice', Arteriosclerosis, Thrombosis, and Vascular Biology, 29(2), 173–179.
- Wardle, Carnell, Haworth, Plomin (2008) 'Evidence for a strong genetic influence on childhood adiposity despite the force of the obesogenic environment.', The American journal of clinical nutrition, 87(2), 398–404.
- Weisberg, McCann, Desai, Rosenbaum, Leibel, Ferrante (2003) 'Obesity is associated with macrophage accumulation in adipose tissue', Journal of Clinical …, 112(December), 1796–1808.
- Wen, Wang, Kho, Rinkiko, Sheng, Shen, Zhu (2013) 'Hydrogen Sulfide Protects HUVECs against Hydrogen Peroxide Induced Mitochondrial Dysfunction and Oxidative Stress', PLoS ONE, 8(2), e53147.
- Wensveen, Jelenčić, Valentić, Šestan, Wensveen, Theurich, Glasner, Mendrila, Štimac, Wunderlich, Brüning, Mandelboim, Polić (2015) 'NK cells link obesity-induced adipose stress to inflammation and insulin resistance.', Nature immunology, 16(4), 376–385.
- Wentworth, Naselli, Brown, Doyle, Phipson, Smyth, Wabitsch, Brien, Harrison (2010) 'Pro-inflammatory CD11c+CD206+ adipose tissue macrophages are associated with insulin resistance in human obesity', Diabetes, 59(July), 1648–1656.
- West, Boozer, Moody, Atkinson (1992) 'Dietary obesity in nine inbred mouse strains.', The American journal of physiology, 262(6 Pt 2), R1025-32.
- Whiteman, Armstrong, Chu, Jia-Ling, Wong, Cheung, Halliwell, Moore (2004) 'The novel neuromodulator hydrogen sulfide: an endogenous peroxynitrite "scavenger"?', Journal of neurochemistry, 90(3), 765–8.

- Whiteman, Gooding, Whatmore, Ball, Mawson, Skinner, Tooke, Shore (2010) 'Adiposity is a major determinant of plasma levels of the novel vasodilator hydrogen sulphide.', Diabetologia, 53(8), 1722–6.
- Whiteman, Li, Rose, Tan, Parkinson, Moore (2010) 'The effect of hydrogen sulfide donors on lipopolysaccharide-induced formation of inflammatory mediators in macrophages.', Antioxidants & redox signaling, 12(10), 1147–54.
- Wilson, Mudra, Furne, Levitt (2008) 'Differentiation of the roles of sulfide oxidase and rhodanese in the detoxification of sulfide by the colonic mucosa.', Digestive diseases and sciences, 53(1), 277–83.
- Wintner, Deckwerth, Langston, Bengtsson, Leviten, Hill, Insko, Dumpit, Vandenekart, Toombs, Szabo (2010) 'A monobromobimane-based assay to measure the pharmacokinetic profile of reactive sulphide species in blood', British Journal of Pharmacology, 160(4), 941–957.
- Wolins, Brasaemle, Bickel (2006) 'A proposed model of fat packaging by exchangeable lipid droplet proteins', FEBS Letters, 580(23), 5484–5491.
- Wong, Krawczyk, Kitidis-Mitrokostas, Revett, Gimeno, Lodish (2008) 'Molecular, biochemical and functional characterizations of C1q/TNF family members: adipose-tissue-selective expression patterns, regulation by PPAR-gamma agonist, cysteine-mediated oligomerizations, combinatorial associations and metabolic functions.', The Biochemical journal, 416(2), 161–77.
- Wormser, Kaptoge, Di Angelantonio, Wood, Pennells, Thompson, Sarwar, Kizer, Lawlor, Nordestgaard, Ridker, Salomaa, Stevens, Woodward, Sattar, Collins, Thompson, Whitlock, Danesh (2011) 'Separate and combined associations of body-mass index and abdominal adiposity with cardiovascular disease: Collaborative analysis of 58 prospective studies', The Lancet, 377(9771), 1085–1095.
- Wu, Molofsky, Liang, Ricardo-Gonzalez, Jouihan, Bando, Chawla, Locksley (2011) 'Eosinophils sustain adipose alternatively acitvated macrophages associated with glucose homeostasis', Science, 332(6026), 243–247.
- Wu, Zheng, Qi, Cheng, Sun, Gao, Zhang, Pang, Huangfu, Ji, Xue, Ji, Li (2015) 'Exogenous hydrogen sulfide mitigates the fatty liver in obese mice through improving lipid metabolism and antioxidant potential', Medical Gas Research, 5(1), 1.
- Xie, Shi, Xie, Wu, Li, Hua, Bian (2014) 'Sulfhydration of p66Shc at cysteine59 mediates the antioxidant effect of hydrogen sulfide.', Antioxidants & redox signaling, 21(18), 2531–42.
- Xu, Barnes, Yang, Tan, Yang, Chou, Sole, Nichols, Ross, Tartaglia, Chen (2003) 'Chronic inflammation in fat plays a crucial role in the development of obesity-related insulin resistance', Journal of Clinical Investigation, 112(December), 1821–1830.
- Xu, Grijalva, Skowronski, Van Eijk, Serlie, Ferrante (2013) 'Obesity activates a program of lysosomal-dependent lipid metabolism in adipose tissue macrophages independently of classic activation', Cell Metabolism, 18(6), 816–830.
- Xu, Wang, Keshaw, Yi Xu, Lam, Cooper (2003) 'The fat-derived hormone adiponectin alleviates alcoholic and nonalcoholic fatty liver diseases in mice', Journal of Clinical …, 112, 91–100.
- Xue, Hao, Sun, Li, Zhao, Li, Chen, Zhu, Ding, Liu, Zhu (2013) 'Hydrogen sulfide treatment promotes glucose uptake by increasing insulin receptor sensitivity and ameliorates kidney lesions in type 2 diabetes.', Antioxidants & redox signaling, 19(1), 5–23.
- Yamagishi, Edelstein, Du, Kaneda, Guzmán, Brownlee (2001) 'Leptin Induces Mitochondrial Superoxide Production and Monocyte Chemoattractant Protein-1 Expression in Aortic Endothelial Cells by Increasing Fatty Acid Oxidation via Protein Kinase A', Journal of Biological Chemistry, 276(27), 25096–25100.
- Yamauchi, Kamon, Waki, Terauchi, Kubota, Hara, Mori, Ide, Murakami, Tsuboyama-Kasaoka, Ezaki, Akanuma, Gavrilova, Vinson, Reitman, Kagechika, Shudo, Yoda, Nakano, Tobe, Nagai, Kimura, Tomita, Froguel, Kadowaki (2001) 'The fat-derived hormone adiponectin reverses insulin resistance associated with both lipoatrophy and obesity.', Nature Medicine, 7(8), 941–946.
- Yang, Graham, Mody, Preitner, Peroni, Zabolotny, Kotani, Quadro, Kahn (2005) 'Serum retinol binding protein 4 contributes to insulin resistance in obesity and type 2 diabetes', Nature, 436(7049), 356–362.
- Yang, Tang, Zhang, Wu, Wang (2011) 'The pathogenic role of cystathionine y-lyase/hydrogen sulfide in streptozotocin-induced diabetes in mice', American Journal of Pathology, 179(2), 869–879.
- Yang, Yang, Jia, Wu, Wang, Wang (2005) 'Activation of K-ATP channels by H2S in rat insulin-secreting cells and the underlying mechanisms', J Physiol, 5692, 519–531.
- Yang, Zhao, Ju, Mani, Cao, Puukila, Khaper, Wu, Wang (2013) 'Hydrogen Sulfide Protects Against Cellular Senescence via S-Sulfhydration of Keap1 and Activation of Nrf2', Antioxid. Redox Signal., 18(15), 1906–1919.
- Yant, Ran, Rao, Van Remmen, Shibatani, Belter, Motta, Richardson, Prolla (2003) 'The selenoprotein GPX4 is essential for mouse development and protects from radiation and oxidative damage insults', Free Radical Biology and Medicine, 34(4), 496–502.
- Yaswen, Diehl, Brennan, Hochgeschwender (1999) 'Obesity in the mouse model of pro-opiomelanocortin deficiency responds to peripheral melanocortin', Nature medicine, 5(9), 1066–1070.

- Ye, Gao, Yin, He (2007) 'Hypoxia is a potential risk factor for chronic inflammation and adiponectin reduction in adipose tissue of ob/ob and dietary obese mice.', American journal of physiology. Endocrinology and metabolism, 293(4), E1118–E1128.
- Yki-Jarvinen (2002) 'Ectopic fat accumulation: an important cause of insulin resistance in humans.', Journal of the Royal Society of Medicine, 95 Suppl 4, 39–45.
- Yokota, Oritani, Takahashi, Ishikawa, Matsuyama, Ouchi, Kihara, Funahashi, Tenner, Tomiyama, Matsuzawa (2000) 'Adiponectin, a new member of the family of soluble defense collagens, negatively regulates the growth of myelomonocytic progenitors and the functions of macrophages', Blood, 96, 1723–1732.
- Yu, Javorschi, Hevener, Kruszynska, Norman, Sinha, Olefsky (2002) 'The effect of thiazolidinediones on plasma adiponectin levels in normal, obese and type 2 diabetic subjects', Diabetes, 51(October), 2968–2974.
- Zarkesh-Esfahani, Pockley, Metcalfe, Bidlingmaier, Wu, Ajami, Weetman, Strasburger, Ross (2001) 'High-Dose Leptin Activates Human Leukocytes Via Receptor Expression on Monocytes', The Journal of Immunology, 167, 4593–4599.
- Zarrouki, Soares, Guichardant, Lagarde, Géloën (2007) 'The lipid peroxidation end-product 4-HNE induces COX-2 expression through p38MAPK activation in 3T3-L1 adipose cell', FEBS Letters, 581(13), 2394–2400.
- Zhang, Basinski, Beals, Briggs, Churgay, Clawson, DiMarchi, Furman, Hale, Hsiung, Schoner, Smith, Zhang, Wery, Schevitz (1997) 'Crystal structure of the obese protein leptin-E100.', Nature.
- Zhang, Guo, Wu, Zhang, Gu, Wang, Wang (2012) 'Hydrogen sulfide inhibits the development of atherosclerosis with suppressing CX3CR1 and CX3CL1 expression', PLoS ONE, 7(7), 1–18.
- Zhang, Guo, Zhang, Fan, Gu, Wu, Sparatore, Wang (2012) 'Effect of S-aspirin, a novel hydrogen-sulfide-releasing aspirin (ACS14), on atherosclerosis in apoE-deficient mice', European Journal of Pharmacology, 697(1–3), 106–116.
- Zhang, Pan, Zhou, Yuan, Wang, Cui, Zhang (2015) 'Hydrogen Sulfide as a Potential Therapeutic Target in Fibrosis', Oxidative Medicine and Cellular Longevity, Epub, ID: 593407.
- Zhang, Proenca, Maffei, Barone, Leopold, Friedman (1994) 'Positional cloning of the mouse obese gene and its human homologue.', Nature, 372(6505), 425–432.
- Zhang, Yang, Untereiner, Ju, Wu, Wang (2013) 'Hydrogen sulfide impairs glucose utilization and increases gluconeogenesis in hepatocytes.', Endocrinology, 154(1), 114–26.
- Zhao, Wang, Li, Wang, Tan, Cao, Suo, Jiang (2011) 'Hydrogen sulfide inhibits macrophage-derived foam cell formation.', Experimental biology and medicine (Maywood, N.J.), 236(2), 169–176.
- Zhao, Zhang, Lu, Wang (2001) 'The vasorelaxant effect of H2S as a novel endogenous gaseous KATP channel opener', The EMBO Jounrnal, 20(21), 6008–6016.
- Zheng, Li, Wang, Cang, Song, Liu, Li, Mohan, Wu, Hu, Peng (2015) 'PSTK is a novel gene associated with early lung injury in Paraquat Poisoning', Life Sciences, 123, 9–17.
- Zhou, Lu, Hajifathalian, Bentham, Di Cesare, Danaei, Bixby, Cowan, Ali, Taddei, Lo, Reis-Santos, Stevens, Riley, Miranda, Bjerregaard, Cisneros, et al. (2016) 'Worldwide trends in diabetes since 1980: A pooled analysis of 751 population-based studies with 4.4 million participants', The Lancet, 387(10027), 1513–1530.